Master Thesis

Fulfillment of the Requirements for the Degree of
Diplom-Ingenieurs (Dipl.-Ing.)
in the field of Bergwesen
Masterstudium Rohstoffgewinnung und Tunnelbau
Schwerpunktfach Geotechnik und Tunnelbau

Submitted to the
Chair of Subsurface Engineering
at the Montanuniversität Leoben

Ing. Heiko-Marc Mödlhammer, BSc

Leoben, Juni 2011

Topic

“Numerical Methods for Tunneling using ABAQUS and Investigations of Long-Time-Effects of the Shotcrete Shell and its Impact on the Combined Support System”

Affidavit

I declare in lieu of oath, that I wrote this thesis and performed the associated research myself, using only literature cited in this volume.

Eidesstattliche Erklärung

Ich erkläre an Eides statt, dass ich diese Arbeit selbständig verfasst, andere als die angegebenen Quellen und Hilfsmittel nicht benutzt und mich auch sonst keiner unerlaubter Hilfsmittel bedient habe.

(Unterschrift)

Datum	Ing. Heiko-Marc Mödlhammer, BSc

Acknowledgements

My long journey has finally come to an end. I truly appreciate every moment and time I had the great opportunity to learn so much and get to know so much excellent people making my studying memorable and to a great part of my life.

First, for the excellent education at the Montanuniversität Leoben and for the unique opportunity to develop my master thesis at the MIT I would like to express my thanks to Univ.-Prof. Dipl.Ing. Dr.mont Robert Galler.

For supervising this thesis I would like to extend my sincere thanks to Univ.-Prof. Dipl.Ing. Dr.tech. Herbert H. Einstein. He supported me with valuable suggestions and a wealth of advice during this research. It was a great honor and pleasure for me to be under the guidance of such an experienced and great professor.

I also would like to thank my friends – Bernhard, Stefan, Thomas, Marty, Peter, Gunter and all others for making my live at MIT special and unforgettable.

Most importantly, I would like to give a special thank to my family for their continuous support and encouragement throughout this long and challenging phase of my live.

Danksagung

Meine lange Reise kommt schließlich zu einem Ende. Ich bin sehr dankbar für jeden Augenblick und die Zeit in der ich die großartige Möglichkeit hatte so viel zu lernen, sowie so viele hervorragende Menschen kennenlernen zu dürfen, welche mein Studium unvergesslich und zu einem großartigen Teil meines Lebens machten.

Als erstes möchte ich mich für die hervorragende Ausbildung an der Montanuniversität Leoben, sowie für die einzigartige Möglichkeit meine Master Thesis am MIT zu erarbeiten bei Univ.-Prof. Dipl.Ing. Dr.mont. Robert Galler bedanken.

Meinen aufrichtigen Dank für die Betreuung dieser Arbeit möchte ich Univ.-Prof. Dipl.Ing. Dr.tech. Herbert H. aussprechen. Er unterstütze mich mit wertvollen Anregungen und einer Fülle von Ratschlägen während meiner gesamten Diplomarbeit. Es war eine große Ehre und Freude für mich von einem so erfahrenen und routinierten Professor lernen zu dürfen.

Ich möchte mich auch bei meinen Freunden bedanken – Bernhard, Stefan, Thomas, Marty, Peter, Gunter und allen anderen welche mein Leben am MIT und in Leoben bereicherten und unvergesslich machten.

Insbesondere möchte ich mich ganz speziell bei meiner Familie für ihre ununterbrochene Unterstützung und Ermutigung während dieser langen und herausfordernden Phase meines Lebens bedanken.

Abstract

This thesis uses the finite element method to investigate the effect of tunnel support deterioration on the performance of tunnels. First, different methods to simulate tunnel excavation and the installation of a dual-lining system (primary shotcrete shell / secondary cast-in-place concrete inner liner) using the general-purpose of the finite element program ABAQUS are discussed. The second aim of this study is to understand the influence of long-time deterioration of tunnel supports and its impact on the stability of the combined support system (surrounding ground, shotcrete shell and inner liner). Using a parametric study, different deterioration processes are simulated, assuming elastic as well as elasto-plastic material behavior. This includes the simulation of tunnel excavation, the interaction between the shotcrete shell and the ground, and the interaction between the shotcrete shell and the inner liner. This allows one to interpret the main characteristics of the analyzed deterioration processes on the basis of the obtained stress distributions and displacements of the support elements.

Kurzfassung

Diese Arbeit verwendet die Finite Elemente Methode zur Untersuchung der Verwitterung der Tunnelausbauelemente sowie die daraus folgenden Auswirkungen auf das gesamte Tunnelsystem. Als erstes werden verschiedene Techniken zur Simulation eines zweischaligen Tunnelvortriebes (primäre Spritzbetonschale / sekundäre Ortbeton-Innenschale), welche mit dem Finite Elemente Programm ABAQUS simuliert werden, diskutiert. Das zweite Hauptaugenmerk dieser Arbeit liegt auf Langzeit-Verwitterungsprozessen bestehender Tunnelauskleidungen, sowie deren Auswirkungen auf das kombinierte Tragsystem (Gebirge, Spritzbetonschale und Innenschale). Anhand einer Parameterstudie werden verschiedene Verwitterungsszenarien simuliert, wobei elastisches sowie elasto-plastisches Materialverhalten berücksichtigt werden. Dabei wird besonders auf den Tunnelvortrieb, die Kontaktbedingungen zwischen Gebirge und Spritzbetonschale sowie zwischen Spritzbetonschale und Innenschale Wert gelegt. Die Hauptcharakteristiken der Verwitterungsprozesse werden aufgrund der Verschiebungen und der Spannungen der Ausbauelemente interpretiert.

Table of Contents

I. Introduction and Problem Statement

Due to the increasing age of road and railway tunnels, maintenance becomes more important. Nowadays, many Austrian road tunnels with a dual-lining system including shotcrete as primary liner are around 30 to 40 years old. Since the long-time behavior of shotcrete, considering deterioration processes, is not well known, assumptions are made from zero to total deterioration of the shotcrete shell (Stadelmann, Pfeffer, & Wei, 2009). Guidelines like the RVS 09.01.42, (2004) consider the shotcrete shell to be a temporary support, which looses its effect after the construction of the inner liner.

There are two reasons for the deterioration of shotcrete. On the one hand, there can be an increase of the ground-pressure. For example, this can occur by sintering processes in the tunnel drainage system, which cause an increase of the water-pressure and induce greater stresses on the support elements. Another example for the increase of the ground-pressure is based on the suggestion of Pacher, (1964) who says that the load on the tunnel-crown may be estimated by simply considering the weight of the plastic zone. As a result of weathering processes, the plastic zone around the tunnel may grow and so does the load that the tunnel support has to bear.

On the other hand, deterioration of the shotcrete may occur through an attack of aggressive groundwater (e.g. sulphates corrosion, calcium leaching). To get a clear picture about these processes, it is necessary to understand the characteristics and mechanisms of deterioration of shotcrete and to identify their causes and effects. Deterioration can be associated with physical, chemical and other processes:

1. Physical processes are time-dependent changes of loading conditions. Both, support elements and ground are affected. In most cases, the influence of groundwater causes these processes and induces larger stresses in the support elements.

2. Chemical processes change the chemical composition of support elements and ground with time. Aggressive groundwater is often the reason for these processes. Due to the fact, that most tunnels with a dual-lining system have a waterproofing membrane between shotcrete shell and inner liner, only the shotcrete shell is affected by these processes. The consequence of chemical processes is a change in the support characteristics.

3. Other processes like ice- and frost-action and rare events such as fire and car-collisions may also change the tunnel support and should be considered.

Using this classification, a tunnel constructed with a dual-lining system is investigated in a numerical parametric study to analyze the long-time deterioration processes of the shotcrete shell and their impacts on the combined support system, i.e. the ground plus shotcrete shell plus inner liner. The results are discussed in terms of stresses and displacements of the support elements, which evolve during deterioration.

II. Research objectives and approach

The main objectives of this research are to create a numerical model with the general-purpose finite element program ABAQUS to simulate deterioration processes and their impacts on the tunnel.

In order to achieve this goal, a literature study investigates the main deterioration processes of tunnels. Based on the knowledge that groundwater very often is the driving force of deterioration, different tunnel support systems are analyzed to figure out, which ones are commonly built when groundwater is present. In the following step, possible methodologies and solutions to simulate dual-lining tunnel support systems will be studied.

A tunnel construction method, which allows not only considering contact mechanisms between the primary- and secondary liner, but also to simulate deterioration of individual support elements, is used in the parametric study. As a result of this research, one can determine the effects of long-time deterioration processes of tunnel support systems.

III. Structure of Thesis

This thesis is structured as follows:

Chapter 1 presents an overview of the main deterioration processes of tunnels. The deterioration consists of physical-, chemical-, and other processes.

In Chapter 2, a brief introduction to modern tunnel support systems, which includes single-lining- and dual-lining-systems, is presented. Furthermore, it is shown which systems are commonly used in environments where deterioration may occur.

Chapter 3 presents the numerical model, which includes a general part, a part that investigates the construction of a tunnel with a dual-lining system in detail, and a part about the deterioration of the primary shotcrete shell.

In Chapter 4 the results of the parametric study, showing different deterioration processes of the primary shotcrete shell, are presented.

Finally, the conclusions of this research and the recommendations for future researches are outlined in Chapter 5.

1 DETERIORATION OF TUNNELS

Structural and mechanical characteristics during the life-time of a tunnel change. There are many kinds of degradation processes, which may affect tunnels and reduce their safety and serviceability. Due to the increasing age of tunnels in Europe an investigation of long-term-effects becomes more important. Points, which have to be considered, are:

- Monitoring of the tunnel during construction and its life-time. This includes information such as material properties of support elements (initial support and final support) and ground, measurements of deformation, geology and groundwater conditions.
- Investigation of the long-time deterioration processes. This includes understanding their causes and their effects on the support elements and ground.

This thesis investigates deterioration processes, which may affect the support elements. For a better overview these processes are divided into three categories:

- Physical processes
- Chemical processes
- Other processes

1.1 Physical processes

The properties of support elements and ground are affected by several aging processes. Sandrone & Labiouse (2009) recommended calculating these effects by a stiffness reduction or a strain increase.

Physical processes are time-dependent changes of conditions and tectonic effects. For example, time-dependent conditions are water-pressure and water-flow around the tunnel as well as over-consolidation. Changing conditions may lead to swelling or creeping of the ground:

Zachow (1995) argued that an increase of the water-pressure may be the result of sintering of the tunnel drainage system, which causes higher stresses on the support elements.

For deep tunnels, Pacher (1964) suggested the load on the tunnel crown by considering the weight of the plastic zone. According to the German guideline DS 853 (2007) water ingress may lead to a deterioration of ground around the opening by the fact that a tunnel, which is built in an aquifer can act like a drainage system. As a result the ground is eroded and the plastic zone around the tunnel grows. Accordingly, the entire support elements receive additional load.

Marcher & Jiricny (2004) state that over-consolidation of highly cohesive soils may influence the load on tunnel supports. As a result of the tunnel excavation in highly cohesive soils, negative pore-water-pressure may initially build up and first loads the support to a small extent. Through reduction of the negative pore water-pressure over time, the tunnel support elements are loaded. Also, considering the geological conditions, impacts from tectonic movements and viscoplastic deformations, which lead to creep-displacements, have to be taken into account. (Marcher & Jiricny, 2004)

The main physical processes can be summarized:

- Support elements:
  - Ageing
- Ground:
  - Change of water-pressure
  - Water-flow around the opening
  - Over-consolidation of highly cohesive soil
  - Swelling
  - Creeping
  - Tectonic movements

1.2 Chemical processes

Support elements as well as the surrounding ground are affected by chemical processes. In many cases aggressive water causes chemical reactions in the surrounding ground or the support elements. The chemical composition of ground and support elements changes with time and in most instances leads to changed stability conditions. A reduction of rock mass strength properties due to long-time deterioration caused by chemical processes is analyzed by Ladanyi, (1974) and Daemen, (1975). Sandrone & Labiouse (2009) recommend calculating these effects by reducing the material's strength. Also a thickness reduction of the inner liner (final support), which may be caused by deterioration due to de-icing salt corrosion, is discussed.

The main attention is paid to the exposed surfaces of the support elements. These surfaces may be affected first by aggressive groundwater (e.g. sulphates corrosion, calcium leaching, and so on). However, one has to distinguish between a tunnel system with and without sealing. When a waterproofing membrane is placed between the shotcrete shell (part of initial support) and the inner liner, only the initial support (shotcrete shell, rock bolts and anchors) and the inner liner intrados can be affected by chemical deterioration processes. Sandrone & Labiouse (2009) state that in case of a sealing, the deterioration of the shotcrete occurs much faster. This is based on the fact that between the shotcrete shell intrados and the sealing, the aggressive groundwater is concentrated.

An assumption for long-time failure behavior of the support elements is based on the fact that the structural steel elements (rock bolts, anchors, wire mesh and steel ribs)

are not perfectly protected against corrosion. A concrete cover is feasible during construction, but subsequent deformations of the ground may cause cracks in the shotcrete / concrete cover and as a result the protection effect is abolished. (Marcher & Jiricny, 2004)

The main chemical processes can be summarized:

- Support element:
  - Aggressive groundwater
  - De-icing salt corrosion affecting inner liner intrados
  - Steel corrosion
- Ground:
  - Weathering

1.3 Other processes

Ice- and frost-action and rare events such as fire and car-collisions may also change the equilibrium of a tunnel with time and should be considered.

1.4 Research approach

Since a detailed description of all aspects (deterioration of support elements and ground, caused by physical, chemical and other processes) would go beyond the scope of this thesis, only the deterioration of the shotcrete shell caused by physical and chemical processes is investigated.

Hence, to simulate the physical deterioration processes, a degradation of the Young's modulus is used and to simulate the chemical deterioration processes the compressive strength is reduced. For detailed values of the reduction of the Young's Modulus and the compressive strength see chapter 3.7.

2 MODERN TUNNEL SUPPORTS

Basically, one can distinguish simple single-lining systems and dual-lining systems. Both support systems are designed and implemented today. In this study the main attention will be paid to a lining system, which uses shotcrete as the primary liner (shell). Moreover, the focus is on the simulation of the construction process followed by the deterioration of the primary shotcrete shell. However, to provide an overview of the tunnel support systems that use shotcrete, this chapter describes single-lining and dual-lining systems.

2.1 Single-lining systems

Generally, single-lining systems can be implemented with different construction methods. Shotcrete is applied when using the conventional (drill and blast) tunneling methods as well as when using the mechanical tunneling methods with roadheaders or open tunnel boring machines (TBMs). Pre-cast tunnel segments are mostly used with shielded TBMs. Thus, single-lining systems can be realized with every tunneling method. Fig. 2–1 provides an overview of common tunneling methods, whereby the tunneling methods which use shotcrete are highlighted.

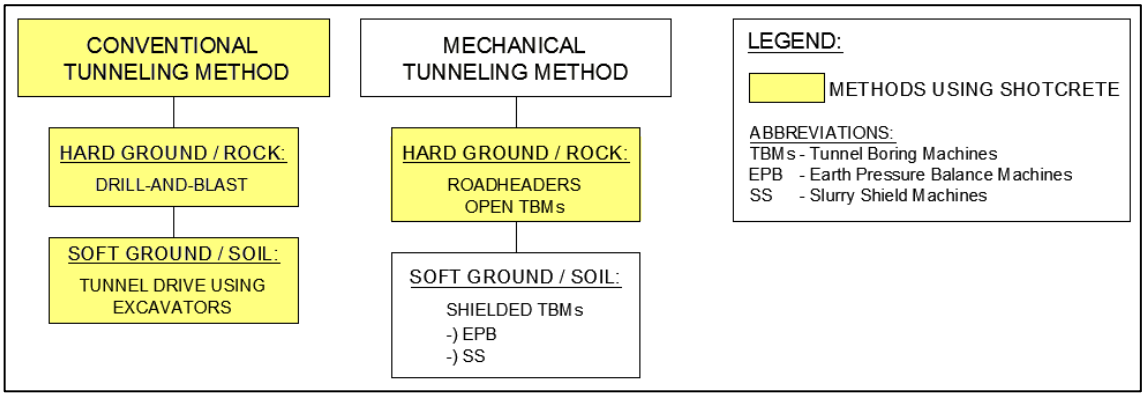

Fig. 2–1: Overview of tunneling methods; yellow colored methods provide the possibility to use shotcrete as support.

Single-lining systems in infrastructure tunnels (e.g. road-tunnels, railway-tunnels) are only used in exceptional cases since they are not watertight. To guarantee the tunnel's long-time watertightness, the shotcrete should be applied in several layers to the tunnel wall and to minimize cracking, reinforcement should be used either with wire mesh or steel fiber shotcrete. Watertightness can be reached by sub-sequent grouting. Nevertheless, one has to be aware of the fact that single-lining systems are not ideal when groundwater is present. Fig. 2–2 presents two different types of single-lining systems.

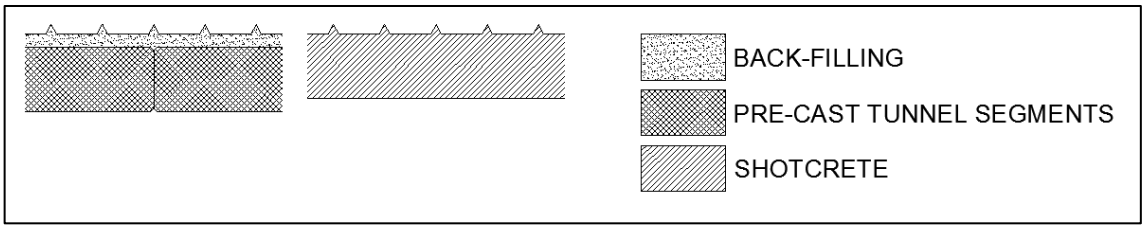

Fig. 2–2: different types of single-lining systems; adapted from RVS 09.01.31, (2003)

2.2 Dual-lining systems – composite lining (C-DLS)

Dual-lining systems with composite linings (C-DLS) consist of two tied liners (primary liner and secondary liner), which are applied one after the other. “Tied” implies that the tunnel liners are in tight mechanical contact with each other. The primary liner can be shotcrete or pre-cast tunnel segments. Cast-in-place concrete is usually used for the secondary inner liner. Fig. 2–3 shows different types of C-DLS. Since all liners are tied, C-DLS have a higher load-bearing capacity than other dual-lining systems, in which the primary- and secondary liner are separated by a waterproofing membrane, i.e. S-DLS (see section 2.3). As a consequence, the drainage effect of S-DLS does not occur and additional water-pressure can act on the tunnel support. Furthermore, since the primary shotcrete shell is not watertight, the secondary liner is not protected against aggressive groundwater. Therefore, C-DLS are not recommended when aggressive groundwater is present.

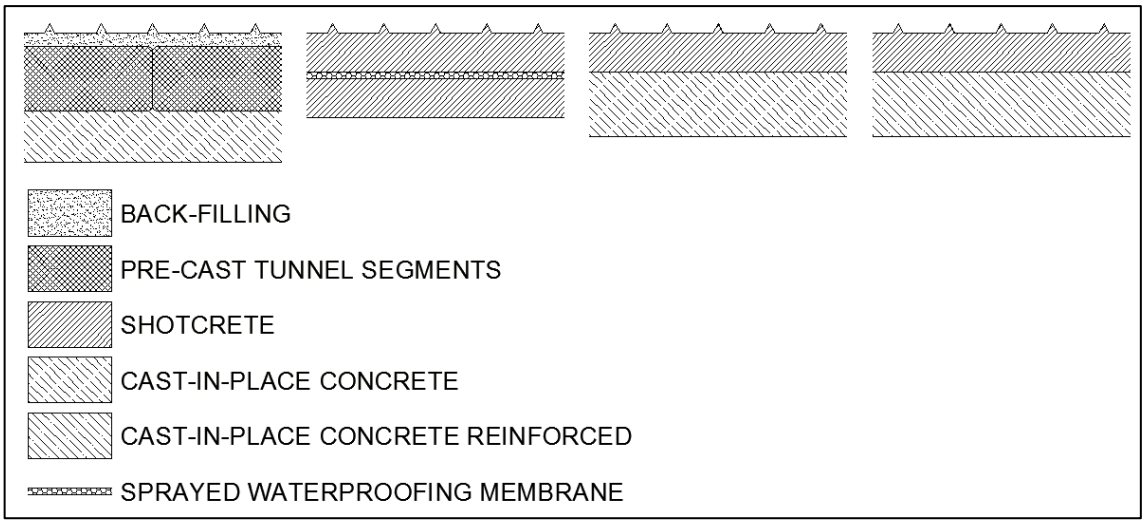

Fig. 2–3: different types of dual-lining systems with composite linings (C-DLS); note that C-DLS consist of different connected components; adapted from RVS 09.01.31, (2003)

Special types of C-DLS are systems with a sprayed waterproofing membrane between primary and secondary liner. The advantages of sprayed waterproofing membranes are that they can be easily applied when complex tunnel-geometries are present (e.g. junctions, bays) and that the tied contact between primary and secondary liner can be maintained. One has to be aware of the fact that there are other C-DLS than those shown in Fig. 2–3.

2.3 Dual-lining systems – separate linings (S-DLS)

Dual-lining systems with separate linings (S-DLS) consist of two independent liners (primary liner and secondary liner), which are applied one after the other. The separation of the primary and the secondary liner with a waterproofing membrane, which is applied after the primary liner is installed, is the main characteristic of S-DLS; S-DLS can be used with all tunneling methods. For the conventional, drill and blast tunneling method, the primary liner is a shotcrete shell, and when the mechanical tunneling method is used, the primary liner can be made of shotcrete or pre-cast tunnel segments. Regarding both tunneling methods (conventional, and mechanical), the secondary liner usually consists either of non-reinforced or of reinforced cast-in-place concrete. Fig. 2–4 illustrates different types of S-DLS. After the waterproofing membrane is installed, the secondary liner is constructed. Thus, watertightness of the primary liner is not absolutely necessary.

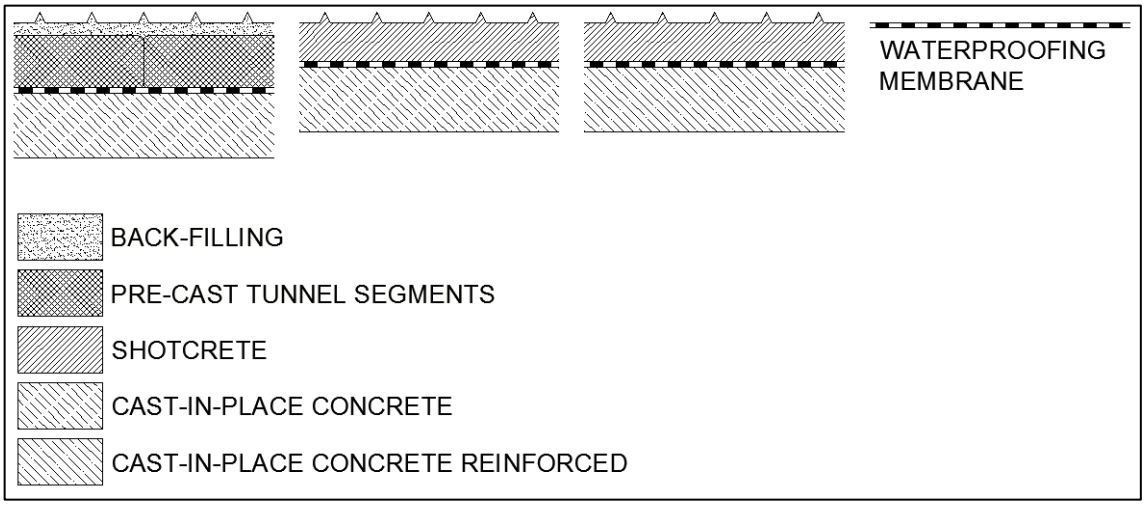

Fig. 2–4: different types of dual-lining systems with separate linings (S-DLS); note that S-DLS always include a waterproofing membrane; adapted from (RVS 09.01.31, 2003)

The secondary lining has to guarantee long-term stability and fulfill requirements regarding fire-resistance. Depending on the presence and chemical composition of the groundwater as well as on the quality of the primary shotcrete shell, including the primary shotcrete shell in the long-term stability of the tunnel is possible (RVS 09.01.31, 2003). However, since long-time behavior of shotcrete in combination with groundwater is not well known, and to ensure a higher level of safety, the secondary cast-in-place concrete inner liner is often designed to fulfill all requirements regarding long-term stability of the tunnel.

2.4 Application – single-lining systems vs. dual-lining systems

The German guideline DS 853, (2007) states that in case of dual-lining systems with composite linings (C-DLS) the cast-in-place concrete inner liner has to be thicker than in case of dual-lining systems with separate linings (S-DLS). Furthermore, concerning C-DLS, the German guideline states that the inner liner can be shotcrete when groundwater is absent.

The Austrian guideline for shotcrete ÖVBB, (2009) outlines that single-lining systems with shotcrete are only recommended when no or only little groundwater is present. In addition, the Austrian guideline for shotcrete ÖVBB, (2009) recommends for single-lining systems with shotcrete that the possibility for subsequent grouting, to guarantee watertightness, should be provided and that a sufficient tunnel-drainage system is present. When aggressive groundwater is present, the Austrian guideline for shotcrete suggests a dual-lining system with waterproofing membrane (S-DLS) and a special shotcrete-quality to achieve resistance against deterioration of the shotcrete shell.

The Austrian guideline for inner liner ÖVBB, (2003) suggests a higher inner-liner-concrete-quality for C-DLS than for S-DLS. Furthermore, a special quality waterproofing membrane is recommended when aggressive groundwater is present.

The Austrian guideline for tunnels RVS 09.01.31, (2003) states that single-lining systems consisting of shotcrete shall be applied only if no water-pressure can act on the tunnel. Moreover, to guarantee the long-term stability of the tunnel, a reinforced shotcrete shell should be applied in several layers. Concerning S-DLS, the long-term stability of the tunnel has to be provided by a cast-in-place concrete inner liner. For watertightness, a waterproofing membrane has to be placed between the primary shotcrete shell and secondary inner liner. The requirements regarding fire-resistance are also fulfilled by the inner liner. Thus, the primary shotcrete shell has to only ensure the stability of the tunnel during the construction process.

Very importantly, all listed guidelines state that single-lining systems are assuming no deterioration of the shotcrete. This is based on the fact that single-lining systems are only recommended when no or little groundwater is anticipated. Dual-lining systems are the state-of-the-art construction method for transportation tunnels in much of Europe. Apart from the distinction between C-DLS and S-DLS, two types of dual-lining systems can be distinguished in that the primary liner can be constructed either with shotcrete or with pre-cast tunnel segments. In most cases, a cast-in-place concrete inner liner is applied as secondary liner and a waterproofing membrane separates the primary- and secondary liner.

2.5 Conclusion – single-lining systems vs. dual-lining systems

Single-lining systems and dual-lining systems with composite linings (C-DLS) are not ideal and are not used when aggressive groundwater, which is the major cause of deterioration, is present. Thus, this study investigates dual-lining systems with separate linings (S-DLS), whereby the waterproofing membrane between the primary shotcrete shell and secondary cast-in-place concrete inner liner is considered in the numerical calculation using contact formulations that allow slipping.

3 NUMERICAL MODEL

The numerical model is elaborated in three parts:

- Chapter 3.1 to 3.4: general
- Chapter 3.5 to 3.6: tunnel construction
- Chapter 3.7: deterioration of the shotcrete shell

The first part, general, deals with the model and model-parts, which includes the mesh, the boundary conditions, material properties and material behavior. Contact formulations as well as sources of nonlinearity of the finite element (FE) method are also treated.

The second part, tunnel construction, deals with the excavation progress, which includes the installation of the shotcrete shell and inner liner. Several procedures for the 2D numerical simulation of tunnel excavation as well as several methods for the installation of support elements (shotcrete shell and inner liner) are discussed.

The third part, deterioration of the shotcrete shell, deals with the degradation of the material properties to simulate a deterioration of the shotcrete. The aim of this part is to determine the interaction between the shotcrete shell and inner liner during the deterioration progress.

3.1 Investigation of the FE model

The tunnel is assumed to have a circular shape with an outer diameter of 10 m and should be constructed at a depth of 250 m below the ground surface. The stress field around the tunnel is applied with uniform vertical and horizontal stresses.

Considering the symmetric conditions of the tunnel, a quarter portion of the tunnel is used for the numerical analysis. The thickness of the shotcrete shell is 20 cm and the thickness of the inner liner is 30 cm. The excavation method is simplified to a full-face excavation. The size of the FE mesh is chosen in such a way, that the boundary effects are minimized. This is the case when the horizontal mesh length is 4 to 5 times the tunnel diameter (Meißner, 1991; 1996). To simulate a quarter of the tunnel with a diameter of 10 m, an absolute model size of 55 m x 55 m is chosen (Fig. 3–1). The calculations are done using the ABAQUS 6.7-1 FE program (Hibbitt et al., 2007).

To consider the time dependent behavior of the shotcrete (creeping and hardening), two different Young's moduli are used. According to the guideline RVS 09.01.42, (2004), for a short time after application of the so called "young" shotcrete, a Young's modulus of E_{S1} = 10,000 MN/m² is used, and to represent a "hardened" shotcrete, a Young's modulus of E_{S2} = 15,000 MN/m² is applied.

3.1.1 Boundary conditions

The model is bounded on the right vertical and the bottom side with roller supports. These axes are also planes of symmetry. The vertical earth-pressure is applied on the top side and the horizontal earth-pressure is applied on the left vertical side (Fig. 3–1).

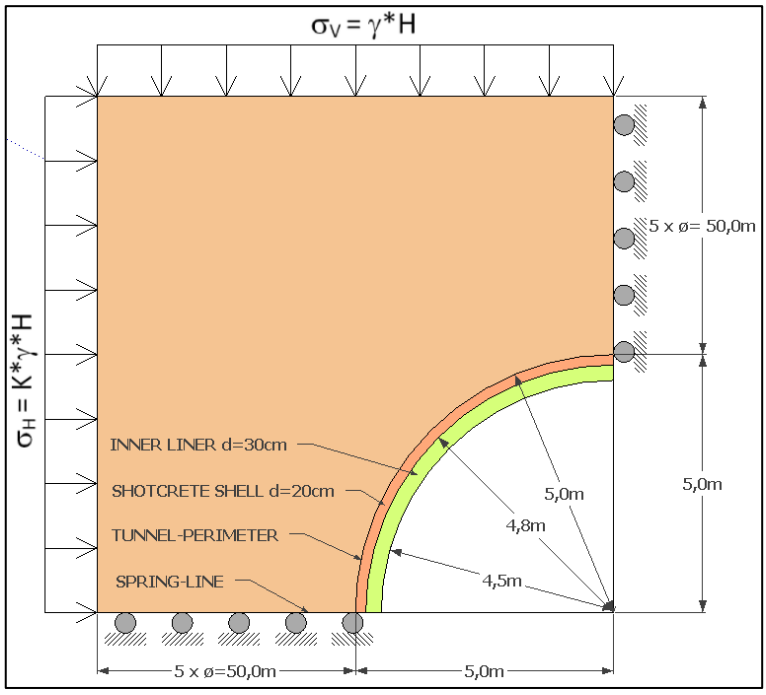

Fig. 3–1: Schematic representation of model size, boundary conditions, system load and model parts

3.1.2 Elements, nodes and mesh

The ground, the shotcrete shell and the inner liner are usually modeled with 4-node bilinear plane strain continuum elements (CPE4) (Fig. 3–2). For the parametric studies also 8-node biquadratic plane strain continuum elements with reduced integration (CPE8R) are used.

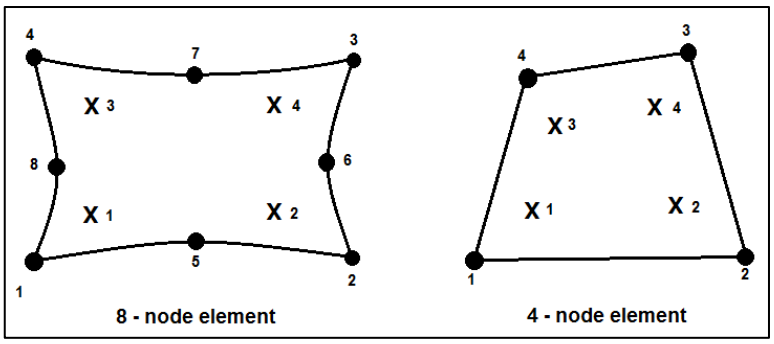

Fig. 3–2: Numbering of integration and node points for output; CPE8R (left) and CPE4 (right); Source: Hibbitt, Karlson, & Sorenson, 2007

4-node bilinear plane strain continuum elements:

Fig. 3–3 and Fig. 3–4 show the structured mesh, which was chosen according to Einstein et al. (1995). To model the ground, 624 elements are used. The shotcrete shell is modeled using 48 elements and the inner liner is modeled with 72 elements.

The contact interface between the ground and the shotcrete shell, as well as between the shotcrete shell and inner liner are modeled using the same number of nodes (25). (See also chapter 3.3)

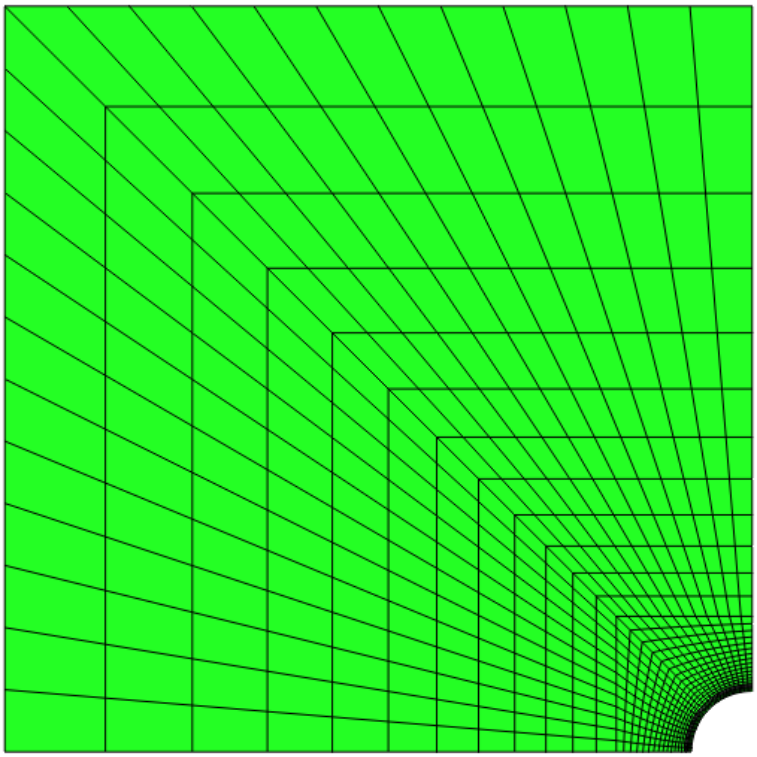

Fig. 3–3: FE mesh CPE4

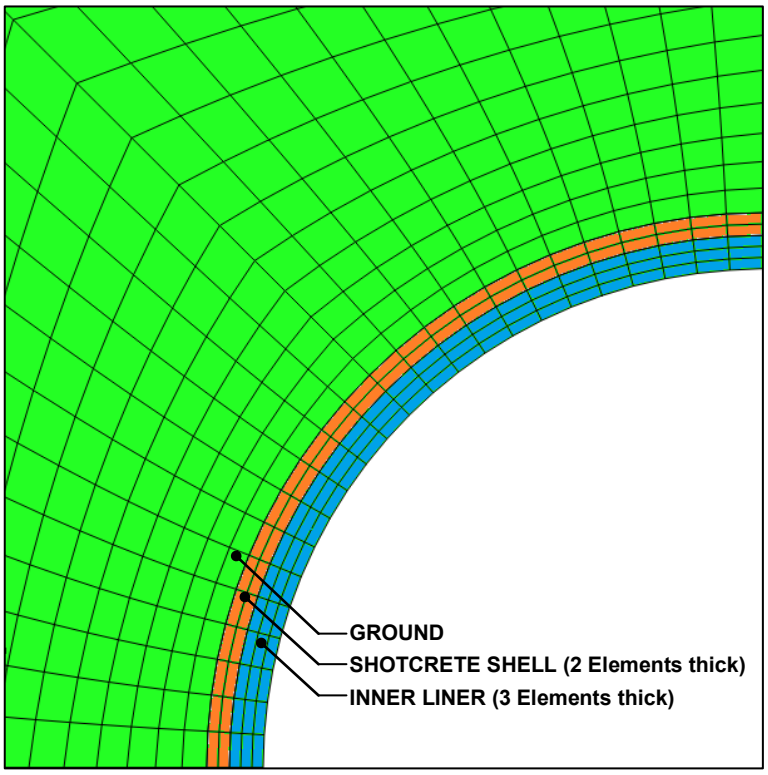

Fig. 3–4: mesh CPE4 – detail tunnel

8-node biquadratic plane strain continuum elements with reduced integration:

Based on a convergence study CPE8R elements are chosen. The convergence study investigates the use of 8-node biquadratic plane strain elements with and without reduced integration, using a mesh which can be created with so called FREE, STRUCTURED and SWEEP techniques. The best results were obtained with the FREE technique and the CPE8R elements. The element number around the tunnel is double that of the CPE4 elements. Accordingly, to model the ground, 1738 elements are used. The shotcrete shell is modeled using 96 elements and the inner liner is modeled with 144 elements. The contact interfaces between ground and shotcrete shell, as well as between shotcrete shell and inner liner are modeled using the same number of nodes (97). (See also chapter 3.3) (Fig. 3–5 & Fig. 3–6)

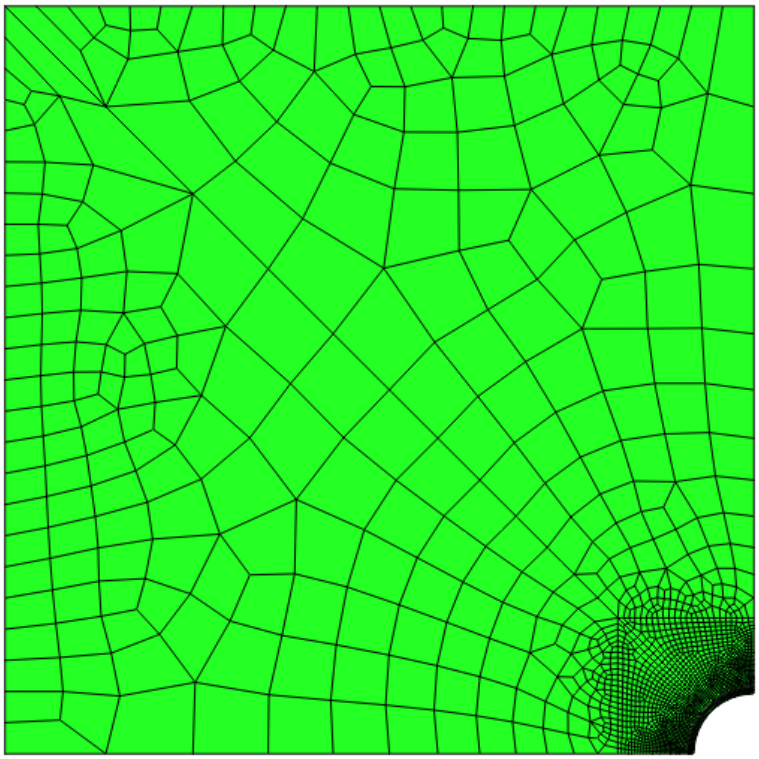

Fig. 3–5: FE mesh CPE8R

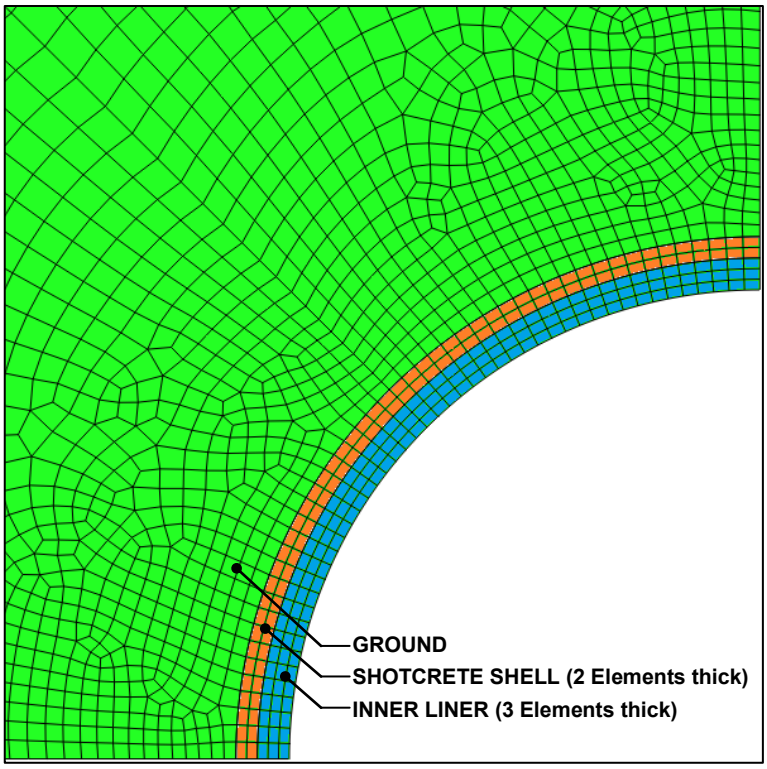

Fig. 3–6: mesh CPE8R – detail tunnel

3.2 Parameters for the numerical analysis

The model consists of different materials:

1. ground
2. “young” shotcrete (for: shotcrete shell)
3. “hardened” shotcrete (for: shotcrete shell)
4. concrete (for: inner liner)

The ground is assumed to be marl and is idealized homogenous and isotropic. The unit weight is assumed as γ = 27 kN/m³. The overburden above the crown of the tunnel is 250 m. The horizontal ground stress is obtained assuming Poisson’s ratios of ν = 0.5 and ν = 0.4 and no lateral deformation.

In the first part of this paper, the material behavior of the ground is assumed to be governed by a linear elastic relationship. Later on, a linearly elastic – perfectly plastic relation based on the Coulomb criterion is investigated. The basic principle of this behavior is to separate the strains and stresses into an elastic and a plastic part:

$$\varepsilon = \varepsilon^{e} + \varepsilon^{pl} \tag{3.1}$$

3.2.1 Investigation of dilatation of ground (soil and rock)

Dilatation is defined as volume-increase due to loosening of the ground.

The plastic strain increments are assumed to be normal to the yield surface, i.e. using the associated flow rule. However, for soil to use an associated flow rule with a

Coulomb yield function leads to an overestimating of dilatation. Fig. 3–7 shows a non-associated flow rule using the Coulomb criterion.

Fig. 3–8 illustrates that the dilatation behavior only occurs in the plastic state. In short, the volume increase only occurs in the plastic state and concerns only the plastic strain ε^{pl}.

The friction-angle (φ) is defined by the angle of internal-friction (φ_i) and the dilatation-angle (ψ):

$$\varphi = \varphi_i + \psi \tag{3.2}$$

Generally it can be assumed that cohesive soils, except extremely over-consolidated soils, have no dilatation behavior (ψ = 0).

The dilatation angle of non-cohesive soils is dependent on the friction angle as well as on their density. It is possible to estimate the dilatation angle by subtracting a constant factor from the friction angle (Bolton, 1986; Brinkgreve & Veermeer, 2002):

$$\psi \cong \varphi - 30° \tag{3.3}$$

For friction-angles less than 30° the dilatation-angle is assumed to be zero.

For rock, the dilatation is defined as volume increase due to riding over asperities (Fig. 3–8). F_N, F_S, l and d are the normal-force, the shear-force, the shear-displacement and the dilatation. For the dilatation-angle of rock the notation (i) is used. (Brosch, 1990)

To limit the number of input variables for the parametric studies a dilatation-angle of ψ = 0° is used.

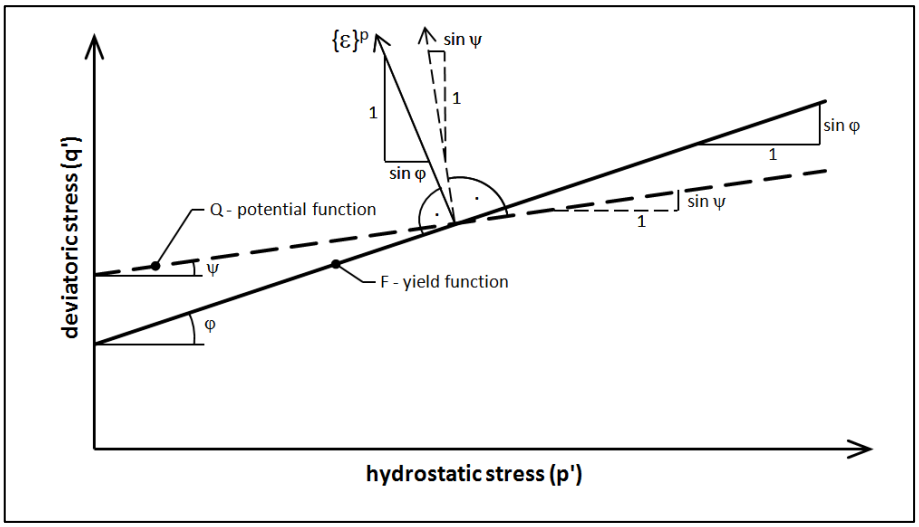

Fig. 3–7: Basic principle of a non-associated flow rule

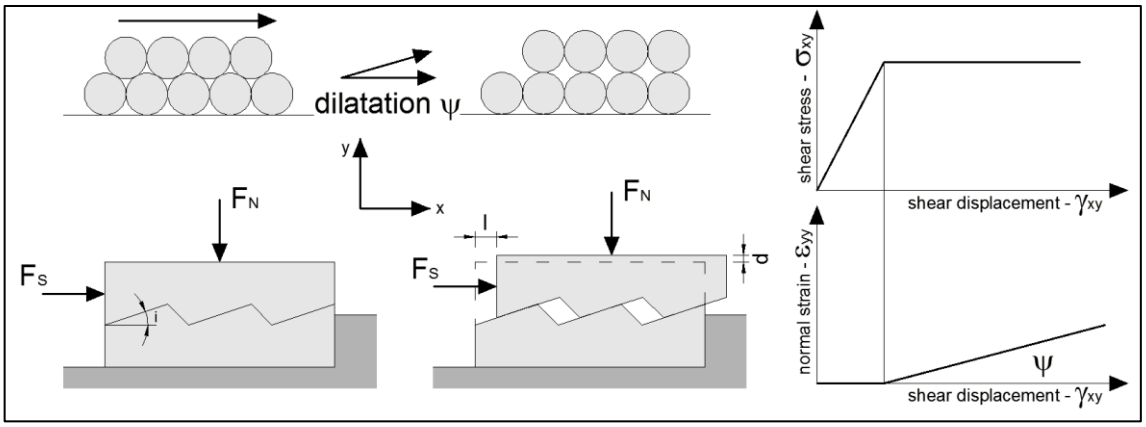

Fig. 3–8: Dilatation behavior of soil and rock

3.2.2 Material properties

Table 1 shows the main physical mechanical parameters, where E, ν, c, φ and ψ are the Young's modulus, the Poisson's ratio, the cohesion, the friction-angle and the dilatation-angle.

The material behavior of the ground is, as mentioned above, first assumed to be governed by a linear elastic relationship and in a second investigation by a linearly elastic – perfectly plastic relationship using the Coulomb constitutive law.

The material behavior of the shotcrete shell and inner liner are assumed to be governed by a linear elastic relationship. Furthermore for the shotcrete, a yield stress of 20 MN/m² is assumed. All support elements (shotcrete shell and inner liner) are also assumed to be homogenous and isotropic. The shotcrete shell has a uniform thickness of 20 cm and the quality is assumed to be a SpC 25/30-J2 (MPa). The inner liner has a uniform thickness of 30 cm and the quality is assumed to be a C 25/30 (MPa).

SpC 25 / 30 - J2

- J2 → Early strength (ÖVBB, 2009)
- 30 → Characteristic cube compressive strength, after 28 days; (MPa)
- 25 → Characteristic cylinder compressive strength, after 28 days; (MPa)
- SpC → Sprayed concrete or shotcrete

C 25 / 30

- 30 → Characteristic cube compressive strength, after 28 days; (MPa)
- 25 → Characteristic cylinder compressive strength, after 28 days; (MPa)
- C → Concrete

Table 1: Physical mechanical properties of ground, shotcrete shell and inner liner

Material	Material Detail	E (MN/m²)	ν (-)	c (MN/m²)	φ (deg)	ψ (deg)
GROUND	MARL	500	0.4 + 0.5	3.0	35	0
SHOTCRETE SHELL (YOUNG)	SpC 25/30-J2	10,000	0.2			
SHOTCRETE SHELL (HARDENED)		15,000	0.2			
INNER LINER	C25/30	30,500	0.2			

3.3 Contact formulation

For the numerical calculation, contact conditions have to be defined between all interacting surfaces. An overview of the contact conditions for the numerical model is provided below:

- ground and shotcrete shell (3.3.1)
- shotcrete shell and inner liner (3.3.2)

3.3.1 Contact formulation between ground and shotcrete shell

Tangential behavior:

- The Coulomb friction law is assumed with a very large friction coefficient of μ = 100 (ρ = 89.43°) and no cohesion. This value (μ = 100) is recommended in the ABAQUS User's Manual (Hibbitt et al., 2007) to simulate a contact with no slip. (Fig. 3–9 left)
- To achieve better convergence, an elastic slip of $\gamma_{elast.}$ = 1 mm is defined. In other words, the maximum transferable shear stress ($\tau_{crit.}$) is reached after a displacement of 1 mm. (Fig. 3–9 right)

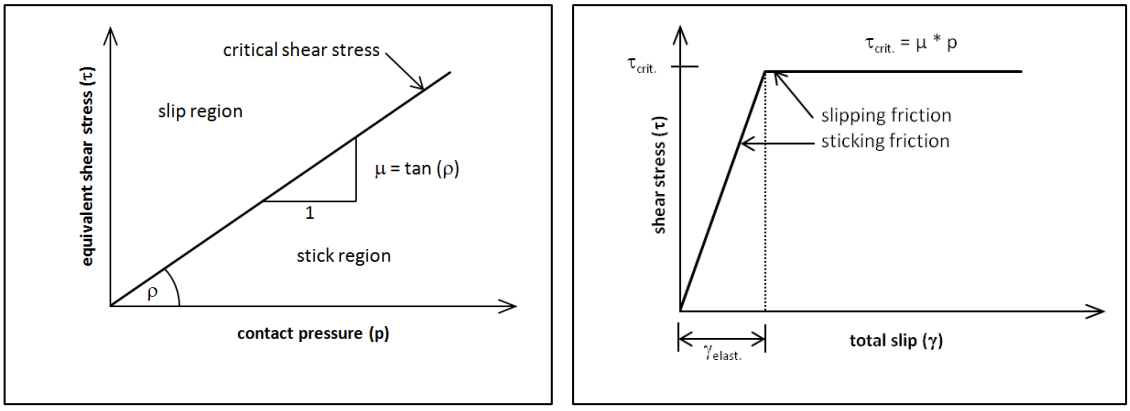

Fig. 3–9: Coulomb friction law (left) and elastic slip behavior (right); adapted from Hibbitt, Karlson, & Sorenson, (2007)

Normal behavior:

- Separation of the two surfaces is prevented once contact has been established. In other words, a transfer of tensile stresses is possible after the surfaces got into contact.

- To ensure numerical convergence a so called “hard contact” is implemented. After the clearance between the two surfaces is closed a transfer of normal stresses – contact pressure or tensile stress – is possible. (Fig. 3–10)

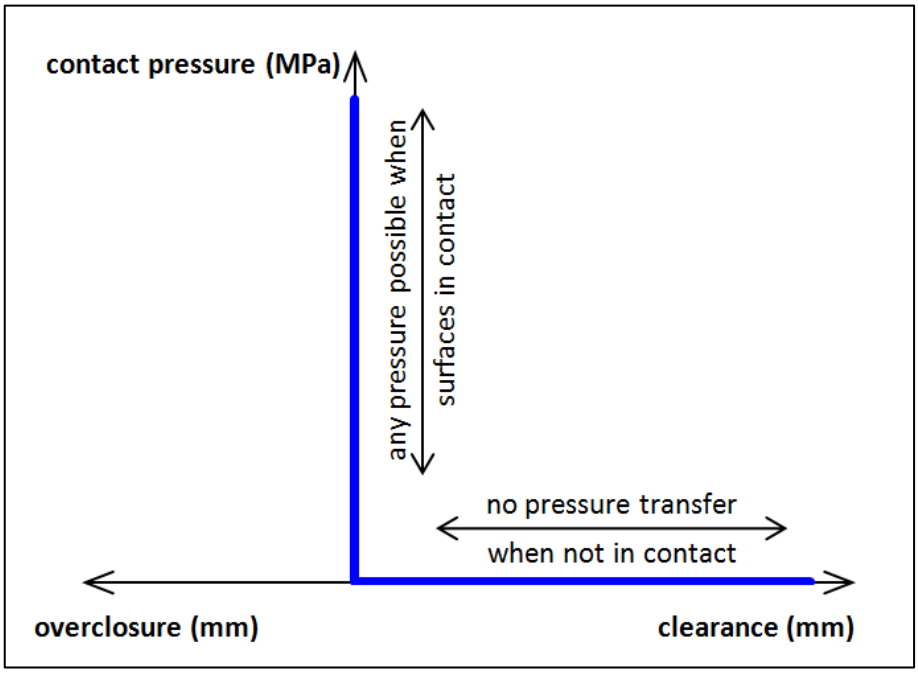

Fig. 3–10: Contact normal behavior: “hard contact”; tensile stresses are not considered; adapted from Hibbitt, Karlson, & Sorenson, (2007)

3.3.2 Contact formulation between shotcrete shell and inner liner

Tangential behavior:

- The Coulomb friction law is assumed with a friction coefficient of μ = 1 and no cohesion. Hence, the possibility for slippage is provided. (Fig. 3–9 left)
- To achieve better convergence, an elastic slip of $\gamma_{elast.}$ = 1 mm is defined. In other words, the maximum transferable shear stress ($\tau_{crit.}$) is reached after a displacement of 1 mm. (Fig. 3–9 right)

Normal behavior:

- Separation of the two surfaces is allowed once contact has been established. In other words, there is no possibility for a transfer of tensile stresses.
- To ensure numerical convergence a so called “hard contact” is implemented. After the clearance between the two surfaces is closed a transfer of normal stresses – contact pressure – is possible. (Fig. 3–10)

3.3.3 Removing and reactivation of elements and contact pairs

Removing of elements and contact pairs is a useful technique for uncoupling several parts (ground, shotcrete shell and inner liner) of a model until they are brought together. This option is recommended in the ABAQUS User’s Manual (Hibbitt et al., 2007) when complicated processes with deformation are simulated:

After excavation, the tunnel-perimeter moves inward until the shotcrete shell is installed and before the inner liner is installed, the ground and the shotcrete shell move inward. To simulate the installation of the support elements (shotcrete shell and inner liner), the corresponding elements are removed in the first step of the calculation and reactivated later on. Hence, the contact pairs are also removed, until the support elements get installed. (See Fig. 3–25 to Fig. 3–27)

This procedure is used for the two contact pairs:

- Ground – shotcrete shell
- Shotcrete shell – inner liner

Another advantage is that significant computational time can be saved by eliminating unnecessary calculations of a non-existing contact.

3.4 Sources of nonlinearities

There are three different kinds of nonlinearities occurring with finite element simulations:

- Geometric nonlinearities
- Nonlinear material behavior
- Contact and friction

Geometric nonlinearities are introduced by large displacements. Displacements and strains may be so large that it is no longer admissible to use small strain theory. This also entails that new equilibrium of the system is formulated on the deformed structure. In this study, the nonlinearity results from the excavation of the tunnel, where large displacements are expected.

Virtually all materials show a nonlinear behavior. Examples are hyperelasticity for materials like rubber or polymers, nonlinear plasticity or viscoplasticity in concrete or bitumen, materials showing phase transformations for thermo-mechanical simulations and various other materials.
This thesis mostly deals with linear elastic material behavior. However, it has to be noted that the elastic parameters are time dependent, thus requiring an incremented solution scheme.

Contact and friction mostly occur together. Friction changes with contact pressure. In this study contact and friction problems exist at the interfaces between the ground and shotcrete shell as well as between the shotcrete shell and the inner liner.

The basic idea for the solution of nonlinear relationships of the displacement based FE-method is given by the incremental- iterative concept. Thereby the load is applied step-by-step (incrementally), and the tangent stiffness matrix is calculated from displacements and stresses of the last increment. (Bathe, 1996)

In ABAQUS the increments are defined by a “time period of one step”, an “initial time increment”, a “minimum time increment” and a “maximum time increment”. Assuming linearity, one step can be calculated using one increment (“time period of one step” = “initial time increment”). In case of nonlinearities, a smaller “initial time increment” should be chosen (“initial time increment” < “time period of one step”). If the chosen increment size is too large, the time increment is reduced to within the previously selected range (“minimum/maximum time increment”).

3.5 Simulation of the tunnel excavation

The excavation of a tunnel is basically a three dimensional problem. However, it can be reduced to a 2D plane strain problem considering the fact that a given tunnel section essentially behaves like its neighboring section. It is hence sufficient to only regard a single slice of the entire tunnel with the additional constraint that the slice thickness remains constant. At the tunnel’s face, however, plane strain conditions are no longer applicable, since the not excavated ground in front of the tunnel has some load carrying capacity supporting the tunnel’s face. This so called “3D effect” can be simulated by two methods (Golser & Schubert, 2003; Schwartz & Einstein, 1980):

- Load reduction method (β-method) (3.5.1)
- Stiffness reduction method (α-method) (3.5.2)

In tunneling usually ground displacements occur prior the support can be applied. This displacement mobilizes the resistance of the ground and reduces the load, which the support installed later has to carry.

3.5.1 Load reduction method (β-method)

In the load reduction method (Panet, 1978), an initial state is assumed, where the internal pressure (p_0) in the opening equals the external earth-pressure (Fig. 3–11a). Before the shotcrete shell is introduced, this internal pressure is reduced by a β-factor (between 0 and 1; 0 = full internal pressure; 1 = no internal pressure). According to Fig. 3–11a, $\beta_0 = 0$, $\beta_1 > \beta_0$, $\beta_2 > \beta_1$, and so on.

Fig. 3–11a_1 shows the installation of the shotcrete shell with a Young’s modulus (E_{S1}) of a “young” shotcrete. Before this is done, the unloading factor (β-factor) is set to β_1. Hence, the internal pressure is reduced and the ground moves radially inward. Subsequently, the shotcrete shell is installed.

Fig. 3–11a_2 illustrates a further reduction step of the internal pressure. Hence, the unloading factor is set to β_2. After the internal pressure is reduced a second time, the material property of the shotcrete is changed to a “hardened” (E_{S2}) one.

Fig. 3–11a_3 shows the installation of the inner liner with a Young’s modulus of E_L. Before this is done, the unloading factor is set to β_3. Hence, the internal pressure is

reduced a third time and the combined system, ground plus shotcrete shell, moves radially inward. Subsequently, the inner liner is installed.

Fig. 3–11a_4 illustrates the last reduction of the internal pressure. Hence, the unloading factor (β) is set to one and consequently the internal pressure is reduced to zero.

A realistic magnitude of the β-factor must be obtained from measurements.

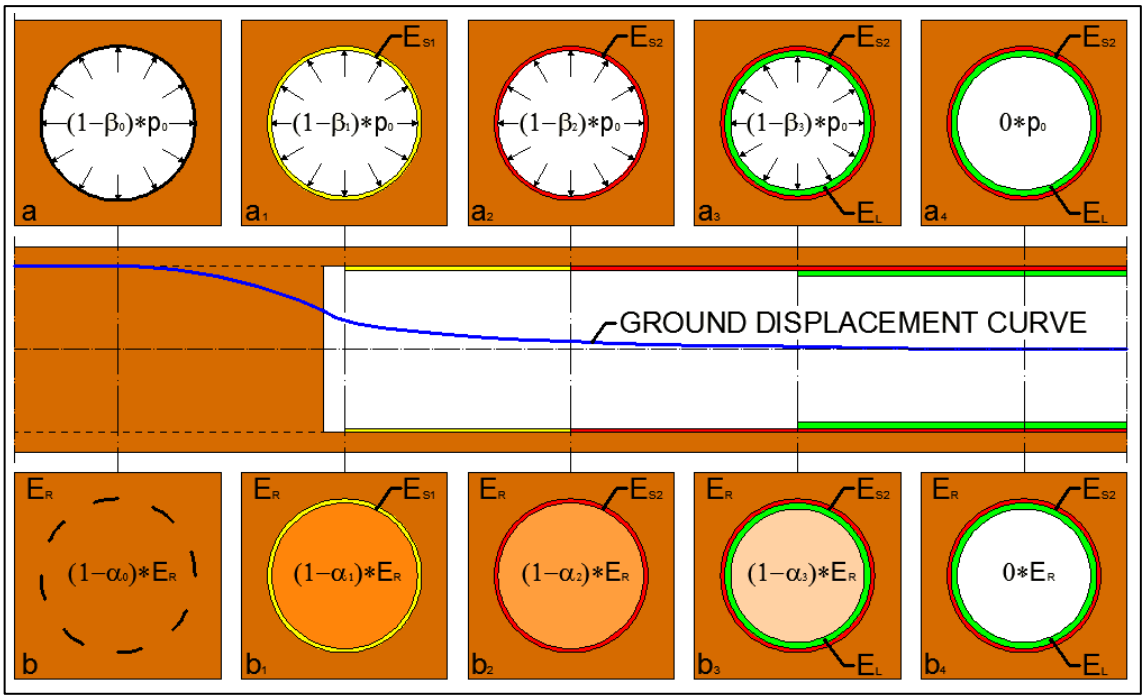

Fig. 3–11: Load and stiffness reduction method with implementation of shotcrete shell and inner liner

3.5.2 Stiffness reduction method (α-method)

In the stiffness reduction method (Fig. 3–11b) (Laabmayr & Swoboda, 1978), the tunnel construction simulation is conducted by reducing the stiffness of the material in the future opening gradually. Between these steps, the shotcrete shell and inner liner are installed similarly to the scheme of the load reduction method mentioned above.

The material in the future opening is reduced by an α-factor (between 0 and 1; 0 = same stiffness of material inside as around the outside of the opening zone; 1 = no stiffness of material in the opening). According to Fig. 3–11b, $\alpha_0 = 0$, $\alpha_1 > \alpha_0$, $\alpha_2 > \alpha_1$, and so on.

In the first excavation step (Fig. 3–11b_1) a stiffness reduction factor of $\alpha = 50\%$ is recommended by Laabmayr & Swoboda, (1978).

The advantage of the stiffness reduction method is that it works well with all values of the lateral earth-pressure coefficient K being $\frac{\nu}{1-\nu}$. In comparison, the load reduction method, which assumes a uniform internal pressure applied at the tunnel-perimeter, can only be used to calculate a uniform earth stress field with K = 1.

3.5.3 Evaluation and critique of the reduction factor

Nowadays it is very common to use 2D numerical analyses for the design of tunnels. The main advantage over this, compared to 3D analyses, is its lower computational costs for modeling the calculations. However, some assumptions have to be made to consider the so called “3D effects”. Displacements occur in the ground before the tunnel is excavated. Therefore, the support can often only be constructed with a delay behind the excavation face. Subsequently the tunnel-perimeter deforms before shotcrete or other support material can be applied. Fig. 3–11 shows a schematic ground displacement curve for this pre-displacements[1] and support delay[2]. This behavior can be simulated by the load- or stiffness reduction method. However, assumptions concerning the unloading factor have to be made in both methods.

Several authors have suggested different values for pre-displacements and support delay, either based on measurements or engineering practice. Panet (1976) derives an unloading factor of β = 33% at the tunnel face, and β = 100% at a distance “four times the radius” behind the tunnel face. Laabmayr et al. (1978) determined an unloading factor of β = 50% at the tunnel face based on measurements. For partial excavation they come up with a factor between β = 20% and β = 50% for top heading excavation and with a factor between β = 40% and β = 80% for side drift excavation (Laabmayr & Swoboda, 1986). Golser (2008) simulated the Brenner base tunnel in rock with a very high overburden using an unloading factor of β = 95%. Möller et al. (2010) simulated a tunnel drift in a cohesive soil using a load reduction factor of β = 70% for the top heading and a load reduction factor of β = 50% for the bench and invert. Baudendistel, (1979) quoted in Möller, (2006) says that the unloading factor for full excavation of a horse-shoe profile depends on the round length[3].

This short review makes clear that the load reduction factor varies and that it is very difficult to ascertain an exact value.

The load reduction factor is dependent on the opening size (S. Möller, 2006), the round length and the material behavior of the surrounding ground, the overburden, the advance method, and much more. Hence, assumptions of the load reduction factors have to be made for each separate case. The best way to do this is using dilatometer measurements ahead of the tunnel face as well as displacement measurements at the tunnel wall after excavation. Another possibility is to compare the results with a three dimensional numerical analysis, in which the excavations are simulated step-by-step. Last but not least, a third way would be to calibrate the load reduction factor with the use of an analytical or empirical method. For instance it is possible to use the

[1] Movement of ground (rock or soil) into the future opening before tunnel is excavated.
[2] Displacement on tunnel-perimeter behind tunnel face and before initial support is installed.
[3] Length of one excavation cycle

characteristic curve concept to determine the pre-excavation displacements as well as the support delay (Lombardi, 1973).

This thesis does not consider measurements or uses three dimensional numerical calculations. Hence, a calibration of the load reduction factor is done based on the characteristic curve concept.

3.5.4 Conclusion

For this investigation the load reduction method is used. This method is chosen on the basis of conceptual considerations of contact problems. Using the stiffness reduction method, two parts are in contact with the ground's tunnel-perimeter at the same time:

- Part of future opening
- Part of shotcrete shell

This ambiguous contact pair definition causes numerical problems. For this reason, the load reduction method is chosen.

To remove the above mentioned disadvantage of the load reduction method (not all values of K can be simulated), the internal pressure is simulated by concentrated forces in the vertical and horizontal direction at each node of the tunnel-perimeter. Their values are obtained as reaction forces from an independent calculation, where all nodes at the tunnel-perimeter are fixed. (See also chapter 3.6.4)

3.6 Simulation of the tunnel construction

Different methods have been proposed in the literature (Einstein et al., 1995; Hibbitt et al., 2007) to simulate in ABAQUS the implementation of support elements (i.e. shotcrete shell and inner liner) during the calculation.

- Model Change Method (3.6.1)
- Dummy Node Method (3.6.2)
- Changing Stiffness Method (3.6.3)
- Four Calculation Method (3.6.4)

The task of this chapter is to determine a method, which provides a stress-free activation of support elements and the possibility to simulate contact conditions. This is not straight- forward in ABAQUS due to the fact that displacements occur before the support elements are included. Each of these methods involves a different approach to deal with this task.

Each of these methods requires either the stiffness reduction method or the load reduction method (see chapter 3.5) to simulate pre-displacement, support delay and the loading on the support elements (shotcrete shell and inner liner).

For the Model Change Method (3.6.1) and the Dummy Node Method (3.6.2), for the sake of simplicity only the implementation of the shotcrete shell is discussed.

For the Changing Stiffness Method (3.6.3) and the Four Calculation Method (3.6.4), the implementation of the shotcrete shell and the inner liner are discussed, including a detailed description of the calculation steps.

The conclusion (3.6.5) provides an overview of properties and behaviors, which can be simulated using these methods. One of the four methods has eventually been chosen for all further investigations for reasons presented in the following sections.

3.6.1 Model Change Method

This method is recommended in the ABAQUS Example Problems Manual (Hibbitt et al., 2007).

A half circle for the tunnel is simulated. The tunnel is situated at the left hand side of the model (Fig. 3–12). The excavation and construction of the tunnel are simulated in four steps.

In the initial step, a geostatic stress field is applied. It is assumed that the stress increases linearly with the depth. Moreover, the vertical stress is two times higher than the horizontal stress. Ground and shotcrete shell are implemented in this step. The load reduction method is realized by means of the function AMPLITUDE, which allows one to decrease the prescribed forces at the tunnel-perimeter during several calculation steps. Additionally the interaction between ground and shotcrete shell is defined by means of a so called TIE contact, where no slippage is allowed.

Fig. 3–15a shows a section of the ground and the shotcrete shell in detail. Fig. 3–15b shows the same as Fig. 3–15a, focusing on the interaction between ground and shotcrete shell. Note that the nodes at the tunnel-perimeter have the same coordinates as the nodes on the outside of the shotcrete shell and are connected during the entire calculation. Fig. 3–13a illustrates the FE-mesh around the tunnel.

In the first step the shotcrete shell is removed using the method MODEL CHANGE (Fig. 3–15c & Fig. 3–13b). A gravity field is activated with a predefined unit weight. Symmetry conditions are specified, i.e. the degree of freedom 1 (Fig. 3–18) is fixed at every node at the entire left vertical side of the model. Moreover, vertical and horizontal concentrated forces are prescribed at the nodes at the tunnel-perimeter to prevent any displacement.

The forces are obtained from an independent analysis where the displacements on the tunnel-perimeter are fully constrained, i.e. the first and second degree of freedom (D.O.F) at the tunnel-perimeter are fixed. (See also chapter 3.6.4)

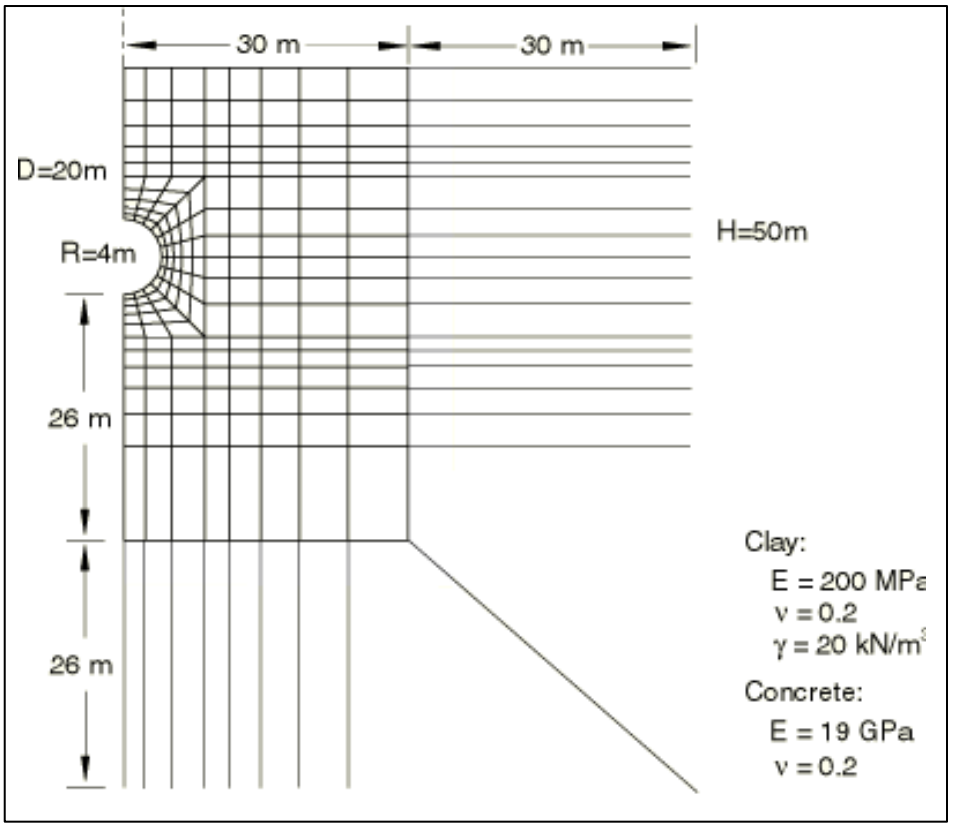

Fig. 3–12: Geometry and finite element discretization; Source: Hibbitt, Karlson, & Sorenson, (2007)

In the second step the internal pressure is reduced to 60% of its initial value. As a result the ground moves inward (Fig. 3–13c). Fig. 3–15d illustrates the movements, which occur at the ground-tunnel interface. The hatching shows the undeformed geometry. Note that the nodes of the tunnel-perimeter and the outside of the shotcrete shell are connected by means of a TIE contact, even when the shotcrete shell is deactivated. It can be seen that the original thickness of the shotcrete shell changes during this step (Fig. 3–14).

In the third step, the shotcrete shell is reactivated in a stress-free state. Fig. 3–15e shows again that the thickness of the now activated shotcrete shell (solid-part) changed in comparison to its original geometry (hatched-part).

In the fourth step the internal pressure is reduced to zero (Fig. 3–15f & Fig. 3–13d). As a result, the combined system (ground plus shotcrete shell) moves inward.

Between Fig. 3–13b and Fig. 3–13c, which corresponds to the first load reduction step, the bottom part of the tunnel moves significantly upwards (see marked areas). Comparing the thickness of the shotcrete shell, at the tunnel-crown and the bottom, one can see that the thickness changes. Note: The shotcrete shell, represented in white, is not included (activated) at this calculation step.

Summarizing, the tunnel moves radially inward before the shotcrete shell can be constructed (see chapter 3.5). During this first load reduction step, the nodes at the outer edge of the shotcrete shell are connected to the nodes at the tunnel-perimeter.

Since all other deactivated nodes of the shotcrete shell stay at their initial coordinates during this reduction step, the thickness of the shotcrete shell is reduced by the amount of displacement, which occurs on the tunnel-perimeter. By reactivation of the deformed shotcrete shell and further unloading, all nodes of the shotcrete shell displace uniformly. However, since that the shotcrete shell is thinner than it should be, it exerts less support-resistance. As a result, more deformation of the combined system occurs.

Concluding, the disadvantages of this method are that

- a constant thickness of the shotcrete shell cannot be ensured,
- realistic displacements of the shotcrete shell cannot be achieved,
- no other contact formulation than a TIE contact can be realized.

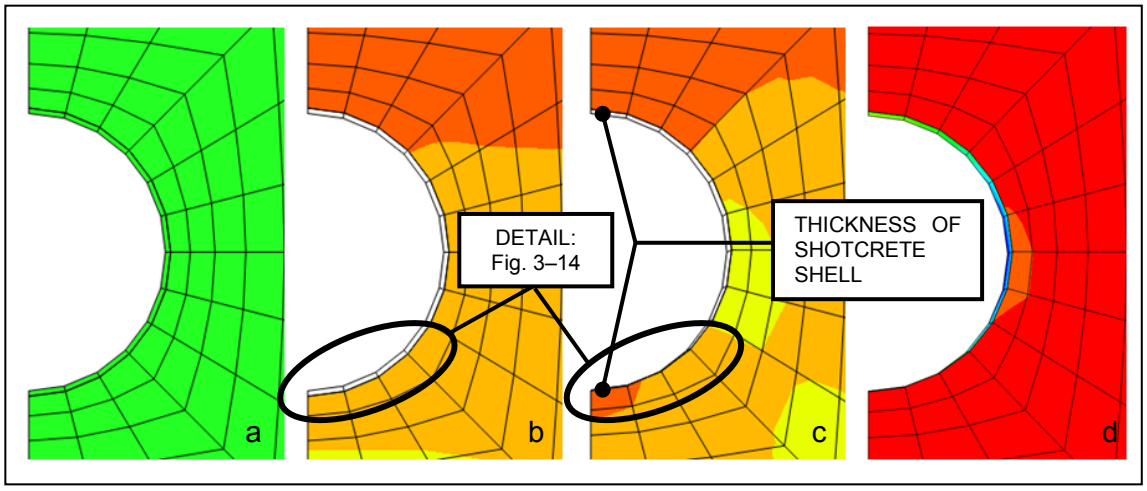

Fig. 3–13: Vertical stress (S22) and displacements; a) model; b) initial step, the shotcrete shell is not activated; c) first load reduction step, the shotcrete shell is not activated, deformation on deactivated the shotcrete shell; d) reactivation of the shotcrete shell and subsequently second load reduction step

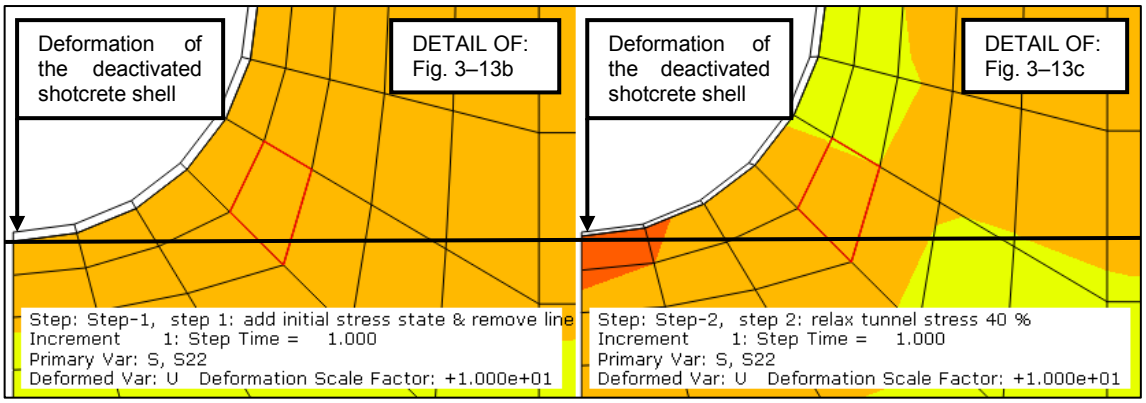

Fig. 3–14: Comparison: Fig. 3–13b and Fig. 3–13c; contours of vertical stresses (S22) and displacement; white part = deactivated shotcrete shell, colored part = ground; Note: displacement – bottom of tunnel moves up, thickness – thickness of deactivated shotcrete shell gets reduced, stress – decrease of vertical stress at bottom;

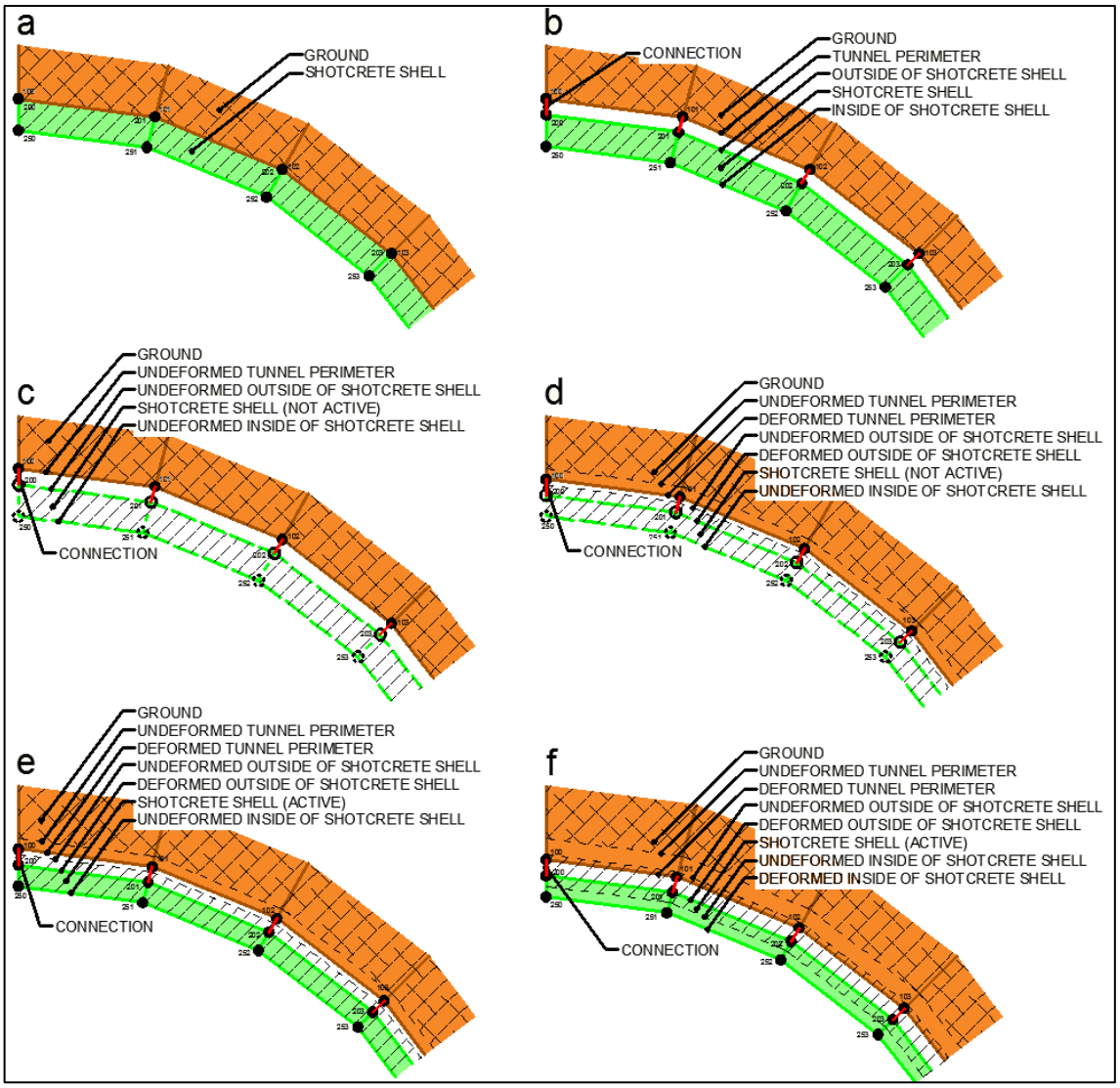

Fig. 3–15: Steps of the construction process using the Model Change Method; only a single shotcrete shell is considered (no inner liner)

3.6.2 Dummy Node Method

Dummy Nodes can be used to connect the deformed tunnel-perimeter to the corresponding nodes of the shotcrete shell using the equation (3.4) (Einstein et al., 1995). Therefore, it is necessary that in the initial step, three sets of different nodes, but with the same nodal coordinates are defined (Fig. 3–16). The first node-set belongs to the ground-interface, the second one to the shotcrete shell-interface and the third node-set represents the dummy nodes. The equation is set up in terms of displacements:

$$displacement\ vector\ of\ ground\ interface\ nodes = displacement\ vector\ of\ shotcrete\ shell\ interface\ nodes + displacement\ vector\ of\ dummy\ nodes \quad (3.4)$$

In the initial step the shotcrete shell is removed (Fig. 3–17a). Hence, the displacements of the ground-interface nodes are equal to those of the dummy nodes. The load reduction method can be simulated in the same way as described in chapter 3.5.1. As

a result, the ground-interface and the dummy nodes move inward ($\Delta 1$), while the shotcrete shell stays at its initial position (Fig. 3–17b).

Subsequently, the shotcrete shell is reactivated and the dummy nodes are fixed (D.O.F. 1 and 2; (Fig. 3–18)) at their positions. According to equation (3.4), the further displacements of the ground-interface are equal to those of the shotcrete shell-interface. Fig. 3–17c shows an overlapping of the ground with the shotcrete shell as result of the preceding displacements of the ground-interface. (Note that an overlapping of the ground with the shotcrete shell is also shown in Fig. 3–17b. This has not emphasized, because the shotcrete shell was not activated)

Fig. 3–17d illustrates further reduction of the internal pressure and inward movement ($\Delta 2$). The nodes of the ground-interface are still connected to the nodes of the shotcrete shell-interface. Consequently the overlapping of the ground and the shotcrete shell-interface still exists.

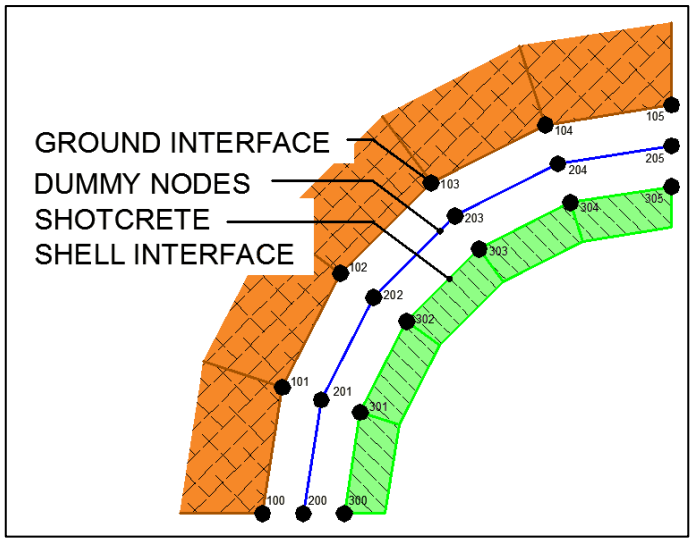

Fig. 3–16: Dummy Node Model; only a single liner is considered

The advantage of the Dummy Nodes Method compared to the Model Change Method (3.6.1) is that a constant thickness of the liner can be maintained. A disadvantage of this method is that specific contact conditions cannot be taken into account.

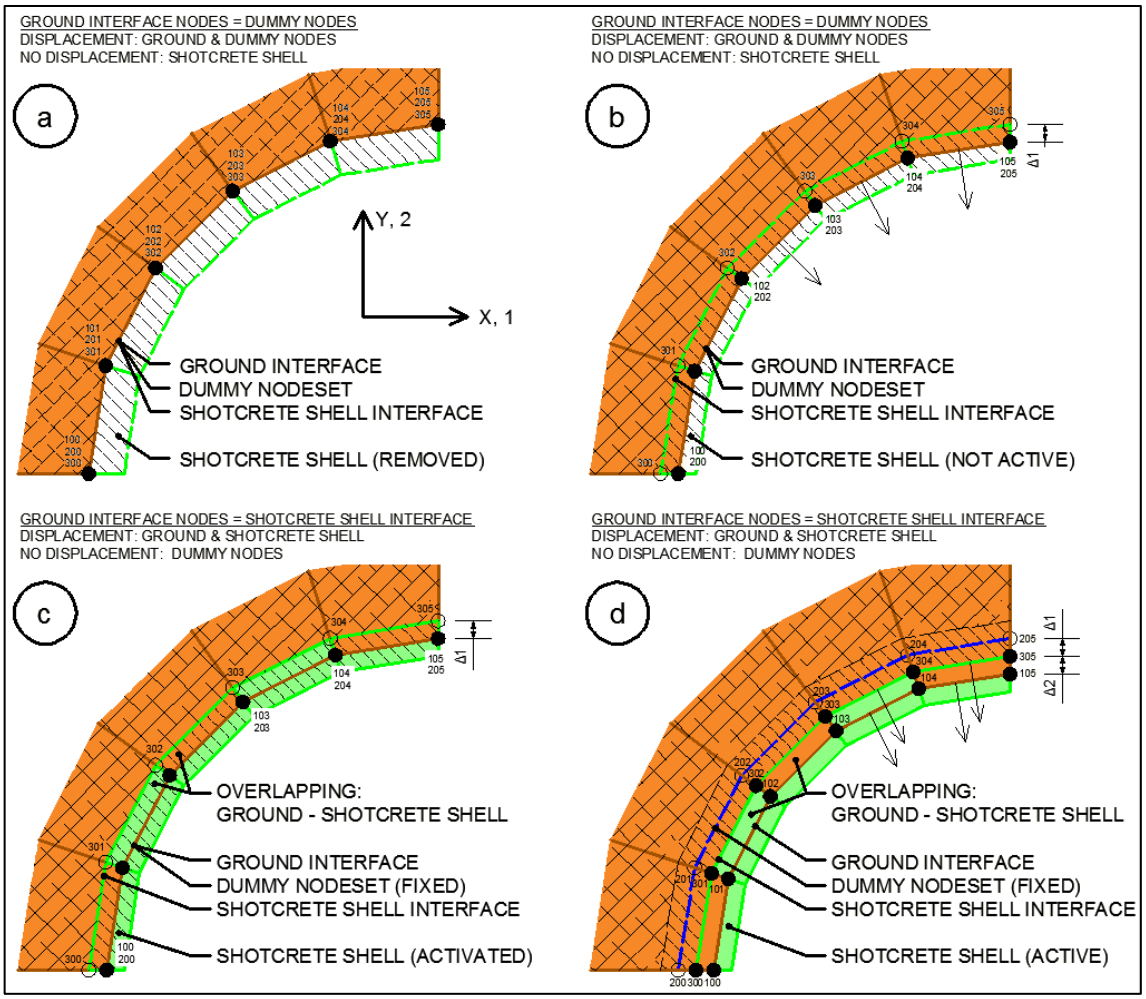

Fig. 3–17: Steps of the construction process using the Dummy Node Method; only a single liner is considered; hatching symbolizes initial (no displacement) geometry of ground and shotcrete shell; a: the shotcrete shell is removed; according to equation (3.4) the ground interface and the dummy nodes are connected; b: inward movement of ground and dummy nodes (Δ1); no displacement of deactivated shotcrete shell; c: the shotcrete shell is activated and the dummy nodes are fixed; hence, according to equation (3.4) the ground interface and the shotcrete interface are connected; note an overlapping of the ground and the shotcrete shell as a result of the displacements (Δ1), which occur on the ground in step b; d: inward movement of ground and shotcrete shell (Δ2); no displacement of now fixed dummy nodes;

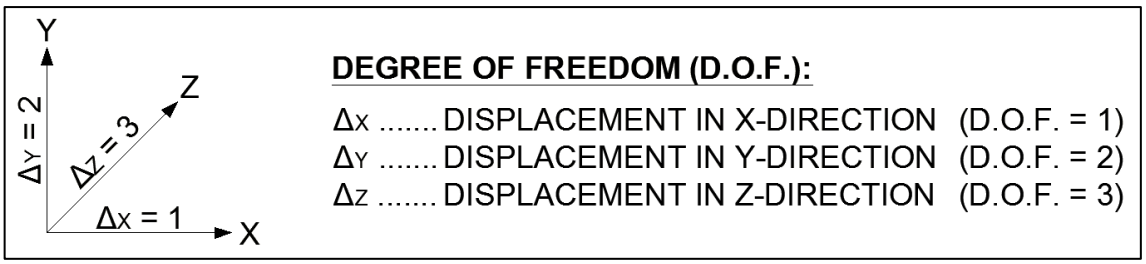

Fig. 3–18: Degree of freedom formulation in ABAQUS

3.6.3 Changing Stiffness Method

This method should prohibit geometrical problems. The basic idea is to make material properties dependent on field variables. Therefore, in the initial step, the shotcrete shell and inner liner have a Young's modulus of 50 N/m² (i.e. very low). Accordingly, they do not influence the displacement of the tunnel-perimeter during a decrease of the internal

pressure by the load reduction method. To avoid numerical problems, the Young's modulus is set to a small value rather than zero.

After a first reduction with the β-factor, the shotcrete shell is activated by setting the Young's modulus to E_{S1} = 10,000 MN/m². After a second reduction of the internal pressure, the Young's modulus of the shotcrete shell is set to E_{S2} = 15,000 MN/m². To ensure a loading on the inner liner, it is activated after a third load reduction step. Finally the internal pressure is set to zero in a last reduction step.

Changing material properties (i.e. stiffness) during the calculation is not straightforward in ABAQUS. First the material properties have to be made dependent on field variables. To call them in later steps, the user subroutine USER DEFINED FIELD is used.

The calculation steps for the simulation of the construction progress are listed below:

INITIAL: Imposing the initial stress field; fix degree of freedom (D.O.F.) 1 (Fig. 3–18) for the right vertical boundary; fix D.O.F. 2 for the bottom boundary; Young's modulus of shotcrete shell (E_{S0}) and inner liner (E_{L0}) is initialized with 50 N/m²; the load reduction method is implemented by means of the function AMPLITUDE, which allows the decrease of concentrated forces at the tunnel-perimeter during the calculation; additionally the interactions between ground and shotcrete shell as well as between shotcrete shell and inner liner are defined by a Coulomb friction law with a friction coefficient of μ = 100 (ρ = 89,43°) and μ = 1.0, respectively.

STEP 1: Apply σ_V at the top boundary; apply σ_H at the left vertical boundary; apply p_0 * (1-β) at the tunnel-perimeter; set β to zero; (Fig. 3–19a)

STEP 2: Set β to 20%; (Fig. 3–19b)

STEP 3: The shotcrete shell is introduced. Therefore, D.O.F. 1, 2 at the tunnel-perimeter are fixed and the Young's modulus of shotcrete is set to E_{S1} = 10,000 MN/m².

STEP 4: D.O.F. 1, 2 at the tunnel-perimeter are released; (Fig. 3–19c shows STEP 3 and 4)

STEP 5: Set β to 40%; (Fig. 3–19d)

STEP 6: Idle step (for evaluation purposes)

STEP 7: Changing material behavior of the shotcrete from a "young" to a "hardened" one. Therefore, D.O.F. 1, 2 at the tunnel-perimeter are fixed and the Young's modulus of shotcrete is set to E_{S2} = 15,000 MN/m². (Fig. 3–19e)

STEP 8: D.O.F. 1, 2 at the tunnel-perimeter are released; set β to 60%; (Fig. 3–19f)

STEP 9: The inner liner is activated; Therefore, D.O.F. 1, 2 at the tunnel-perimeter are fixed and E_L is set to 30,500 MN/m². (Fig. 3–19g)

STEP 10: D.O.F. 1, 2 at the tunnel-perimeter are released; set β to 80%; (Fig. 3–19h)

STEP 11: β is set to 100%; end of tunnel construction; (Fig. 3–19i)

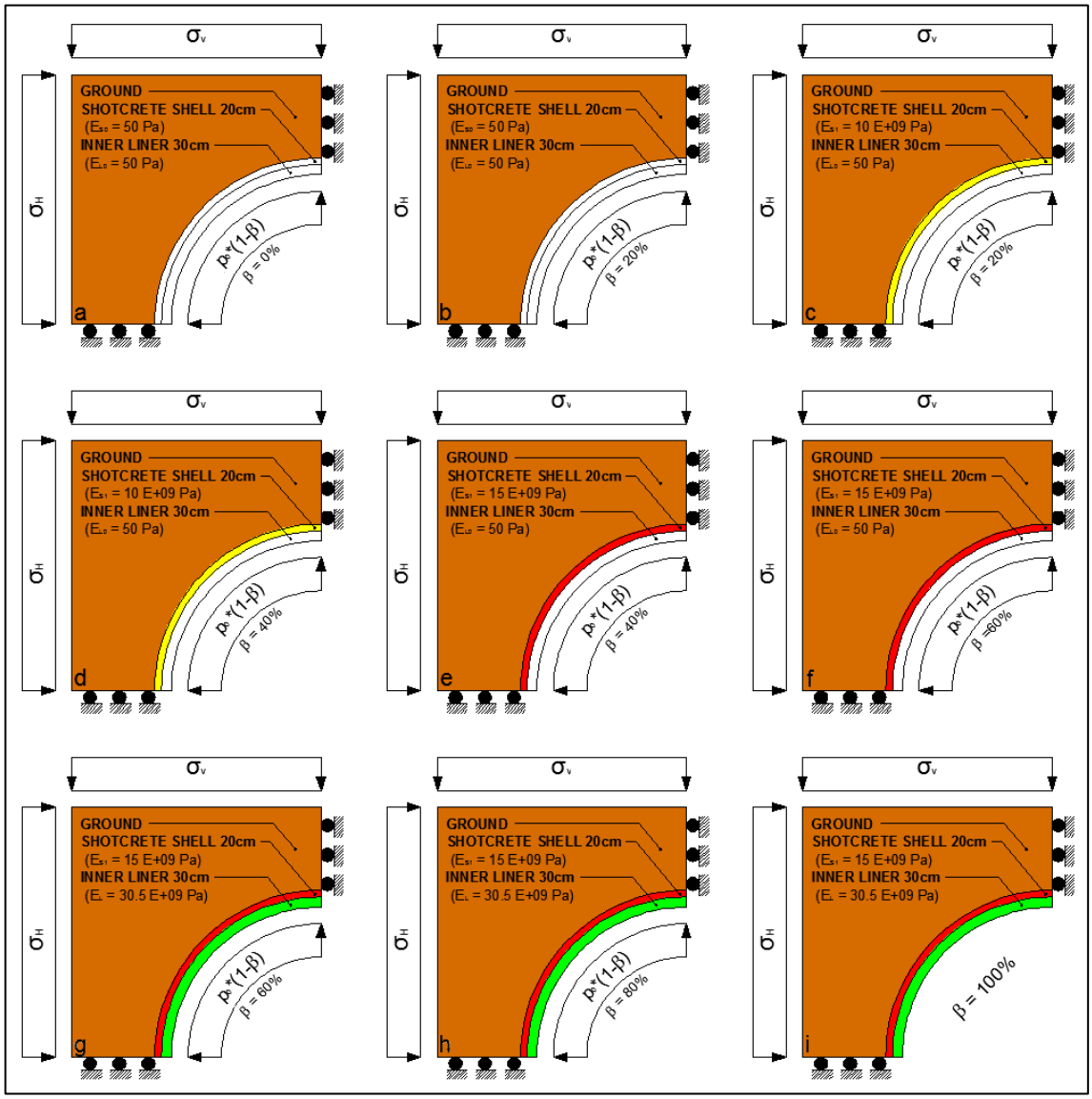

Fig. 3–19: Changing Stiffness Method – construction process; (Note: figure sub-numbering in left lower corner)

Fixing the boundary at the tunnel-perimeter during installation of the support elements (shotcrete shell and inner liner) was demonstrated by Einstein et al., (1995). It should ensure that no numerical problems during changing of the material properties occur. Fig. 3–20 shows a plot of tangential stresses (S22)[4] in the support elements as well as

[4] Note: All results of the shotcrete shell and inner liner are transformed into an user defined cylindrical coordinate system, but also called S22, U1 and so on.

the radial displacements (U1) of the tunnel-perimeter during the above mentioned calculation steps. All results are obtained at the spring-line (Fig. 3–1).

In the third step (Fig. 3–20) a significant increase of the stresses in the shotcrete shell occurs. In the fourth step a significant decrease of those stresses occurs. For comparison purposes, a calculation in which D.O.F. 1, 2 at the tunnel-perimeter are not fixed during the modification of the material properties is performed (Fig. 3–21). (Note that D.O.F. 1, 2 are fixed for STEP 3, STEP 7 and STEP 9 in Fig. 3–20) The first calculation with fixed D.O.F. 1, 2 at the tunnel-perimeter during the modification of material properties (same as in Fig. 3–20; black dashed lines) is compared to a second calculation in which D.O.F. 1, 2 at the tunnel-perimeter are not fixed during the modification of material properties (colored solid lines).

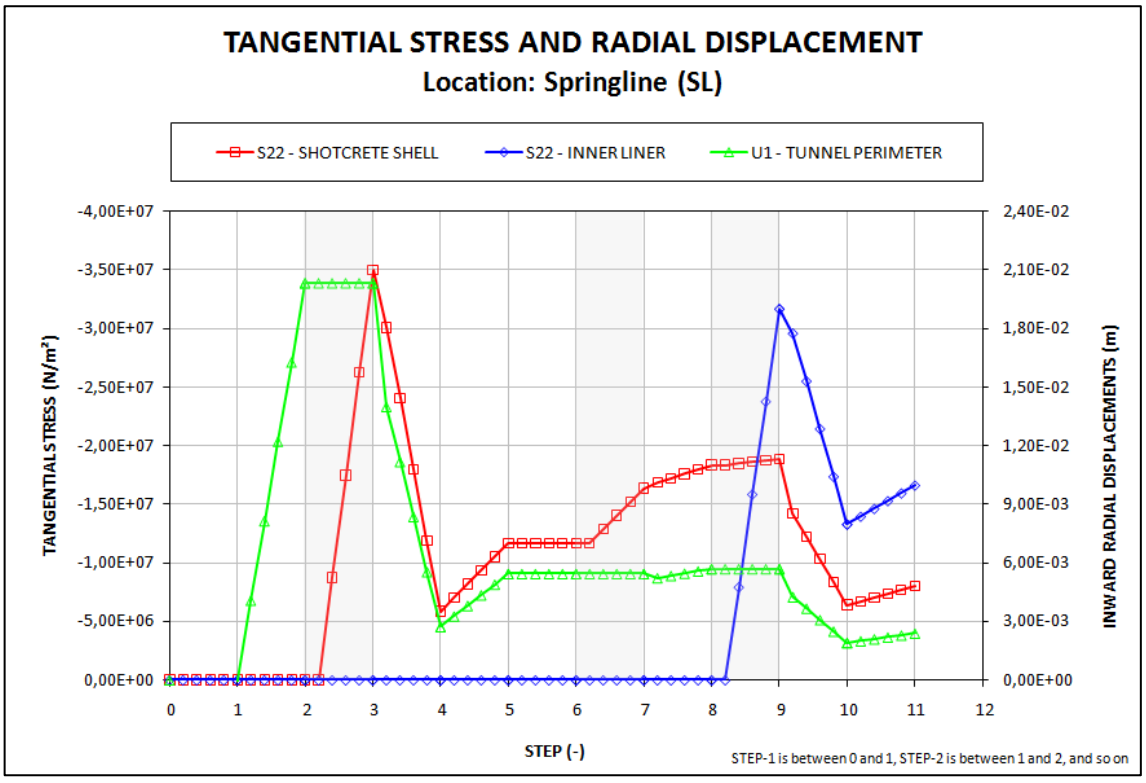

Fig. 3–20: Result of Changing Stiffness Method; in the gray marked STEP 3, 7 and 9 the D.O.F. 1, 2 at the tunnel-perimeter are fixed;

With regards to Fig. 3–20 and Fig. 3–21 the curves with the squared (□) markers are the averaged stresses of the shotcrete shell, the diamond (◊) markers indicate the averaged stresses of the inner liner and the triangular (Δ) ones are the radial displacements (positive = inward) of the tunnel-perimeter at the spring-line. Regarding the simulation steps mentioned above, STEP 1 extends the horizontal axis between 0 and 1, STEP 2 between 1 and 2, and so on.

Table 2 gives a detailed description of Fig. 3–21, providing a comparison of tangential stresses in the shotcrete shell and the inner liner, and of the radial displacements of the tunnel-perimeter at the spring-line.

Parentheses are used in Table 2 to make comments about the real behavior. Square brackets are used to insert notes. Note that the only differences between these two calculations are the constraints on the tunnel-perimeter nodes in STEP 3, -7 and -9.

Looking at the values of STEP 11 (end of tunnel construction progress) it is obvious that the stresses and displacements of the two calculations (with and without fixing the nodal displacements in STEP 3, -7 and -9) are exactly the same. (Fig. 3–21)

A comparative calculation, in which all support elements are simulated using their final material parameters from the very beginning, shows the same values of stresses and displacements at STEP 11 as the two discussed calculations shown in Fig. 3–21, which makes sense as long as all material are linear elastic. However, the stress and displacement history in the preceding steps will be entirely different due to the change of material properties.

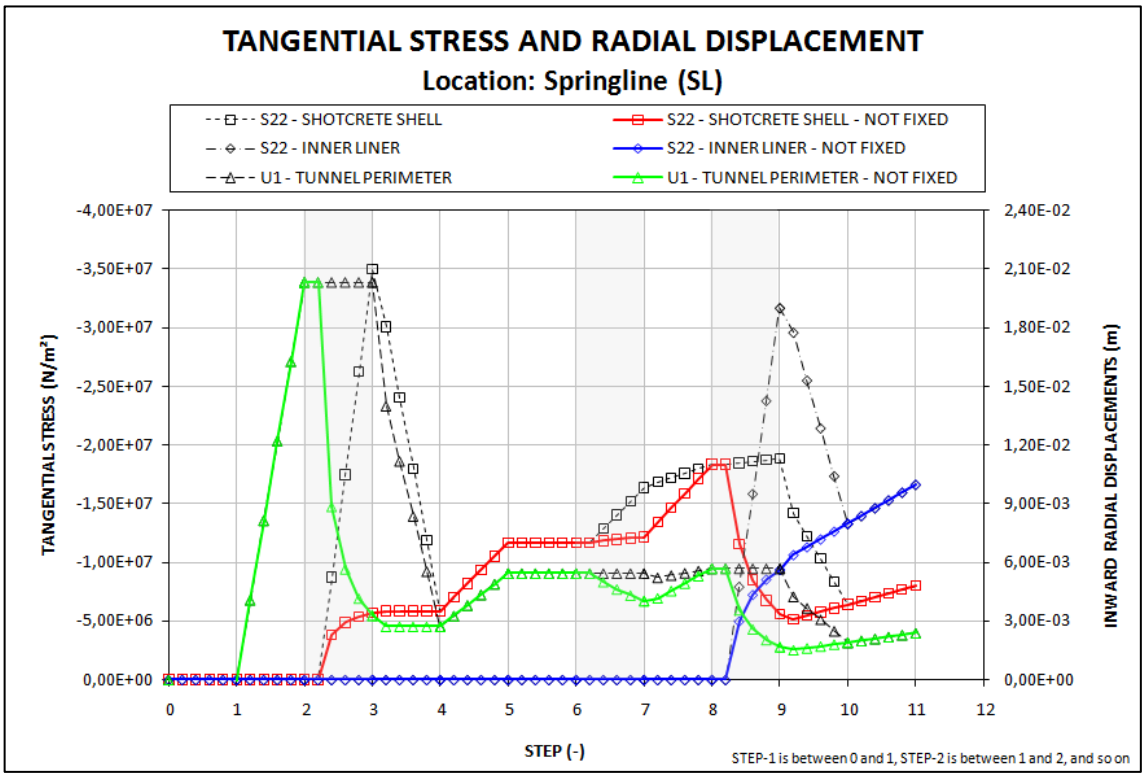

Fig. 3–21: Comparison: Changing Stiffness Method with and without fixed D.O.F. 1 and 2 at the tunnel-perimeter during the change of properties;

Table 2: Interpretation Fig. 3–21; distribution of stresses and displacements; Comparison: Changing Stiffness Method with and without fixed D.O.F. 1, 2 at tunnel-perimeter;

	TANGENTIAL STRESSES SHOTCRETE SHELL		TANGENTIAL STRESSES INNER LINER		RADIAL DISPLACEMENTS TUNNEL-PERIMETER	
	FIXED D.O.F.	D.O.F. NOT FIXED	FIXED D.O.F.	D.O.F. NOT FIXED	FIXED D.O.F.	D.O.F. NOT FIXED
STEP 1	no change	no change	no change	no change	no change	no change
STEP 2	no change	no change	no change	no change	Tunnel-perimeter moves 2cm radially inward	Tunnel-perimeter moves 2cm radially inward
STEP 3	Stresses go up to 35MPa; (Reality: no stresses)	Stresses go up to 6MPa; (Reality: no stresses)	no change	no change	no change; [Note: fixed D.O.F.]	Tunnel-perimeter moves 1.7cm radially outward; (Reality: no change)
STEP 4	Stresses go down to 6MPa; (Reality: no stresses)	no change	no change	no change	Tunnel-perimeter moves 1,7cm radially outward; (Reality: no change)	no change
STEP 5	Stresses go up	Stresses go up	no change	no change	Tunnel-perimeter moves radially inward	Tunnel-perimeter moves radially inward
STEP 6	no change	no change	no change	no change	no change	no change
STEP 7	Stresses go up; (Reality: no change)	almost no change; (Reality: no change)	no change	no change	no change; [Note: fixed D.O.F.]	Tunnel-perimeter moves radially inward; (Reality: no change)
STEP 8	Stresses go up; (Reality: greater increase)	Stresses go up	no change	no change	almost no change; (Reality: Tunnel-perimeter moves radially inward)	Tunnel-perimeter moves radially inward
STEP 9	almost no change; (Reality: no change)	stresses go down to 5MPa; (Reality: no change)	Stresses go up to 32MPa; (Reality: no stresses)	Stresses go up to 9MPa; (Reality: no stresses)	no change; [Note: fixed D.O.F.]	Tunnel-perimeter moves radially outward; (Reality: no change)
STEP 10	Stresses go down; (Reality: stresses go up)	Stresses go up	Stresses go down; (Reality: stresses go up)	Stresses go up	Tunnel-perimeter moves radially outward; (Reality: Tunnel-perimeter moves radially inward)	Tunnel-perimeter moves radially inward
STEP 11	Stresses go up	Stresses go up	Stresses go up	Stresses go up	Tunnel-perimeter moves radially inward	Tunnel-perimeter moves radially inward

To summarize, the advantages of this method are

- a constant thickness of the support elements (shotcrete shell and inner liner) can be maintained,
- the possibility for specific contact formulations (i.e. Coulomb friction) exists.

However, the disadvantages of this method are

- the displacements of the support elements cannot be predicted realistically,
- the stresses of the support elements cannot be predicted realistically.

3.6.4 Four Calculations Method

This method uses four separate calculations to simulate the construction of a tunnel:

- calculation to obtain reaction forces (at tunnel-perimeter)
- calculation to obtain coordinates to construct the shotcrete shell
- calculation to obtain coordinates to construct the inner liner
- final calculation of tunnel construction

With ABAQUS it is not straightforward to add new elements based on result values obtained in a previous step without interrupting the calculations. All steps of a simulation have to be defined before the calculation is submitted. This is the major reason for having four separate calculations. The calculations are formulated such that the results of preceding calculations are always included in the subsequent one. The only exception to this rule is the first calculation, where the reaction forces are obtained by applying boundary conditions to the tunnel-perimeter.

The following will give an overview of those four separate calculations. At the end an overview of all steps is presented.

The first calculation is done to obtain reaction forces at each node of the tunnel-perimeter (Fig. 3–24). In case of a uniform earth-pressure (K = 1) this calculation can be omitted and a pressure ($p_0 = \sigma_v = \sigma_H$) can be applied at the tunnel-perimeter. However, in all other cases the D.O.F. 1 and 2 of all nodes at the tunnel-perimeter are fixed. Furthermore, in the initial step, a geostatic stress field is introduced and boundary conditions, here roller support, are applied at the bottom and the right side of the model (see chapter 3.1.1). In the first step the vertical and horizontal earth-pressure are applied at the top and the left side of the model. After full loading of the model, the reaction forces can be obtained at each node of the tunnel-perimeter.

The second calculation is to simulate the pre-displacements and support delay. For this purpose, the previously determined reaction forces are applied as concentrated forces at the tunnel-perimeter (Fig. 3–24). These forces are then reduced using the load reduction method. Upon reaching the load reduction factor at that the shotcrete shell is

to be installed, the calculation is terminated and the nodal-coordinates of the deformed tunnel-perimeter can be read out.

The third calculation is to include the shotcrete shell. The previously determined nodal-coordinates are used to model and apply the shotcrete shell. At the start of the calculation the outer edge of the shotcrete shell has a radius smaller than the tunnel-perimeter. Consequently there is no contact between tunnel-perimeter and shotcrete shell. Therefore, the concentrated forces are reduced with the load reduction method. As a result, the tunnel-perimeter moves inward. Upon reaching the load reduction factor at which the nodal-coordinates were obtained in the second calculation, the contact between tunnel-perimeter and shotcrete shell is closed. Next, the concentrated forces on the combined system, ground plus shotcrete shell, are reduced to a certain value where the inner liner is to be installed.

A brief discussion of contact formulations is necessary:

An accurate formulation of contact is very important to avoid numerical problems. (See chapter 3.4). Contact formulations in ABAQUS have to be set when two parts are interacting. For instance, a contact formulation has to be set between the tunnel-perimeter of the ground and the outer edge of the shotcrete shell. The tunnel-perimeter is defined as master-surface and the outer edge of the shotcrete shell is the slave-surface. The general definition of surfaces in ABAQUS is as follows:

Nodes of the master-surface can penetrate into the slave-surface, but nodes of the slave-surface cannot penetrate into the master-surface (node-to-surface contact) (Fig. 3–23$_{LEFT}$).

A node on the slave-surface cannot penetrate into a node on the master-surface (Fig. 3–23$_{RIGHT}$). Nodes on the tunnel-perimeter have the same position as nodes on the outer edge of the shotcrete shell. Also nodes on the inner edge of the shotcrete shell have the same position as nodes on the outer edge of the inner liner.

Now the question arises: Are the nodes of these interfaces in the same position, or is an interface thickness to consider? For this purpose, two different elements, CPE8R and CPE4 elements are investigated. (Fig. 3–2)

Regarding CPE8R elements, a thickness of the interface has not been implemented, meaning two nodes (one on the master- and one on the slave-surface) have the same coordinates once contact has been established.

By contrast, CPE4 elements require the definition of an interface with a given non-zero thickness. Consequently, two nodes (one on the master- and one on the slave-surface) do not have the same coordinates once contact has been established. As a result, the interface has a finite thickness.

Fig. 3–22 shows how to consider the finite interface thickness (z) during the construction of the shotcrete shell. The new coordinates of the nodes on the outer edge

of the shotcrete shell, considering a finite interface thickness, are extrapolated from the nodal-coordinates of the undeformed initial tunnel-perimeter as well as the deformed tunnel-perimeter:

$$y_3 = y_2 + z * \sin\left[\tan^{-1}\left(\frac{y_1 - y_2}{x_1 - x_2}\right)\right] \tag{3.5}$$

$$x_3 = x_2 + z * \cos\left[\tan^{-1}\left(\frac{y_1 - y_2}{x_1 - x_2}\right)\right] \tag{3.6}$$

Note that the nodal-coordinates of the undeformed initial tunnel-perimeter can be obtained at the beginning of each calculation. The nodal-coordinates of the deformed tunnel-perimeter are calculated by adding or subtracting the vertical (ΔY) and horizontal (ΔX) displacements.

A finite interface thickness can be considered to construct the shotcrete shell and inner liner.

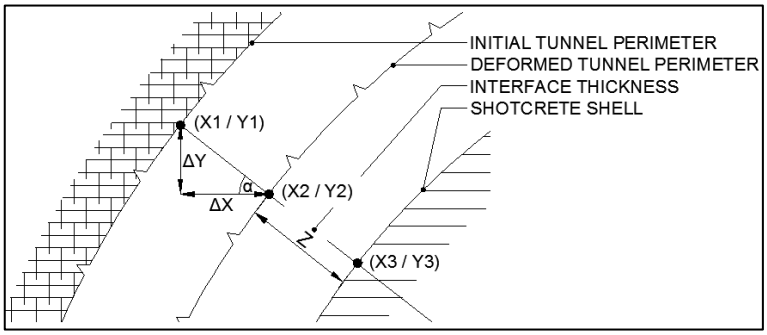

Fig. 3–22: Establish nodal-coordinates of shotcrete shell under consideration of interface thickness

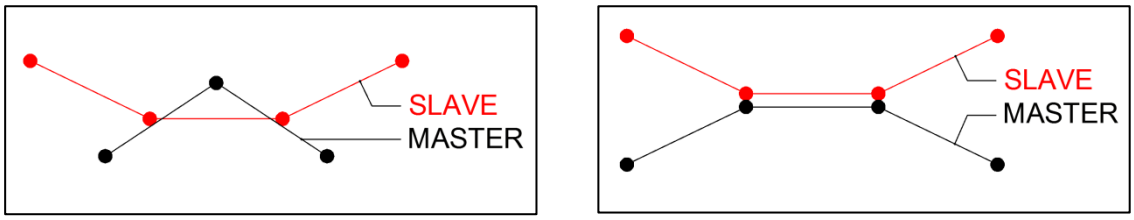

Fig. 3–23: node to surface (left) and node to node contact (right) of MASTER and the SLAVE surface

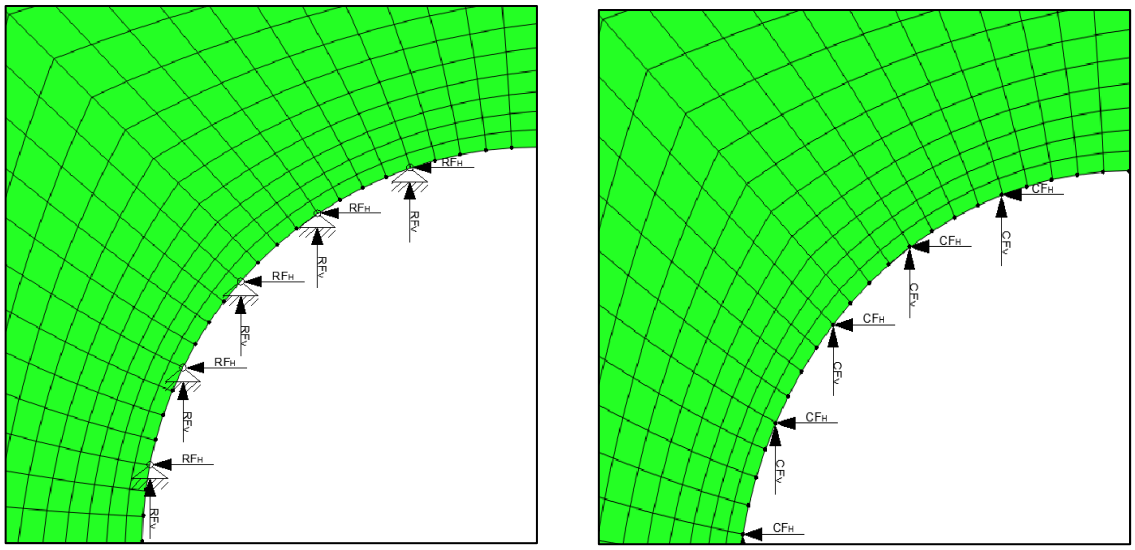

Fig. 3–24: Obtaining reaction forces for fixed D.O.F. 1 and 2 (left), and applying them as concentrated forces at the tunnel-perimeter (right)

The fourth calculation is to include the inner liner. For this purpose, the determined nodal-coordinates of the third calculation are used to model and apply the inner liner in the fourth calculation. At the start of the calculation, the outer edge of the shotcrete shell has a radius smaller than the tunnel-perimeter, and the outer edge of the inner liner has a radius smaller than the inner edge of the shotcrete shell. This can also be interpreted as gaps (Fig. 3–25$_{LEFT}$). First the gap between tunnel-perimeter and shotcrete shell is closed in the same way as in calculation three. Subsequently, the gap between the shotcrete shell and the inner liner is closed as well. Finally the reaction forces, which are still applied at the tunnel-perimeter, are reduced to zero.

In order to provide an overview, all calculation steps are listed in detail in the following:

INITIAL: INITIAL CONDITIONS (PART ONE):

The calculation starts with a gap between tunnel-perimeter and shotcrete shell (SHOT) as well as between shotcrete shell and inner liner (LINER) (Fig. 3–25). Contact formulations in terms of normal and tangential behavior are defined and applied to these interfaces. The D.O.F. 1 is fixed for all three parts (GROUND, SHOT, LINER) of the model at the right vertical boundary and the D.O.F. 2 is fixed for all three parts of the model at the bottom (Fig. 3–18). Furthermore, an initial stress field is applied to the GROUND (Fig. 3–28). The initial stress field is defined by a uniform vertical stress and a horizontal stress, which is defined by the vertical stress and the lateral stress coefficient (K). The initial stress field is to prevent displacements on the model in the first step, when the external vertical and horizontal stresses are applied. The external stress field is to maintain a constant stress in the GROUND during the excavation process. Note that the external stress field is applied in STEP 1. Finally the load reduction method is implemented using the function AMPLITUDE, which allows one

to decrease the concentrated forces at the tunnel-perimeter during the calculation.

STEP 1: INITIAL CONDITIONS (PART TWO):
The vertical stress σ_V is applied at the top boundary of the model and the horizontal stress σ_H is applied at the left vertical side of the model (Fig. 3–28). Concentrated forces are applied at the tunnel-perimeter (Fig. 3–24). The function AMPLITUDE is used to govern those forces to be reduced over several calculation steps. The support elements are removed using the method MODEL CHANGE (Fig. 3–25$_{right}$). Simultaneously the contact formulations between tunnel-perimeter and SHOT as well as between SHOT and LINER are removed.
[Notes regarding the first calculation: Concentrated forces are not applied; D.O.F. 1 and 2 are fixed at tunnel-perimeter]

STEP 2: OBTAIN REACTION FORCES [Note: End of first calculation]:
At this step, the first calculation is terminated and the reaction forces at each node of the tunnel-perimeter are obtained.

EXCAVATION (UNLOADING FACTOR β = 85%):
Here, the support delay is simulated. Hence, the reaction forces are reduced using the load reduction method until the point where the SHOT is to be installed is reached (Fig. 3–11).

STEP 3: OBTAIN NODAL COORDINATES SHOT [Note: End of second calculation]:

At this step, the second calculation is terminated and the coordinates of the nodes at the deformed tunnel-perimeter are obtained.

CONTACT TO YOUNG SHOT:
The contact formulation between tunnel-perimeter and SHOT is reactivated (See chapter 3.3). Moreover, the SHOT is activated with a Young's modulus of E_{S1} = 10,000 MN/m² (Fig. 3–26$_{left}$).

STEP 4: EXCAVATION (UNLOADING FACTOR β = 90%):
This step is to simulate the displacement of the combined system, GROUND plus "young" SHOT. Therefore, the reaction forces are reduced, using the load reduction method, until the point where the material behavior of shotcrete is changed to a hardened one is reached (Fig. 3–11).

STEP 5: CHANGE PROPERTIES FROM YOUNG TO HARDENED SHOTCRETE:

In this step, the Young's modulus of shotcrete is changed from a "young" shotcrete to a "hardened" one (E_{S2} = 15,000 MN/m²). This is done using the

user subroutine USER DEFINED FIELD in the same way as in the Changing Stiffness Method (3.6.3).

STEP 6: EXCAVATION (UNLOADING FACTOR β = 95%):
This step simulates the displacements of the combined system, GROUND plus "hardened" SHOT. Therefore, the reaction forces are reduced, using the load reduction method, until the point is reached at that the LINER is to be installed (Fig. 3–11).

STEP 7: OBTAIN NODAL COORDINATES LINER [Note: End of third calculation]:

At this step the third calculation is terminated and the nodal-coordinates on the inner edge of the deformed SHOT are obtained.

CONTACT TO INNER LINER:
The contact formulation between SHOT and LINER is reactivated. Moreover, the LINER is introduced with a Young's modulus of E_L = 30,500 MN/m² (Fig. 3–26$_{right}$).

STEP 8: EXCAVATION (UNLOADING FACTOR β = 100%):
In practice, when all displacements on the combined system GROUND plus SHOT have abated, the LINER is to be installed. As a result, no load will be carried by the LINER. The loading on the LINER is mostly done by assuming full deterioration of the SHOT. Consequently the LINER has to carry the load that was taken before by the SHOT. However, to ensure a load on the combined system, GROUND plus SHOT plus LINER, the reaction forces that appear at the tunnel-perimeter are set to zero in the last step (STEP 8) of the calculation (Fig. 3–11).

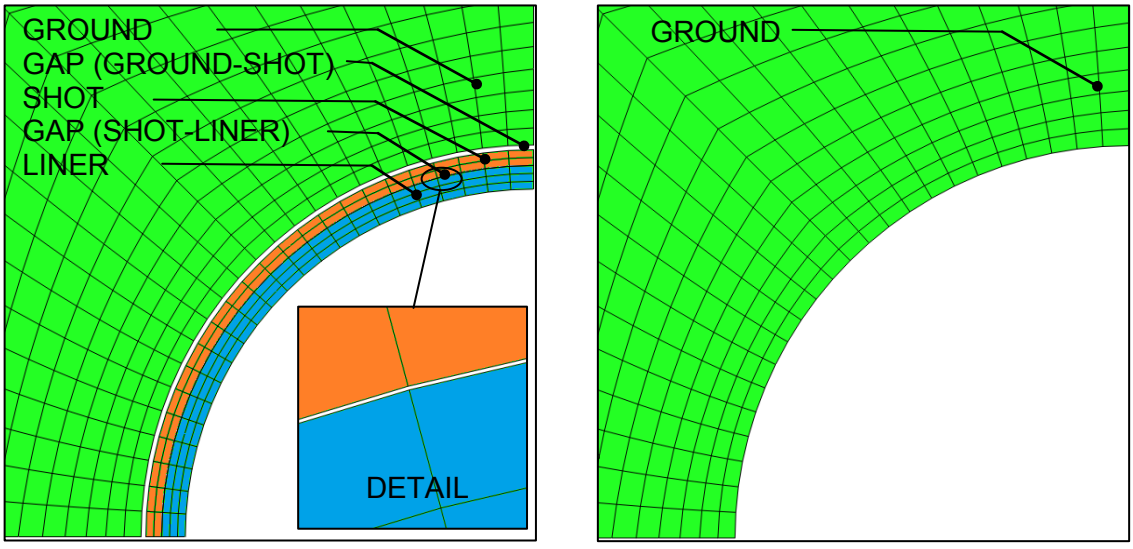

Fig. 3–25: Initial (left) and first step (right) of four calculation method. Support elements (shotcrete shell and inner liner) are removed in first step.

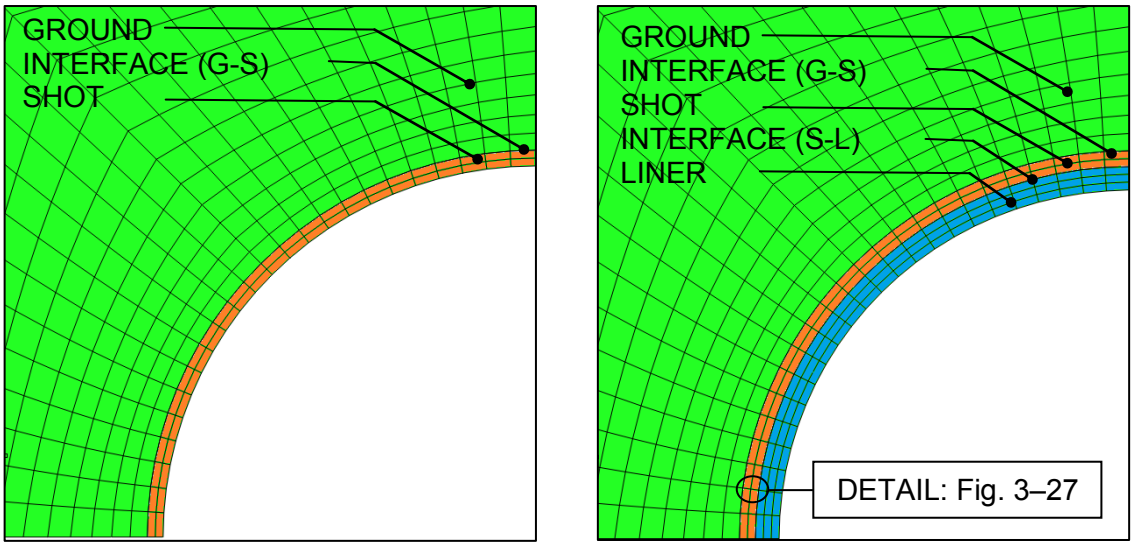

Fig. 3–26: Activation of shotcrete shell as well as the contact formulations at the ground – shotcrete shell (G-S) interface at STEP 3 (left) and activation of inner liner as well as the contact formulations at the shotcrete shell – inner liner (S-L) interface at STEP 7 (right).

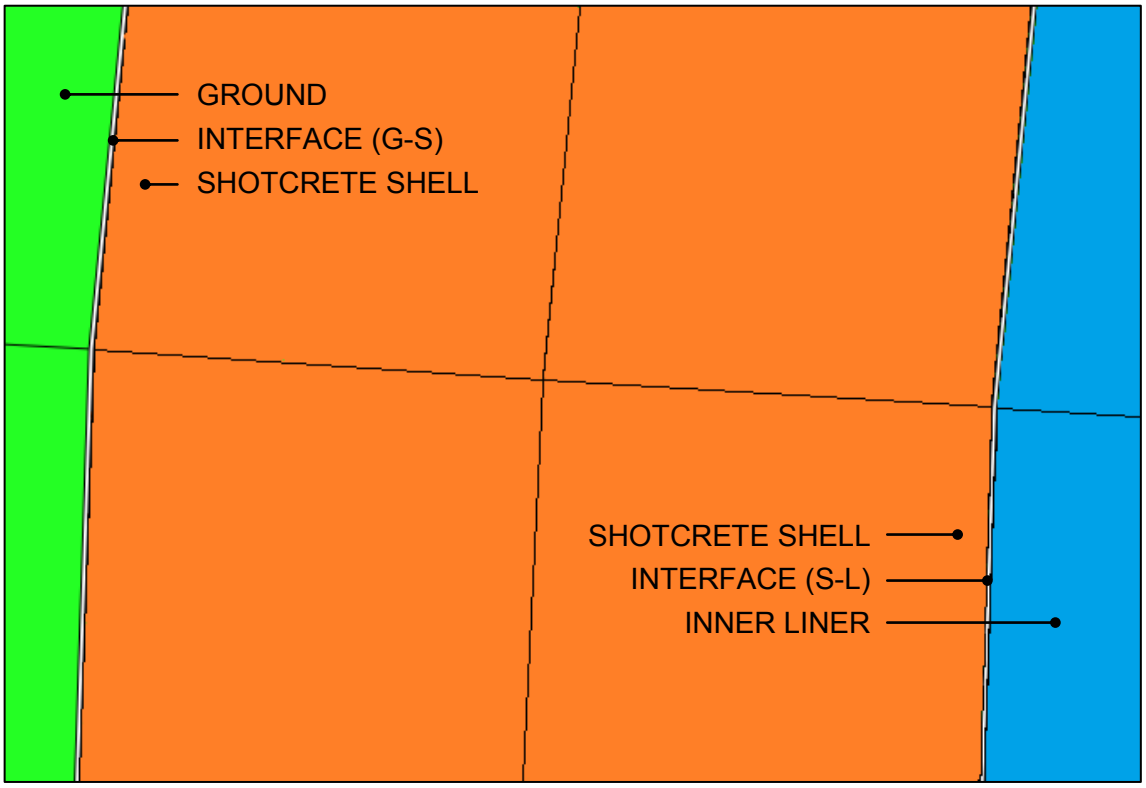

Fig. 3–27: Detail; Interfaces between ground (G), shotcrete shell (S) and inner liner (L)

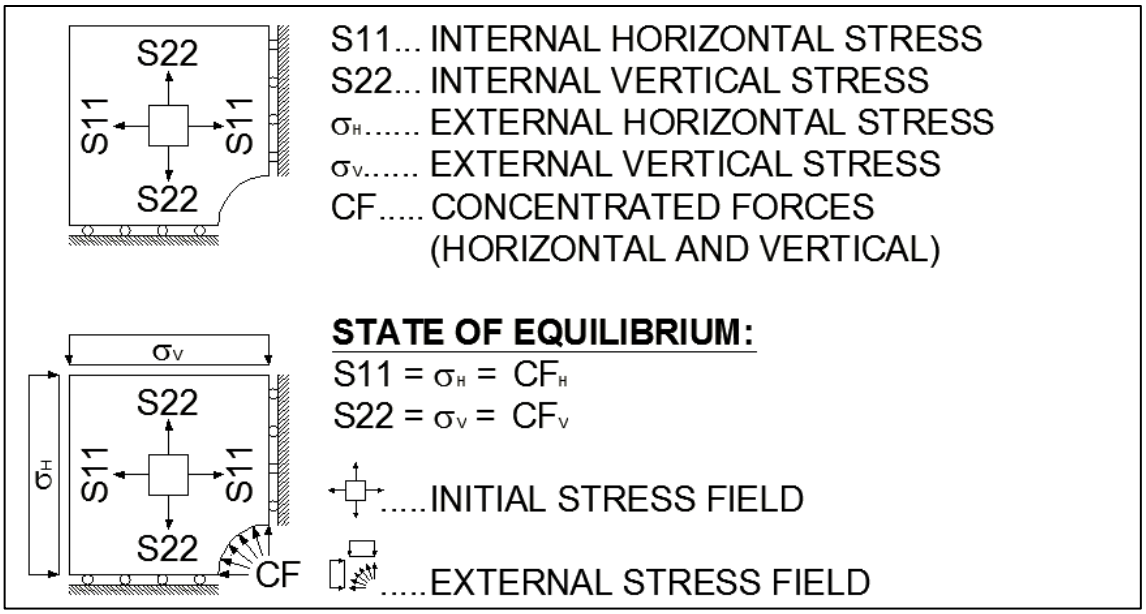

Fig. 3–28: Initial stress field (upper figure) and initial stress field with external stress field in equilibrium (lower figure); reaction forces are separated into horizontal and vertical direction;

The advantages of this method are that

- a constant thickness of the support elements (shotcrete shell and inner liner) can be maintained
- the possibility for contact formulation (i.e. Coulomb friction) exists,
- the displacements of the support elements can be predicted realistically,
- the stresses of the support elements can be predicted realistically.

3.6.5 Conclusion

Different methods to simulate a tunnel construction with a 2D numerical analysis, using ABAQUS, were discussed:

- Model Change Method
- Dummy Node Method
- Changing Stiffness Method
- Four Calculation Method

Depending on the aim and accuracy of the investigation, the best method for each case has to be figured out. Table 3 presents a brief overview of the discussed methods. One aim of this research is to find a method, which considers contact formulations. This is possible using the Changing Stiffness Method or the Four Calculation Method. However, changing material properties during the calculation, as needed for the Changing Stiffness Method, is not straightforward in ABAQUS.

One possibility to simulate the change of material properties is given by the user subroutine USER DEFINED FIELD. This is done in the Changing Stiffness Method to simulate the construction or activation of support elements (shotcrete shell and inner liner). First, the support elements are included in the numerical model with a very low

Young's Modulus, meaning that they can be seen as deactivated. On the basis of this very low Young's Modulus, nearly no stresses exist in the support elements during the first reduction of the concentrated forces. In other words, the support elements can deform without taking stresses. The activation of the support elements is simulated by changing their Young's Moduli. This change leads to stresses in the support. Displacements of support elements, which occur with a very low Young's Modulus, are considered. As a result of this behavior, a stress-free activation of the support elements cannot be performed.

This thesis is based on the Four Calculation Method. It is not the purpose of this thesis to investigate complex material formulations. Indeed, it aims at the simulation of a deterioration of the shotcrete shell considering the combined system, ground plus support elements. Furthermore, a contact formulation between ground and support elements, as well as between the support elements should be provided. All these requirements are fulfilled by the Four Calculation Method.

Table 3: Overview of tunnel construction methods; 1) Model Change Method; 2) Dummy Node Method; 3) Changing Stiffness Method; 4) Four Calculation Method; X = possible, O = partly possible;

PROPERTIES AND BEHAVIOR	1	2	3	4
Constant thickness of the support elements can be maintained		X	X	X
Contact formulation can be set (i.e. Coulomb friction)			X	X
Accurate geometrical definition of the boundaries of the parts (ground; support elements) is possible. (i.e. no overlapping of several parts)	X		X	X
Real behavior in terms of displacement (e.g. pre-displacements, support delay, deformation of the combined system)	O	O		X
Real behavior in terms of tangential stresses of the support elements (inner liner; shotcrete shell)	O	O		X
Divergent deformation behavior of tunnel shape can be simulated	X	X	X	

3.7 Simulation of the shotcrete shell's deterioration

The deterioration of the shotcrete is investigated. In addition, the effects of different Poisson's ratios (ν), element types (CPE4 and CPE8R) as well as simulations with and without the Coulomb (C) constitutive law are analyzed. The numerical model consists of three parts: the ground (GROUND), the shotcrete shell (SHOT), and the inner liner (LINER). The variation of the Poisson's ratio and the Coulomb constitutive law applies only to the material parameters of the GROUND, whereas the variation of the element type applies to all three parts (GROUND, SHOT and LINER).

The degradation of material properties is simulated using the user subroutine USER DEFINED FIELD. Thereby, material properties are linked to field variables. These field variables are related to the calculation steps:

- STEP 1 to STEP 8: Simulation of the tunnel construction
- STEP 9: Idle step between construction and deterioration part
- STEP 10 to STEP 18: Simulation of the shotcrete shell's deterioration

The deterioration is assumed to be linear. Accordingly, the material properties are reduced by 10% in each step of the calculation, beginning with STEP 10. For this investigation the deterioration of the Young's modulus (E) and the deterioration of the compressive strength (f_C) are simulated.

In the following an overview of the applied deterioration methods is shown:

- Young's Modulus (E)
- Compressive strength (f_C)
- Young's Modulus plus compressive strength (E & f_C) simultaneously

Table 4 shows the applied values of E and f_C related to the several calculation steps.

When the deterioration is simulated by reducing the compressive strength, a linearly elastic – perfectly plastic (LE-PP) material behavior for the shotcrete is assumed. The deterioration of the Young's Modulus is simulated based on a linear elastic (LE) material behavior. In a third calculation, the degradation of the Young's Modulus simultaneous with the degradation of the compressive strength is analyzed, which is based on a linearly elastic – perfectly plastic material behavior.

Table 4: Deterioration of Young's Modulus (E) and compressive strength (f_C) of the shotcrete shell; 10% reduction of E and f_c per step; this table is valid for all three cases; note that in Case 1 only the Young's modulus, in Case 2 only the compressive strength and in Case 3 the Young's modulus and the compressive strength are degraded simultaneously;

STEPS	DETERIORATION	E (GPa)	f_C (MPa)
STEP 9	0%	15.0	20.0
STEP 10	10%	13.5	18.0
STEP 11	20%	12.0	16.0
STEP 12	30%	10.5	14.0
STEP 13	40%	9.0	12.0
STEP 14	50%	7.5	10.0
STEP 15	60%	6.0	8.0
STEP 16	70%	4.5	6.0
STEP 17	80%	3.0	4.0
STEP 18	90%	1.5	2.0

Table 5 shows an overview of the possible combinations. The first column shows the combination number, which is quoted in subsequent chapters. The second column

shows the applied deterioration method. Either the Young's modulus or the compressive strength or both material properties are degraded simultaneously. The third column shows the applied element type. The fourth column shows the applied Poisson's ratio. Either a uniform stress state with a Poisson's ratio of $\nu = 0.5$ or a Poisson's ratio of $\nu = 0.4$ is investigated. The last three columns at the right side show the applied material behavior and whether a Coulomb constitutive law is used or not.

Table 5: Combinations of numerical calculations – investigation in deterioration behavior of shotcrete; E – Young's Modulus, f_c – compressive strength, CPE4 – 4-node plane strain elements, CPE8R – 8-node plane strain elements with reduced integration, LE – linear elastic, LE-PP – linearly elastic – perfectly plastic, (C) – Coulomb constitutive law

Combi-nation	Deterior-ation	Element Type	Poisson's ratio (ν)	Material Behavior & Constitutive Law		
				GROUND	SHOT	LINER
C01	E	CPE4	0.5	LE	LE	LE
C02	E	CPE4	0.4	LE	LE	LE
C03	f_c	CPE4	0.5	LE	LE-PP	LE
C04	f_c	CPE4	0.4	LE	LE-PP	LE
C05	E & f_c	CPE4	0.5	LE	LE-PP	LE
C06	E & f_c	CPE4	0.4	LE	LE-PP	LE
C07	E	CPE4	0.5	LE-PP (C)	LE	LE
C08	E	CPE4	0.4	LE-PP (C)	LE	LE
C09	f_c	CPE4	0.5	LE-PP (C)	LE-PP	LE
C10	f_c	CPE4	0.4	LE-PP (C)	LE-PP	LE
C11	E & f_c	CPE4	0.5	LE-PP (C)	LE-PP	LE
C12	E & f_c	CPE4	0.4	LE-PP (C)	LE-PP	LE
C13	E	CPE8R	0.5	LE	LE	LE
C14	E	CPE8R	0.4	LE	LE	LE
C15	f_c	CPE8R	0.5	LE	LE-PP	LE
C16	f_c	CPE8R	0.4	LE	LE-PP	LE
C17	E & f_c	CPE8R	0.5	LE	LE-PP	LE
C18	E & f_c	CPE8R	0.4	LE	LE-PP	LE

4 RESULTS

This chapter shows the results. The interpretation and comments on the results can be obtained from chapter 5.

The main focus of this research is to investigate the stresses in the inner liner during the deterioration of the shotcrete shell. In addition, radial displacements of the tunnel are investigated. Fig. 4–1 shows the stresses in the support elements (shotcrete shell and inner liner) as well as radial displacements at the spring-line (see Fig. 3–1).

Zone Σ, STEP 2 to STEP 8, represents the tunnel construction. Zone Π, STEP 9, represents an idle step between tunnel construction and the deterioration (No process changes occur in this part) and zone Ω, STEP 10 to STEP 18, represents the deterioration of the shotcrete shell and its effects on the inner liner.

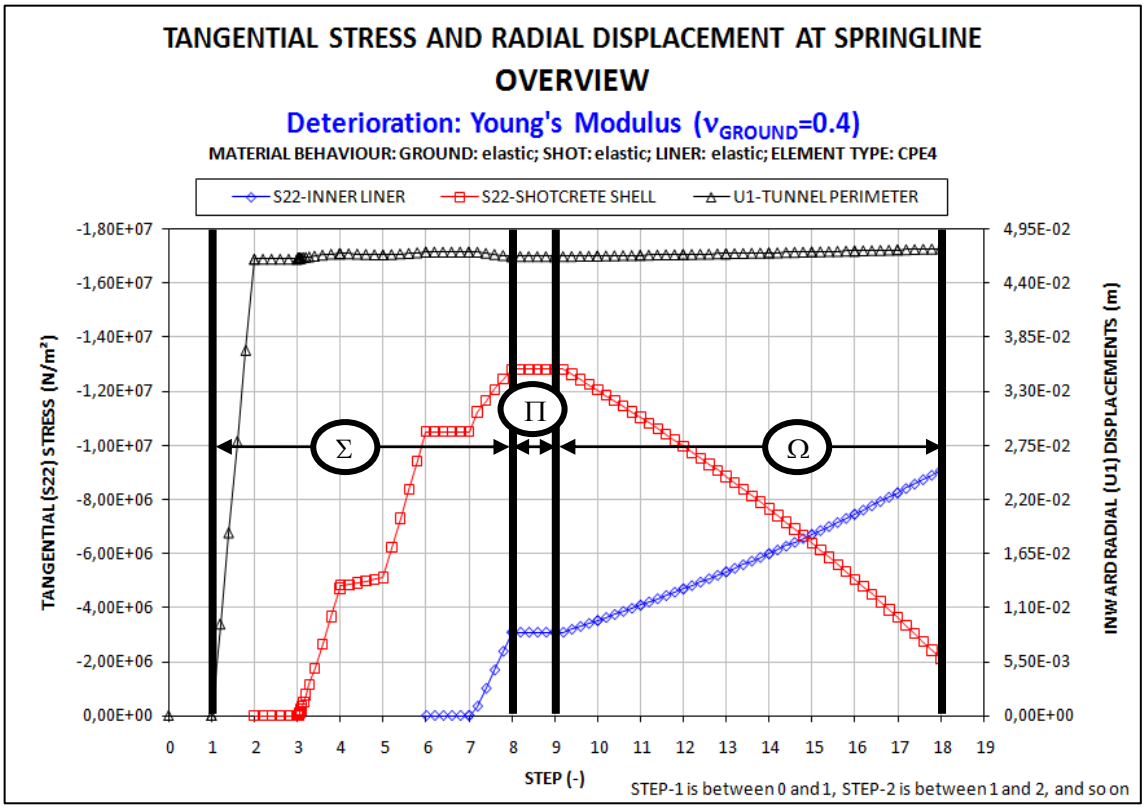

Fig. 4–1: Overview of stresses in inner liner and shotcrete shell as well as radial displacements, all results are obtained at the spring-line; results based on (C02); Zone Σ, Π & Ω; [(C02) relates to the specific calculation used to develop this plot – deterioration: Young's modulus, element-type: CPE4, Poisson's ratio: 0.4, material behavior of ground, shotcrete shell and inner liner: linear-elastic; see Table 5]

Zone Σ & Ω are discussed in subsequent chapters:

- Zone Σ: Tunnel construction (chapter 4.1)
- Zone Ω: Deterioration of the shotcrete shell (chapter 4.2)

Regarding Fig. 4–1, the stresses were averaged over the shotcrete shell and inner liner thicknesses. The red square (□) curve shows the averaged stress in the shotcrete

shell. The averaged stresses in the inner liner are shown by the blue diamond (◊) curve. The black triangular (Δ) curve shows the radial displacements of the tunnel-perimeter at the spring-line. All results are based on the combined system, ground plus shotcrete shell plus inner liner.

Table 5 shows every combination of the parametric study, i.e. material behavior, finite element type, deterioration and Poisson's ratio. Generally, the parametric study can be divided in two parts, dependent on the Poisson's ratio. Subsequently, only results with a Poisson's ratio of $\nu = 0.4$ are discussed. Other results can be obtained from the appendix.

4.1 Tunnel construction

Fig. 4–2 shows the averaged stresses in the shotcrete shell and inner liner. The calculations can be categorized into three cases:

- Case A: Linear elastic material behavior using CPE4 elements
- Case B: Linearly elastic – perfectly plastic material behavior using CPE4 elements
- Case C: Linear elastic material behavior using CPE8R elements

Note that the linearly elastic – perfectly plastic material behavior is based on the Coulomb failure criterion.

CPE4	4-node bilinear plane strain continuum elements
CPE8R	8-node biquadratic plane strain continuum elements with reduced integration
LE-PP (C)	linearly elastic – perfectly plastic material behavior based on the Coulomb failure criterion
LE	linear elastic material behavior
S22	tangential stress in shotcrete shell and inner liner
U1	radial displacement of tunnel-perimeter at spring-line; positive = inward-movement (Fig. 4–3);

Generally, for all three cases, very similar stress-distributions could be obtained in the shotcrete shell and inner liner. Nevertheless, higher stresses occur, using linearly elastic – perfectly plastic material behavior and the Coulomb failure criterion (Case B), than using linear elastic material behavior (Cases A and C). Changing the element types (Case A vs. Case C) does not change the state of stresses significantly.

Fig. 4–2 shows the stresses in the shotcrete shell and in the inner liner for all three cases. More iteration steps are needed in STEP 4 in Case C (see Fig. 4–2). Smaller iteration steps than usual, are caused by effects of nonlinearities (see also chapter 3.4).

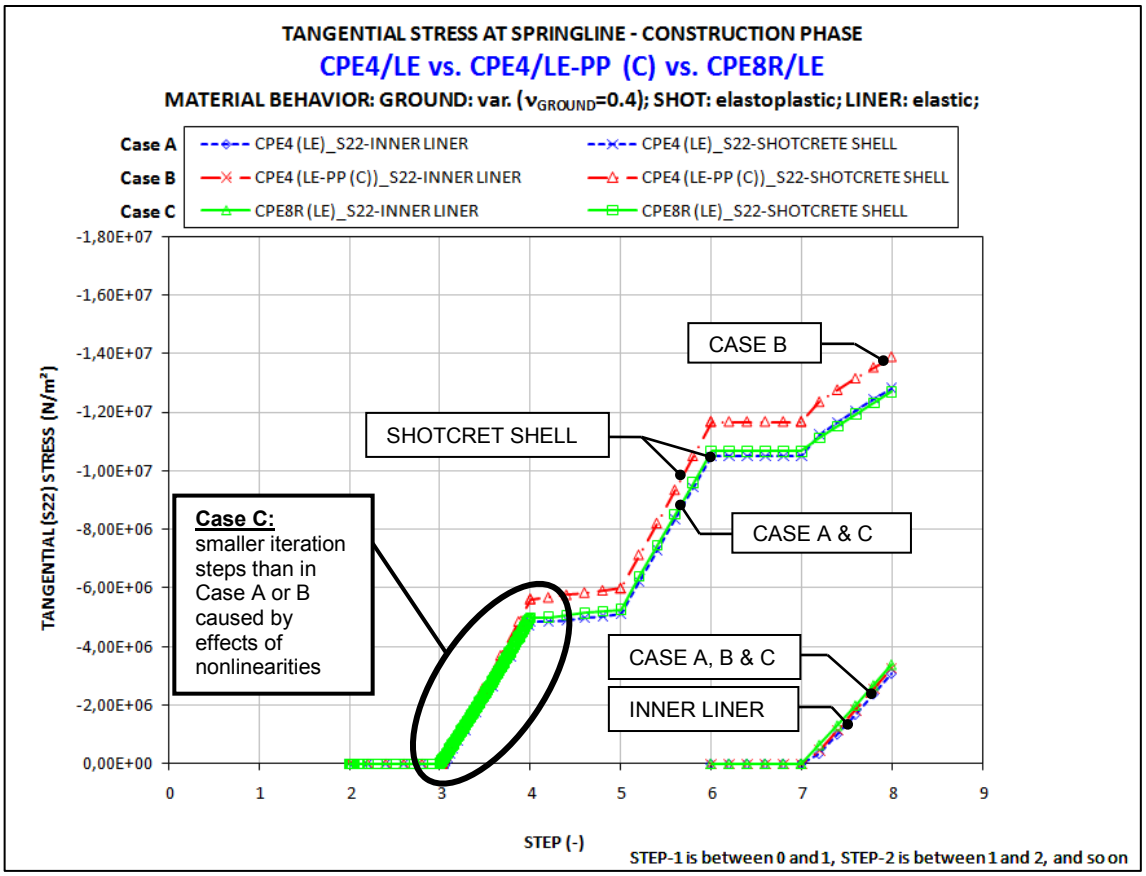

Fig. 4–2: Comparison of Case A (CPE4 elements & LE material behavior), Case B (CPE4 elements & LE-PP material behavior) and Case C (CPE8R elements & LE material behavior); tangential stresses at spring-line in shotcrete shell and inner liner are shown; Case C: smaller iteration steps than in Case A or B, caused by effects of nonlinearities, explanation of symbols see chapter 4.1; results based on (C06+C12+C18);

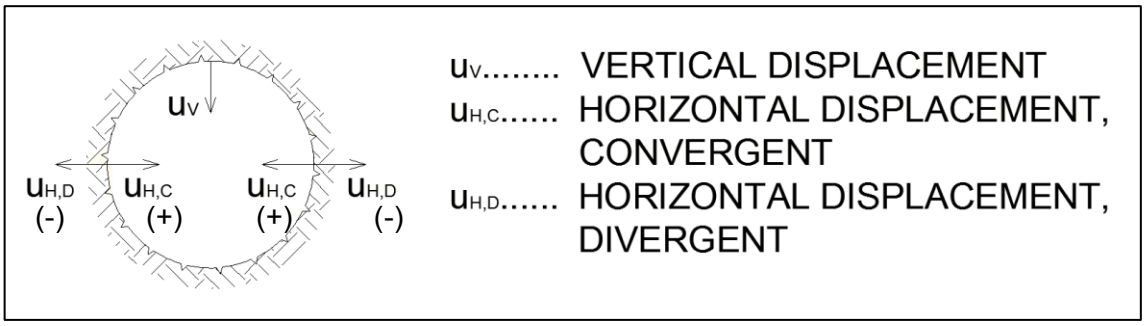

Fig. 4–3: Convergent and divergent deformation behavior

Fig. 4–4 shows the radial displacements. The linearly elastic – perfectly plastic investigation considers plastic strains. (See equation (3.1)) As a result, the displacements are larger than in the linear elastic case. The investigations using different element types are showing no significant changes.

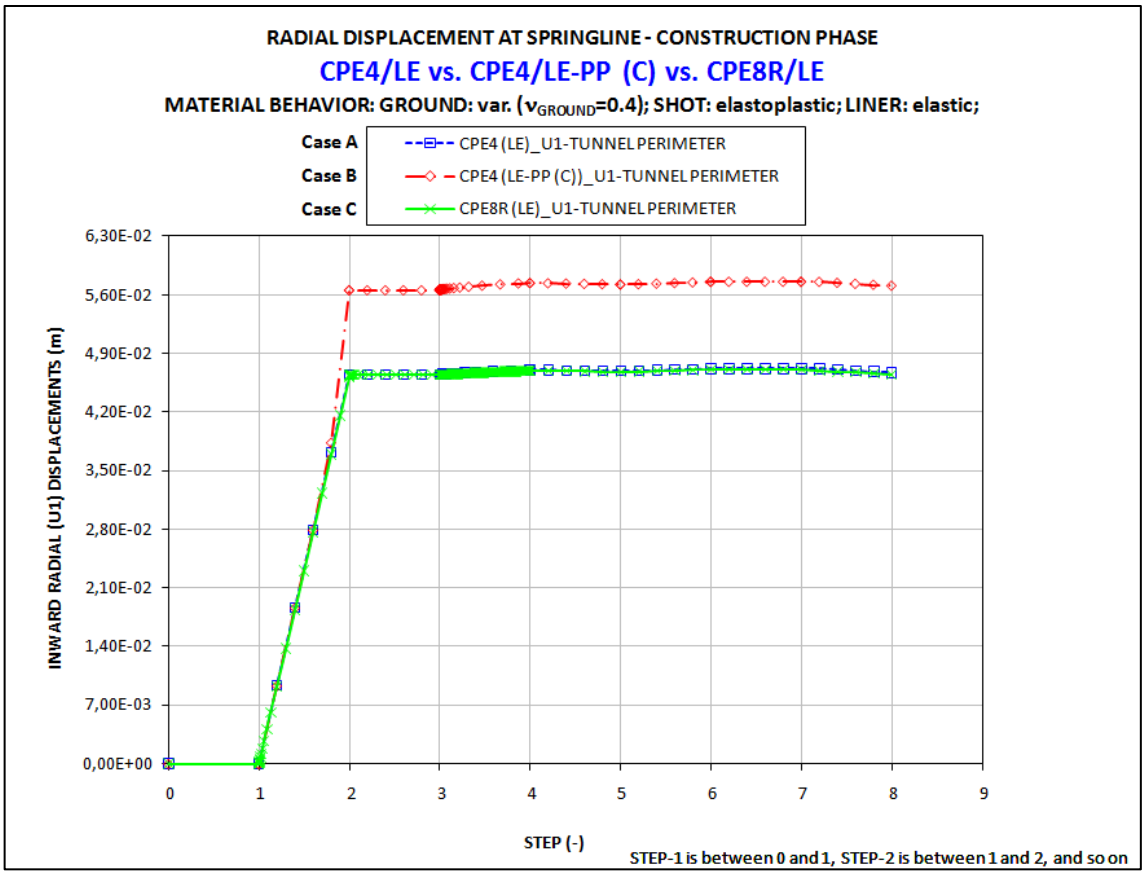

Fig. 4–4: Comparison of Case A (CPE4 elements & LE material behavior), Case B (CPE4 elements & LE-PP (C) material behavior) and Case C (CPE8R elements & LE material behavior); radial displacements of tunnel-perimeter at spring-line; results based on (C06+C12+C18);

Table 6 shows the values of the radial displacements at the spring-line at significant steps for the Cases A, B and C. The column “STEP 2”, “STEP 4”, “STEP 7” and “STEP 8” show the absolute horizontal displacements at the end of the calculation-steps and the columns “Δ” show the relative displacements between the steps.

There are two points of interests, which can be observed from Table 6:

- No plastic deformations of the ground occur after “STEP 4” (after first load reduction with shotcrete shell – see chapter 3.6.4). (Note that plastic deformations can only occur in Case B)
- After including the inner liner (“STEP 7”), the tunnel-perimeter moves radially outward at the spring-line (see Fig. 4–3).

Concerning plastic deformations (Table 6):

In column “Δ” between “STEP 2” and “STEP 4” can be seen that the greatest radial displacements occur in Case B (CPE4 & LE-PP (C)). This is caused by plastic deformations. The column “Δ” between “STEP 4” and “STEP 7” shows that all values are approximately equal and so it can be concluded that no plastic deformations after “STEP 4” occur.

Concerning relative displacements after the inner liner is included (Table 6):

Column "Δ" between "STEP 7" and "STEP 8" shows that all relative displacements have negative values. This means that the tunnel-perimeter at the spring-line moves radially outward (divergent deformation behavior – see Fig. 4–3). Note that this divergent deformation behavior is only relative and occurs only between "STEP 7" and "STEP 8". The absolute displacements of the tunnel-perimeter at the spring-line at the end of the calculation of the tunnel construction ("STEP 8") are positive and convergent (see Fig. 4–3).

Table 6: Comparison: Radial displacements at the spring-line at several steps – tunnel construction

ν_{GROUND} = 0.4	DISPLACEMENT AT TUNNEL-PERIMETER - U1 (m)						
	STEP 2	Δ	STEP 4	Δ	STEP 7	Δ	STEP 8
Case A: CPE4 (LE)	0.04644	*5.59E-04*	0.04699	*1.67E-04*	0.04717	*-4.58E-04*	0.04671
Case B: CPE4 (LE-PP (C))	0.05651	*8.68E-04*	0.05738	*1.49E-04*	0.05753	*-4.64E-04*	0.05706
Case C: CPE8R (LE)	0.04643	*4.88E-04*	0.04691	*1.59E-04*	0.04707	*-5.73E-04*	0.04649

Fig. 4–5 shows the plastic zone around the tunnel at the end of STEP 2. Note that the plastic zone is only in the vicinity of the spring-line.

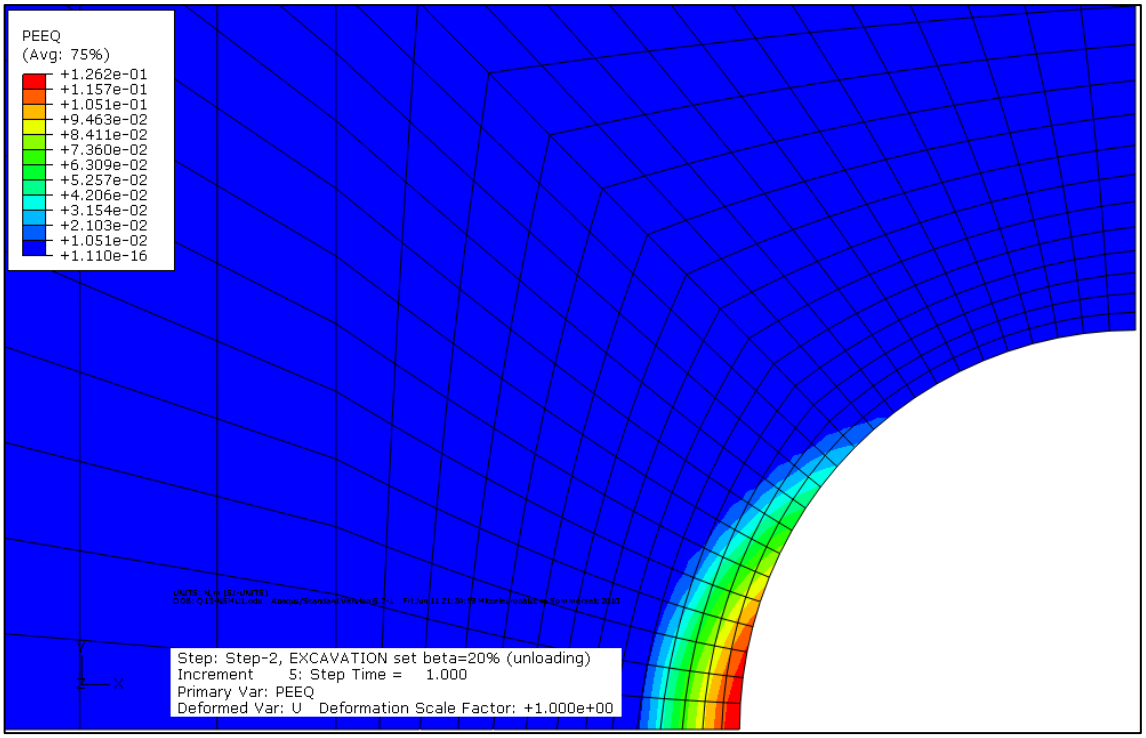

Fig. 4–5: Equivalent plastic strain at integration points – end of STEP 2, the plastic zone is only in the vicinity of the spring-line; result based on (C12)

4.2 Deterioration of the shotcrete shell

The evaluation of the deterioration of shotcrete is divided into three sub-chapters:

- Stress transfer from the shotcrete shell to the inner liner during the deterioration of shotcrete

- Investigation of the effects of element types (CPE4, CPE8R) and of material behavior (LE, LE-PP (C))
- Investigation of the effects of different deterioration processes of shotcrete

First, the effects of different element types and material behavior are investigated. The calculation can be divided into the same three cases as in chapter 4.1:

- Case A: Linear elastic material behavior using CPE4 elements
- Case B: Linearly elastic – perfectly plastic material behavior using CPE4 elements
- Case C: Linear elastic material behavior using CPE8R elements

The explanation of the abbreviations, which are used in the text or in the figures and not listed in the following, can be obtained from chapter 4.1 or from the table of abbreviations.

SCC	support characteristic curve – stresses in shotcrete shell; inner liner is not included in the calculation of these stresses; no deterioration simulated; only used for comparison reasons in Fig. 4–7;
SHOT	numerical model of the shotcrete shell
LINER	numerical model of the inner liner

Table 4 shows the values of the deterioration parameters and their value at each step.

4.2.1 Stress transfer from the shotcrete shell to the inner liner during the deterioration of shotcrete

Fig. 4–6 illustrates the stress distribution in the shotcrete shell and in the inner liner during deterioration of the shotcrete shell. The deterioration is simulated by a degradation of the Young's modulus. The stress distributions in Fig. 4–6 are calculated using a linear elastic material behavior and 4-node continuum plane strain elements (Case A).

Following the description of Fig. 4–6 in detail:

- Blue diamond (◊) curve: Stress state of the inner liner during degradation of the shotcrete.
- Red squared (□) curve: Stress state of the shotcrete shell during degradation of the shotcrete.
- Green crossed (x) curve: Based on a separate calculation where the inner liner is not included and the shotcrete is not deteriorated. All loads are beared by the shotcrete shell. In other words, the stresses of this support characteristic curve are the sum of the stresses in the shotcrete shell and the inner liner after tunnel construction.

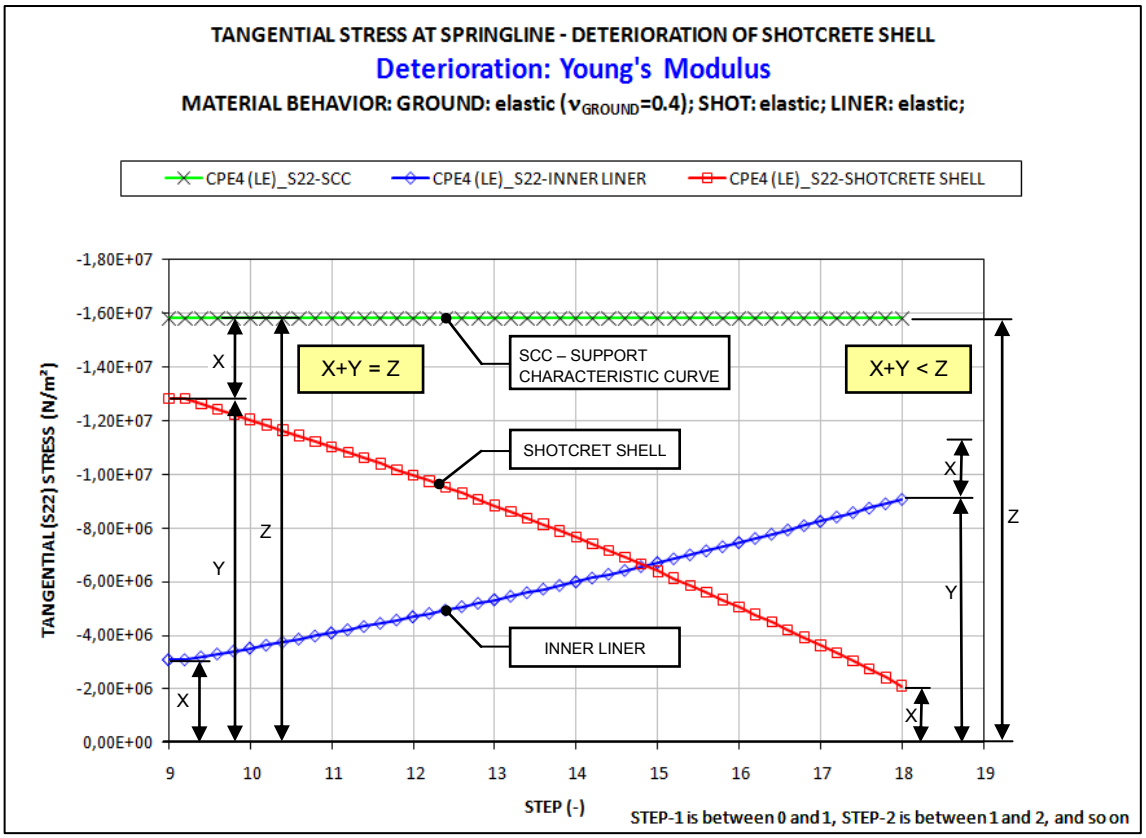

Fig. 4–6: Transfer of stresses from the shotcrete shell to the inner liner during deterioration of the shotcrete; deterioration caused by degradation of the Young's modulus of shotcrete; support characteristic curve is the sum of the stresses in the shotcrete shell and in the inner liner "Z=X+Y" after tunnel construction (STEP 9); a comparison of the stresses in the shotcrete shell and the inner liner to the support characteristic curve shows, that after deterioration of the shotcrete (STEP 18) less stresses exist in the support elements (shotcrete shell and inner liner) "Z>X+Y" than at the end of STEP 9; results based on (C02);

Generally, an increase of the stresses in the inner liner due to the deterioration of the shotcrete shell is obtained. Furthermore, the stresses in the shotcrete shell decrease more than the stresses in the inner liner increase. This can be seen by a comparison of the stresses after STEP 9 and STEP 18. If the stresses of the inner liner (X) and the shotcrete shell (Y) at STEP 9 are summed, the stresses are equal to the stresses of the support characteristic curve (Z). If this is done in STEP 19, the stresses in the shotcrete shell plus the stresses in the inner liner are less than the stresses of the support characteristic curve (Z > X + Y).

4.2.2 Investigation of the effects of element types and of material behavior

Fig. 4–7 shows a comparison of the effects of different element types and different material behaviors during the deterioration of the shotcrete:

- Case A: LE material behavior & CPE4 elements
- Case B: LE-PP (C) material behavior & CPE4 elements
- Case C: LE material behavior & CPE8R elements

The deterioration is simulated by a degradation of the Young's modulus.

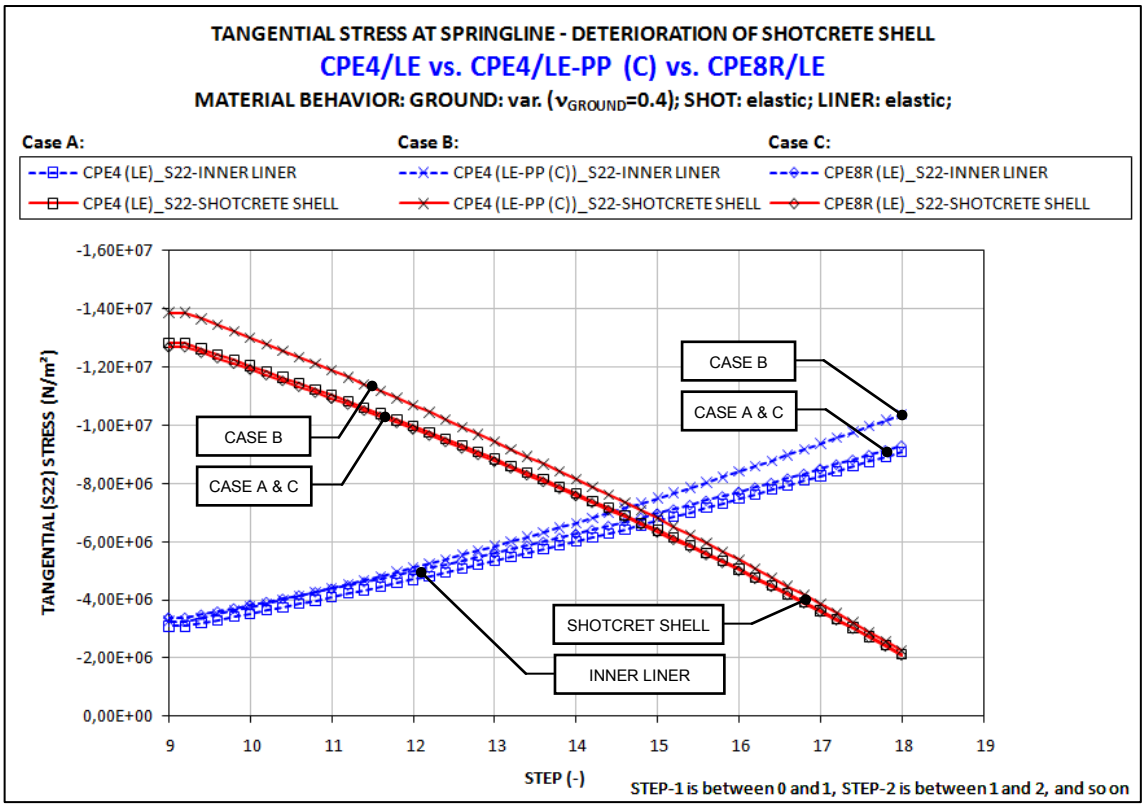

Fig. 4–7: Comparison of Cases A, B and C; tangential stresses in shotcrete shell and inner liner during deterioration of shotcrete; stresses at spring-line; deterioration caused by degradation of Young's modulus; results based on (C02+C08+C14);

Concerning the results of "Case B", the stresses in the shotcrete shell at the beginning of the deterioration process (STEP 9) are higher than the stresses in the shotcrete shell, which are calculated using "Case A or C". The higher stresses in "Case B" are caused by additional plastic deformations of the ground during the construction of the tunnel (see chapter 4.1 and Fig. 4–2). Furthermore, one can observe that at the end of the deterioration process (STEP 18), all stresses in the shotcrete shell are approximately equal (Case A, B & C).

Concerning the load transfer from the shotcrete shell to the inner liner, one obtains higher stresses in the inner liner at the end of the deterioration process (STEP 18) using a linearly elastic – perfectly plastic material behavior (Case B) compared to a linear elastic material behavior (Case A & C).

Table 7 shows the values of the radial displacements during deterioration at the spring-line for all three cases. The deterioration of the shotcrete, which is caused by degradation of the Young's modulus, starts at STEP 9 and ends at STEP 18. The absolute values for these steps are shown. The column "Δ" shows the relative displacements between STEP 9 and STEP 18. Slightly higher relative displacements can be obtained, using a LE-PP (C) material behavior, than using LE material behavior.

Table 7: Comparison of Cases A, B and C; radial displacements of tunnel-perimeter at spring-line before (STEP 9) and after (STEP 18); deterioration of shotcrete; degradation of E and f_C; inner liner is considered; results based on (C02+C08+C14)

ν_{GROUND} = 0.4	DISPLACEMENT – TUNNEL-PERIMETER (m)		
	STEP 9	STEP 18	Δ
Case A: CPE4 (LE)	4.67E-02	4.75E-02	8.01E-04
Case B: CPE4 (LE-PP (C))	5.71E-02	5.80E-02	9.50E-04
Case C: CPE8R (LE)	4.65E-02	4.73E-02	8.14E-04

Considering the stress transfer shown in Fig. 4–7 and the results of Table 7, one can speculate that the released stresses of the shotcrete shell, which are caused by deterioration of the shotcrete, are redistributed to the surrounding ground and the inner liner.

Fig. 4–8, Fig. 4–9 and Fig. 4–10 show the stresses along the circumference of the inner liner. These results are based on the deterioration of the Young's modulus of the shotcrete shell. The dashed lines represent the stresses at the outer boundaries, and the solid lines show the stresses at the inner boundaries of the inner liner. These figures show three different stages of deterioration. The green square (□) lines show the stresses at 10% deterioration, the blue diamond (◊) lines at 50% deterioration, and the red triangular (Δ) lines at 90% deterioration.

Fig. 4–8 shows the stresses, which are obtained by a model based on CPE4 elements and a linear elastic material behavior (Case A). Comparing the stress distributions in the inner liner at a deterioration of 10% with the stress distribution at a deterioration of 90%, one can recognize an increase of the thrusts at the spring-line as well as at the tunnel-crown. The increase of the thrust at the spring-line may be a little bit higher than at the tunnel-crown. Furthermore, one can conclude that the moments in the inner liner change slightly. (See also chapter 4.2.3; Fig. 4–28)

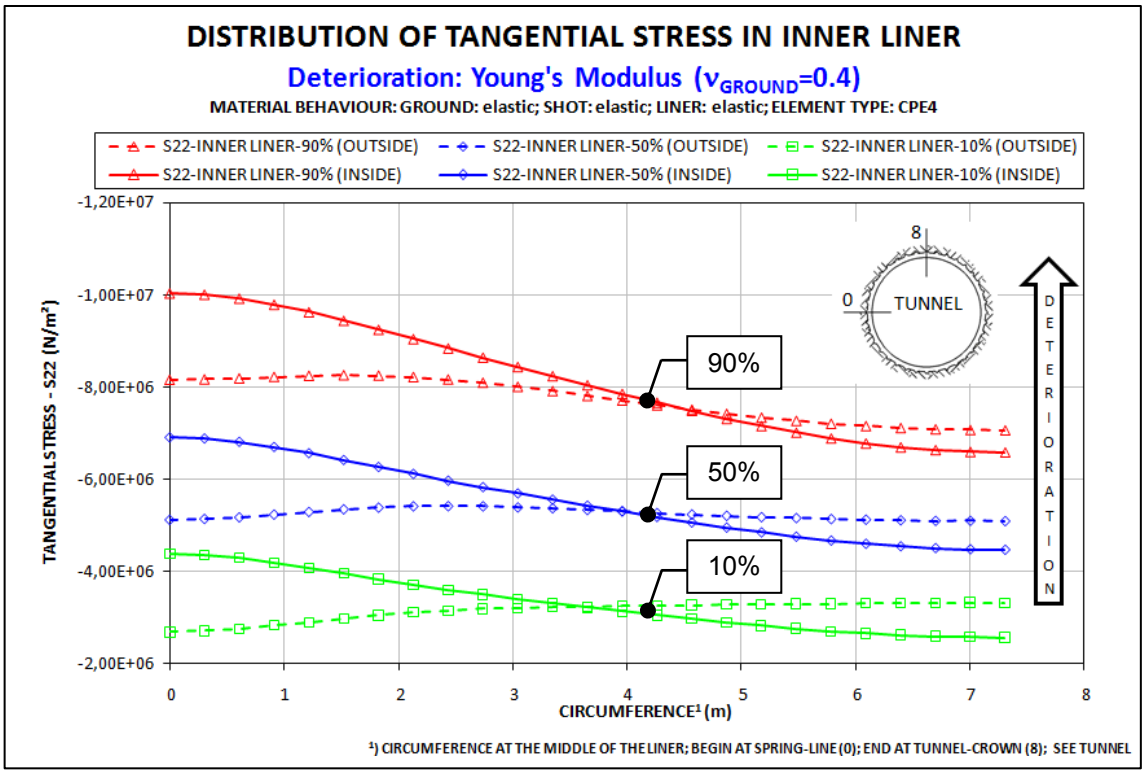

Fig. 4–8: Stresses at the outside and inside of the inner liner for three deterioration steps (10%, 50%, 90%); deterioration caused by degradation of Young's modulus; Case A (CPE4 elements, LE material behavior); results based on (C02)

Fig. 4–9 shows the stresses, which are obtained with a model based on CPE4 elements and a linearly elastic – perfectly plastic material behavior (Case B). The difference between the stresses at the spring-line and at the tunnel-crown at a deterioration of 10% is smaller than at a deterioration of 90%. The maximum stress at a deterioration of 90% along the circumference of the liner changes two times from the inside to the outside of the liner. The change of the maximum stress can be explained by a change of the moment distribution. Additional investigations of this behavior have to be carried out to make more definite statements.

Fig. 4–10 shows the stresses, obtained by a model based on CPE8R elements and linear elastic material behavior (Case C). The main difference between this (Case C) and the other investigations (Cases A and B) is in the usage of 8-node elements instead of 4-node elements. The stresses along the inner liner, which are obtained in Case C are slightly higher than the stresses, which are obtained in Case A.

Generally, the stress distribution based on a linear elastic material behavior is similar using 4-node elements or 8-node elements. However, additional investigations concerning a linearly elastic – perfectly plastic material behavior should be performed.

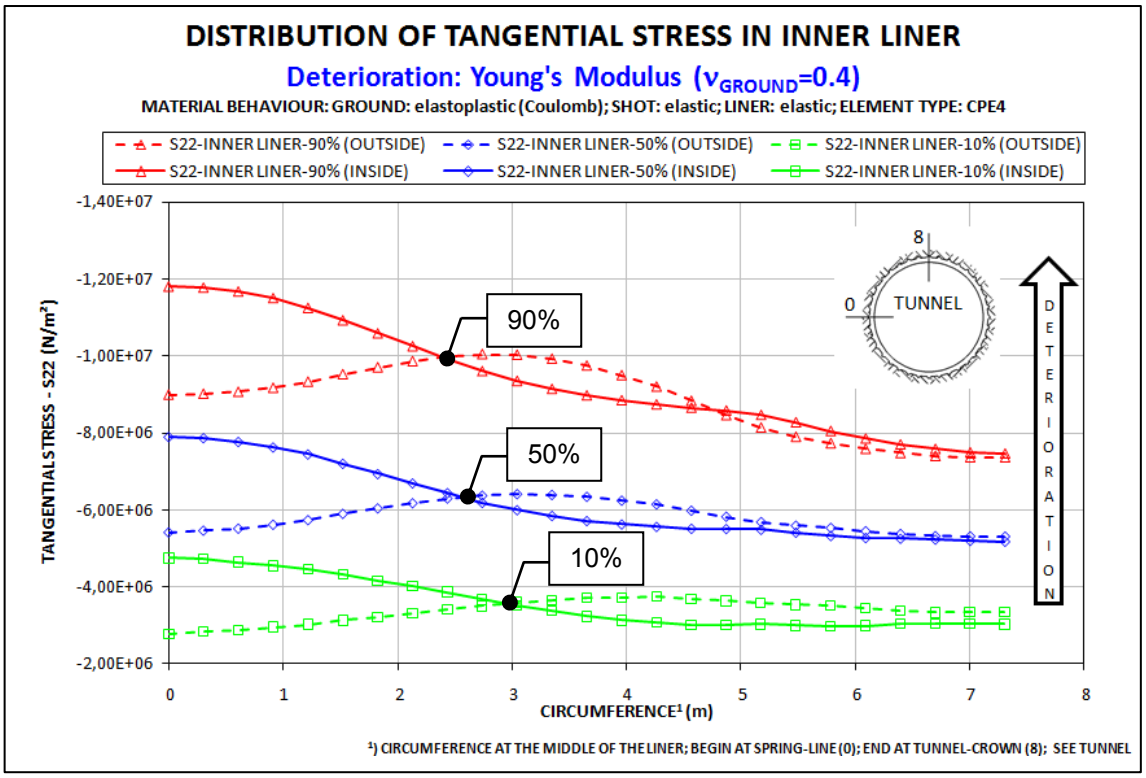

Fig. 4–9: Stresses at the outside and inside of the inner liner for three deterioration steps (10%, 50%, 90%); deterioration caused by degradation of Young's modulus; Case B (CPE4 elements, LE-PP material behavior); results based on (C08)

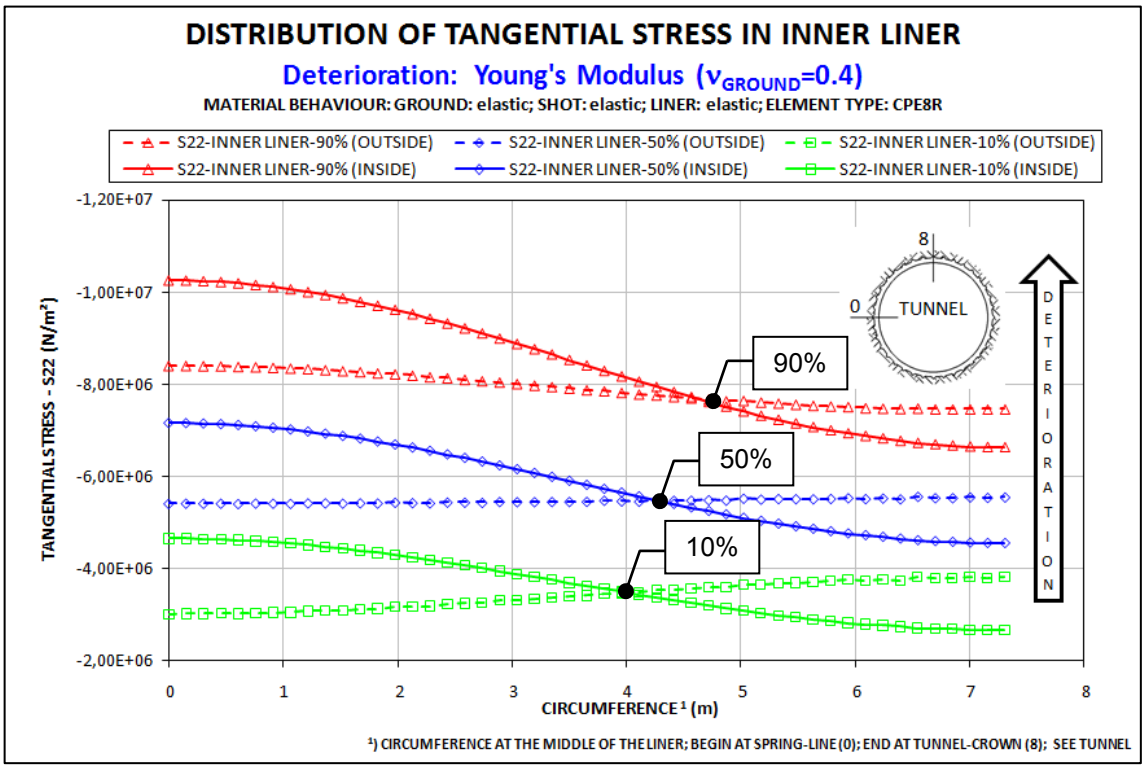

Fig. 4–10: Stresses at the outside and inside of the inner liner for three deterioration steps (10%, 50%, 90%); deterioration caused by degradation of Young's modulus; Case C (CPE8R elements, LE material behavior); results based on (C14)

4.2.3 Investigation of the effects of different deterioration processes of shotcrete

Only results for Case A (CPE4 elements, LE material behavior) are discussed here. The results of the other cases can be seen in appendix A.

As mentioned in chapter 3.7, this investigation uses three different deterioration processes: First, the Young's modulus (E) is degraded, second, the compressive strength (f_C) is degraded, and third, the Young's modulus and the compressive strength (E & f_C) are degraded, simultaneously.

Following the classification of the three deterioration processes (based on Case A) is outlined:

Case A-1:

- Deterioration of the Young's modulus (E)
- Fig. 4–11

Case A-2:

- Deterioration of the compressive strength (f_C)
- Fig. 4–12

Case A-3:

- Simultaneous deterioration of the Young's modulus and the compressive strength (E & f_C)
- Fig. 4–13

Fig. 4–14 illustrates that the stresses in Case A-1 and Case A-3 are exactly the same. In other words, the deterioration of shotcrete caused by lowering the compressive strength has no effect on the combined deterioration in Case A-3. Thus, for Case A-3 the decisive factor to simulate the deterioration of shotcrete is only the Young's modulus.

Now the question arises, can the compressive strength also become the decisive factor in Case A-3? Fig. 4–15 illustrates that the stresses in the inner liner in Case A-1 are always higher than the stresses in the inner liner in Case A-2. Accordingly, the stresses in the shotcrete shell in Case A-1 are always lower than the stresses in the shotcrete shell in Case A-2. This leads to the assumption that the compressive strength could become the decisive factor if the stresses in the inner liner in Case A-1 are lower than in Case A-2, or if the stresses in the shotcrete shell in Case A-1 are higher than in Case A-2, which has to be verified in future investigation.

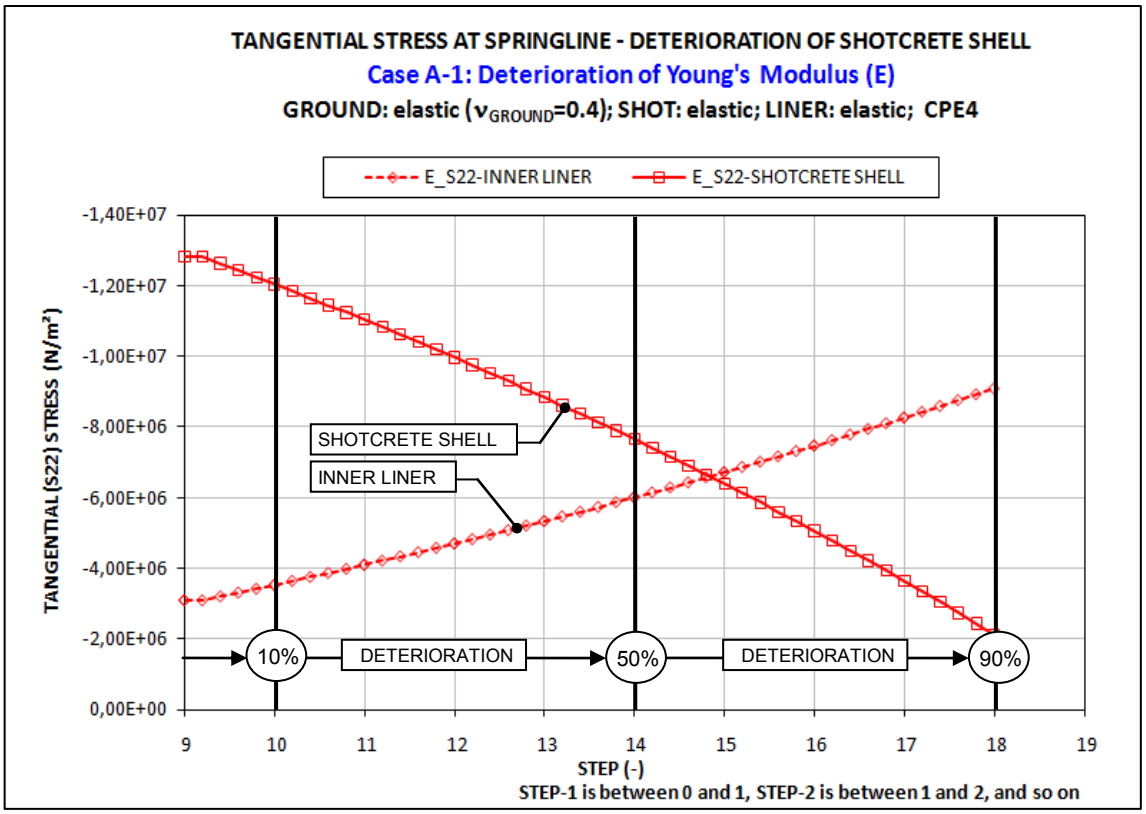

Fig. 4–11: Case A-1; stress transfer from shotcrete shell to inner liner, caused by deterioration of shotcrete; deterioration caused by degradation of Young's modulus; results based on (C02)

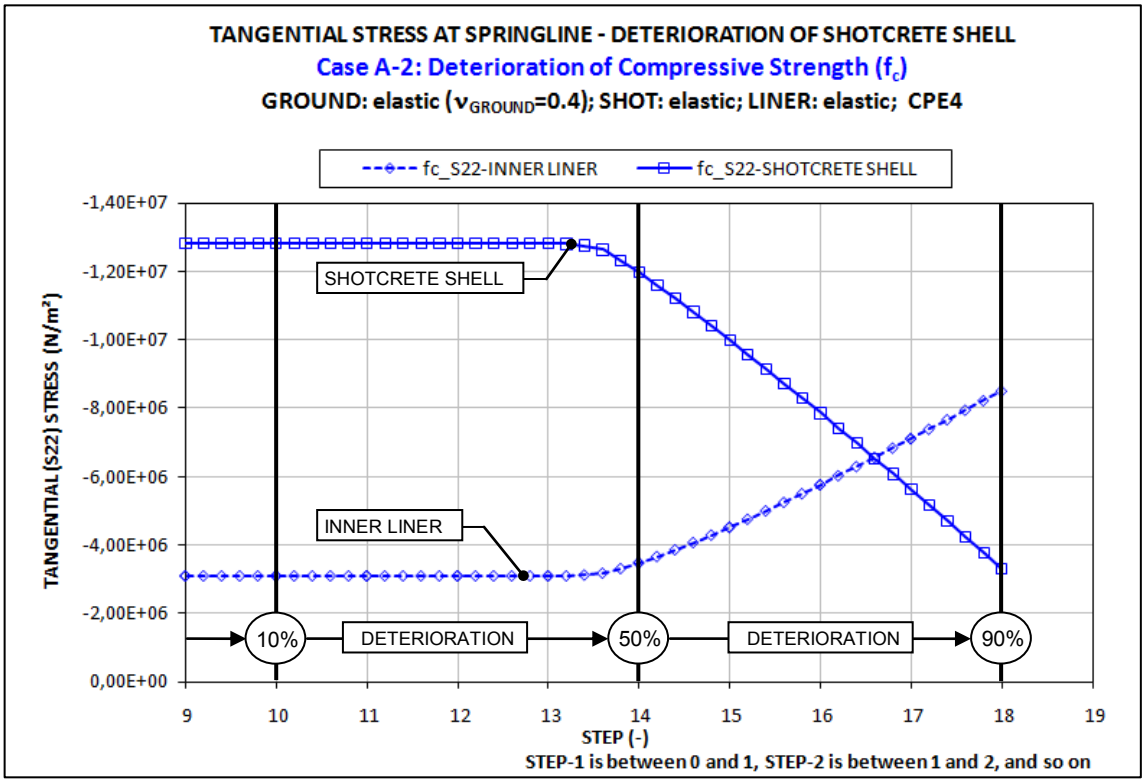

Fig. 4–12: Case A-2; stress transfer from shotcrete shell to inner liner, caused by deterioration of shotcrete; deterioration caused by degradation of compressive strength; results based on (C04)

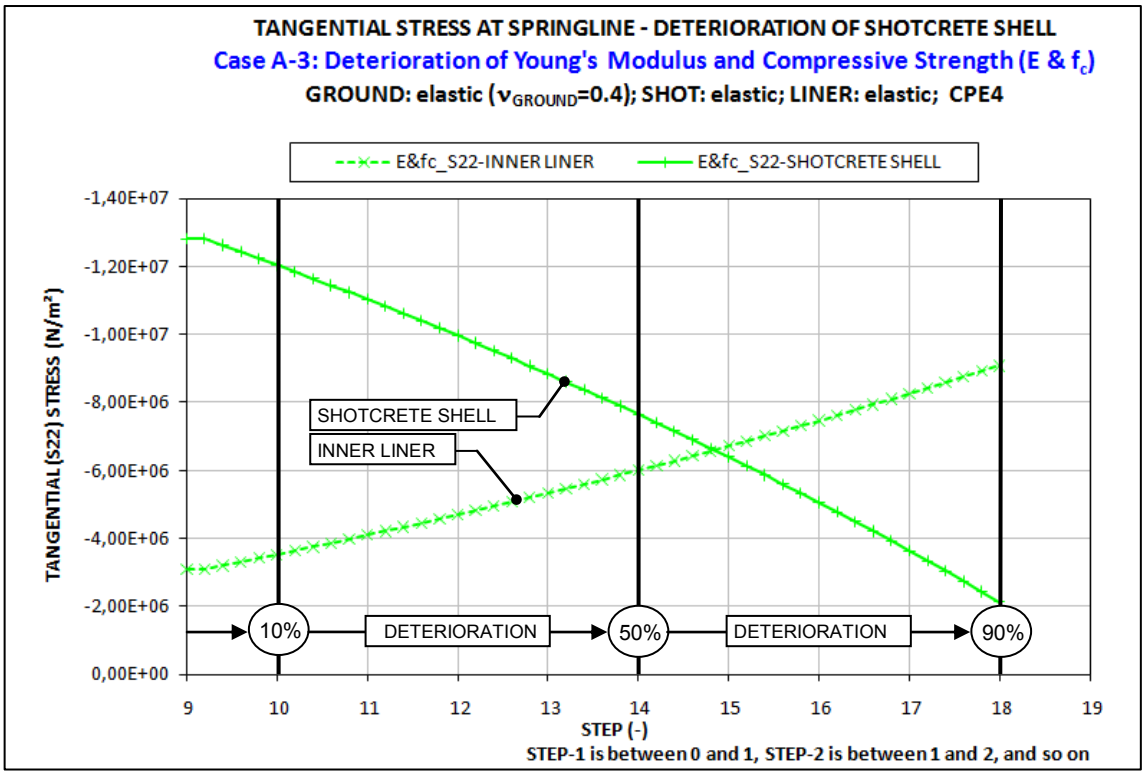

Fig. 4–13: Case A-3; stress transfer from shotcrete shell to inner liner, caused by deterioration of shotcrete; deterioration caused by degradation of E & f_C; results based on (C06)

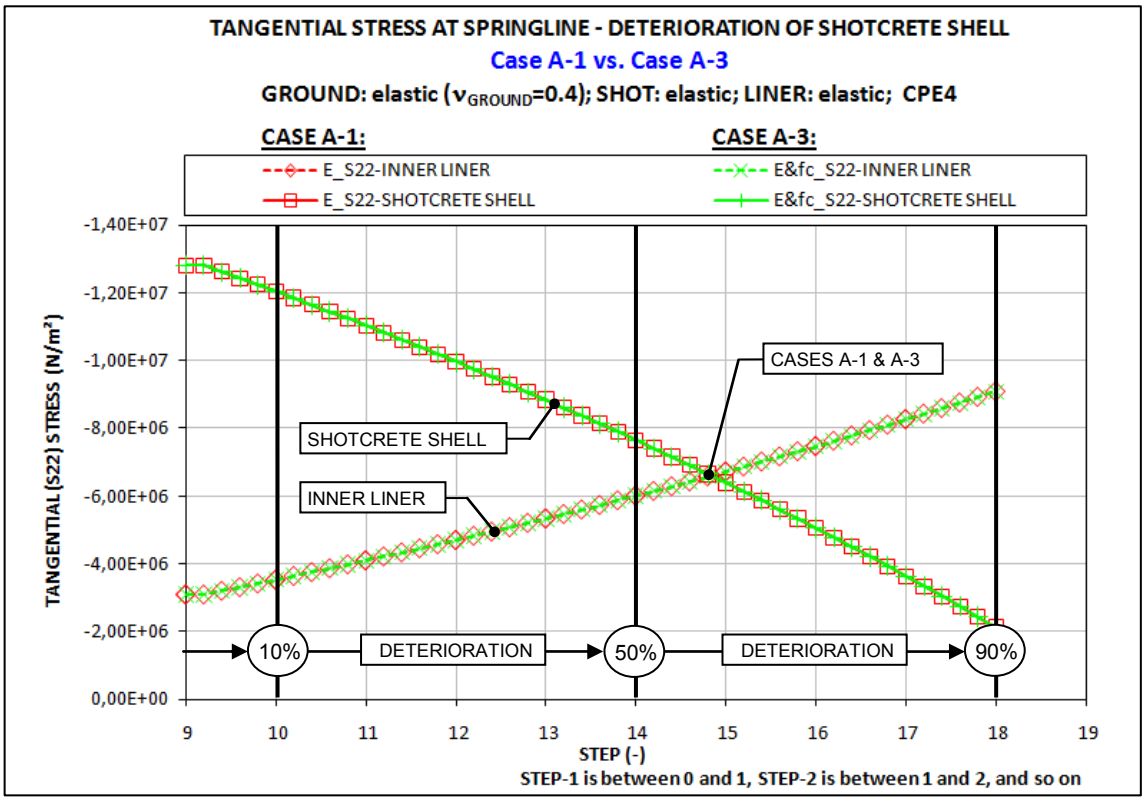

Fig. 4–14: Comparison of Cases A-1 and A-3; transfer of tangential stresses from shotcrete shell to inner liner caused by deterioration of the shotcrete; results based on (C02+C06)

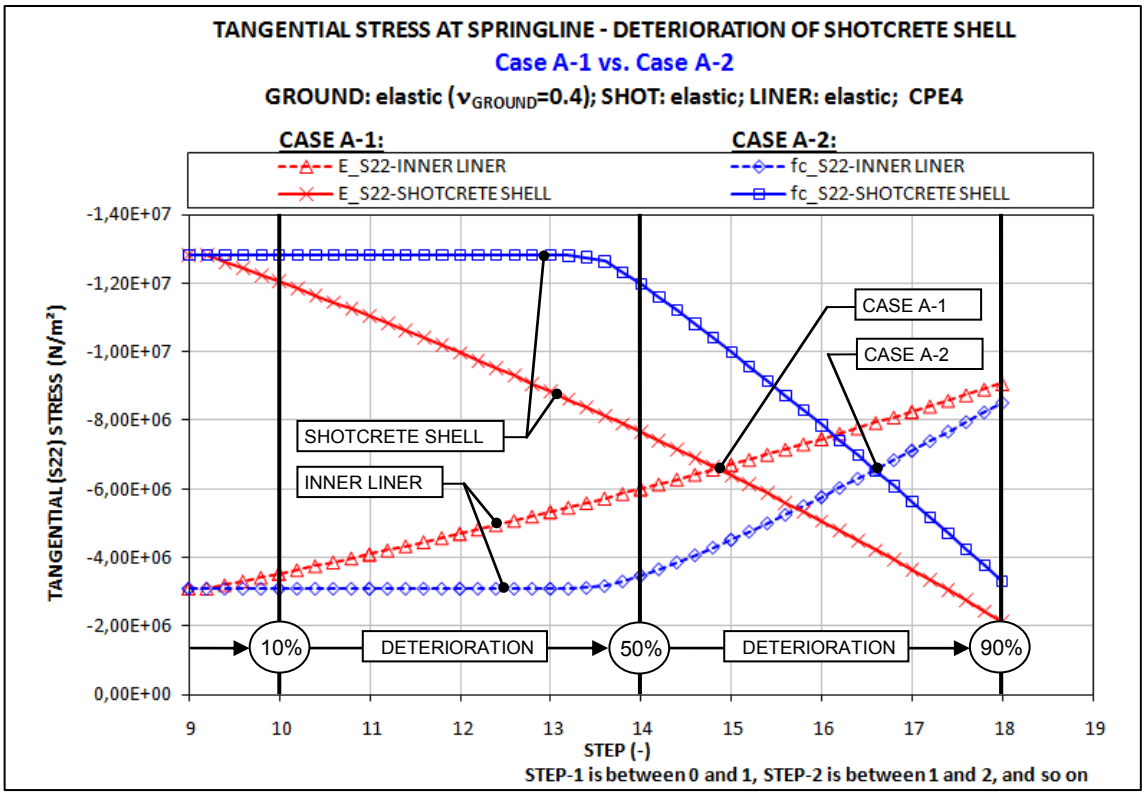

Fig. 4–15: Comparison of Cases A-1 and A-2; transfer of tangential stresses from shotcrete shell to inner liner caused by deterioration of the shotcrete; results based on (C02+C04)

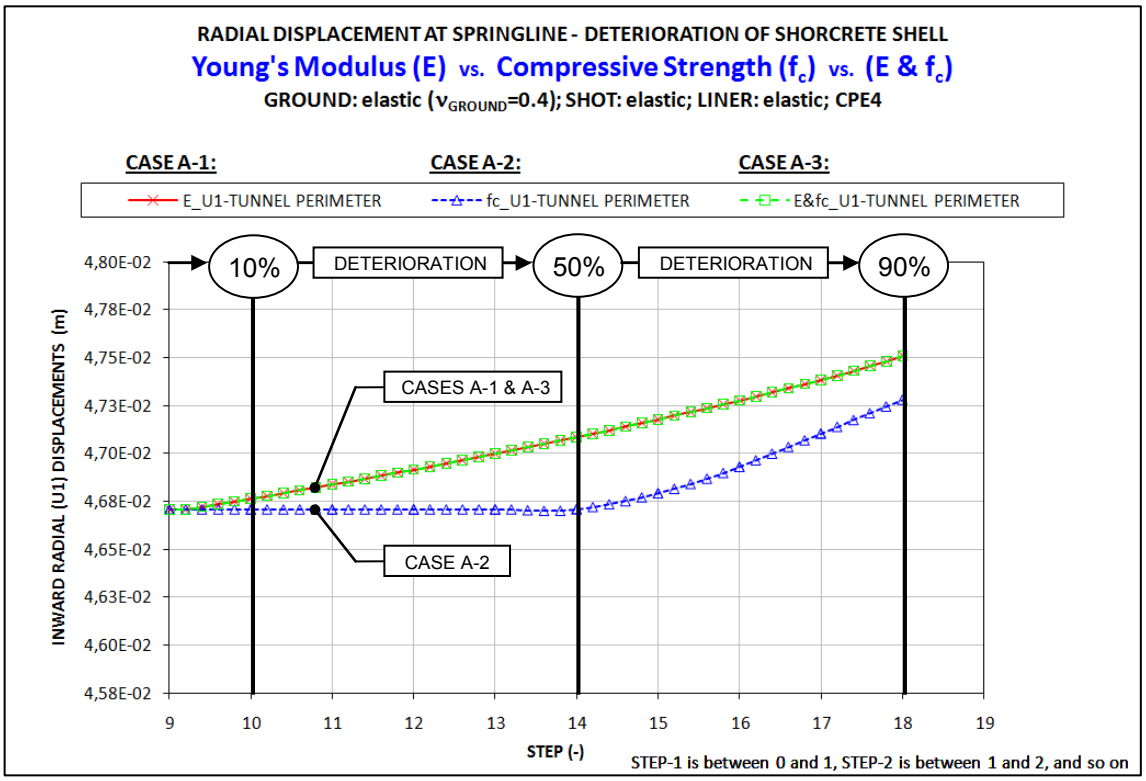

Fig. 4–16: Comparison of Cases A-1, A-2 and A-3; radial displacements at the spring-line caused by deterioration of shotcrete; positive displacements = inward movement; results based on (C02+C04+C06)

Fig. 4–16 shows the corresponding displacements of the tunnel-perimeter at the spring-line in these three cases. A behavior similar to the stresses in the inner liner can be obtained in all three cases. Considering Case A-2, between STEP 9 and STEP 14

the displacements are nearly zero. Between 50% and 90% deterioration, the tunnel-perimeter moves inward. The displacements of Cases A-1 and A-3 are equal. The tunnel-perimeter moves over all steps at a constant rate inward (Cases A-1 and A-3).

Stress distribution along the circumference of the shotcrete shell and the inner liner

Fig. 4–17 shows the stresses in the shotcrete shell along the circumference. These results are based on the combined system, ground plus shotcrete shell plus inner liner, and on the deterioration of the Young's modulus and compressive strength (Case A-3). First, a comparison of the stress distributions at deterioration levels of 10%, 50% and 90% is presented. Note that the deterioration in the combined case is equal to the deterioration of the Young's modulus (Case A-1 = Case A-3).

For a deterioration of 10%, higher stresses in the shotcrete shell are obtained at the spring-line than at the tunnel-crown. For a deterioration of 90%, the stresses in the shotcrete shell are at a lower level than at a deterioration of 10%, and the stresses at the spring-line are approximately equal to the stresses at the tunnel-crown. This means that the stresses at the spring-line decrease more significantly than at the tunnel-crown.

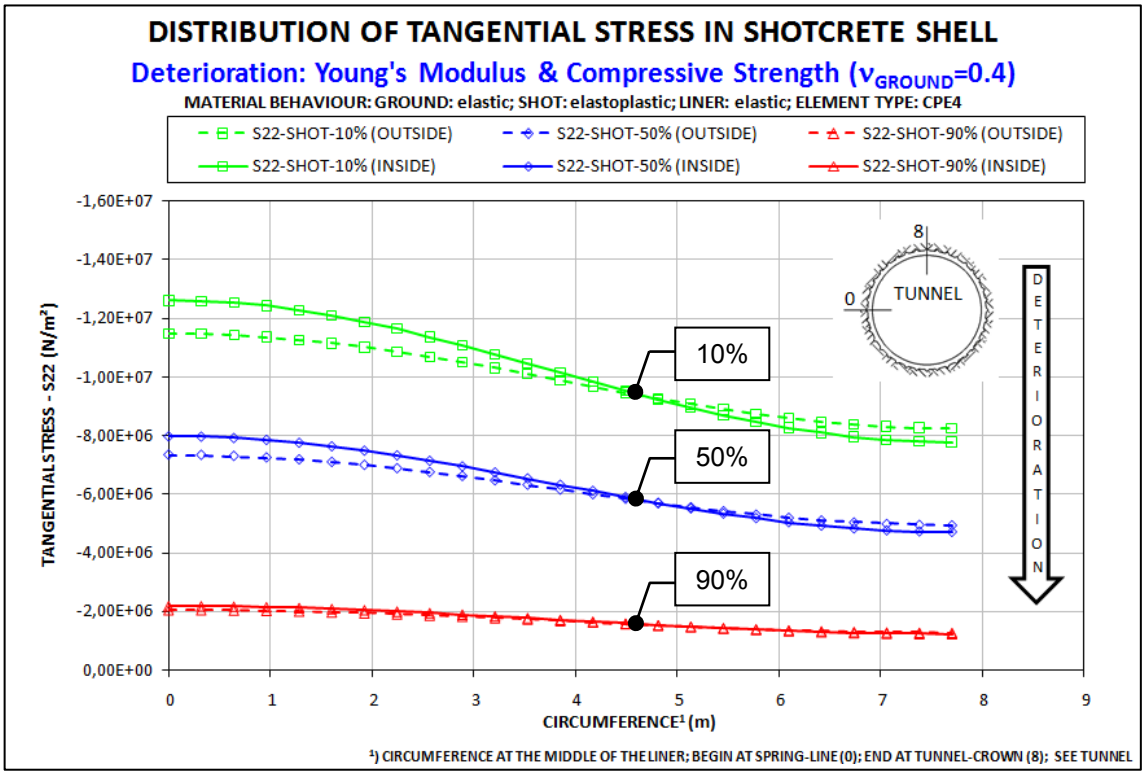

Fig. 4–17: Stresses at the outside and inside of the shotcrete shell for three deterioration steps (10%, 50%, 90%); deterioration caused by simultaneously degrading Young's modulus and compressive strength (Case A-3); (results equal to Case A-1); results based on (C06)

Fig. 4–18 shows the corresponding stresses along the circumference of the inner liner. For a deterioration of 10%, higher outside stresses were obtained at the tunnel-crown than at the spring-line. However, for a deterioration of 90%, the outside stresses at the spring-line are higher than the outside stresses at the tunnel-crown. The stresses at the inside of the inner liner at the spring-line are always higher than at the tunnel-crown.

Generally, during the deterioration of the shotcrete, a larger increase of the stresses in the inner liner at the spring-line than at the tunnel-crown can be recognized. Moreover, at the spring-line the stresses at the inside of the inner liner are higher than at the outside. In contrast to the tunnel-crown, the outside stresses are higher than the inside ones. An interpretation of these results follows in chapter 5.

Fig. 4–19 shows the stresses along the circumference of the shotcrete shell for the deterioration of the compressive strength. The stress distribution at a deterioration of 10% is similar to the 10% deterioration of the combined case (Fig. 4–17). The stress distribution in the shotcrete shell at a deterioration of 90% is uniform, i.e. the stresses at the spring-line are equal to the stresses at the tunnel-crown. The main decrease of the stresses in the shotcrete shell occurs between 50% and 90% deterioration.

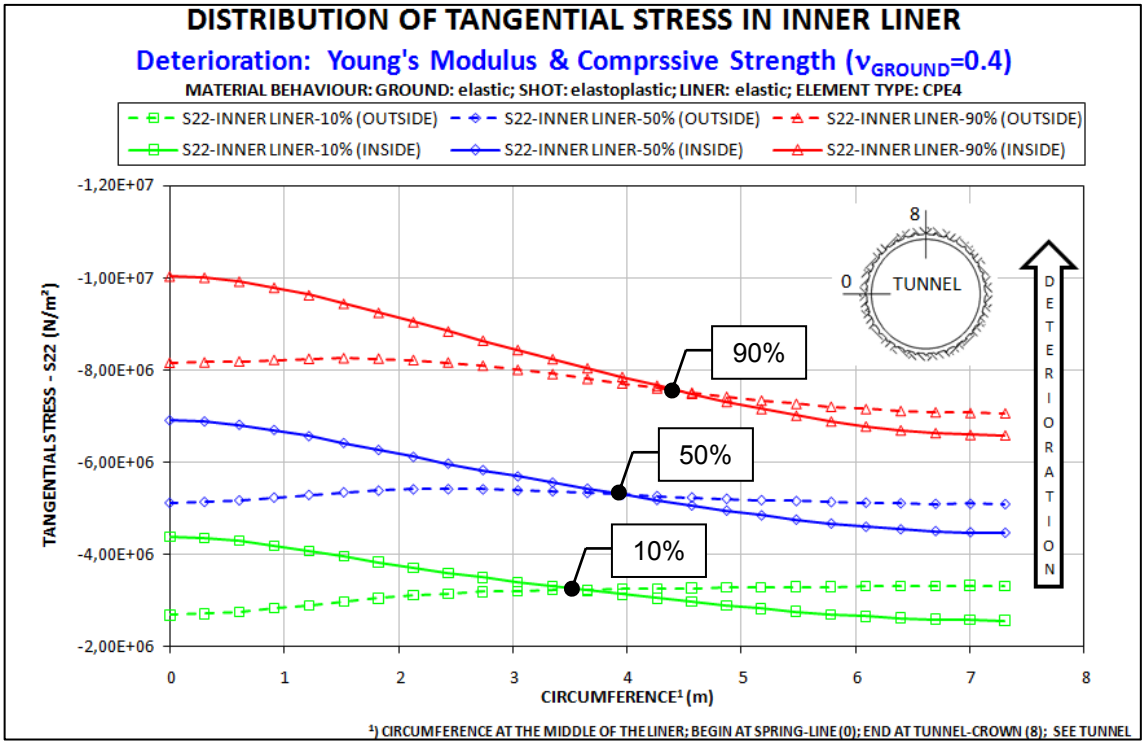

Fig. 4–18: Stresses at the outside and inside of the inner liner for three deterioration steps (10%, 50%, 90%); deterioration caused by simultaneously degrading Young's modulus and compressive strength (Case A-3); (results equal to Case A-1); results based on (C06)

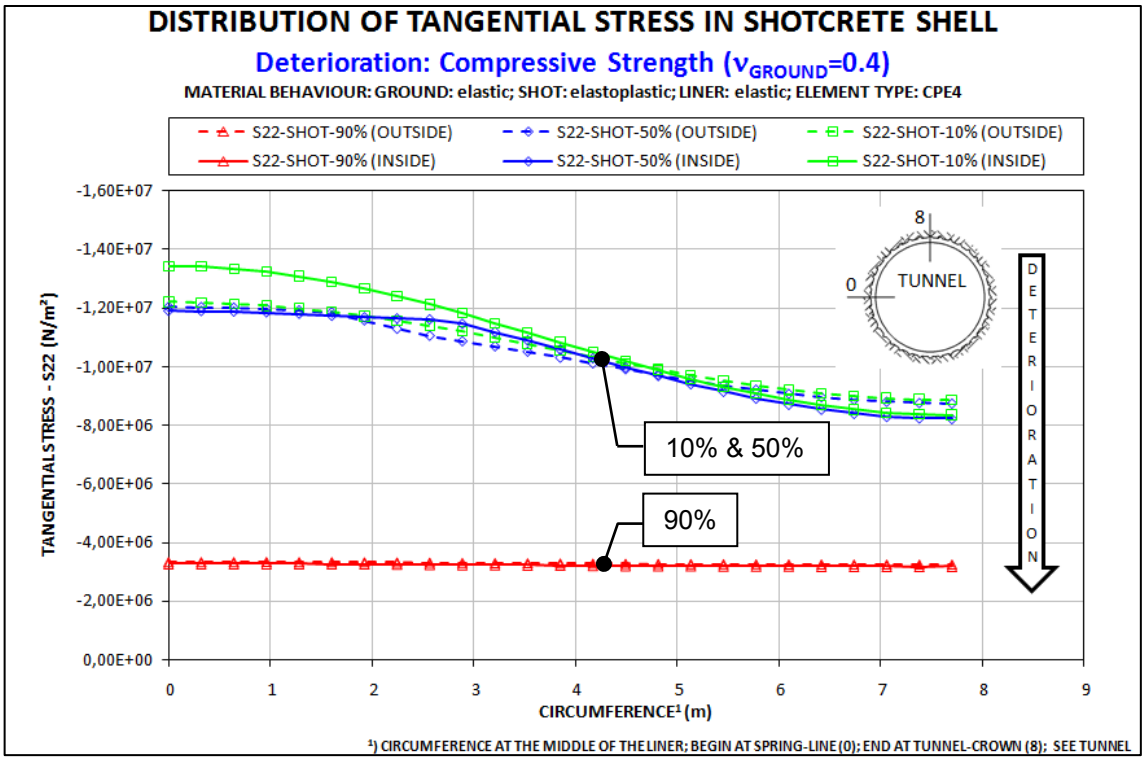

Fig. 4–19: Stresses at the outside and inside of the shotcrete shell for three deterioration steps (10%, 50%, 90%); deterioration caused by degrading compressive strength (Case A-2); results based on (C04)

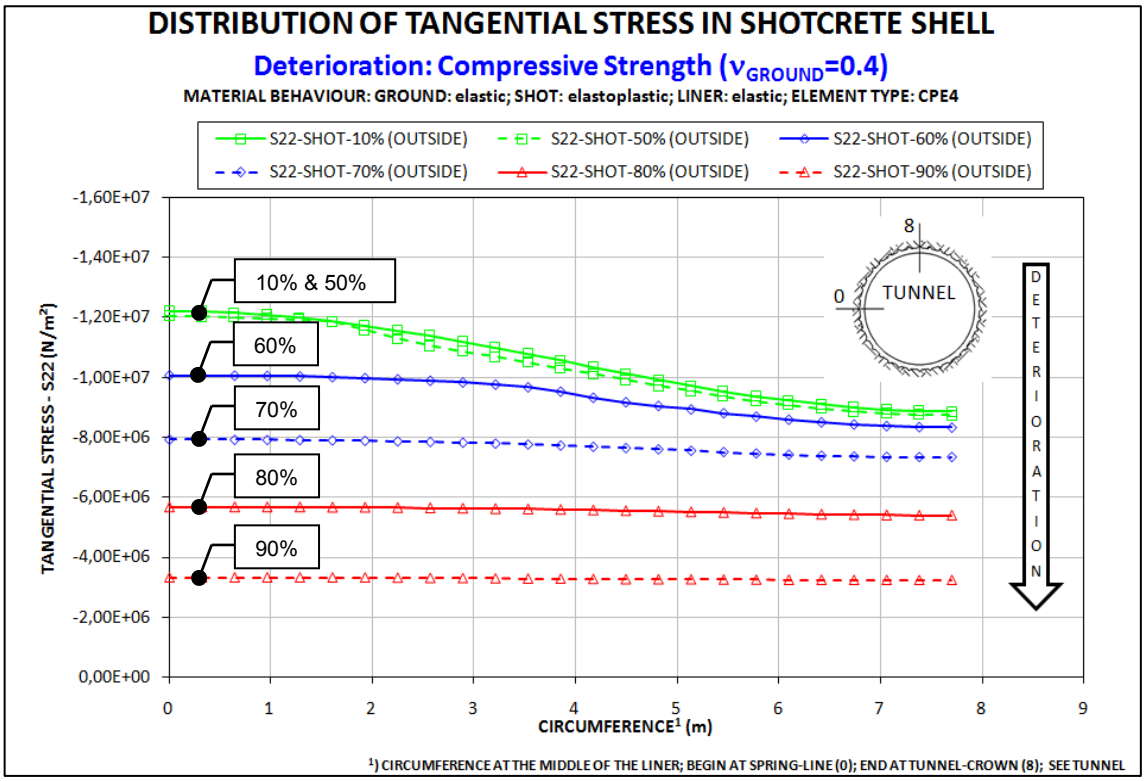

Fig. 4–20: Stresses at the outside of the shotcrete shell for several deterioration steps (10%, 50%, 60%, 70%, 80%, 90%); deterioration caused by degradation of compressive strength (Case A-2); results based on (C04)

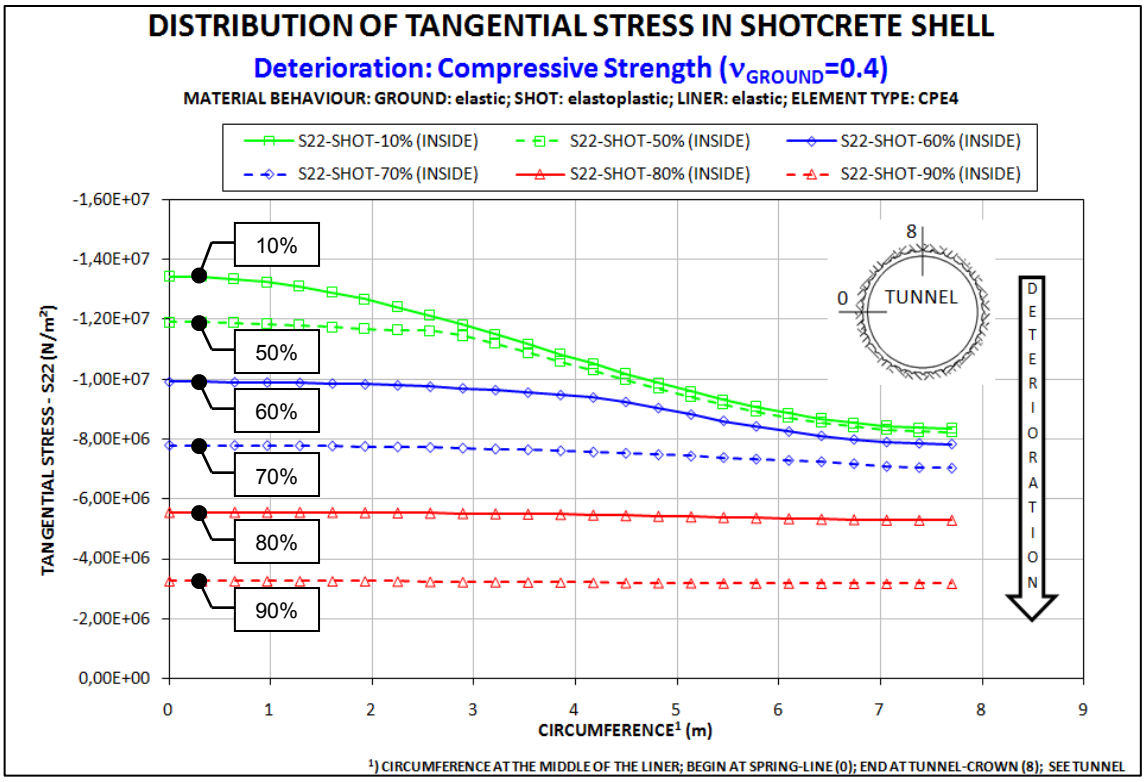

Fig. 4–21: Stresses at inside of the shotcrete shell for several deterioration steps (10%, 50%, 60%, 70%, 80%, 90%); deterioration caused by degradation of compressive strength (Case A-2); results based on (C04)

Comparing Fig. 4–17 to Fig. 4–19 one can observe that an exact uniform stress distribution in the shotcrete shell is only reached by degradation of the compressive strength (Case A-2).

Fig. 4–20 and Fig. 4–21 investigate the degradation of the compressive strength of the shotcrete shell in steps of 10%, from 50% to 90% deterioration. Specifically, the stress distribution at the outside of the shotcrete shell is shown in Fig. 4–20, and the stress distribution at the inside is shown in Fig. 4–21.

Fig. 4–22 shows the stresses along the circumference of the inner liner. These results are based on the deterioration of the compressive strength. Between 10% and 50% deterioration of the shotcrete, nearly no rise of the stresses in the inner liner can be observed. To investigate the stress distribution between 50% and 90% deterioration in more detail, Fig. 4–23 shows the stresses at the outside of the inner liner, and Fig. 4–24 shows the stresses at the inside of the inner liner. Note that the deterioration between 50% and 90% is shown in steps of 10%.

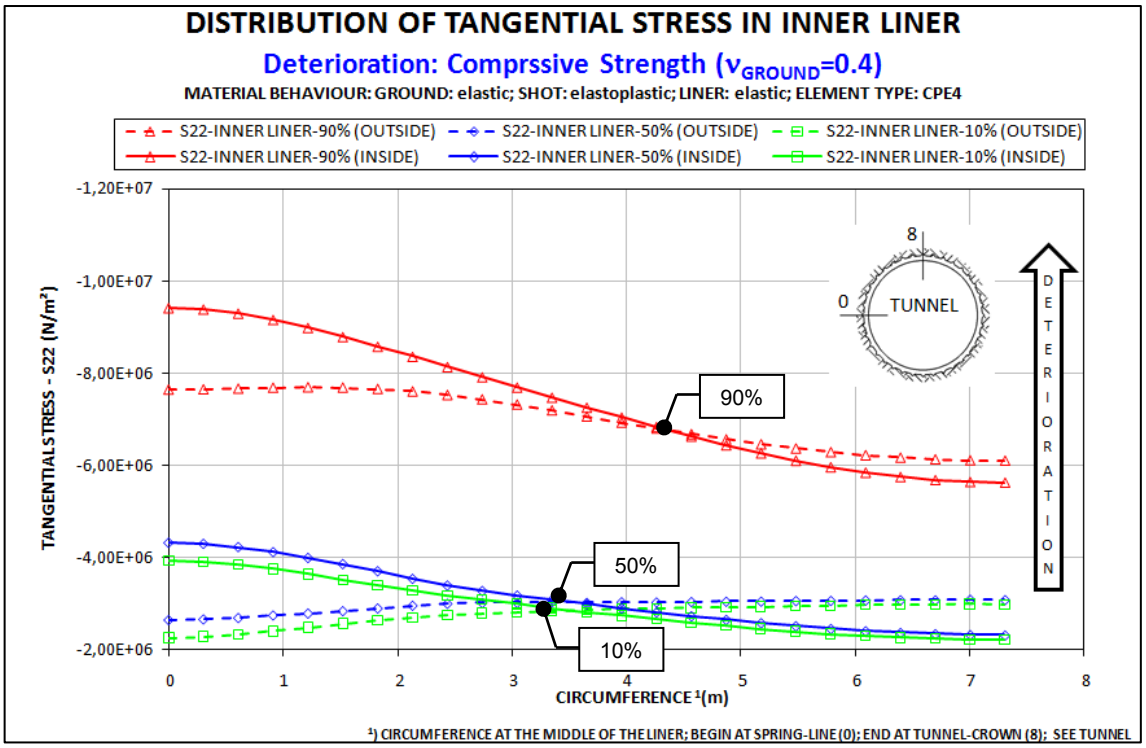

Fig. 4–22: Stresses at the outside and inside of the inner liner for three deterioration steps (10%, 50%, 90%); deterioration caused by degradation of compressive strength (Case A-2); results based on (C04)

From zero deterioration to a deterioration of 50%, the stresses at the outside of the inner liner at the spring-line are less than at the tunnel-crown (Fig. 4–23). At a deterioration of 60%, the stresses at the spring-line are approximately equal to the stresses at the tunnel-crown. At a deterioration of 70% the stresses at the spring-line are higher than the stresses at the tunnel-crown. Note that after a deterioration of 70% the stresses increase at the spring-line by the same amount as at the tunnel-crown. In other words, a more significant increase of the stresses at the spring-line, compared to the tunnel-crown, can only be observed at the beginning of the deterioration process.

Fig. 4–24 shows that the stresses at the inside of the inner liner at the spring-line are always higher than at the tunnel-crown. Furthermore, one can observe a higher increase of the stresses at the spring-line at the beginning of the deterioration process.

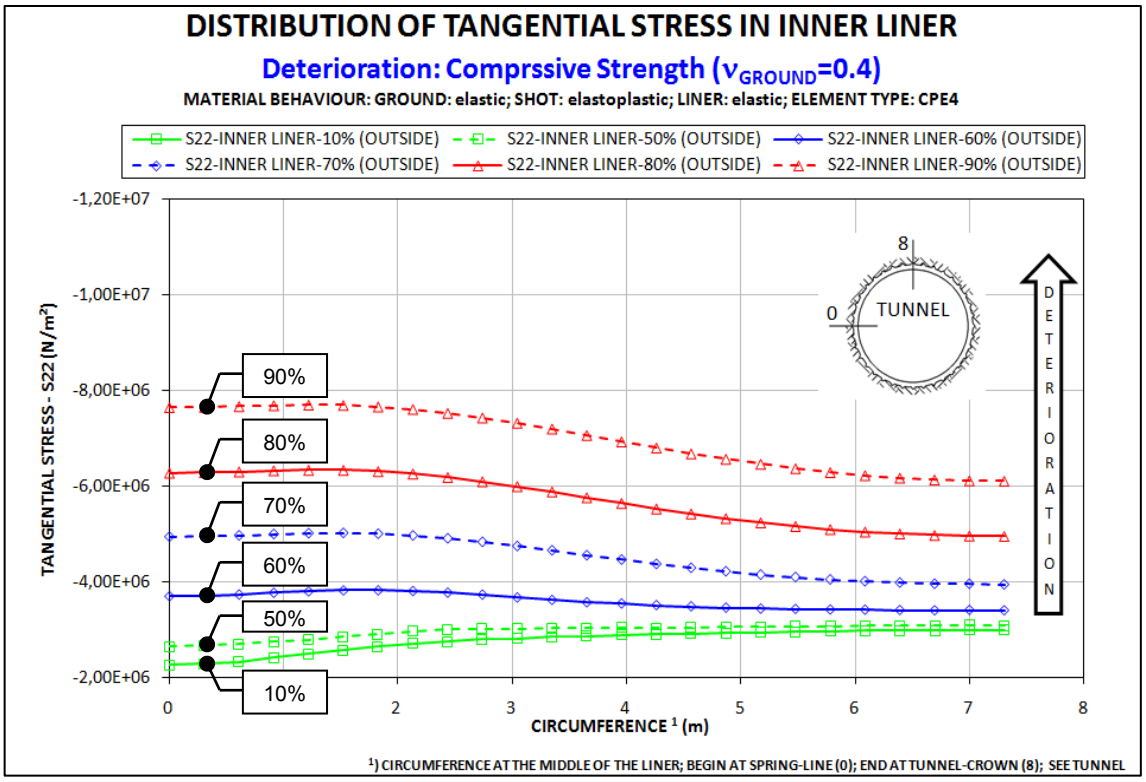

Fig. 4–23: Stresses at the outside of the inner liner for several deterioration steps (10%, 50%, 60%, 70%, 80%, 90%); deterioration caused by degradation of compressive strength (Case A-2); results based on (C04)

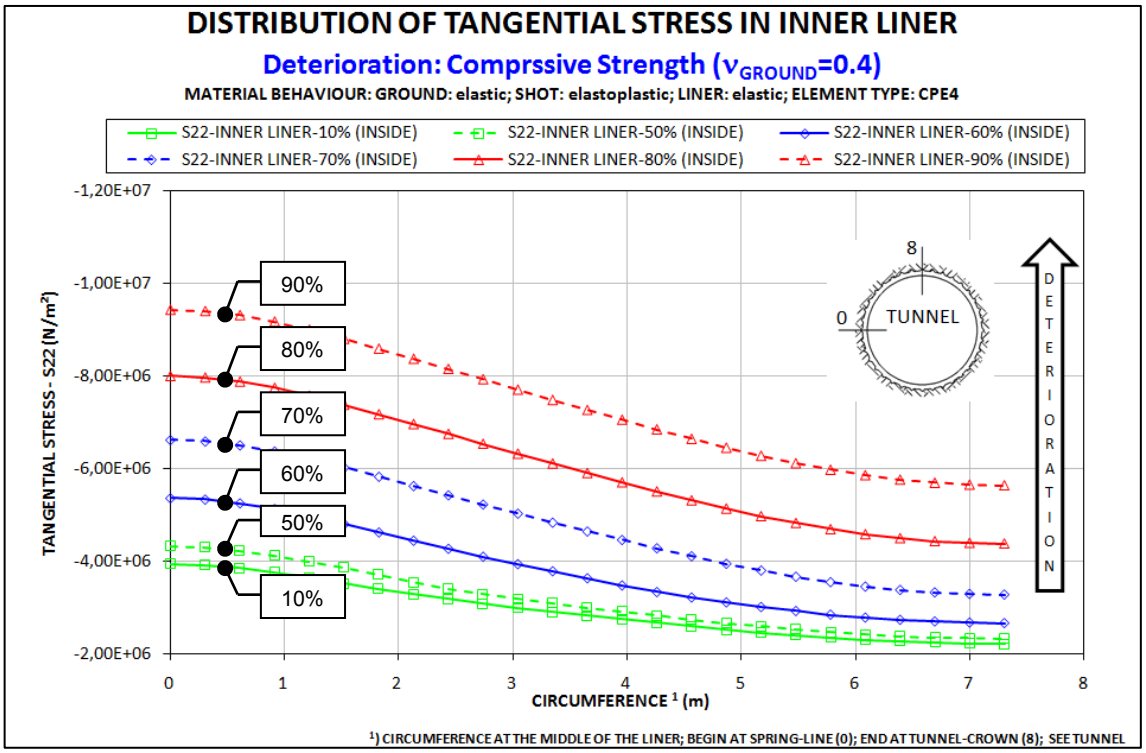

Fig. 4–24: Stresses at the inside of the inner liner for several deterioration steps (10%, 50%, 60%, 70%, 80%, 90%); deterioration caused by degradation of compressive strength (Case A-2); results based on (C04)

Thrusts and moments:

Based on the stress distributions along the shotcrete shell and inner liner, the thrusts and moments along the circumference of the support elements (shotcrete shell and inner liner) are investigated. The same three deterioration levels as above (10%, 50% and 90%) are considered. All graphs, which are subsequently represented, are based on a deterioration of the shotcrete caused by degradation of the Young's modulus (Case A-1). Furthermore, a combined system of ground plus shotcrete shell plus inner liner is assumed for all results. Fig. 4–25 & Fig. 4–26 represent the thrusts and moments along the circumference of the shotcrete shell, followed by Fig. 4–27 & Fig. 4–28, which show the distribution of the thrusts and moments along the inner liner.

Fig. 4–25 illustrates the distribution of the thrusts in the shotcrete shell during deterioration of the shotcrete. After tunnel construction, the thrusts at the spring-line are higher than at the tunnel-crown. During the deterioration of shotcrete, a higher decrease of the thrusts can be observed at the spring-line compared to the tunnel-crown.

Fig. 4–27 shows the distribution of the thrusts in the inner liner during deterioration of the shotcrete. After the tunnel construction, the thrusts at the spring-line and the tunnel-crown are approximately equal. During the deterioration of the shotcrete, the thrusts at the spring-line increase more than the thrusts at the tunnel-crown.

Comparing the thrusts at the spring-line in the shotcrete shell (Fig. 4–25) at a deterioration of 10% and the thrusts at the spring-line in the inner liner (Fig. 4–27) at a deterioration of 90%, one can note higher thrusts in the inner liner after the deterioration of 90% than in the shotcrete shell after a deterioration of 10%. Thus, one can assume that after deterioration of the shotcrete, the inner liner has to carry more load than the shotcrete shell did after tunnel construction, but one has to be aware that the shotcrete shell has a thickness of 20 cm and the inner liner has a thickness of 30 cm. Thus, the stresses at the spring-line in the shotcrete shell (Fig. 4–17) after tunnel construction are higher than the stresses at the spring-line in the inner liner after deterioration (Fig. 4–10).

Fig. 4–26 illustrates the distribution of the moments in the shotcrete shell during deterioration of the shotcrete. After tunnel construction, the moments at the spring-line are higher and act in opposite direction than the moments at the tunnel-crown. During deterioration, the moments at the spring-line as well as the moments at the tunnel-crown decrease.

Fig. 4–28 shows the distribution of the moments in the inner liner during deterioration of the shotcrete. After the tunnel construction, the moments at the spring-line are higher and act in opposite direction than the moments at the tunnel-crown. During deterioration of the shotcrete, one can observe a slight increase of the moments in the

inner liner at the spring-line as well as a slight decrease of the moments in the inner liner at the tunnel-crown.

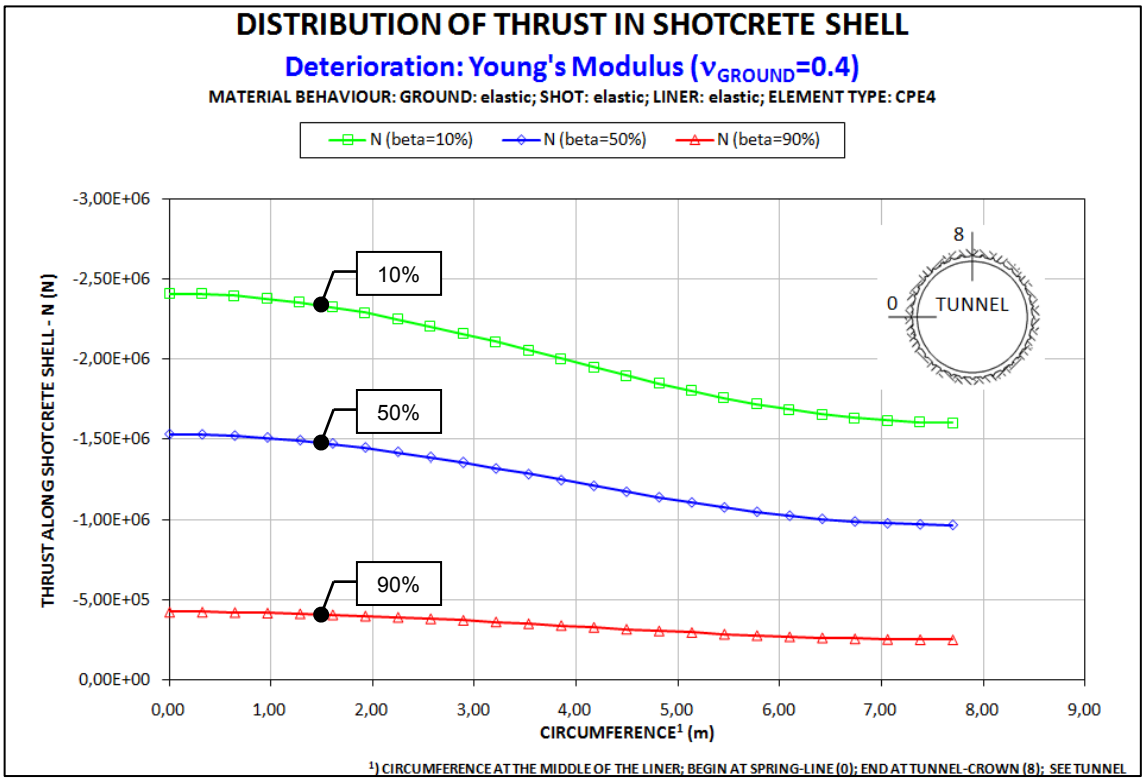

Fig. 4–25: Thrust along the circumference of the shotcrete shell for three deterioration steps (10%, 50%, 90%); deterioration caused by degradation of Young's modulus (Case A-1); results based on (C02)

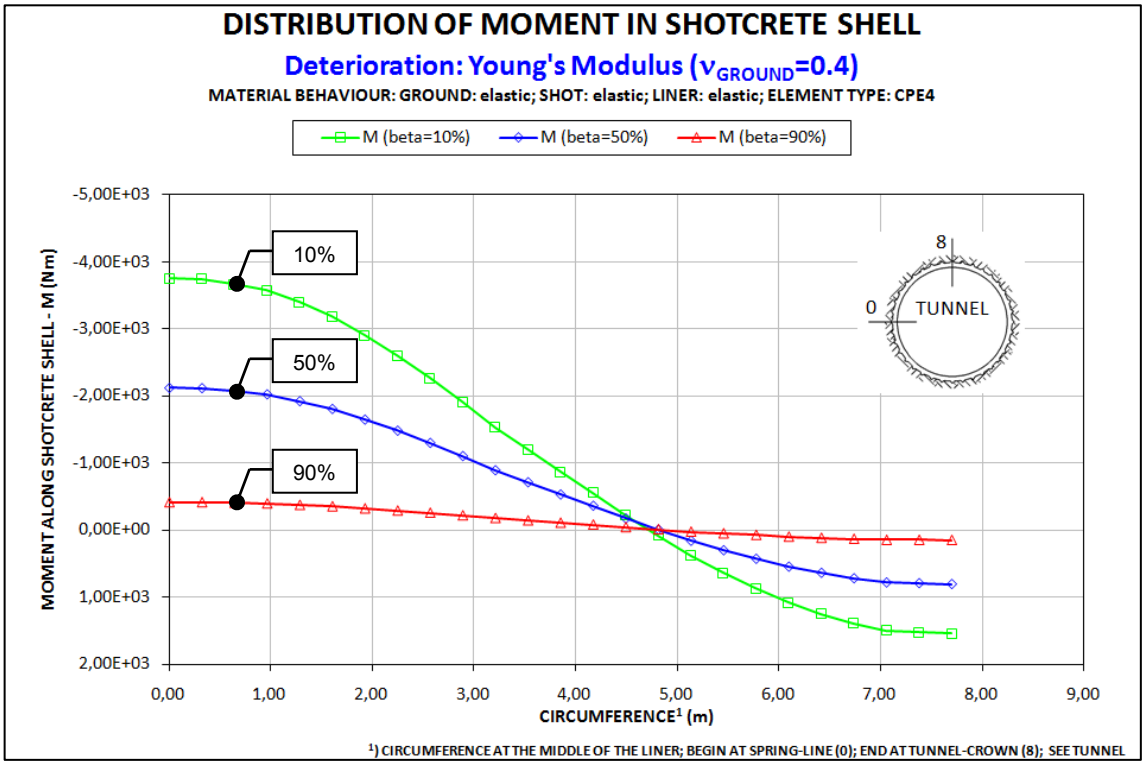

Fig. 4–26: Moments along the circumference of the shotcrete shell for three deterioration steps (10%, 50%, 90%); deterioration caused by degradation of Young's modulus (Case A-1); results based on (C02)

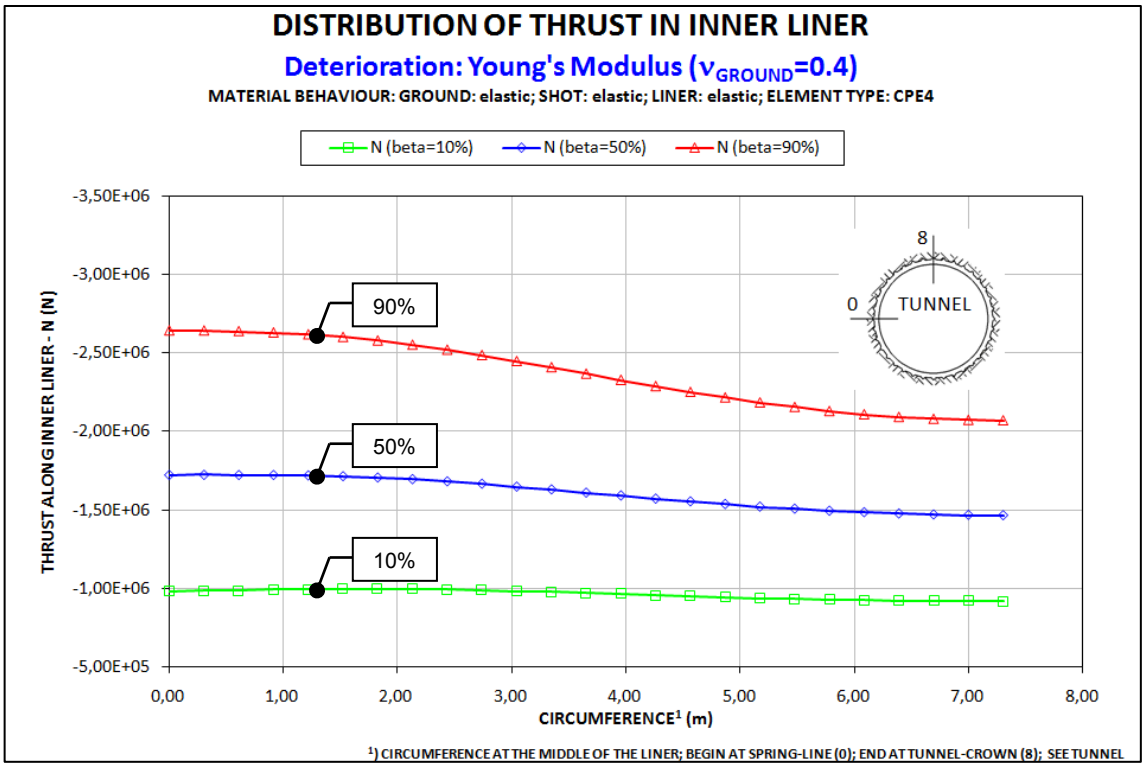

Fig. 4–27: Thrust along the circumference of the inner liner for three deterioration steps (10%, 50%, 90%); deterioration caused by degradation of Young's modulus (Case A-1); results based on (C02)

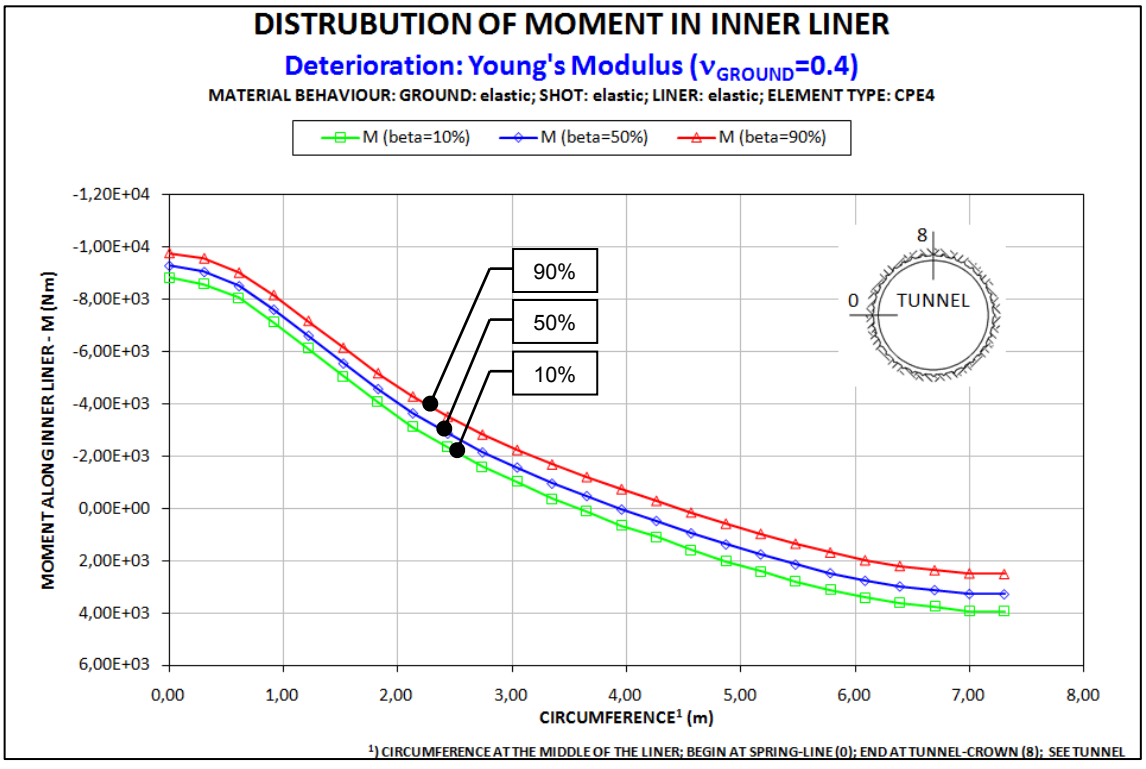

Fig. 4–28: Moments along the circumference of the inner liner for three deterioration steps (10%, 50%, 90%); deterioration caused by degradation of Young's modulus (Case A-1); results based on (C02)

5 CONCLUSION

5.1 Summary of Research Approach

The aim of the research is to establish a Finite Element (FE) model, simulate the deterioration of the shotcrete shell and find out how this affects the inner liner.

Simulation of the tunnel construction

Pre-displacements and support-delay are considered by the Load Reduction Method. The simulation of the placement of support elements can be done by four different methods, the Model Change Method, the Dummy Node Method, the Changing Stiffness Method and the Four Calculation Method. In this thesis the Four Calculation Method is chosen for the following reasons:

- Possibility for contact formulations between support elements is provided (i.e. Coulomb friction)
- Realistic behavior in terms of tangential stresses of the support elements can be obtained

(For details see chapter 3.5.4 and chapter 3.6.5)

Simulation of the effects of deterioration of shotcrete

Using this method (Four Calculation Method), in which stresses are introduced in the primary shotcrete shell and secondary inner liner, a parametric study is carried out. The investigation of the deterioration of the shotcrete shell is done by degradation of the Young's modulus and the compressive strength.

The following combinations of Finite Element types, material behavior and deterioration parameters are used:

- 4-node Finite Elements (CPE4) plus linear elastic material behavior (LE)
    - Deterioration of shotcrete by degradation:
        - Young's Modulus (E)
        - compressive strength (f_C)
        - Young's Modulus and compressive strength simultaneously (E & f_C)

- 4-node Finite Elements (CPE4) plus linearly elastic – perfectly plastic material behavior considering a Coulomb failure criterion (LE-PP (C))
    - Deterioration of shotcrete by degradation:
        - Young's Modulus (E)
        - compressive strength (f_C)
        - Young's Modulus and compressive strength simultaneously (E & f_C)

- 8-node Finite Elements with reduced integration (CPE8R) plus linear elastic material behavior (LE)
    - Deterioration of shotcrete by degradation:
        - Young's Modulus (E)
        - compressive strength (f_C)
        - Young's Modulus and compressive strength simultaneously (E & f_C)

5.2 Interpretation and discussion

The major conclusions of this investigation are as followed:

Simulation of the tunnel construction:

To ensure loading of the inner liner after the simulation of the tunnel construction process is finished (STEP 8), the liner is included before the concentrated forces are set to zero, i.e. at load reduction factor of β = 95%. (Fig. 5–1)
As a consequence of considering of the combined system "ground plus shotcrete shell plus inner liner" lower stresses in the shotcrete are obtained compared to only considering a combined system of "ground plus shotcrete shell" ("SCC" in Fig. 5–1).

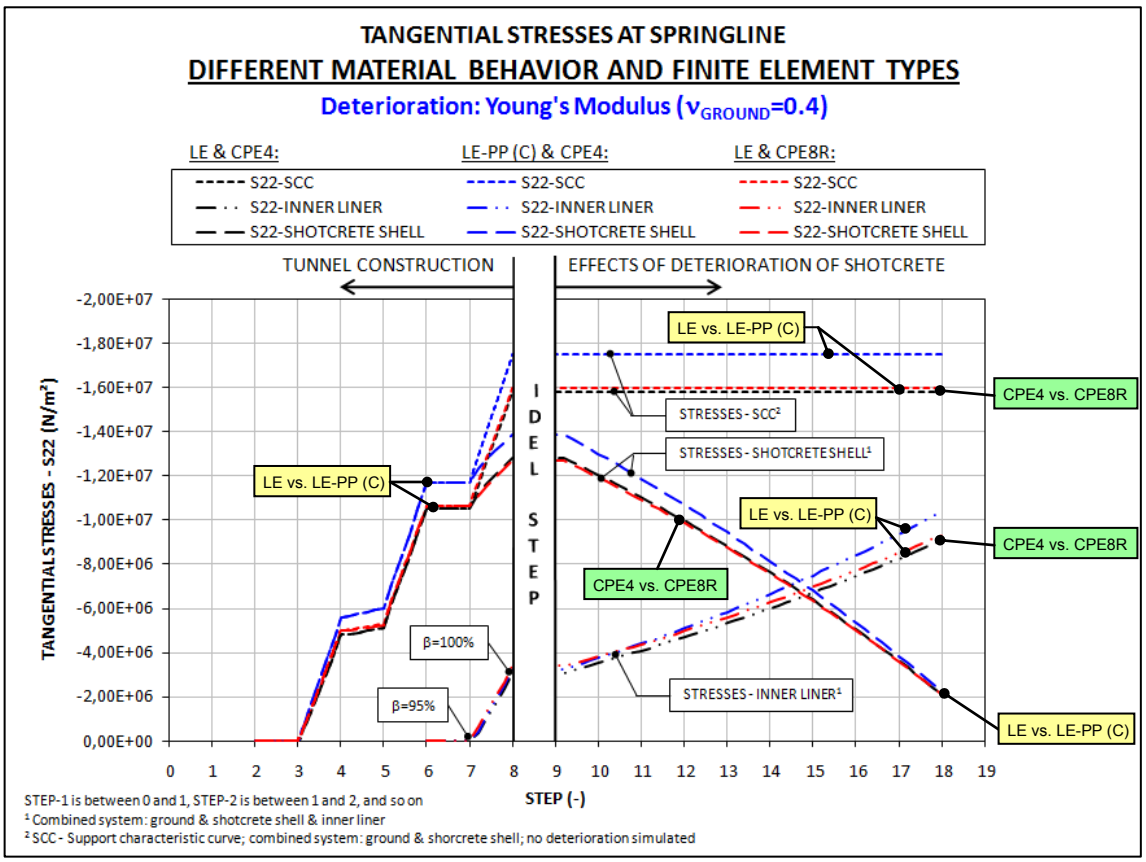

Fig. 5–1: Tangential stresses at spring-line in inner liner and shotcrete shell during the "tunnel construction" process and the "deterioration" process; deterioration caused by degrading the Young's modulus; different material behaviors and finite element types are compared; results based on (C02+C08+C14)

Simulation of the effects of deterioration of shotcrete

The effect of deteriorating material properties, E and f_C, is investigated separately and in combination. Thus, three different cases are considered.

Fig. 5–2 shows the load transfer from the shotcrete shell to the inner liner in terms of tangential stresses for these three sub-cases:

Case A-1: Deterioration of the Young's modulus (E)
Case A-2: Deterioration of the compressive strength (f_C)
Case A-3: Simultaneous deterioration of the Young's modulus and the compressive strength (E & f_C)

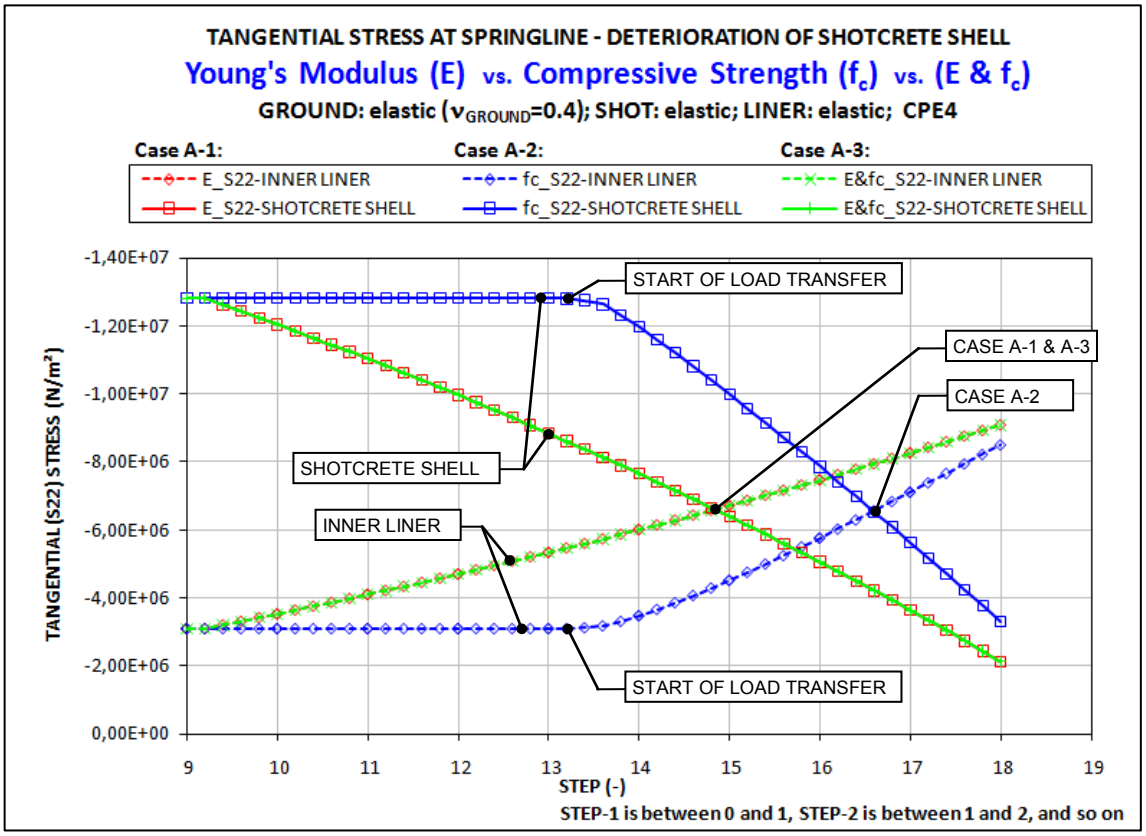

Fig. 5–2: Comparison of Cases A-1, A-2 and A-3; transfer of tangential stresses from shotcrete shell to inner liner caused by deterioration of the shotcrete; results based on (C02+C04+C06)

Exactly the same results were obtained in Case A-3 and Case A-1. Comparing the deteriorations, which are caused by the degradation of E and f_C, one can observe that using f_C as deterioration-factor, the load transfer starts later and at a higher rate than using E as deterioration-factor. However, during deterioration, the stresses in the inner liner, which are caused by degrading the compressive strength of the shotcrete (Case A-2) remain lower than the stresses in the inner liner, which are caused by degrading the Young's modulus of the shotcrete (Case A-1). Moreover, the stresses in the shotcrete shell, which are caused by degrading the compressive strength of shotcrete (Case A-2) remain higher than the stresses in the shotcrete shell, which are caused by degrading the Young's modulus of the shotcrete (Case A-1). Thus, one can assume that the stresses in the inner liner, which are caused by degrading the compressive

strength of the shotcrete (Case A-2), are higher (or lower in case of the shotcrete shell) than the stresses, which are caused by degrading the Young's modulus of the shotcrete (Case A-1), the compressive strength becomes the decisive factor in the combined case (Case A-3) and so the stresses in the combined case are exactly the same as the stresses, which are obtained by degrading the compressive strength (Case A-3 = Case A-2). Additional investigations are necessary to prove this.

The key features of the comparison of the deterioration-factors are:

- As mentioned before, one of the deterioration-factors, E or f_C, is decisive, i.e. deterioration caused by simultaneously degrading E and f_C show exactly the same stresses in the support elements than either by degrading E or by degrading f_C.
- Using the same deterioration-rate, the load-transfer, which is caused by the deterioration of the compressive strength, is faster than the load transfer, which is caused by the deterioration of the Young's modulus.
- The load transfer, which is caused by a deterioration of f_C can start with a delay[5].

Fig. 5–3 and Fig. 5–4 show the stress distribution along the circumference of the inner liner during deterioration of the shotcrete. Fig. 5–3 illustrates the stress distribution in the inner liner, which is caused by degrading the Young's modulus of the shotcrete and Fig. 5–4 shows the stress distribution in the inner liner, which is caused by degrading the compressive strength of the shotcrete. At 90% deterioration of the shotcrete, both stress distributions (caused by degrading the Young's modulus and by degrading the compressive strength) in the inner liner are approximately similar. The stresses in the inner liner at 90% deterioration of the shotcrete (Fig. 5–3), which is caused by degrading the Young's modulus, are slightly higher than the stresses in the inner liner at 90% deterioration of the shotcrete (Fig. 5–4), which are caused by degrading the compressive strength.

[5] See Fig. 5–2: Load transfer, which is caused by degrading f_C starts between STEP 13 and STEP 14

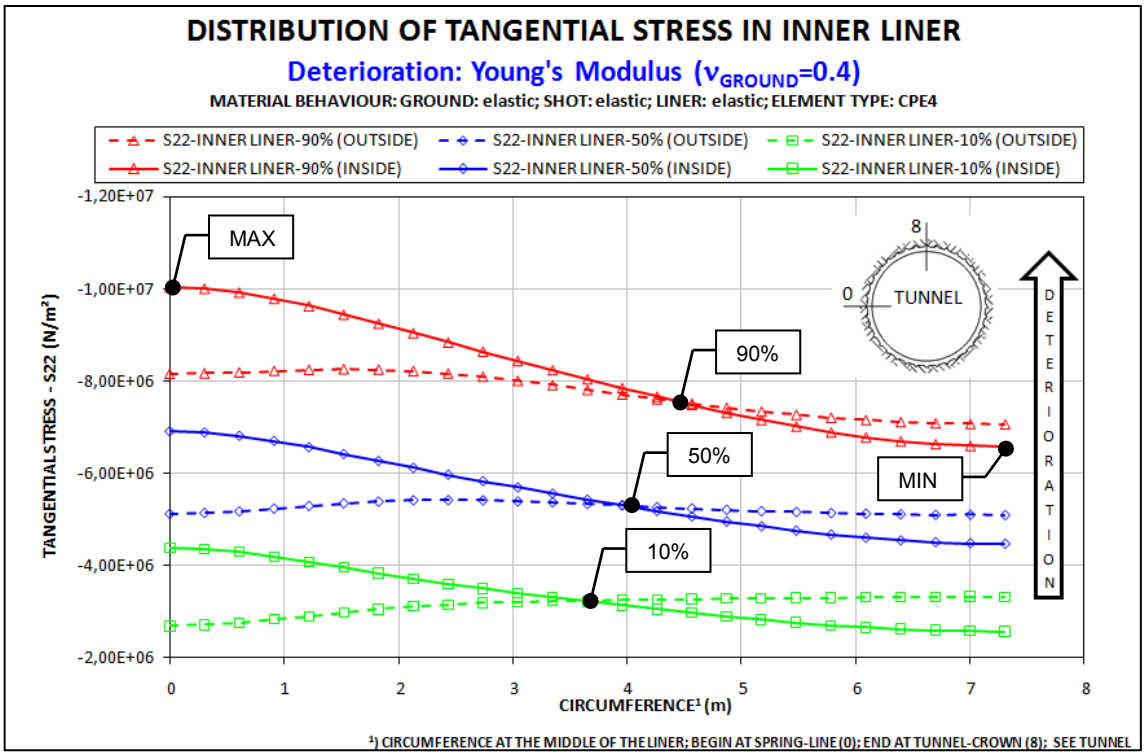

Fig. 5–3: Stresses at the outside and inside of the inner liner for three deterioration steps (10%, 50%, 90%); deterioration caused by degrading Young's modulus (Case A-1); results based on (C02)

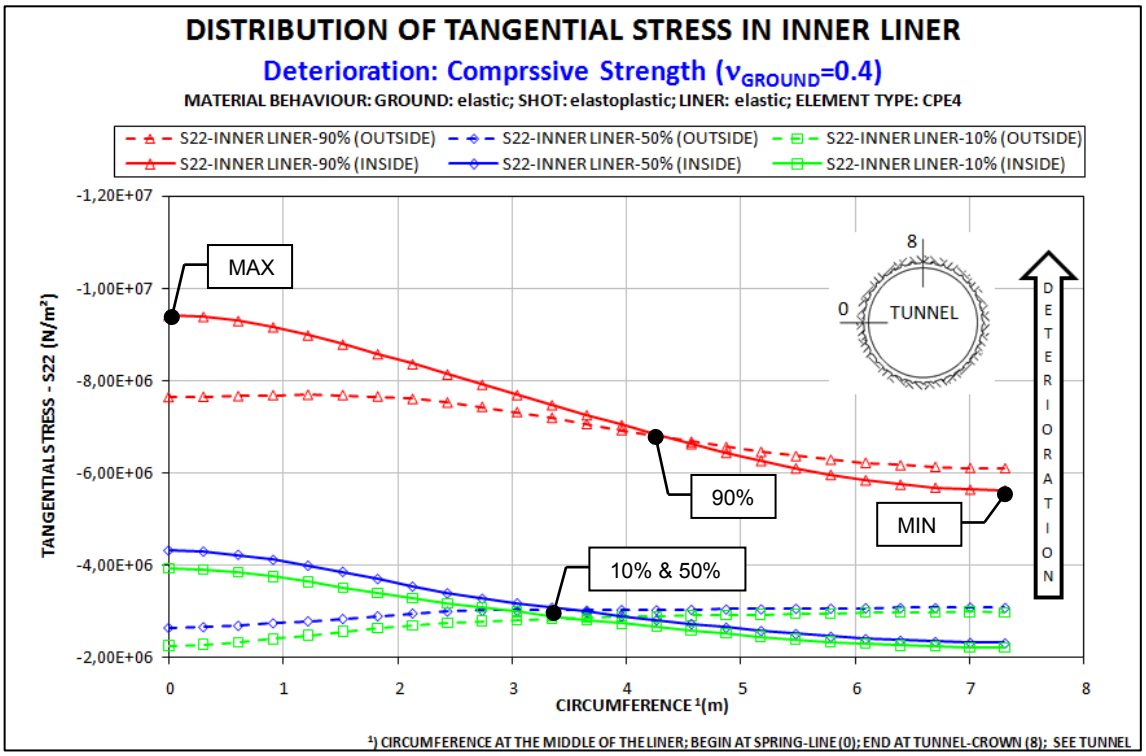

Fig. 5–4: Stresses at the outside and inside of the inner liner for three deterioration steps (10%, 50%, 90%); deterioration caused by degrading compressive strength (Case A-2); results based on (C04)

Generally, lateral earth-pressure-coefficients of K < 1.0 lead to tangential compressive-stresses in the liner, which are higher at the spring-line than at the tunnel-crown. In both cases (Case A-1 (Fig. 5–3) & Case A-2 (Fig. 5–4)), the maximum stresses after deterioration of the shotcrete are observed at the spring-line at the inner liner interior.

Accordingly, the minimum stresses for both cases (Case A-1 & Case A-2) are observed at the tunnel-crown at the inner liner interior.

Fig. 5–5 compares the absolute values of the relative increase of the stresses in the inner liner to the absolute values of the relative decrease of the stresses in the shotcrete shell. The stresses were obtained at deterioration levels of 10% and 90% of the shotcrete. All investigated calculations (C01 to C18, see Table 5) are included in this scattergram. A linear relationship for all calculations can be determined, i.e. the increases of stresses in the inner liner and decreases of stresses in the shotcrete shell have a linear relationship.

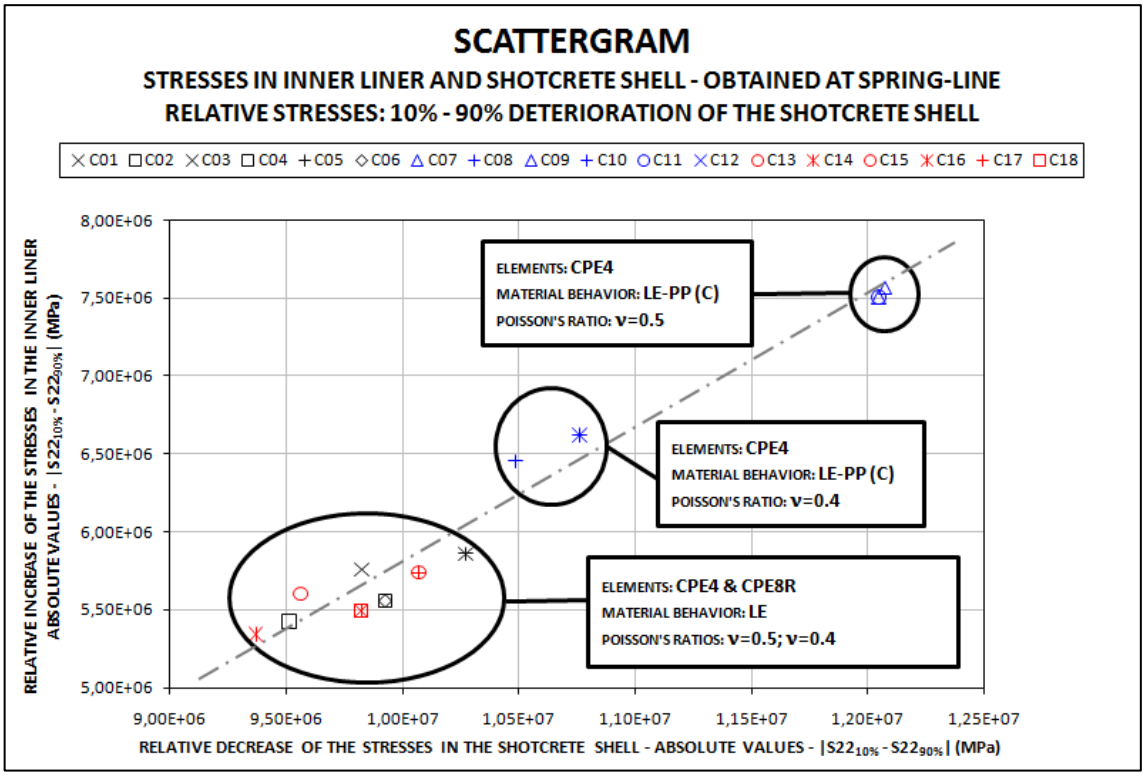

Fig. 5–5: Scattergram, absolute values of relative stresses in shotcrete shell and inner liner at a deterioration levels of 10% and 90% of shotcrete; results based on (C01 to C18, see Table 5);

Other aspects

Fig. 5–1 illustrates that different element types (“CPE4” and “CPE8R”) have only minor effects on the stresses in the support elements (shotcrete shell and inner liner) and Fig. 5–6 presents that different element types (“CPE4” vs. “CPE8R”) have only minor effects on the displacements of the tunnel-perimeter.

Furthermore, Fig. 5–1 shows that changing material behavior (“LE” vs. “LE-PP (C)”) of the ground is affecting the stresses in the support elements. The best way to explain these effects is to look at the radial displacements of the tunnel-perimeter at the spring-line during the “tunnel construction” and the “deterioration” processes (Fig. 5–6).

The main difference is that plastic deformation occurs during the “tunnel construction” process (Fig. 5–6), which causes higher tangential stresses in the shotcrete shell after

the “tunnel construction” process (STEP 8, Fig. 5–1) using “LE-PP (C)” material behavior than using “LE” material behavior. Furthermore, one can observe that in all cases (“LE” & “LE-PP (C)”) at the end of the “deterioration” process (STEP 18, Fig. 5–1), the stresses in the shotcrete shell are approximately similar.

Concerning the stresses in the inner liner at the end of the “deterioration” process (STEP 18, Fig. 5–1) one can observe higher stresses using a linearly elastic – perfectly plastic material behavior compared to a linear elastic material behavior. (Note that after the “tunnel construction” process, the stresses in the inner liner, which are obtained using a linear elastic material behavior, are approximately equal to the stresses, which are obtained using a linearly elastic – perfectly plastic material behavior.)

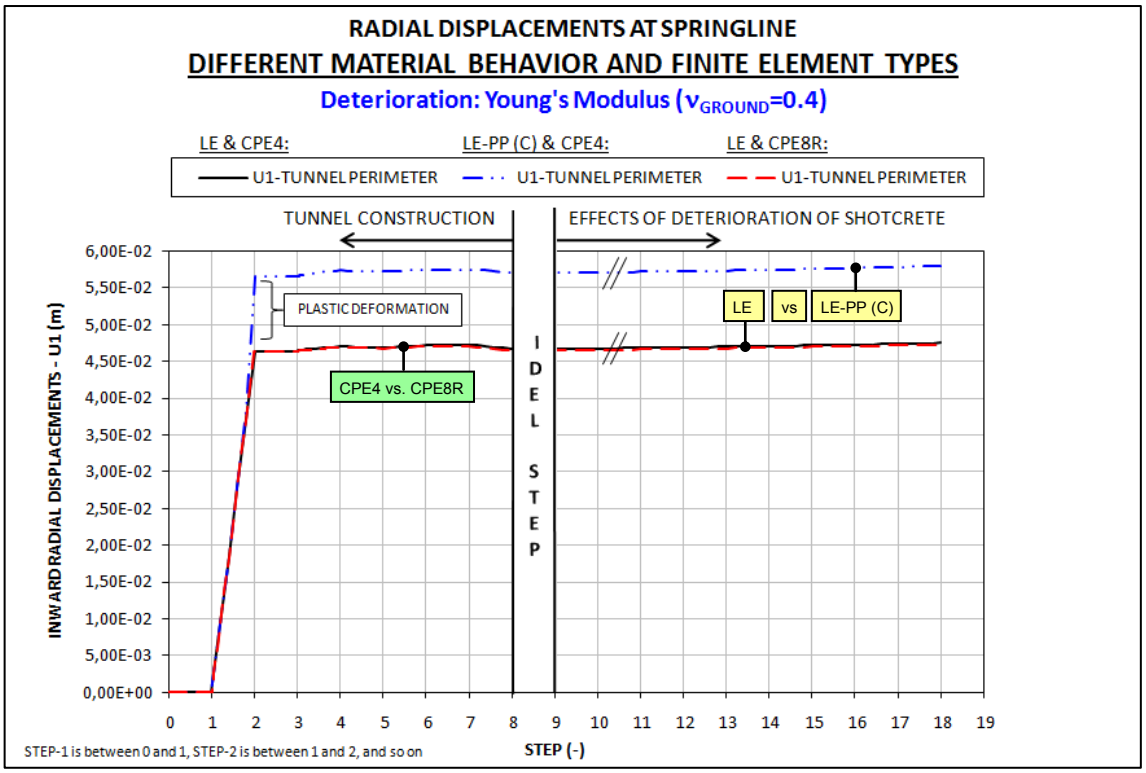

Fig. 5–6: Overview of inward radial displacements at the spring-line of the tunnel-perimeter during the “tunnel construction” process and the “deterioration” process; deterioration caused by degrading the Young’s modulus; different material behaviors and finite element types are compared; results based on (C02+C08+C14)

5.3 Recommendations for future research

Several potential areas for research can enhance the investigation of the deterioration of shotcrete presented in this thesis:

Deterioration of different components of the tunnel support system

It is very likely that not only the shotcrete is affected by deterioration. Also the contact between the ground and the shotcrete shell and the contact between the shotcrete shell and the inner liner can be affected. Further, the properties of the ground around the opening may change with time. The material properties and load-bearing thickness of the inner liner might be reduced by environmental effects such as de-icing and salt

corrosion. All of this should be considered in the main degradation processes and their effects on long-term stability of tunnels.

Variation of other parameters

The parametric study can be expanded to consider, for instance, different ground parameters and overburden as well as different thicknesses of the shotcrete shell and of the inner liner. Also varying the load reduction factors to simulate pre-displacements and support-delay or varying other constitutive laws for ground and support elements might be useful (Walter, 2009).

Further developments of the numerical methods

The Four Calculation Method allows one to consider “contact friction” but not for divergent deformation behavior (Fig. 5–7). The Changing Stiffness Method can handle “contact friction” for divergent and convergent deformation behavior, but does not allow obtaining realistic behaviors in terms of displacements and stresses of the support elements during the simulation of the tunnel construction. Hence, these two methods have to be further developed.

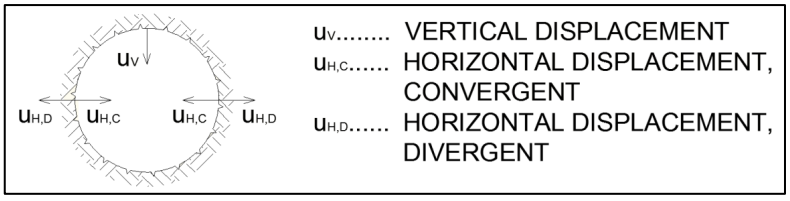

Fig. 5–7: Convergent and divergent deformation behavior

Improving the background knowledge about deterioration

Most importantly, the natural properties should be investigated. Specimens of the support elements and the ground should be tested as or immediately after the tunnel is constructed, as well as from time to time during operation. It is also important that the specimens are obtained at the same locations and that the geology of the surrounding ground is known well.

IV. List of Abbreviations

(C)	Coulomb constitutive law
2D	two dimensional
3D	three dimensional
C	concrete
c	cohesion
C01-C18	combinations of parameters; parametric study
C-DLS	dual lining systems with composite linings
CF_H	horizontal concentrated forces
CF_V	vertical concentrated forces
CPE4	4-node bilinear plane strain continuum element
CPE8R	8-node biquadratic plane strain continuum element with reduced integration
D.O.F.	degree of freedom
DS	Druckschriften (Guideline of German railways AG)
E	Young's modulus
E_L	Young's modulus of inner liner
E_{L0}	very low Young's modulus of inner liner (close to zero)
EPB	earth-pressure balance machines
E_{S0}	very low Young's modulus of shotcrete shell (close to zero)
E_{S1}	Young's modulus of "young" shotcrete
E_{S2}	Young's modulus of "hardened" shotcrete
f_C	compressive strength
FE	finite element
G	ground
GROUND	numerical model of ground
G-S	interface ground – shotcrete shell
H	overburden
K	lateral earth-pressure coefficient
L	inner liner
LINER	numerical model of inner liner
ÖVBB	Österreichische Vereinigung für Beton- und Bautechnologie
p	contact pressure
p_0	internal pressure (load reduction- or stiffness reduction method)
RF	reaction force
RF_H	horizontal reaction force
RF_V	vertical reaction force

RVS	Richtlinien und Vorschriften für das Straßenwesen
S	shotcrete shell
S22	tangential stress in shotcrete shell or inner liner
SCC	support characteristic curve; stresses in shotcrete shell; inner liner is not included in the calculation of these stresses; no deterioration is simulated;
S-DLS	dual lining systems with separate linings
SHOT	numerical model of shotcrete shell
SL	spring-line
S-L	interface shotcrete shell – inner liner
SpC	sprayed concrete or shotcrete
SS	slurry shield machines
TBM	tunnel boring machine
U1	horizontal displacements (radial displacements at spring-line)
$u_{H,C}$	horizontal displacements, convergent
$u_{H,D}$	horizontal displacements, divergent
u_V	vertical displacements
X	nodal X-coordinate
Y	nodal Y-coordinate
Z	interface thickness

List of Abbreviations (Greek symbols)

α	stiffness reduction factor
β	load reduction factor
Δx	displacements in X-direction
Δy	displacements in Y-direction
Δz	displacements in Z-direction
ε	strain
ε^{e}	elastic strain
ε^{pl}	plastic strain
γ	specific weight; unit weight
$\gamma_{elast.}$	elastic slip
φ	friction angle
φ_i	internal friction angle
μ	friction coefficient
ν	Poisson's ratio
Π	idle-step (for evaluation purposes)
ρ	friction angle of two surfaces
Σ	zone of tunnel construction
σ_H	horizontal stress field
σ_V	vertical stress field
τ	shear stress
$\tau_{crit.}$	maximal transferable shear stress
Ω	zone of deterioration of the shotcrete shell
Σ	zone of tunnel construction

V. List of Tables

List of Tables (Appendix)

VI. List of Figures

List of Figures (Appendix)

VII. List of References

Bathe, K.-J. (1996). *Finite Element Procedure* (p. 1050). Upper Saddle River, Ney Jersy: Prentice-Hall, Inc.

Baudendistel, M. (1979). Zum Entwurf von Tunnel mit großem Ausbruchsquerschnitt. *Rock Mechanics*, *8*, 75-100.

Bolton, M. D. (1986). The strength and dilatancy of sands. *Geotechnique*, *36*(1), 65-78.

Brinkgreve, R. B. J., & Veermeer, P. A. (2002). *PLAXIS 3D Tunnel, Version 8: General Information, Tutorial Manual, Reference Manual, Material Model Manual, Scientific Manual, Validation and Verification Manual* (8th ed.). Lisse/Abdingdon/Exton(PA)/Tokyo: A.A. Balkema Publishers.

Brosch, F. J. (1990). Anisotropy of dilation, 3-D stress state and the talobre friction cone. *Rock Mechanics and Rock Engineering*, *23*(2), 113-121.

Daemen, J. J. K. (1975). *Rational Design of Tunnel Supports: Tunnel Support Loading Caused by Rock Failure*. Dissertation; University of Minnesota, Minneapolis.

DS 853. (2007). Richtlinie 853; Eisenbahntunnel planen, bauen und instand halten. Frankfurt am Main: Deutsche Bahn AG.

Einstein, H. H., Bobet, A., & Aristorenas, G. (1995). *Feasibility Study Opalinuston - Text and Appendix 1* (p. 234). Cambridge, MA: Massachusetts Institute of Technology.

Golser, H. (2008). BBT SE: Technischer Bericht, Geomechanische Planung, Zusammenfassende Darstellung. Retrieved 2010, from http://www.bmvit.gv.at/verkehr/eisenbahn/verfahren/bbt/bbt3b/index.html.

Golser, H., & Schubert, W. (2003). Application of numerical simulation at the tunnel site. In G. Beer (Ed.), *Numerical Simulation in Tunnelling* (pp. 427-474). Wien: Springer-Verlag.

Hibbitt, H. D., Karlson, K., & Sorenson, S. (2007). *ABAQUS Version 6.7: CAE User's Manual, Analysis User's manual, Example Problems Manual, Keyword Reference Manual, Theory Manual, User Subroutines Reference Manual*. Rhode Island: HKS Inc.

Laabmayr, F., & Swoboda, G. (1978). Beitrag zur Weiterentwicklung flachliegender Tunnelbauwerke im Lockergestein. In H. Lessmann (Ed.), *Moderner Tunnelbau bei der Münchner U-Bahn* (pp. 55-71). Wien - New York: Springer-Verlag.

Laabmayr, F., & Swoboda, G. (1986). Grundlagen und Entwicklung bei Entwurf und Berechnung im seichtliegenden Tunnel - Teil 1. *Felsbau*, *4*(3), 138-143.

Ladanyi, B. (1974). Use of the long-term strength concept in the determination of ground pressure on tunnel linings. *3rd International Congress on Rock Mechanics* (pp. 1150-1156). Denver: National Academy of Sience.

Lombardi, G. (1973). Dimensioning of Tunnels Linings with regards to Construction Procedure. *Tunnels & tunnelling*, *5*(4), 340-351. Progressive Media Markets, Ltd.

Marcher, T., & Jiricny, F. (2004). Interaction of primary lining and final lining of a NATM tunnel with respect to relevant long-term effects. *Winter Workshop of Rock Mass Mechanic*. Poland.

Meißner, H. (1991). Empfehlungen des Arbeitskreises “Numerik in der Geotechnik” der Deutschen Gesellschaft für Erd- und Grundbau e.V.

Meißner, H. (1996). Tunnelbau unter Tage, Empfehlungen des Arbeitskreises “Numerik in der Geotechnik” der Deutschen Gesellschaft für Erd- und Grundbau e.V. *Numerik in der Geotechnik*.

Möller, S. (2006). *Tunnel induced settlements and structural forces in linings*. Dissertation; Universitaet Stuttgart.

Möller, S. C., Krajewski, W., & Wawrzyniak, C. (2010). Bemessung von Tunnelbauwerken in bindigem Boden - Erfahrung mit unterschiedlichen Stoffgesetzen. *Felsbau magazin*, *1*, 70-79.

Pacher, F. (1964). Deformationsmessungen in Versuchstollen als Mittel zur Erforschung des Gebirgsverhalten und zur Bemessung des Ausbaues. *Felsmech Ingenieursgeol Suppl IV*, 149-161.

Panet, M. (1976). *la mècanique des roches - appliquèe aux ouvrages du gènie civil* (p. 235). Lyon: Association Amicale des Ingènieurs.

Panet, M. (1978). Stability Analysis of a Tunnel driven in a Rock Mass in tracking account of the Post-Failure Behavior. *Rock Mechanics*, *Vol. 8*(1), 209-223.

RVS 09.01.31. (2003). *Tunnel - Kontinuierlicher Vortrieb von Strassentunnel*. Wien: Österreichische Forschungsgemeinschaft Straße und Verkehr.

RVS 09.01.42. (2004). *Tunnel - Geschlossene Bauweise im Lockergestein unter Bebauung*. Wien: Österreichische Forschungsgemeinschaft Straße und Verkehr.

Sandrone, F., & Labiouse, V. (2009). Analysis of the evolution of road tunnels equilibrium conditions with a convergence–confinement approach. *Rock Mechanics and Rock Engineering*, *43*(2), 201-218.

Schwartz, C. W., & Einstein, H. H. (1980). *Improved Design of Tunnel Supports: Volume 1 - Simplified Analysis for Ground-Structure Interaction in Tunneling* (p. 450). Cambridge, MA: Massachusetts Institute of Technology.

Stadelmann, R., Pfeffer, A., & Wei, Z. Q. (2009). Design in tunneling, structural design methodss for the inner lining. *Geomechanics and Tunnelling*, *2*(4), 359-368.

Walter, H. (2009). Structural design of tunnel - how reliable are numerical calculations? *Geomechanics and Tunnelling*, *2*(4), 319-332.

Zachow, R. (1995). Dimensionierung zweischaliger Tunnel im Fels auf der Grundlage von in-situ-Messungen. *Forschungsergebnisse aus dem Tunnel- und Kavernenbau der Universität Hannover*. Hannover: Rokahr R. B.

ÖVBB. (2003). *Richtlinie Innenschalenbeton*. Wien: Oesterreichische Vereinigung für Beton- und Bautechnik.

ÖVBB. (2009). *Richtlinie Spritzbeton*. Wien: Oesterreichische Vereinigung für Beton- und Bautechnik.

VIII. APPENDIX

List of Contents - Appendix:

Appendix A

RESULTS OF PARAMETRIC STUDY

All results can be divided into three cases:

- Case A: Linear elastic (LE) material behavior using CPE4 elements
- Case B: Linearly elastic – perfectly plastic (LE-PP) material behavior using CPE4 elements
- Case C: Linear elastic (LE) material behavior using CPE8R elements

Each case can be divided into three sub-cases based on the deterioration (Table 8):

- Case (A/B/C)-1: Deterioration of the Young's modulus (E)
- Case (A/B/C)-2: Deterioration of the compressive strength (f_C)
- Case (A/B/C)-3: Simultaneous deterioration of the Young's modulus and the compressive strength (E&f_C)

Every of this nine cases is calculated with a Poisson ratio of $\nu = 0.5$ and $\nu = 0.4$. Thus, the parametric study investigates 18 different combinations (C01 to C18).

Table 8: structure of cases, sub-cases and combinations of parametric study;

Material Behavior of GROUND	Element Type	CASE	Deteriora-tion	SUB-CASE	Poisson's ratio (ν)	Combi-nation
LE	CPE4	**A**	E	**1**	0.5	**C01**
					0.4	**C02**
			f_c	**2**	0.5	**C03**
					0.4	**C04**
			E&f_c	**3**	0.5	**C05**
					0.4	**C06**
LE-PP	CPE4	**B**	E	**1**	0.5	**C07**
					0.4	**C08**
			f_c	**2**	0.5	**C09**
					0.4	**C10**
			E&f_c	**3**	0.5	**C11**
					0.4	**C12**
LE	CPE8R	**C**	E	**1**	0.5	**C13**
					0.4	**C14**
			f_c	**2**	0.5	**C15**
					0.4	**C16**
			E&f_c	**3**	0.5	**C17**
					0.4	**C18**

Results of Case A

Combination C01

- **Deterioration:** Young's Modulus
- **Element type:** CPE4
- **Ground parameters:**
  - **Poisson's ratio:** $\nu = 0.5$
  - **Material behavior:** linear elastic
- **Shotcrete shell parameters:**
  - **Poisson's ratio:** $\nu = 0.2$
  - **Material behavior:** linear elastic
- **Inner liner parameters:**
  - **Poisson's ratio:** $\nu = 0.2$
  - **Material behavior:** linear elastic

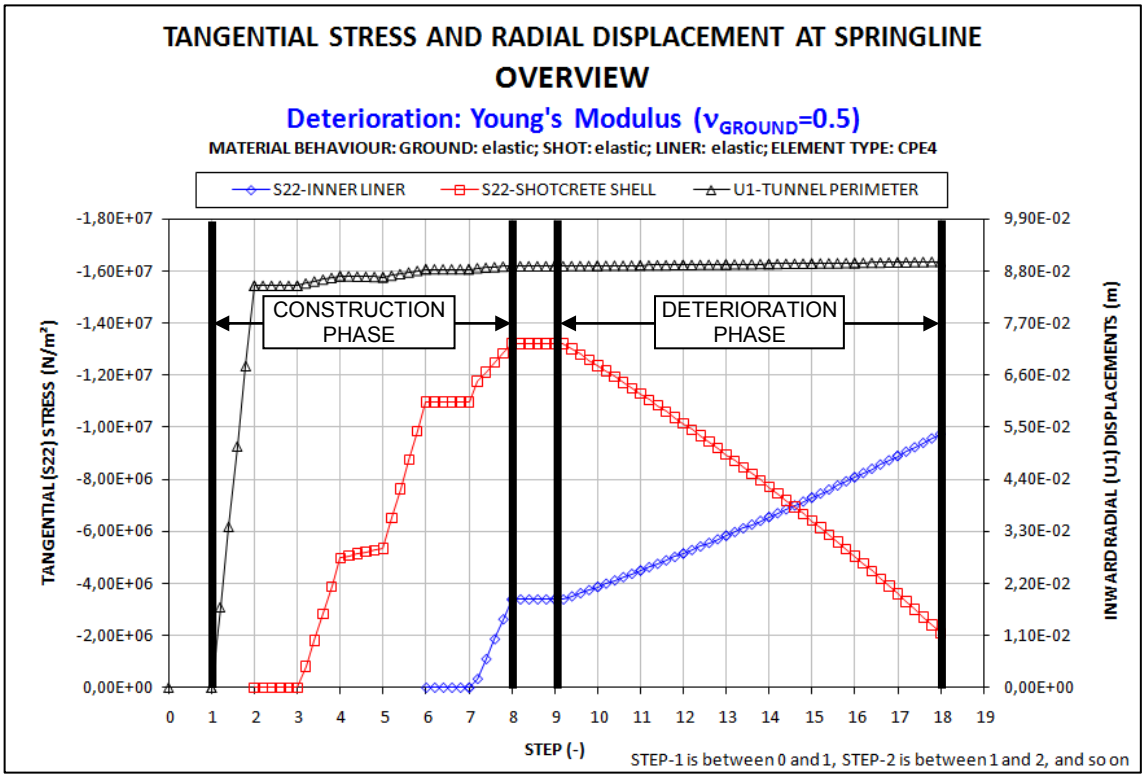

Fig. A–1: Results C01; Overview of stresses in the inner liner and shotcrete shell as well as radial displacements; all results are obtained at the spring-line; construction phase and deterioration phase;

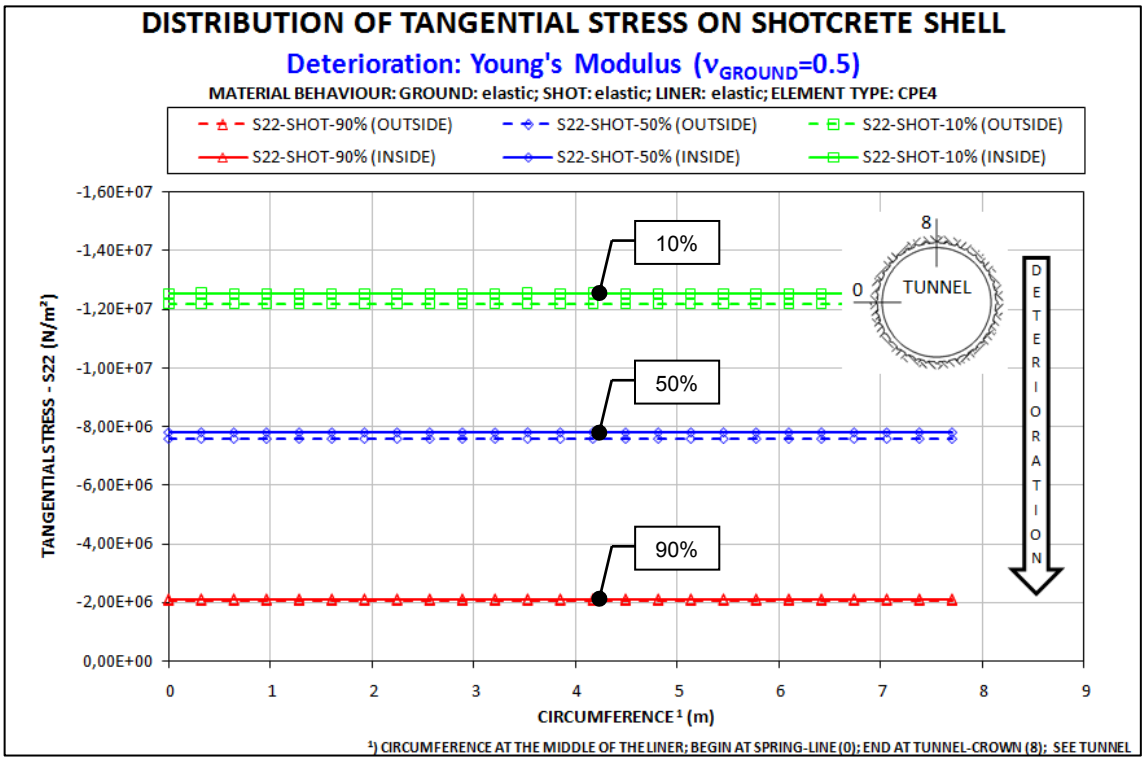

Fig. A–2: Results C01; Stresses at the outside and inside of the shotcrete shell for three deterioration steps (10%, 50%, 90%); deterioration caused by degrading Young's Modulus;

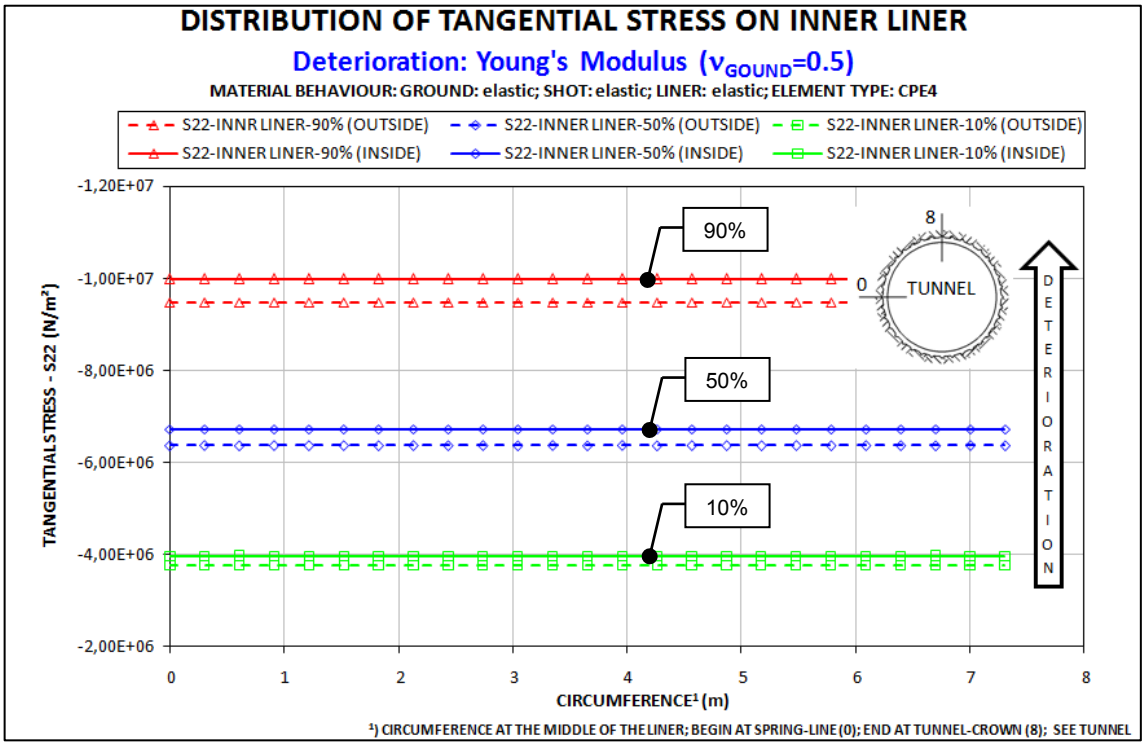

Fig. A–3: Results C01; Stresses at the outside and inside of the inner liner for three deterioration steps (10%, 50%, 90%); deterioration caused by degrading Young's Modulus;

Combination C02

- **Deterioration:** Young's Modulus
- **Element Type:** CPE4
- **Ground parameters:**
  - **Poisson's ratio:** $\nu = 0.4$
  - **Material behavior:** linear elastic
- **Shotcrete shell parameters:**
  - **Poisson's ratio:** $\nu = 0.2$
  - **Material behavior:** linear elastic
- **Inner liner parameters:**
  - **Poisson's ratio:** $\nu = 0.2$
  - **Material behavior:** linear elastic

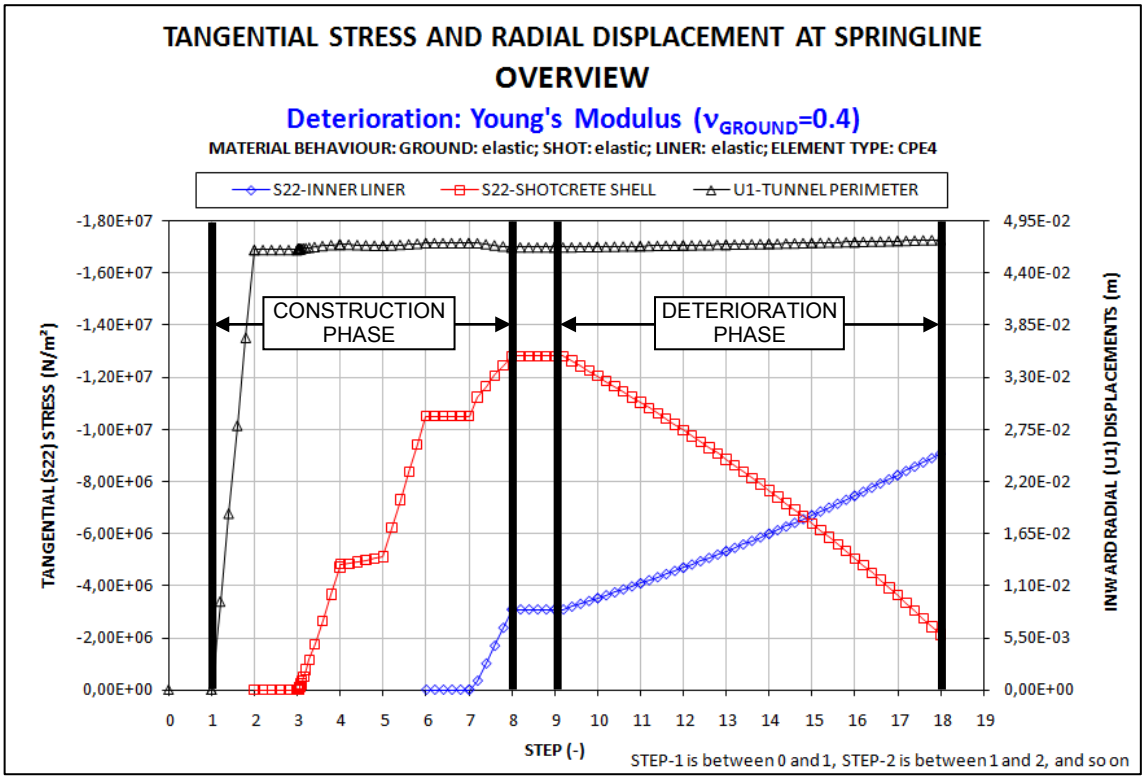

Fig. A–4: Results C02; Overview of stresses in the inner liner and shotcrete shell as well as radial displacements; all results are obtained at the spring-line; construction phase and deterioration phase;

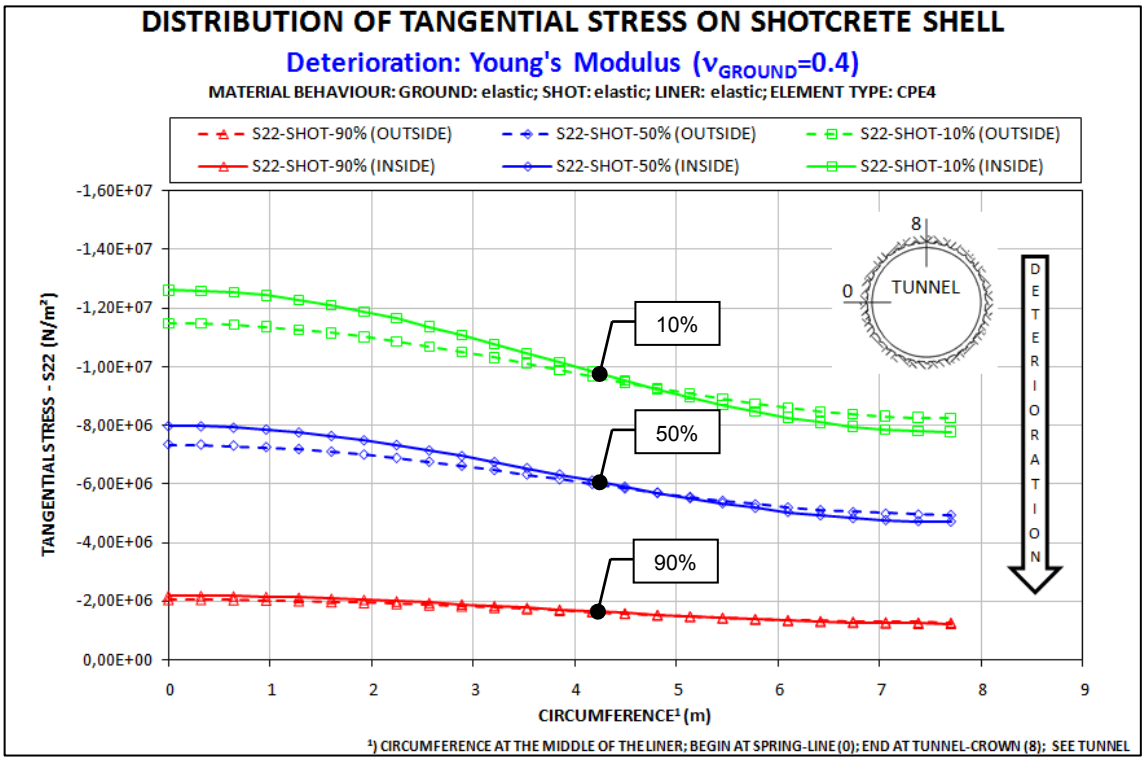

Fig. A–5: Results C02; Stresses at the outside and inside of the shotcrete shell for three deterioration steps (10%, 50%, 90%); deterioration caused by degrading Young's Modulus;

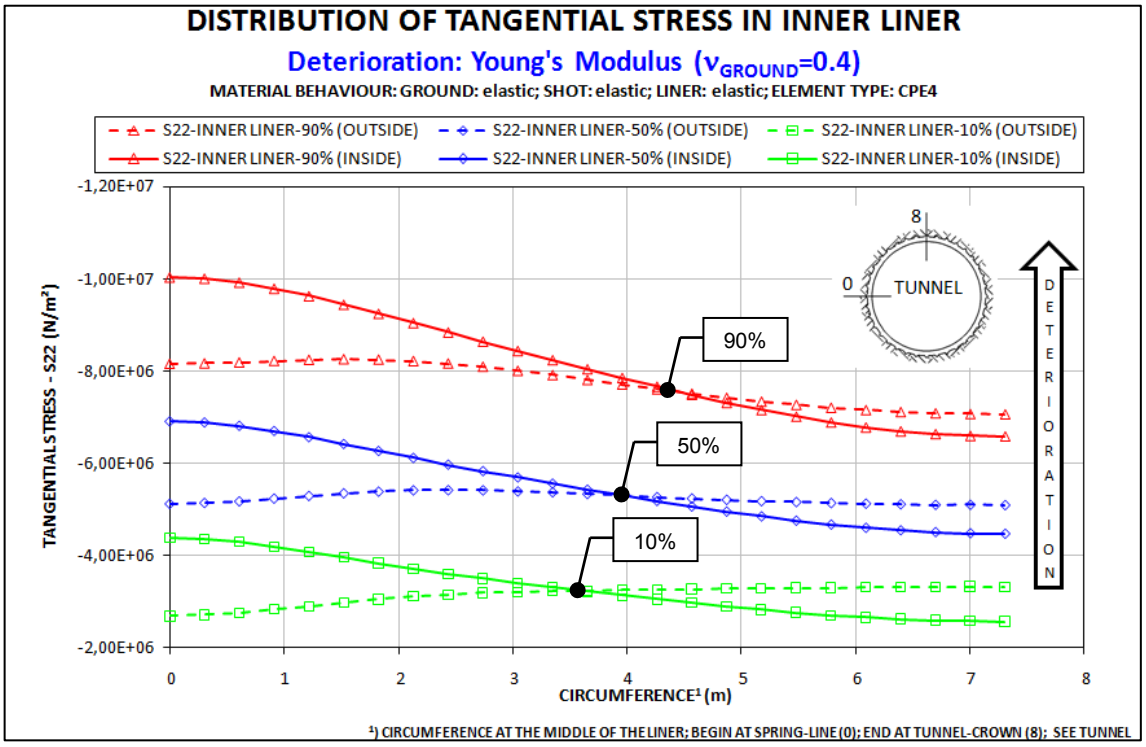

Fig. A–6: Results C02; Stresses at the outside and inside of the inner liner for three deterioration steps (10%, 50%, 90%); deterioration caused by degrading Young's Modulus;

Combination C03

- **Deterioration:** Compressive Strength
- **Element type:** CPE4
- **Ground parameters:**
  - **Poisson's ratio:** $\nu = 0.5$
  - **Material behavior:** linear elastic
- **Shotcrete shell parameters:**
  - **Poisson's ratio:** $\nu = 0.2$
  - **Material behavior:** linear elastic
- **Inner liner parameters:**
  - **Poisson's ratio:** $\nu = 0.2$
  - **Material behavior:** linear elastic

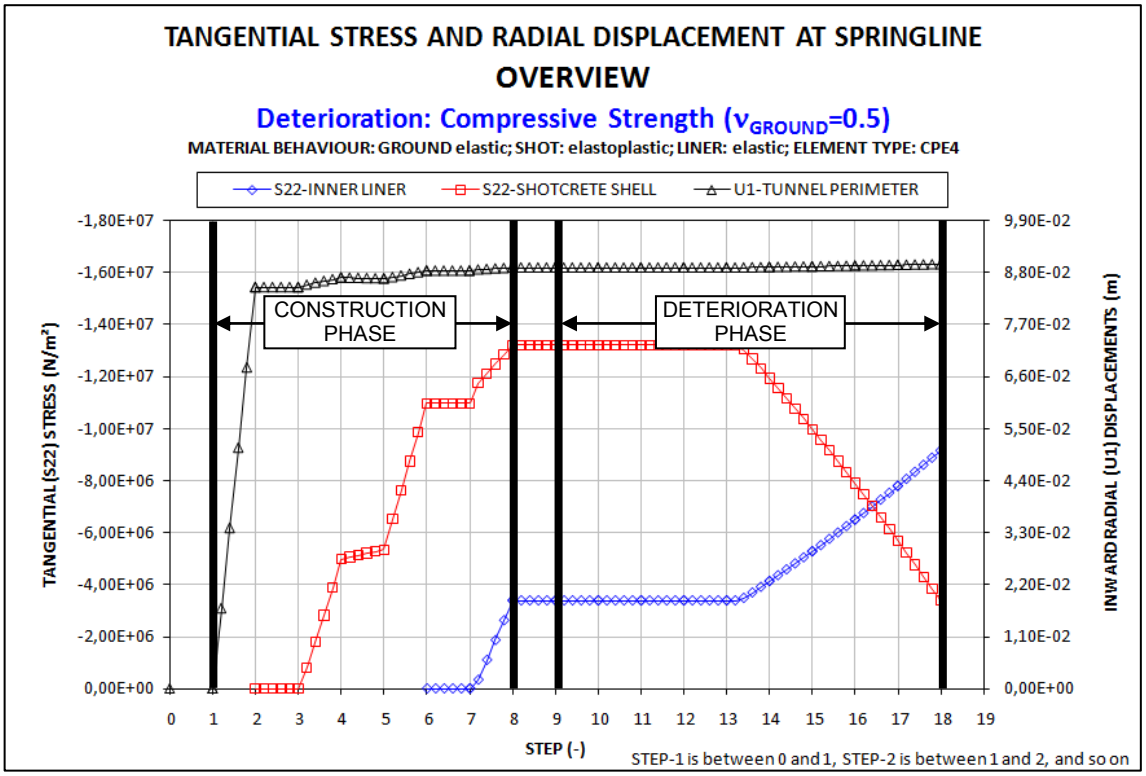

Fig. A–7: Results C03; Overview of stresses in the inner liner and shotcrete shell as well as radial displacements; all results are obtained at the spring-line; construction phase and deterioration phase;

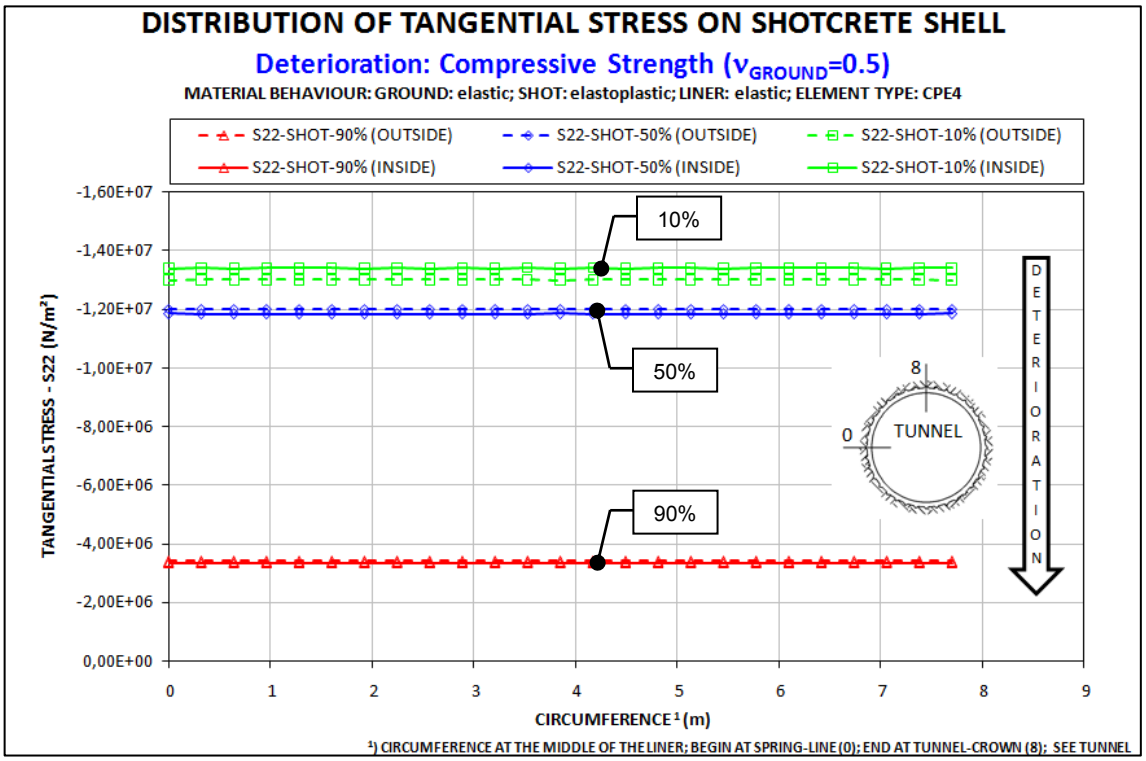

Fig. A–8: Results C03; Stresses at the outside and inside of the shotcrete shell for three deterioration steps (10%, 50%, 90%); deterioration caused by degrading compressive strength;

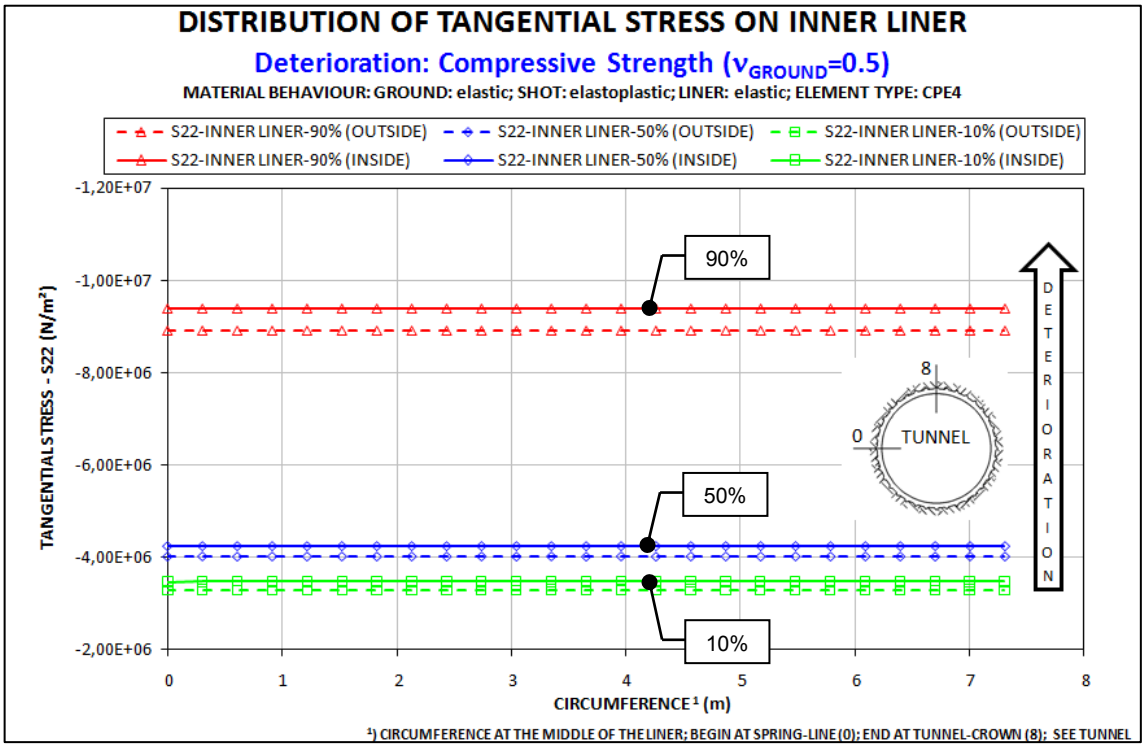

Fig. A–9: Results C03; Stresses at the outside and inside of the inner liner for three deterioration steps (10%, 50%, 90%); deterioration caused by degrading compressive strength;

Combination C04

- **Deterioration:** Compressive Strength
- **Element type:** CPE4
- **Ground parameters:**
  - **Poisson's ratio:** $\nu = 0.4$
  - **Material behavior:** linear elastic
- **Shotcrete shell parameters:**
  - **Poisson's ratio:** $\nu = 0.2$
  - **Material behavior:** linear elastic
- **Inner liner parameters:**
  - **Poisson's ratio:** $\nu = 0.2$
  - **Material behavior:** linear elastic

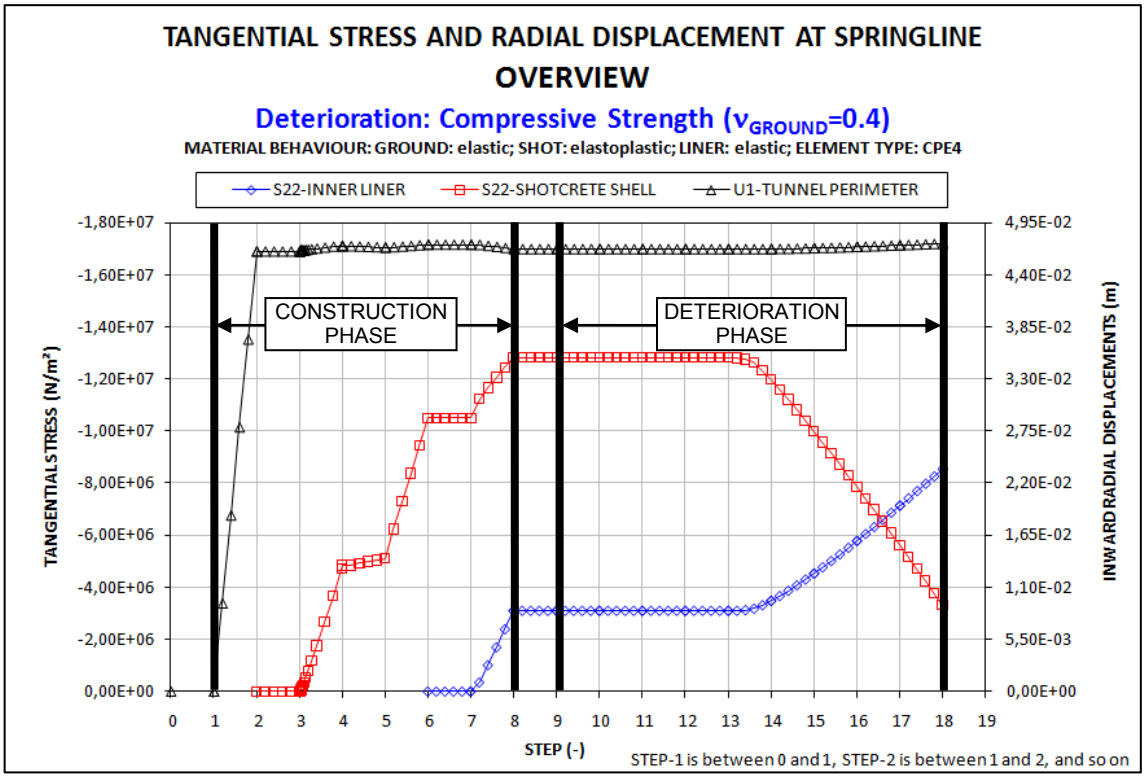

Fig. A–10: Results C04; Overview of stresses in the inner liner and shotcrete shell as well as radial displacements; all results are obtained at the spring-line; construction phase and deterioration phase;

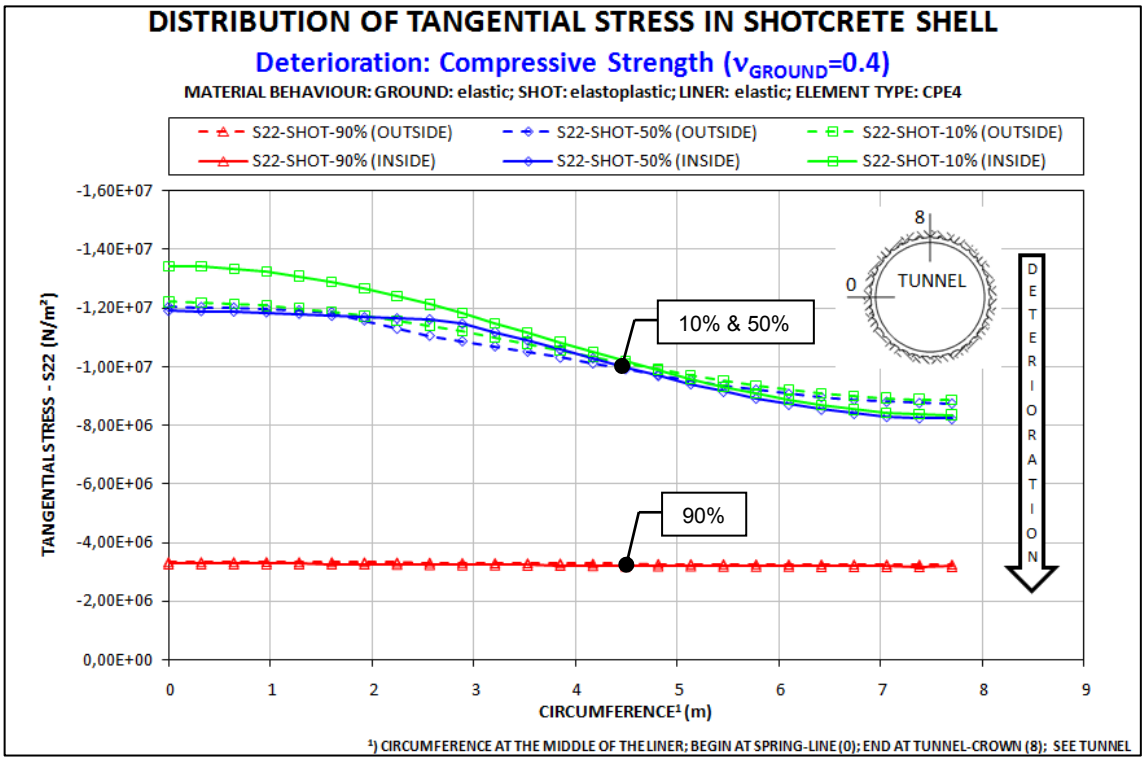

Fig. A–11: Results C04; Stresses at the outside and inside of the shotcrete shell for three deterioration steps (10%, 50%, 90%); deterioration caused by degrading compressive strength;

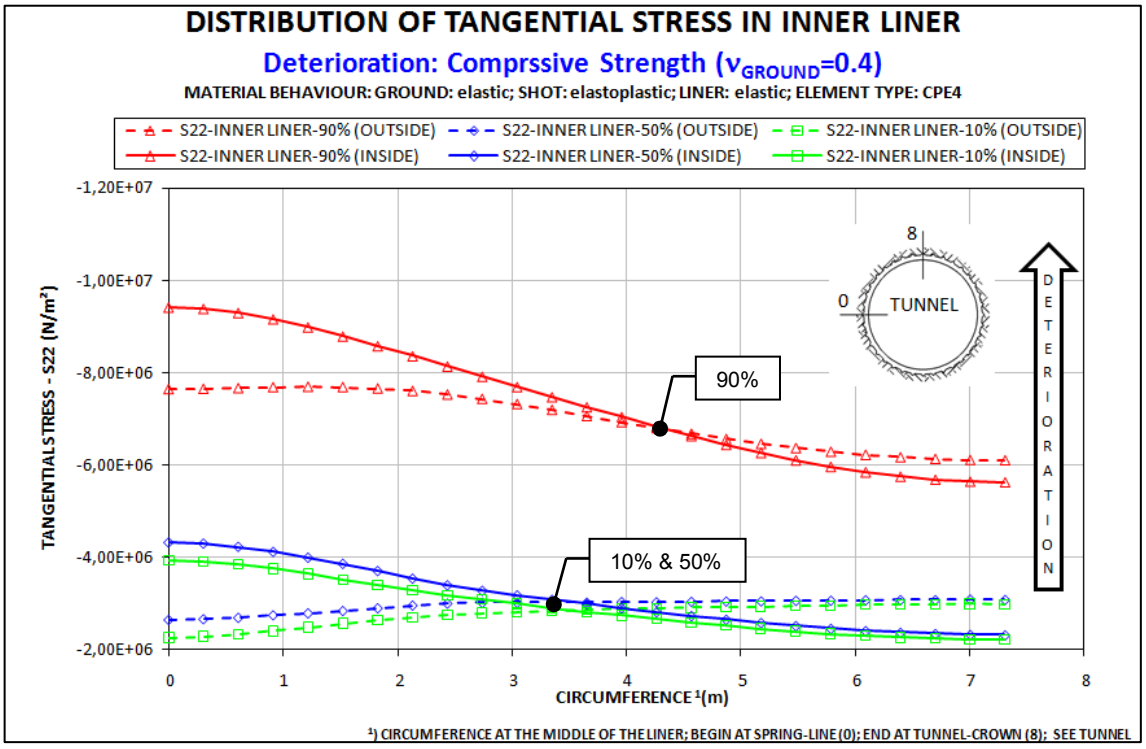

Fig. A–12: Results C04; Stresses at the outside and inside of the inner liner for three deterioration steps (10%, 50%, 90%); deterioration caused by degrading compressive strength;

Combination C05

- **Deterioration:** Young's Modulus & Compressive Strength
- **Element type:** CPE4
- **Ground parameters:**
  - **Poisson's ratio:** $\nu = 0.5$
  - **Material behavior:** linear elastic
- **Shotcrete shell parameters:**
  - **Poisson's ratio:** $\nu = 0.2$
  - **Material behavior:** linear elastic
- **Inner liner parameters:**
  - **Poisson's ratio:** $\nu = 0.2$
  - **Material behavior:** linear elastic

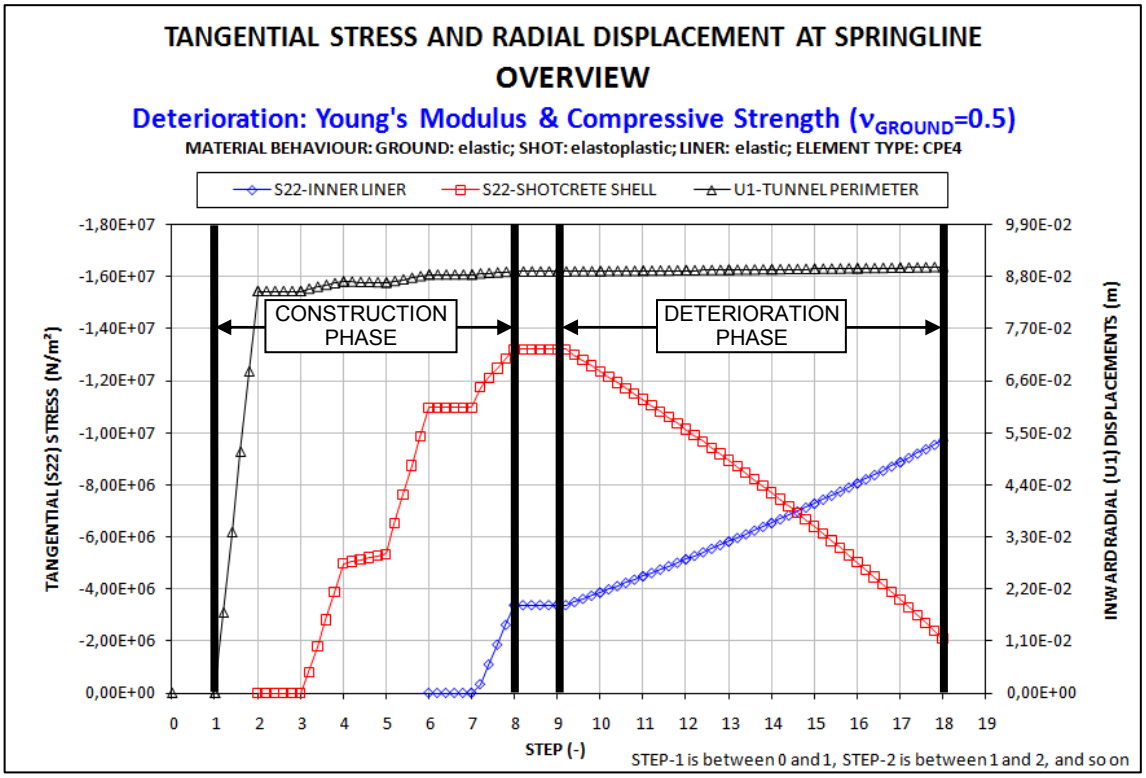

Fig. A–13: Results C05; Overview of stresses in the inner liner and shotcrete shell as well as radial displacements; all results are obtained at the spring-line; construction phase and deterioration phase;

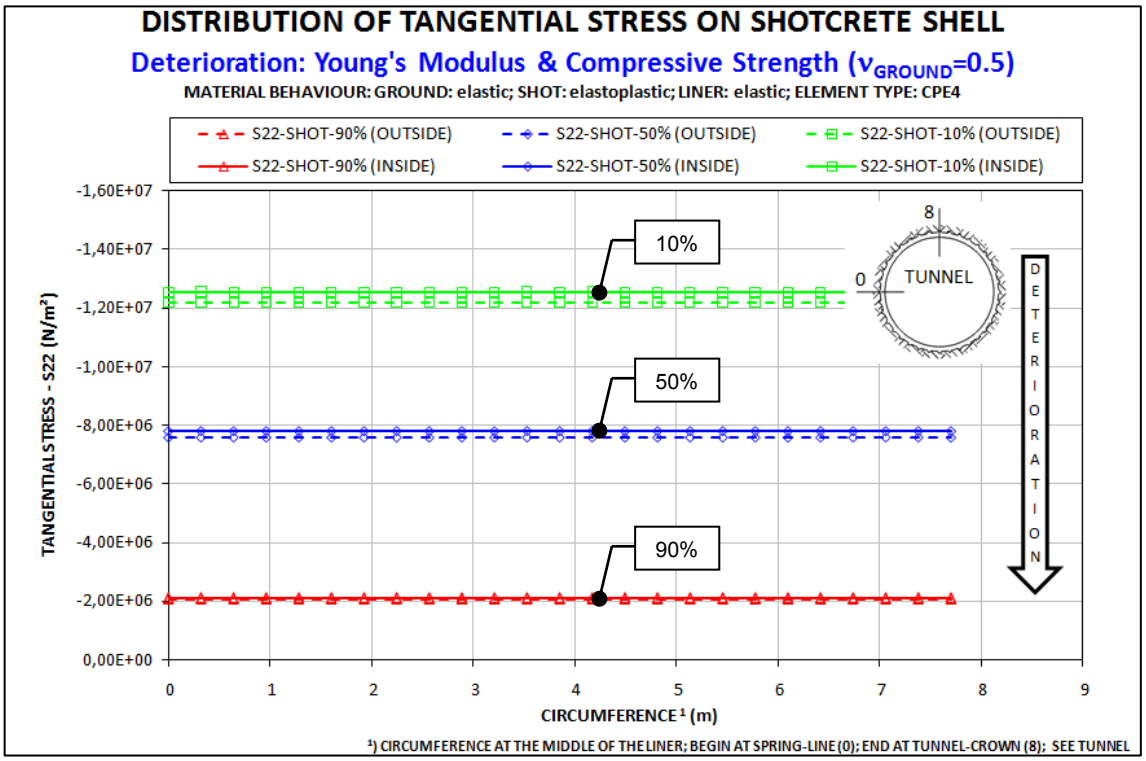

Fig. A–14: Results C05; Stresses at the outside and inside of the shotcrete shell for three deterioration steps (10%, 50%, 90%); deterioration caused by simultaneously degrading Young's modulus and compressive strength;

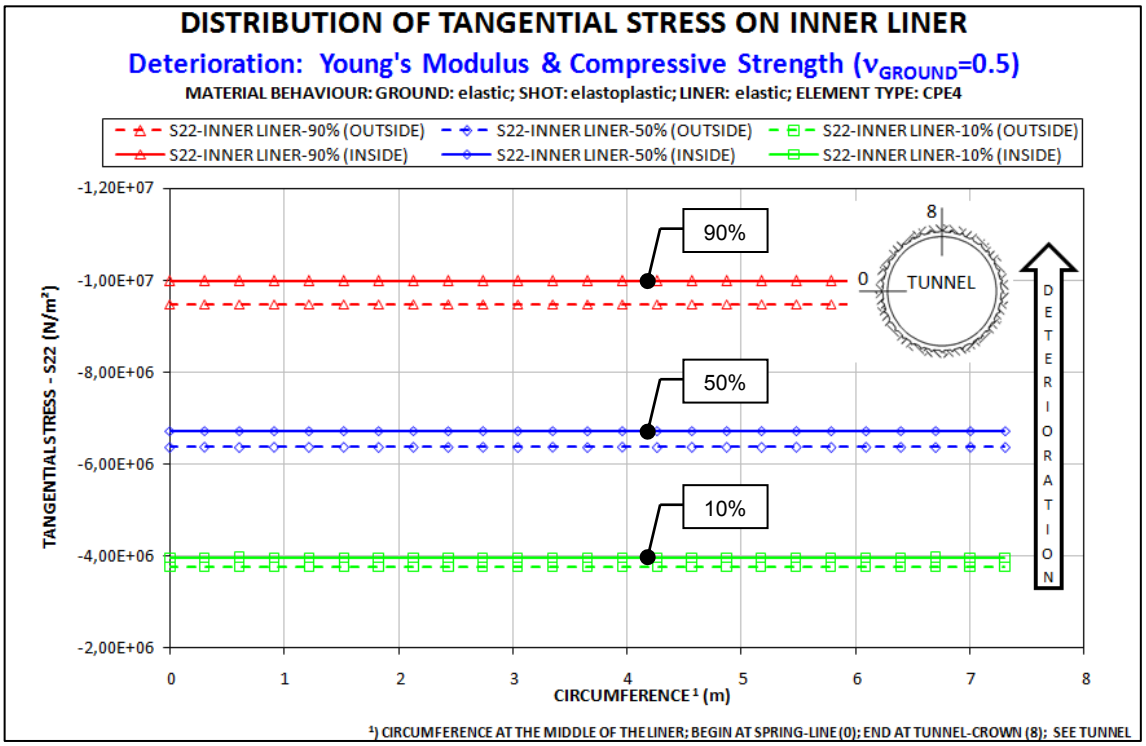

Fig. A–15: Results C05; Stresses at the outside and inside of the inner liner for three deterioration steps (10%, 50%, 90%); deterioration caused by simultaneously degrading Young's modulus and compressive strength;

Combination C06

- **Deterioration:** Young's Modulus & Compressive Strength
- **Element type:** CPE4
- **Ground parameters:**
  - **Poisson's ratio:** $\nu = 0.4$
  - **Material behavior:** linear elastic
- **Shotcrete shell parameters:**
  - **Poisson's ratio:** $\nu = 0.2$
  - **Material behavior:** linear elastic
- **Inner liner parameters:**
  - **Poisson's ratio:** $\nu = 0.2$
  - **Material behavior:** linear elastic

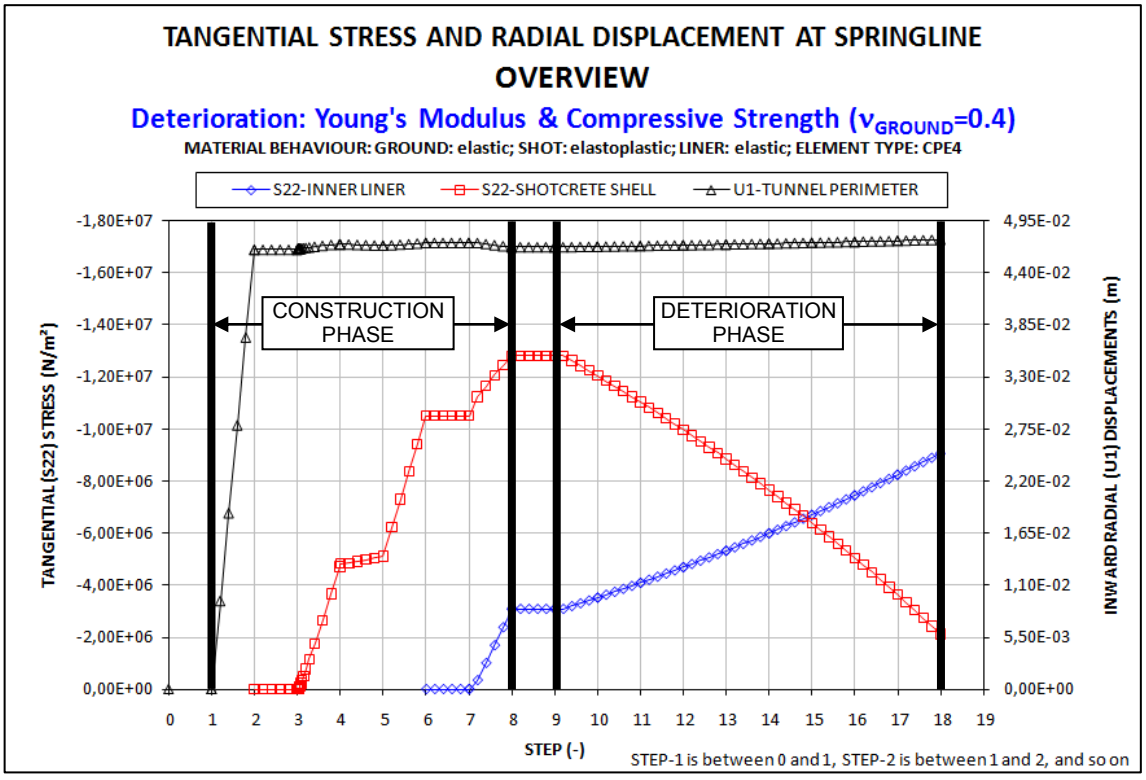

Fig. A–16: Results C06; Overview of stresses in the inner liner and shotcrete shell as well as radial displacements; all results are obtained at the spring-line; construction phase and deterioration phase;

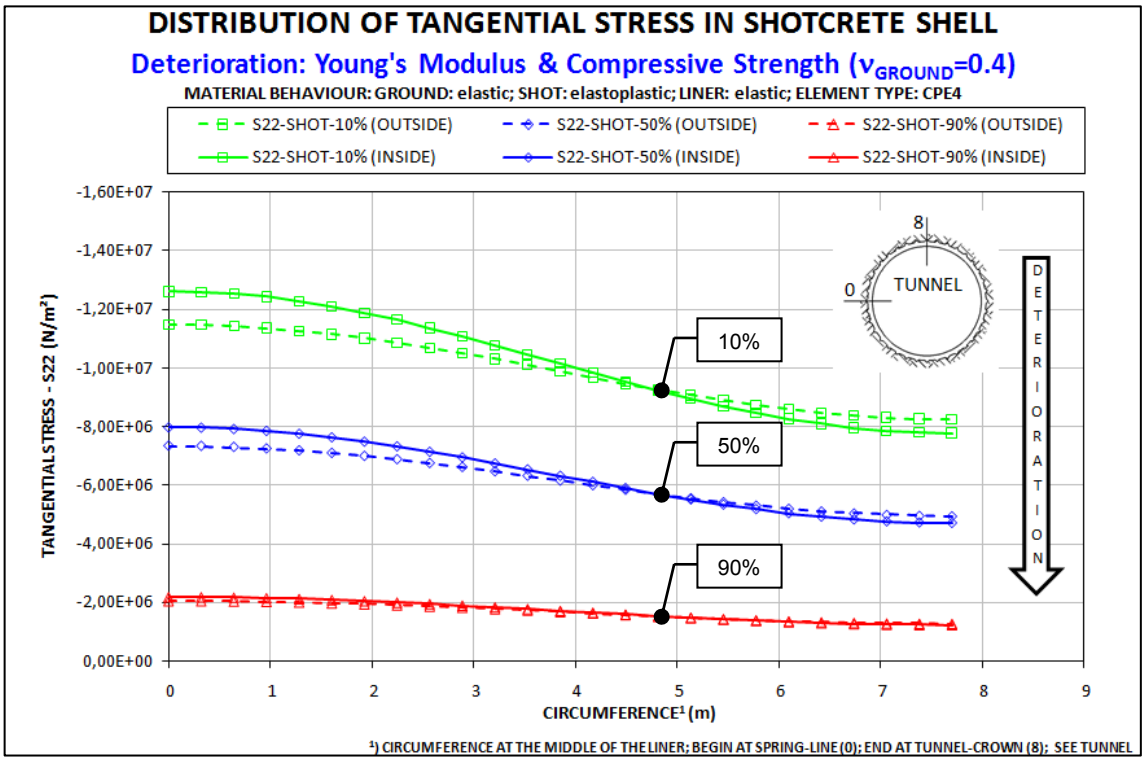

Fig. A–17: Results C06; Stresses at the outside and inside of the shotcrete shell for three deterioration steps (10%, 50%, 90%); deterioration caused by simultaneously degrading Young's modulus and compressive strength;

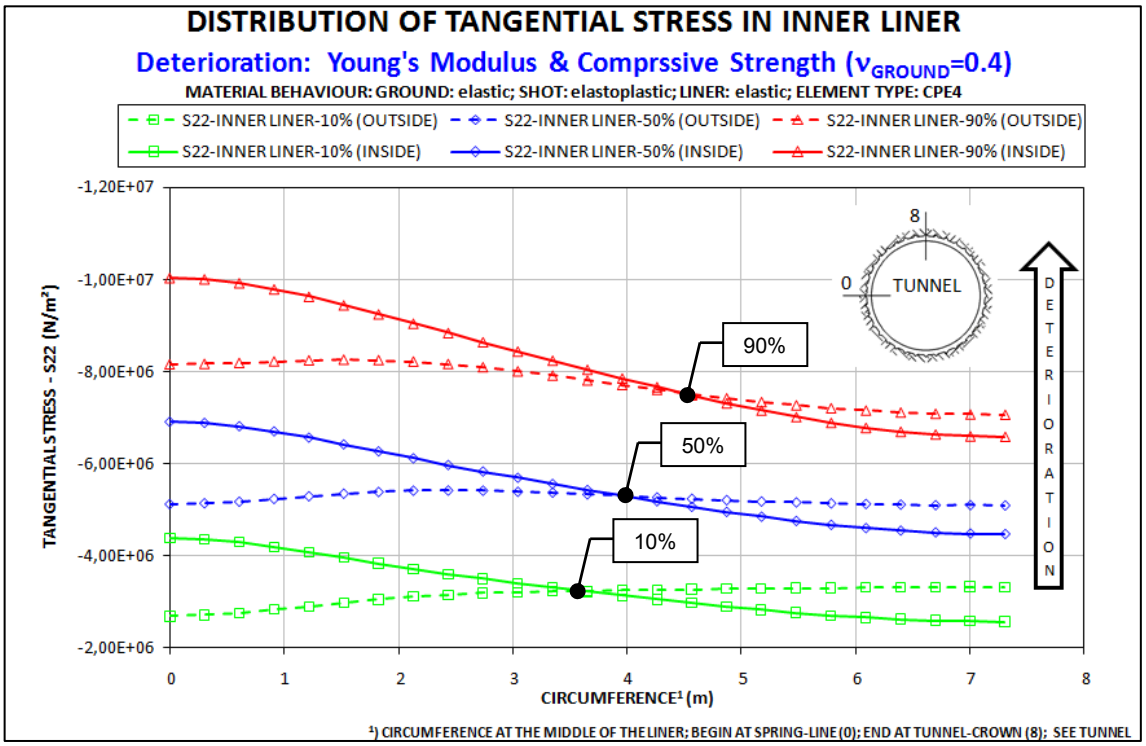

Fig. A–18: Results C06; Stresses at the outside and inside of the inner liner for three deterioration steps (10%, 50%, 90%); deterioration caused by simultaneously degrading Young's modulus and compressive strength;

Results of Case B

Combination C07

- **Deterioration:** Young's Modulus
- **Element type:** CPE4
- **Ground parameters:**
  - **Poisson's ratio:** $\nu = 0.5$
  - **Material behavior:** linearly elastic – perfectly plastic
- **Shotcrete shell parameters:**
  - **Poisson's ratio:** $\nu = 0.2$
  - **Material behavior:** linear elastic
- **Inner liner parameters:**
  - **Poisson's ratio:** $\nu = 0.2$
  - **Material behavior:** linear elastic

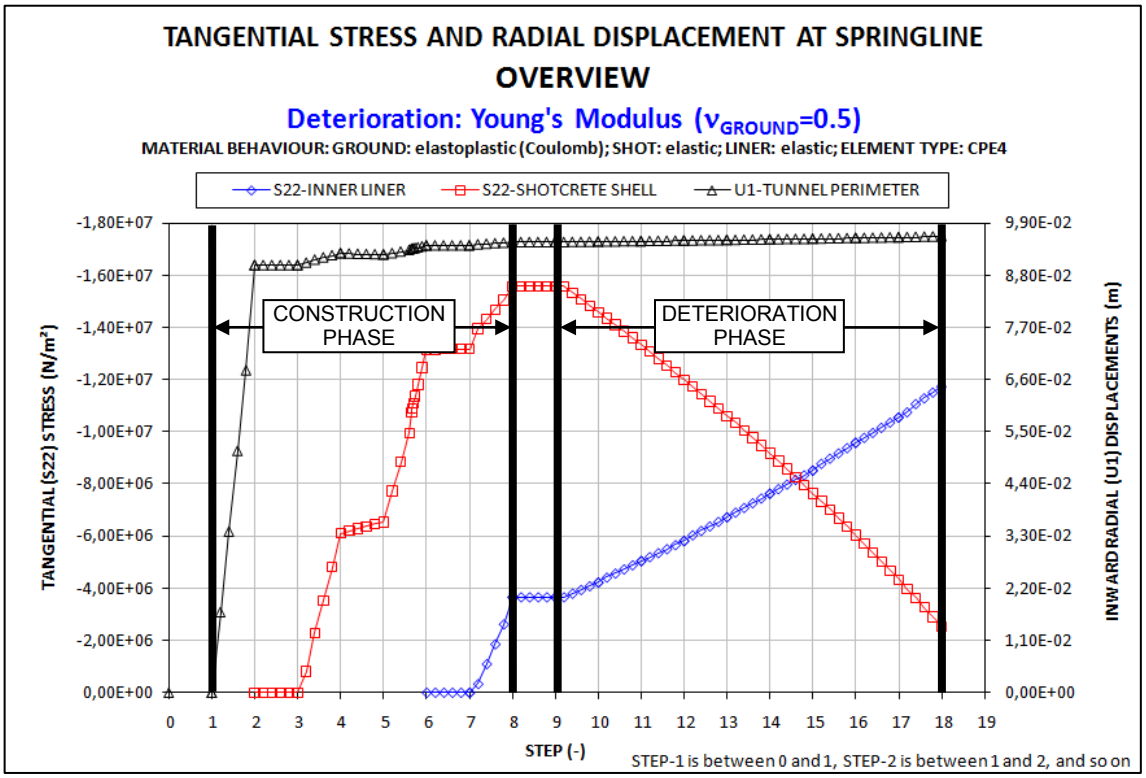

Fig. A–19: Results C07; Overview of stresses in the inner liner and shotcrete shell as well as radial displacements; all results are obtained at the spring-line; construction phase and deterioration phase;

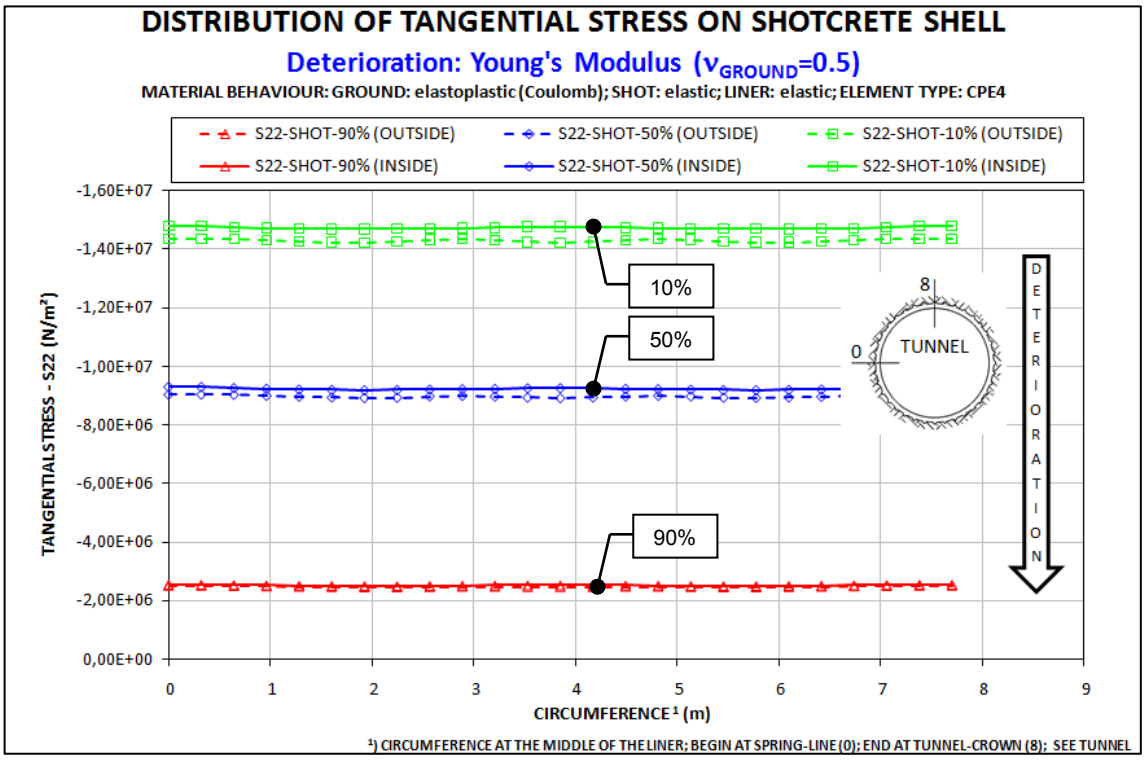

Fig. A–20: Results C07; Stresses at the outside and inside of the shotcrete shell for three deterioration steps (10%, 50%, 90%); deterioration caused by degrading Young's modulus;

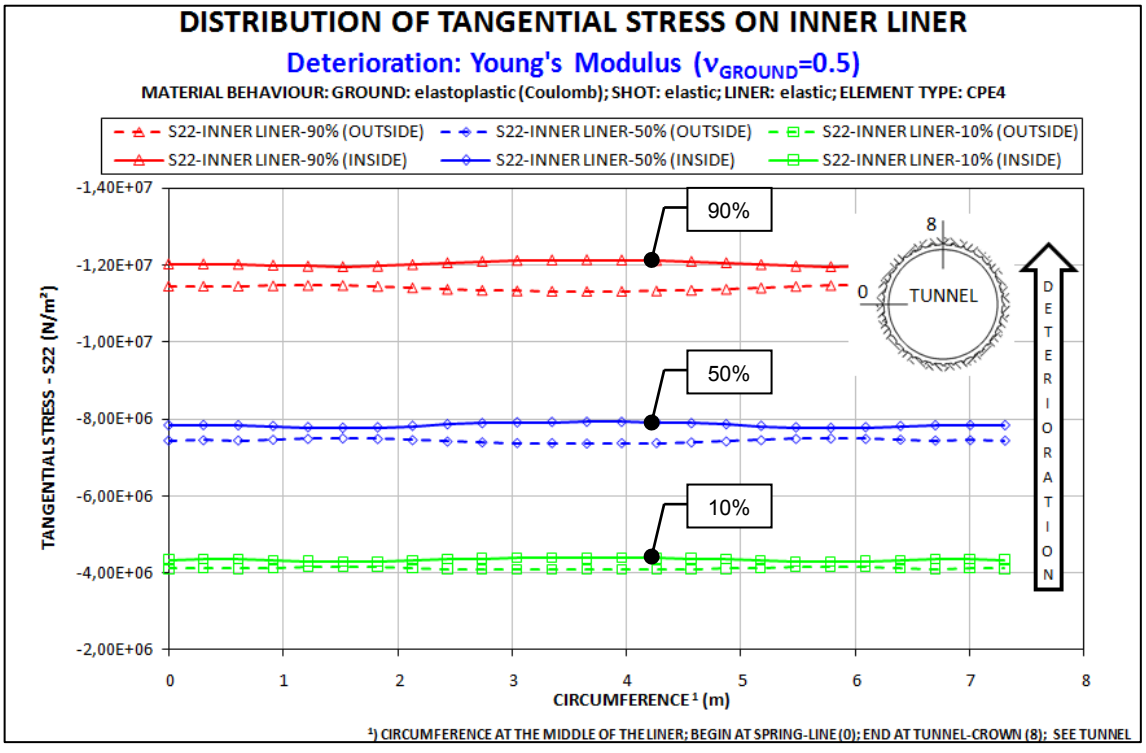

Fig. A–21: Results C07; Stresses at the outside and inside of the inner liner for three deterioration steps (10%, 50%, 90%); deterioration caused by degrading Young's modulus;

Combination C08

- **Deterioration:** Young's Modulus
- **Element type:** CPE4
- **Ground parameters:**
  - **Poisson's ratio:** $\nu = 0.4$
  - **Material behavior:** linearly elastic – perfectly plastic
- **Shotcrete shell parameters:**
  - **Poisson's ratio:** $\nu = 0.2$
  - **Material behavior:** linear elastic
- **Inner liner parameters:**
  - **Poisson's ratio:** $\nu = 0.2$
  - **Material behavior:** linear elastic

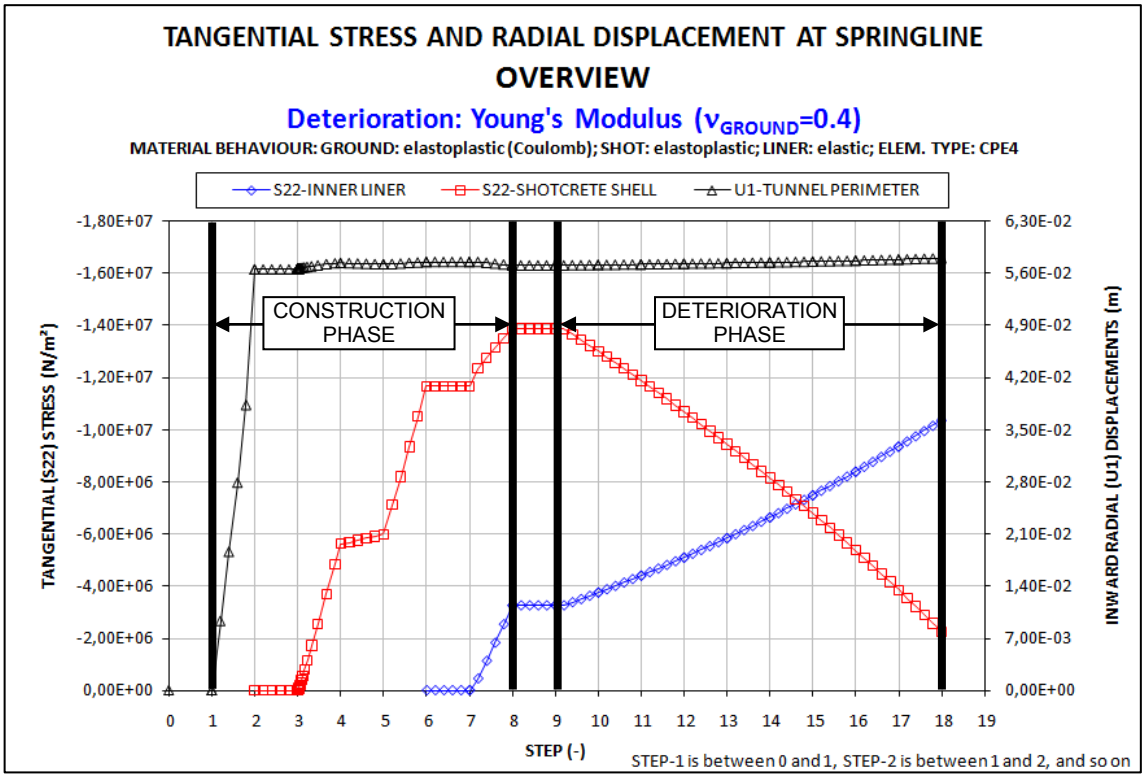

Fig. A–22: Results C08; Overview of stresses in the inner liner and shotcrete shell as well as radial displacements; all results are obtained at the spring-line; construction phase and deterioration phase;

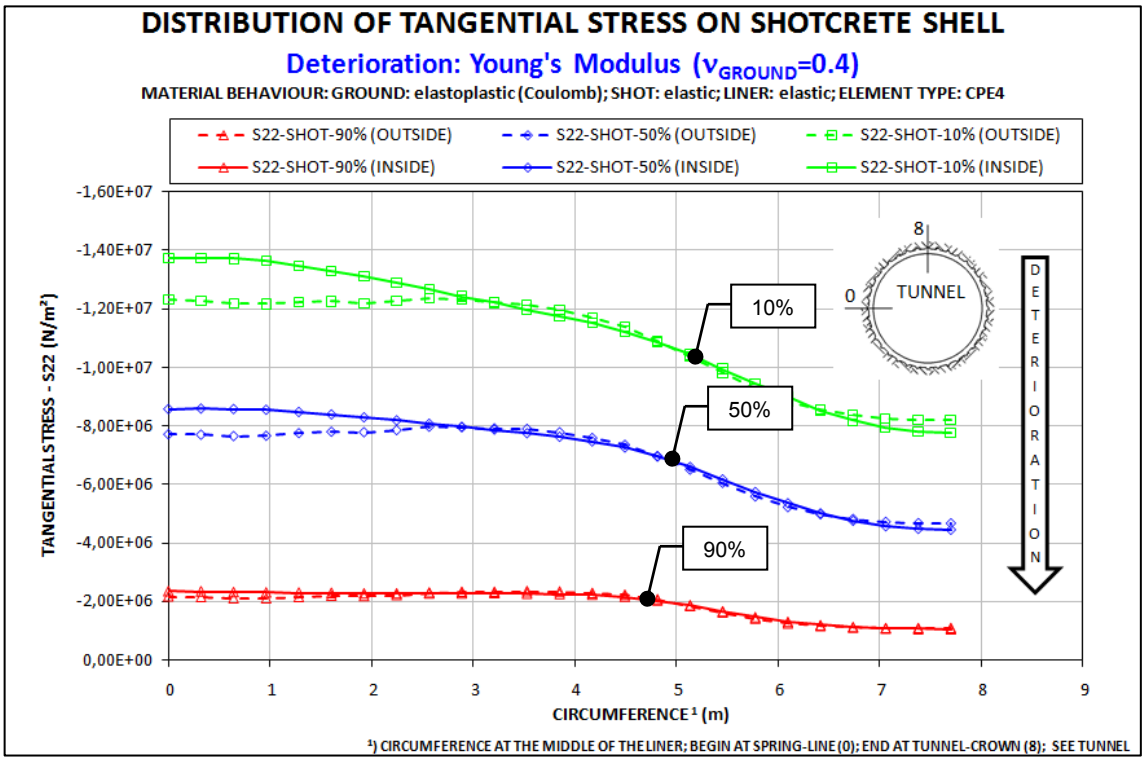

Fig. A–23: Results C08; Stresses at the outside and inside of the shotcrete shell for three deterioration steps (10%, 50%, 90%); deterioration caused by degrading Young's modulus;

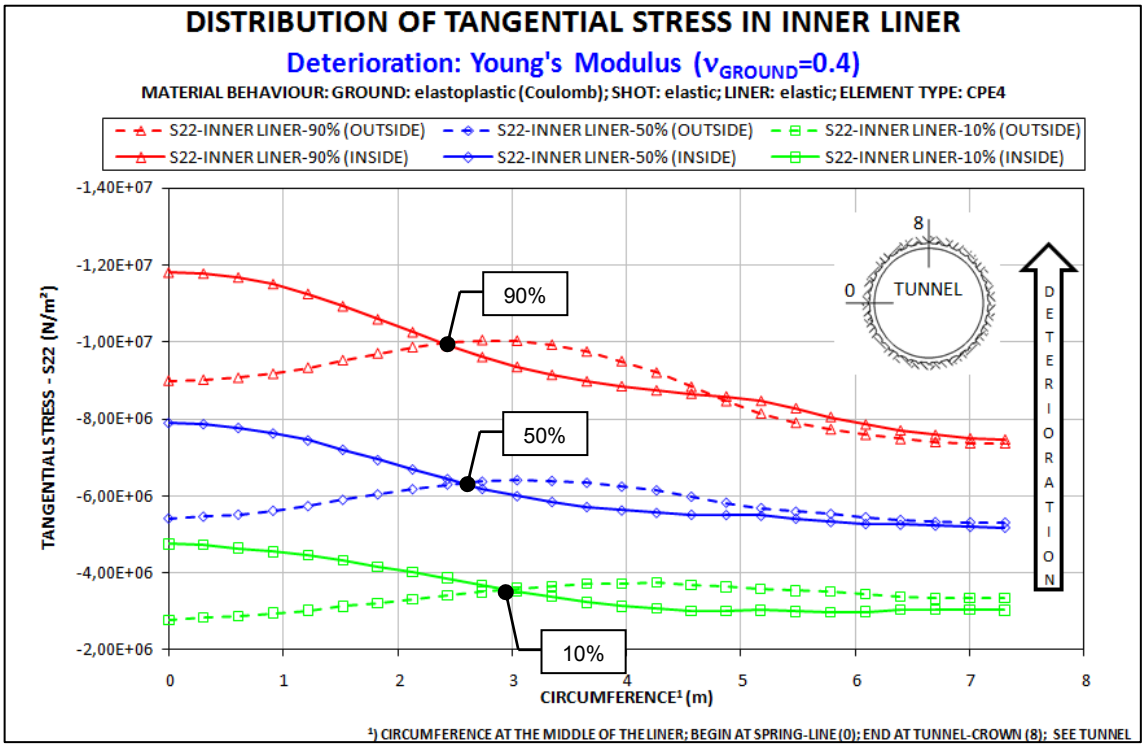

Fig. A–24: Results C08; Stresses at the outside and inside of the inner liner for three deterioration steps (10%, 50%, 90%); deterioration caused by degrading Young's modulus;

Combination C09

- **Deterioration:** Compressive Strength
- **Element type:** CPE4
- **Ground parameters:**
  - **Poisson's ratio:** $\nu = 0.5$
  - **Material behavior:** linearly elastic – perfectly plastic
- **Shotcrete shell parameters:**
  - **Poisson's ratio:** $\nu = 0.2$
  - **Material behavior:** linear elastic
- **Inner liner parameters:**
  - **Poisson's ratio:** $\nu = 0.2$
  - **Material behavior:** linear elastic

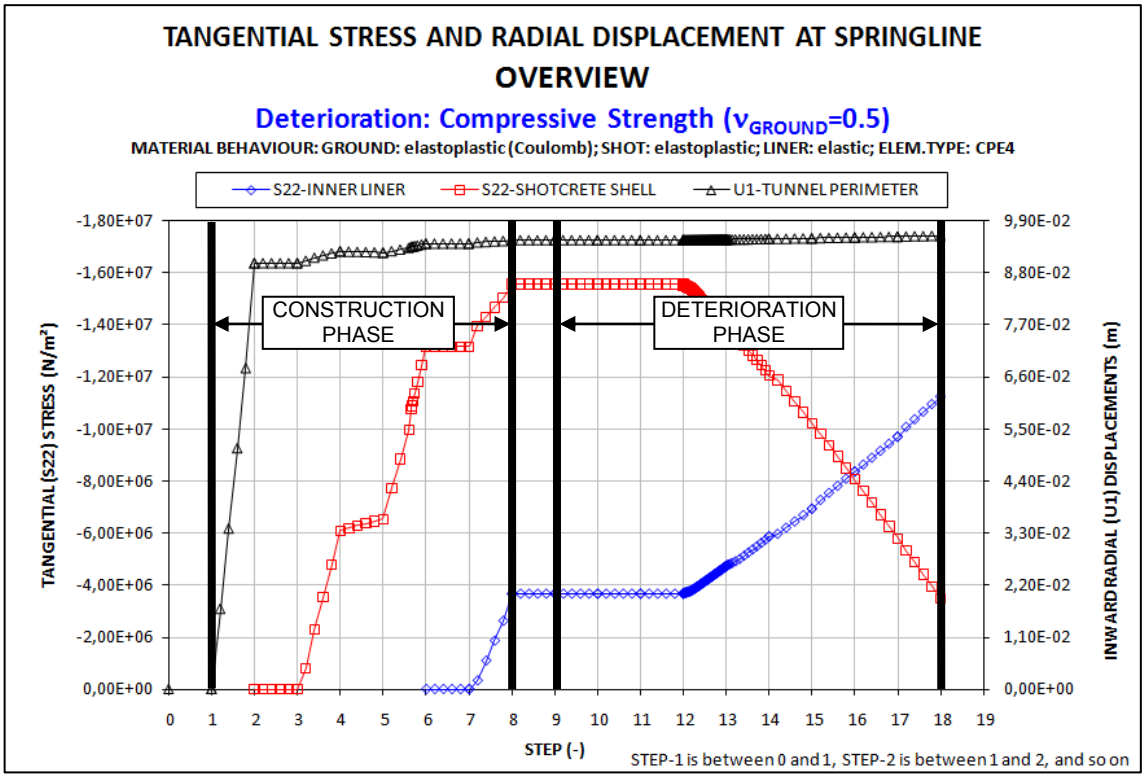

Fig. A–25: Results C09; Overview of stresses in the inner liner and shotcrete shell as well as radial displacements; all results are obtained at the spring-line; construction phase and deterioration phase;

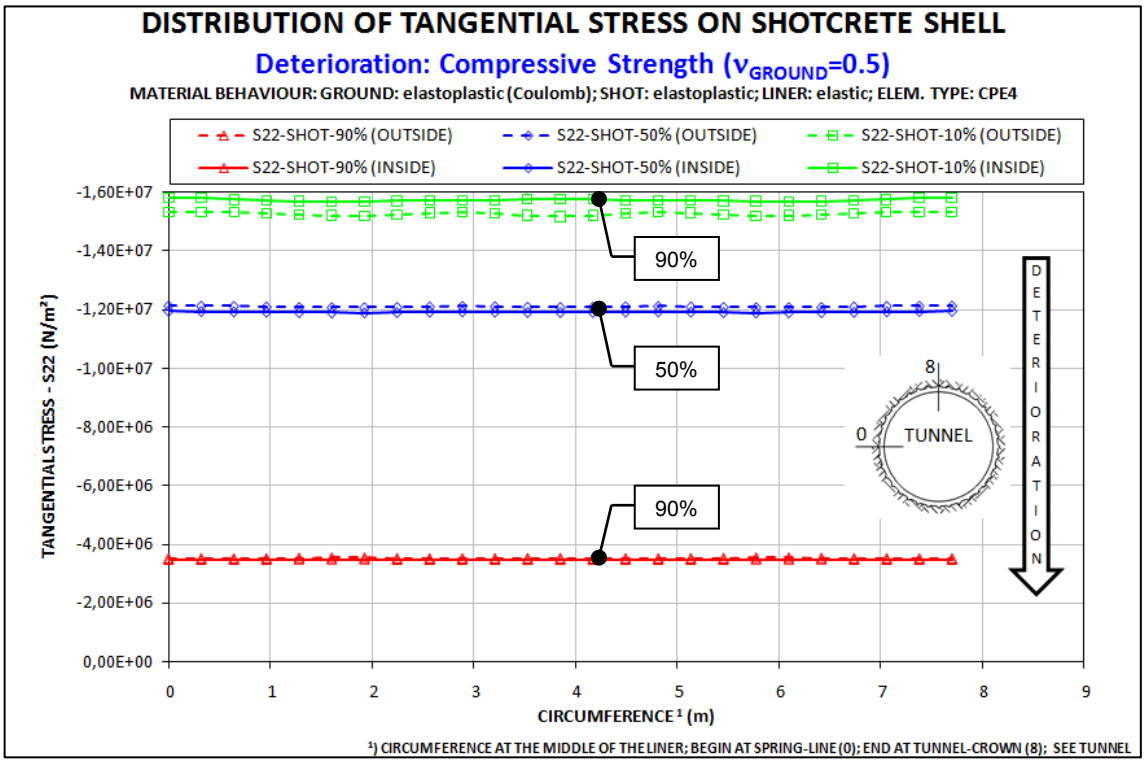

Fig. A–26: Results C09; Stresses at the outside and inside of the shotcrete shell for three deterioration steps (10%, 50%, 90%); deterioration caused by degrading compressive strength;

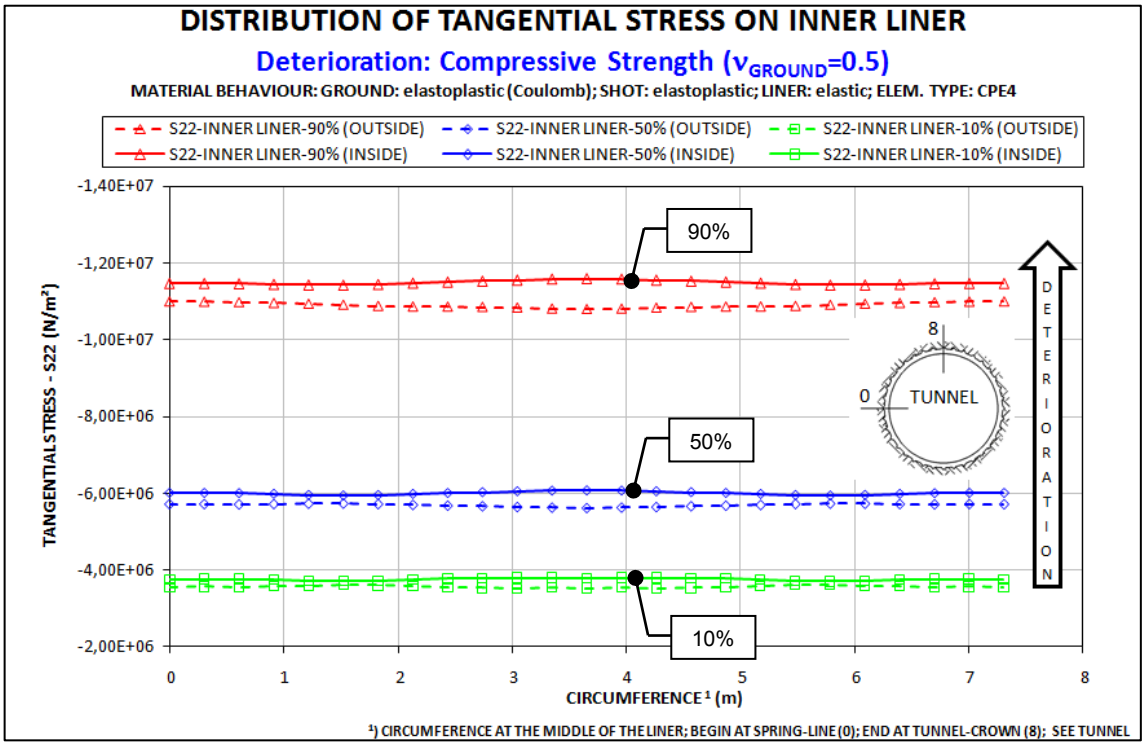

Fig. A–27: Results C09; Stresses at the outside and inside of the inner liner for three deterioration steps (10%, 50%, 90%); deterioration caused by degrading compressive strength;

Combination C10

- **Deterioration:** Compressive Strength
- **Element type:** CPE4
- **Ground parameters:**
  - **Poisson's ratio:** $\nu = 0.4$
  - **Material behavior:** linearly elastic – perfectly plastic
- **Shotcrete shell parameters:**
  - **Poisson's ratio:** $\nu = 0.2$
  - **Material behavior:** linear elastic
- **Inner liner parameters:**
  - **Poisson's ratio:** $\nu = 0.2$
  - **Material behavior:** linear elastic

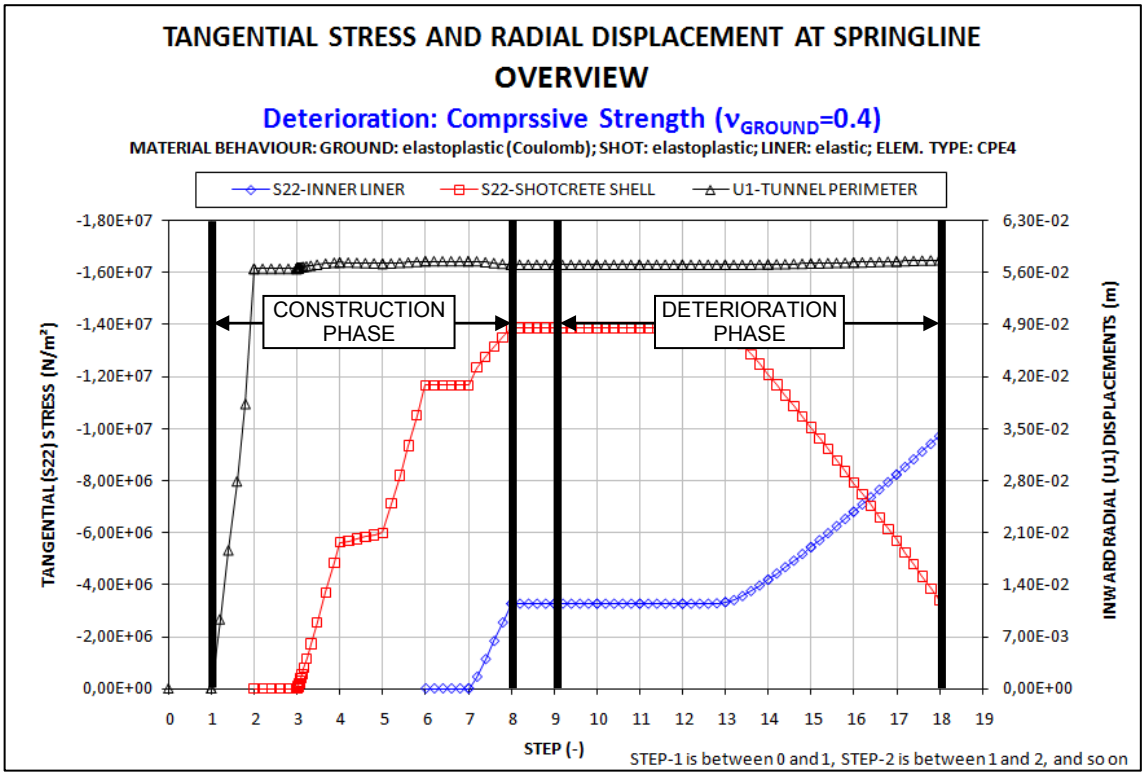

Fig. A–28: Results C10; Overview of stresses in the inner liner and shotcrete shell as well as radial displacements; all results are obtained at the spring-line; construction phase and deterioration phase;

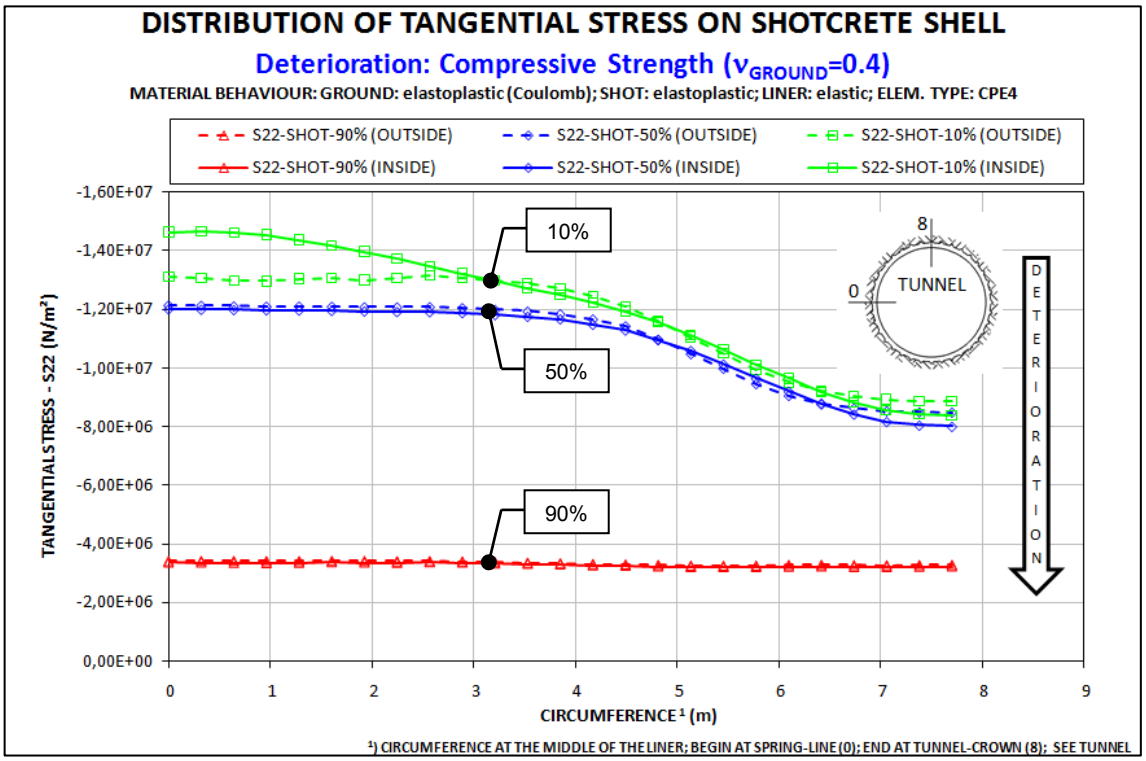

Fig. A–29: Results C10; Stresses at the outside and inside of the shotcrete shell for three deterioration steps (10%, 50%, 90%); deterioration caused by degrading compressive strength;

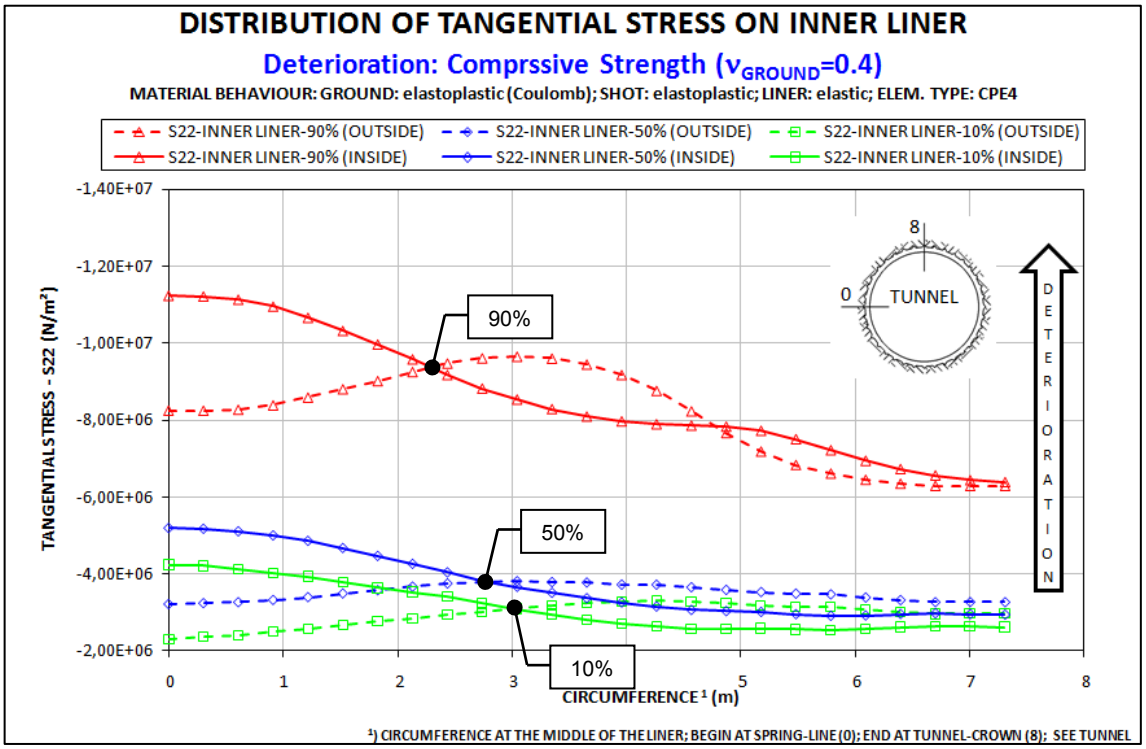

Fig. A–30: Results C10; Stresses at the outside and inside of the inner liner for three deterioration steps (10%, 50%, 90%); deterioration caused by degrading compressive strength;

Combination C11

- **Deterioration:** Young's Modulus & Compressive Strength
- **Element type:** CPE4
- **Ground parameters:**
  - **Poisson's ratio:** $\nu = 0.5$
  - **Material behavior:** linearly elastic – perfectly plastic
- **Shotcrete shell parameters:**
  - **Poisson's ratio:** $\nu = 0.2$
  - **Material behavior:** linear elastic
- **Inner liner parameters:**
  - **Poisson's ratio:** $\nu = 0.2$
  - **Material behavior:** linear elastic

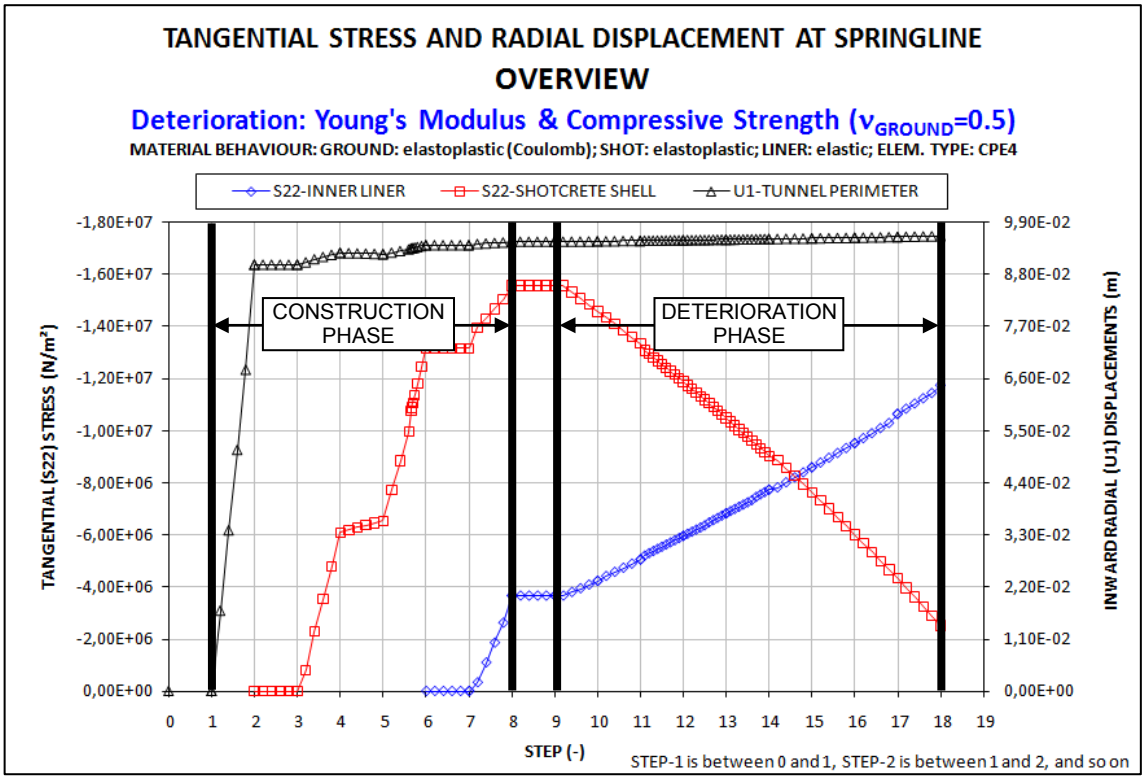

Fig. A–31: Results C11; Overview of stresses in the inner liner and shotcrete shell as well as radial displacements; all results are obtained at the spring-line; construction phase and deterioration phase;

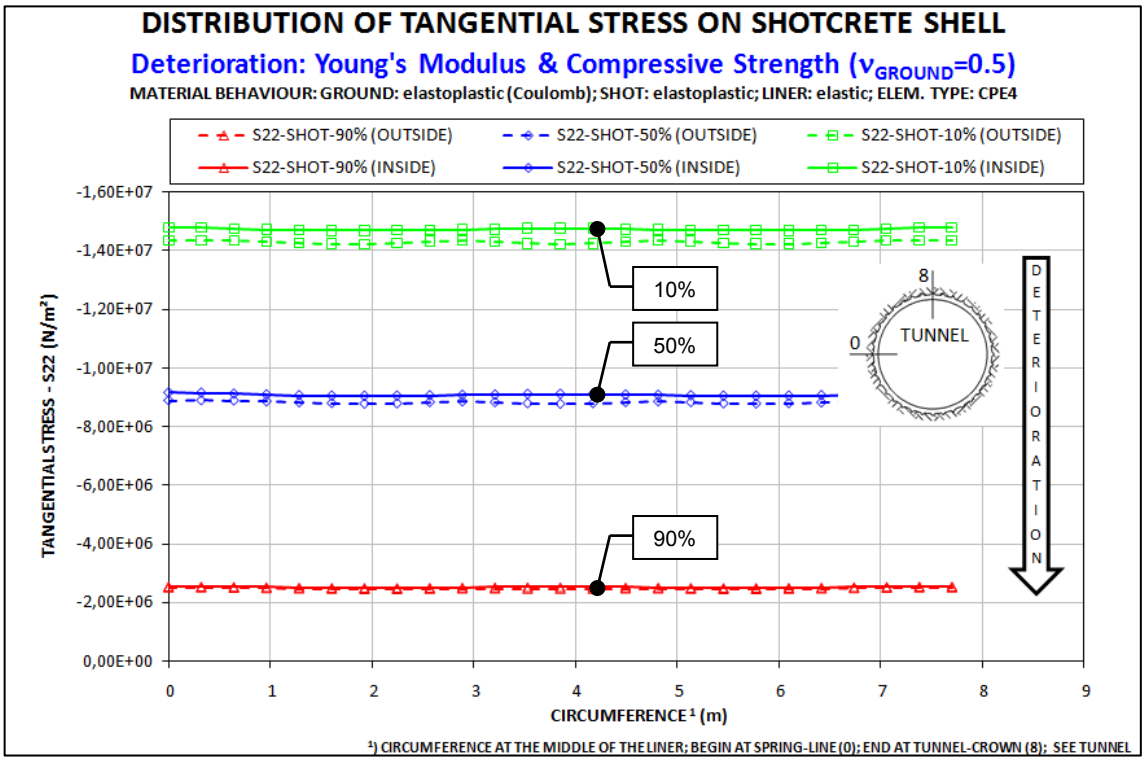

Fig. A–32: Results C11; Stresses at the outside and inside of the shotcrete shell for three deterioration steps (10%, 50%, 90%); deterioration caused by simultaneously degrading Young's modulus and compressive strength;

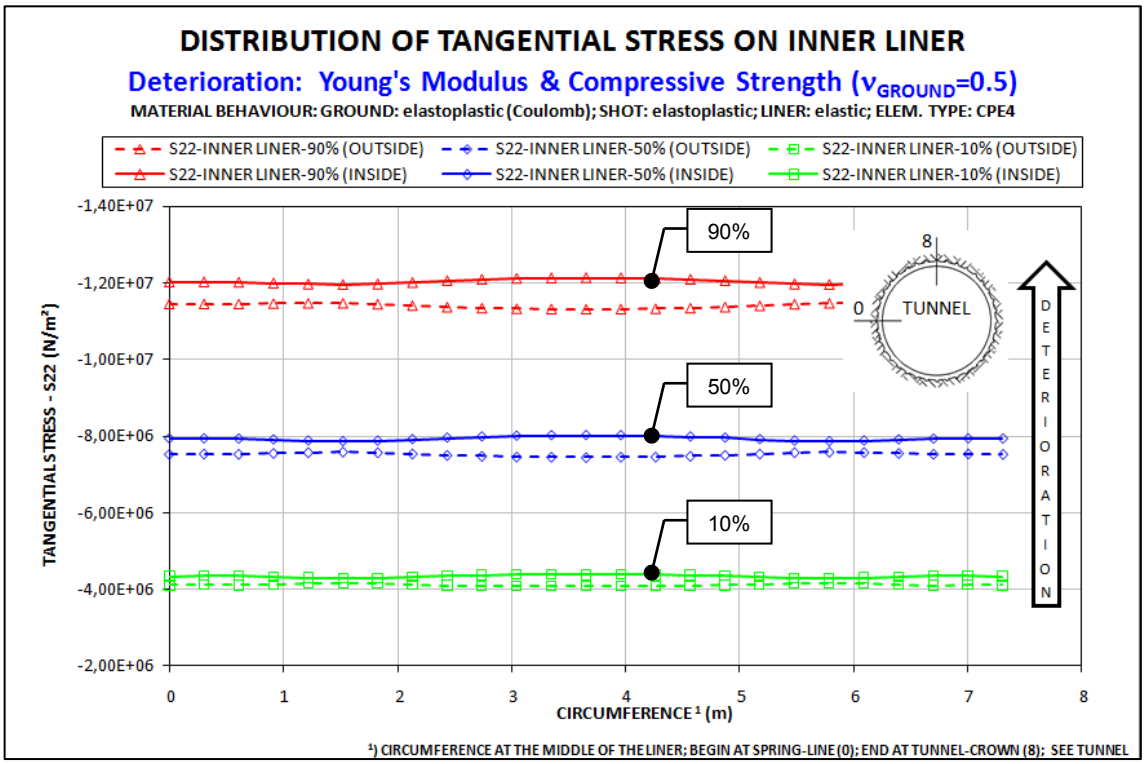

Fig. A–33: Results C11; Stresses at the outside and inside of the inner liner for three deterioration steps (10%, 50%, 90%); deterioration caused by simultaneously degrading Young's modulus and compressive strength;

Combination C12

- **Deterioration:** Young's Modulus & Compressive Strength
- **Element type:** CPE4
- **Ground parameters:**
  - **Poisson's ratio:** $\nu = 0.4$
  - **Material behavior:** linearly elastic – perfectly plastic
- **Shotcrete shell parameters:**
  - **Poisson's ratio:** $\nu = 0.2$
  - **Material behavior:** linear elastic
- **Inner liner parameters:**
  - **Poisson's ratio:** $\nu = 0.2$
  - **Material behavior:** linear elastic

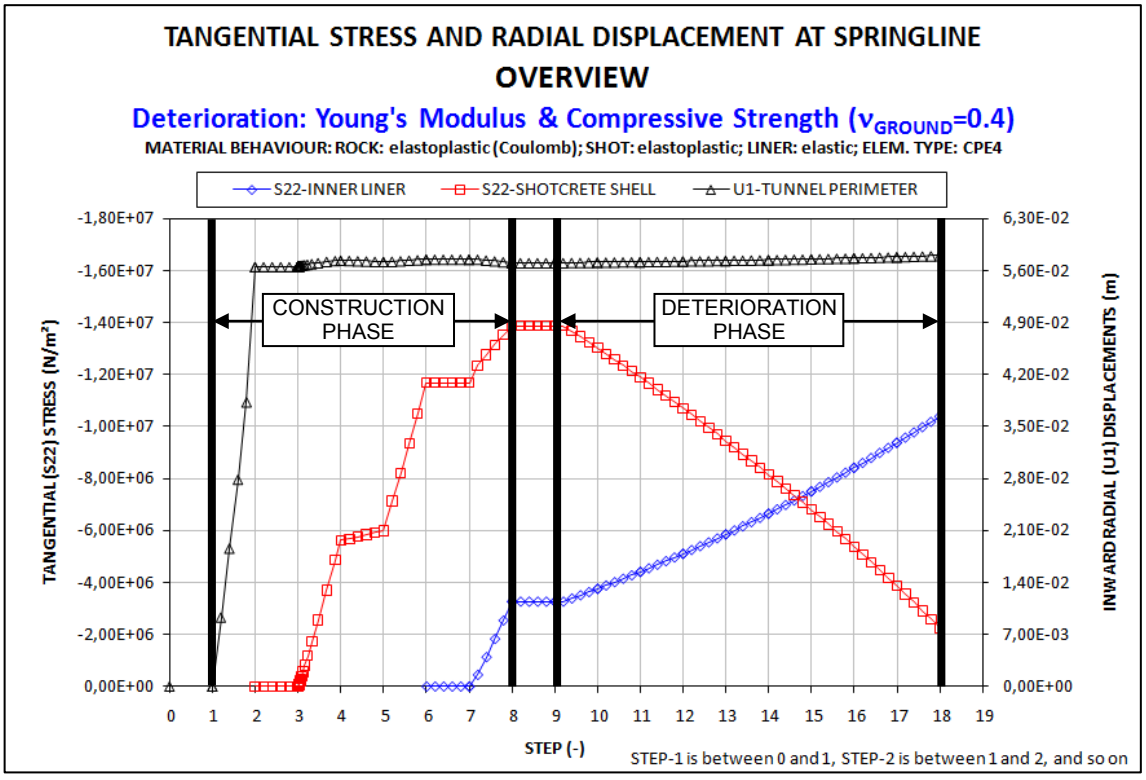

Fig. A–34: Results C12; Overview of stresses in the inner liner and shotcrete shell as well as radial displacements; all results are obtained at the spring-line; construction phase and deterioration phase;

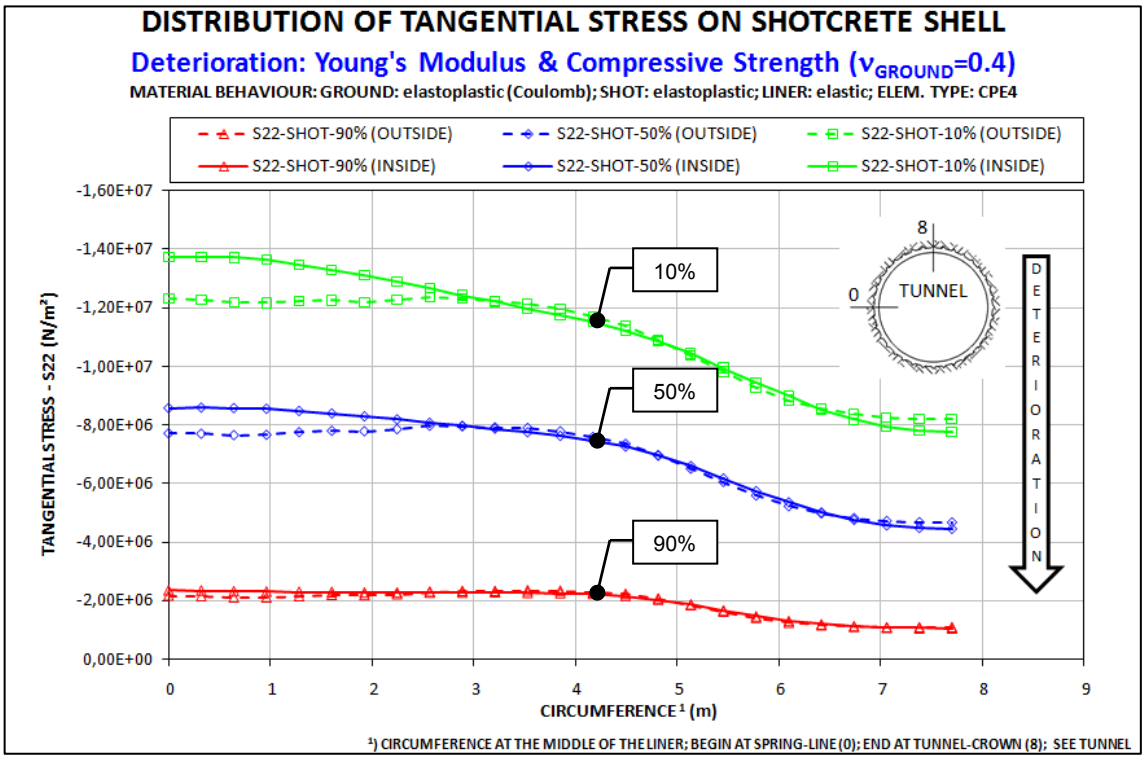

Fig. A–35: Results C12; Stresses at the outside and inside of the shotcrete shell for three deterioration steps (10%, 50%, 90%); deterioration caused by simultaneously degrading Young's modulus and compressive strength;

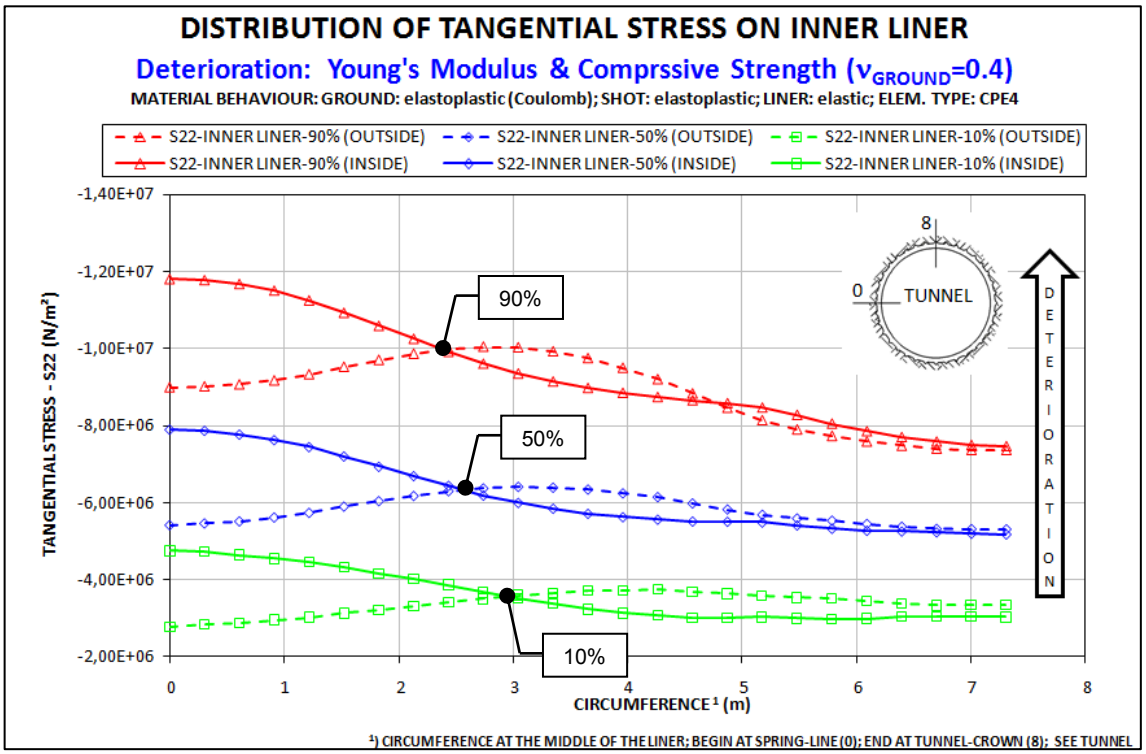

Fig. A–36: Results C12; Stresses at the outside and inside of the inner liner for three deterioration steps (10%, 50%, 90%); deterioration caused by simultaneously degrading Young's modulus and compressive strength;

Results of Case C

Combination C13

- **Deterioration:** Young's Modulus
- **Element type:** CPE8R
- **Ground parameters:**
  - **Poisson's ratio:** $\nu = 0.5$
  - **Material behavior:** linear elastic
- **Shotcrete shell parameters:**
  - **Poisson's ratio:** $\nu = 0.2$
  - **Material behavior:** linear elastic
- **Inner liner parameters:**
  - **Poisson's ratio:** $\nu = 0.2$
  - **Material behavior:** linear elastic

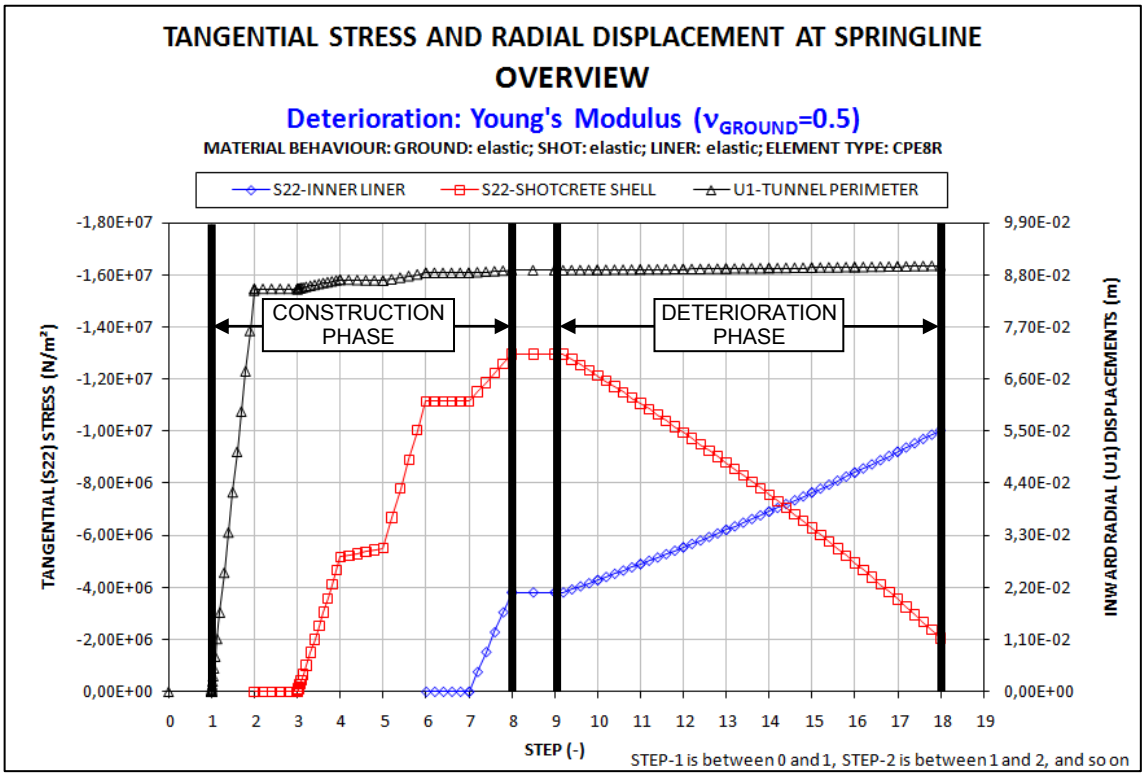

Fig. A–37: Results C13; Overview of stresses in the inner liner and shotcrete shell as well as radial displacements; all results are obtained at the spring-line; construction phase and deterioration phase;

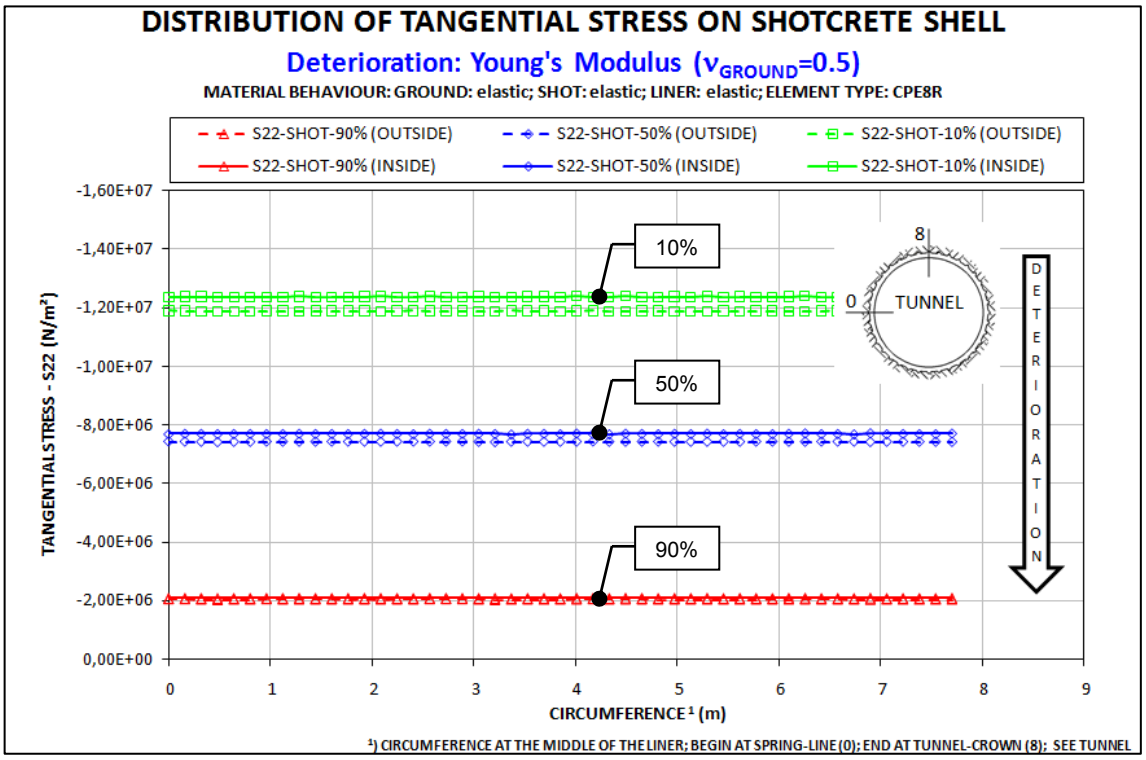

Fig. A–38: Results C13; Stresses at the outside and inside of the shotcrete shell for three deterioration steps (10%, 50%, 90%); deterioration caused by degrading Young's modulus;

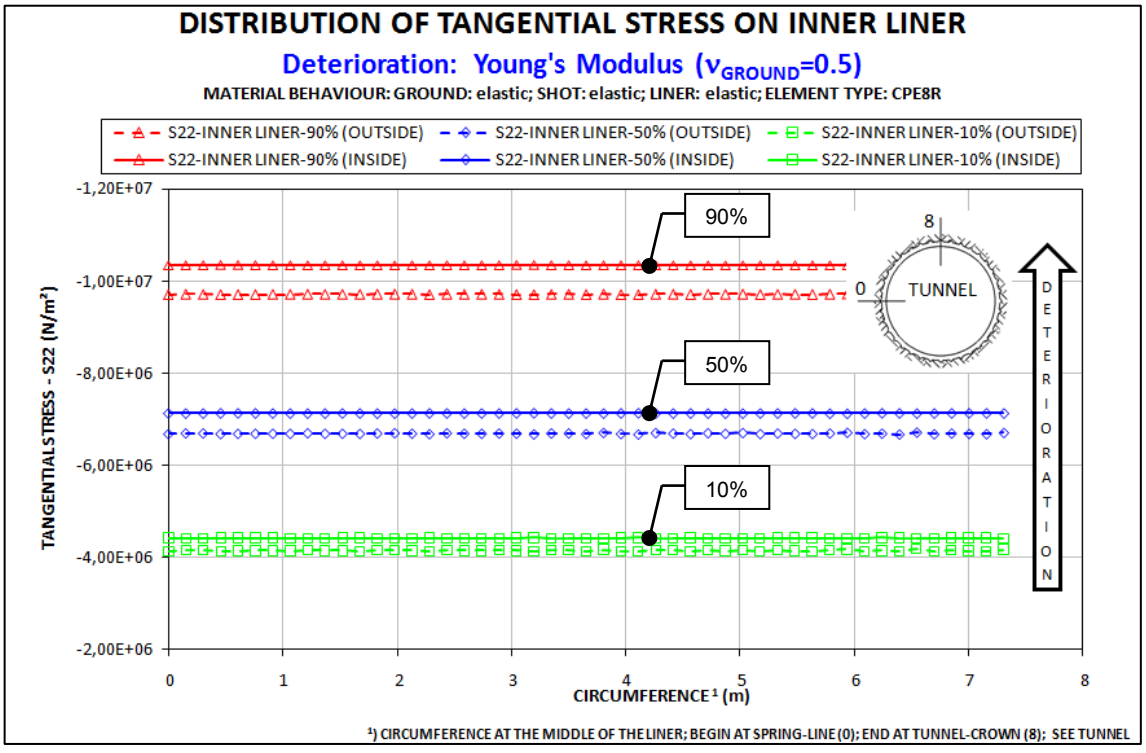

Fig. A–39: Results C13; Stresses at the outside and inside of the inner liner for three deterioration steps (10%, 50%, 90%); deterioration caused by degrading Young's modulus;

Combination C14

- **Deterioration:** Young's Modulus
- **Element type:**CPE8R
- **Ground parameters:**
  - **Poisson's ratio:** $\nu = 0.4$
  - **Material behavior:** linear elastic
- **Shotcrete shell parameters:**
  - **Poisson's ratio:** $\nu = 0.2$
  - **Material behavior:** linear elastic
- **Inner liner parameters:**
  - **Poisson's ratio:** $\nu = 0.2$
  - **Material behavior:** linear elastic

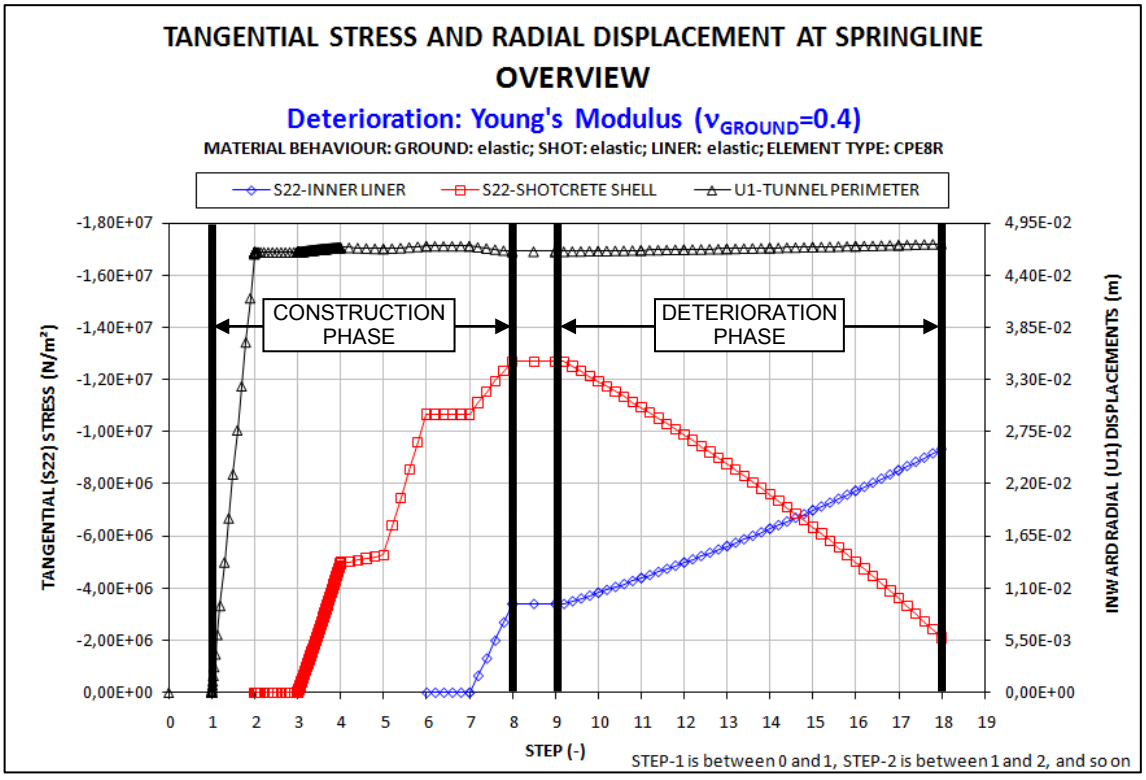

Fig. A–40: Results C14; Overview of stresses in the inner liner and shotcrete shell as well as radial displacements; all results are obtained at the spring-line; construction phase and deterioration phase;

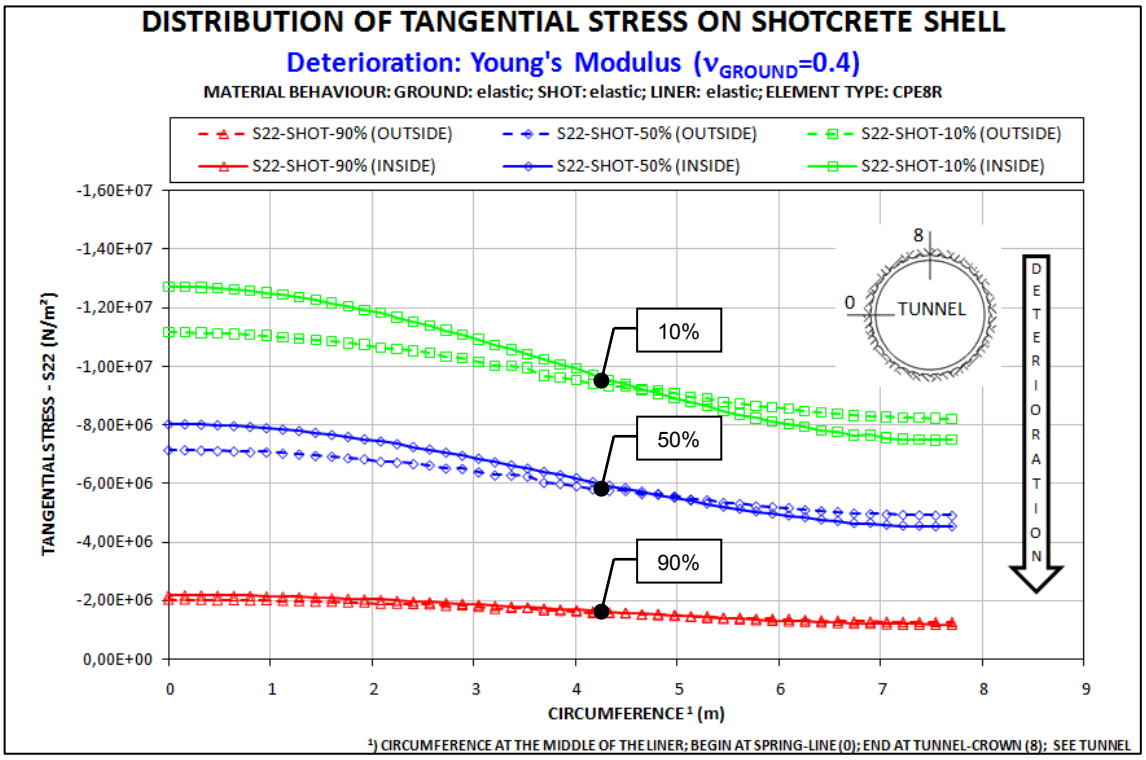

Fig. A–41: Results C14; Stresses at the outside and inside of the shotcrete shell for three deterioration steps (10%, 50%, 90%); deterioration caused by degrading Young's modulus;

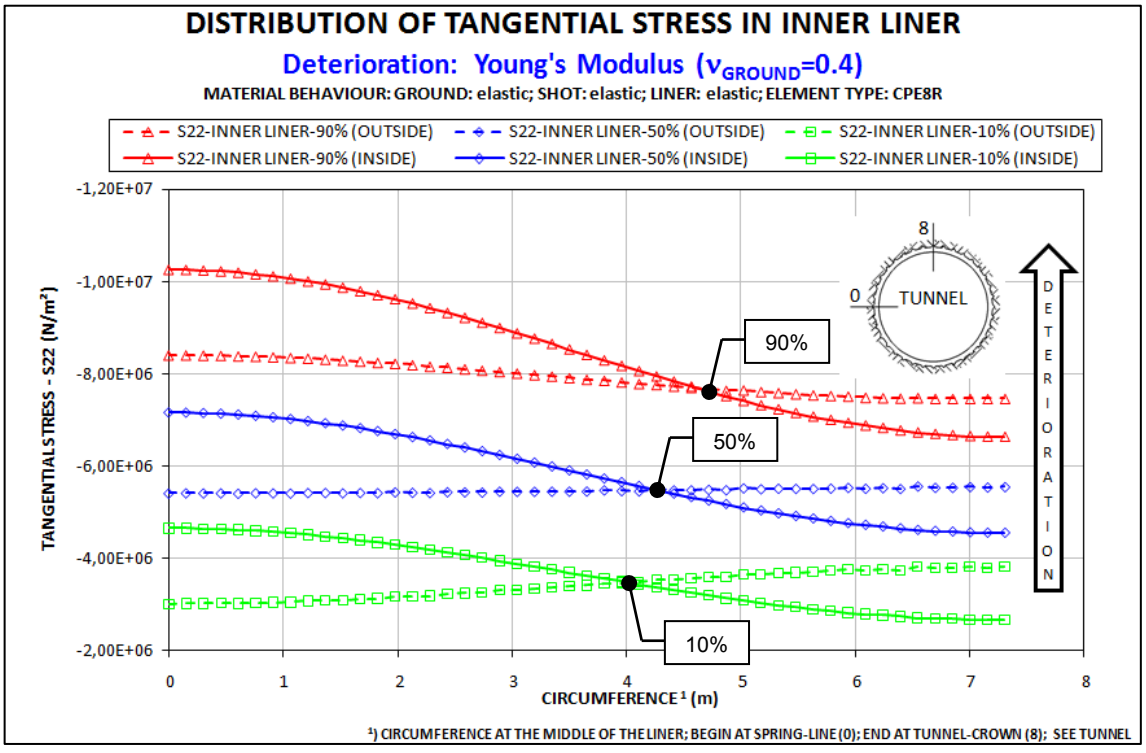

Fig. A–42: Results C14; Stresses at the outside and inside of the inner liner for three deterioration steps (10%, 50%, 90%); deterioration caused by degrading Young's modulus;

Combination C15

- **Deterioration:** Compressive Strength
- **Element type:** CPE8R
- **Ground parameters:**
  - **Poisson's ratio:** $\nu = 0.5$
  - **Material behavior:** linear elastic
- **Shotcrete shell parameters:**
  - **Poisson's ratio:** $\nu = 0.2$
  - **Material behavior:** linear elastic
- **Inner liner parameters:**
  - **Poisson's ratio:** $\nu = 0.2$
  - **Material behavior:** linear elastic

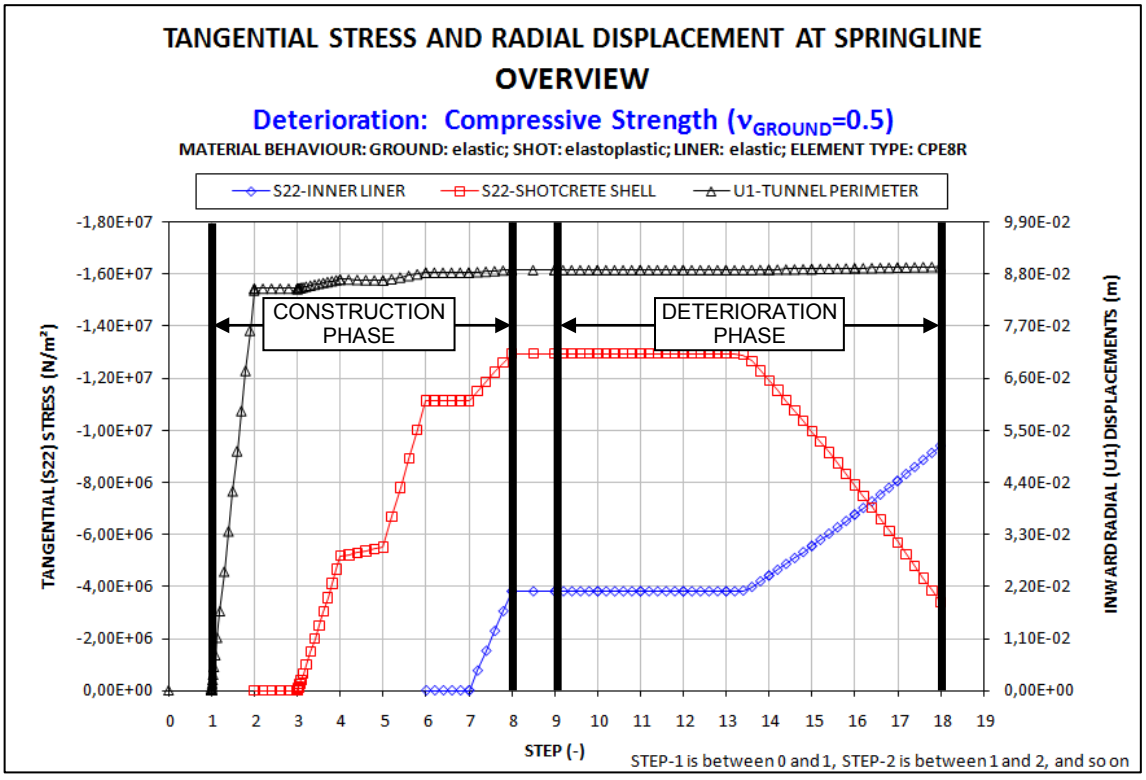

Fig. A–43: Results C15; Overview of stresses in the inner liner and shotcrete shell as well as radial displacements; all results are obtained at the spring-line; construction phase and deterioration phase;

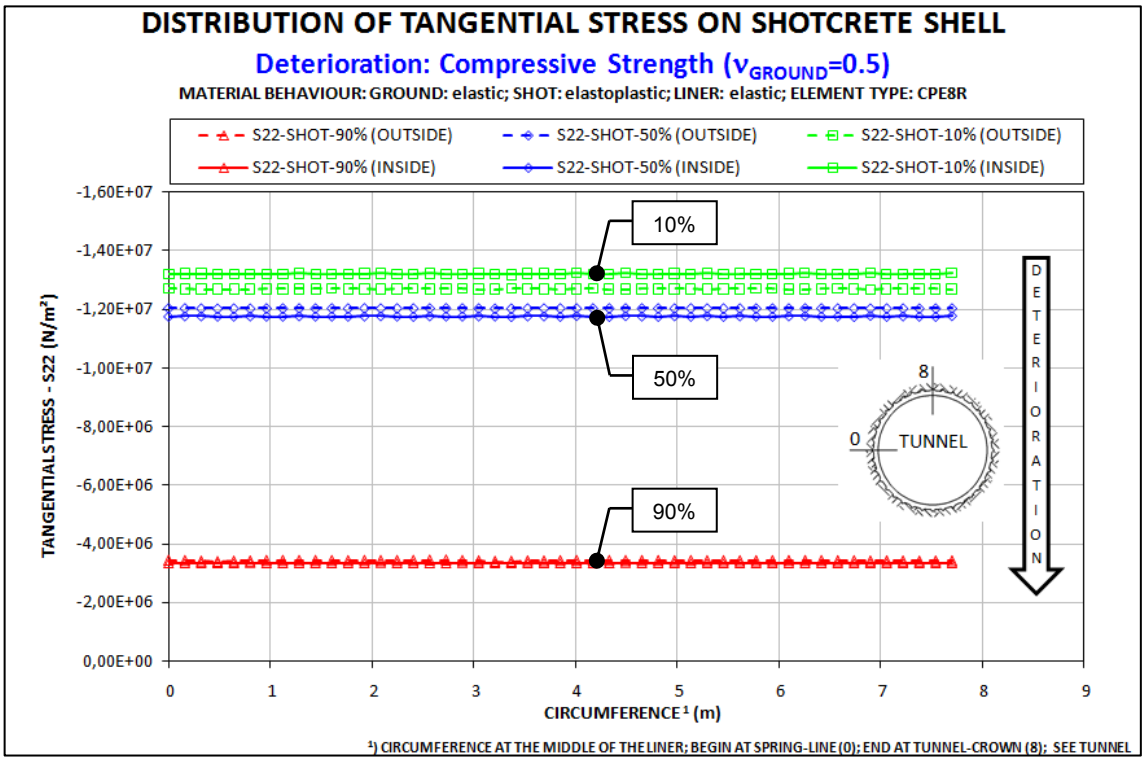

Fig. A–44: Results C15; Stresses at the outside and inside of the shotcrete shell for three deterioration steps (10%, 50%, 90%); deterioration caused by degrading compressive strength;

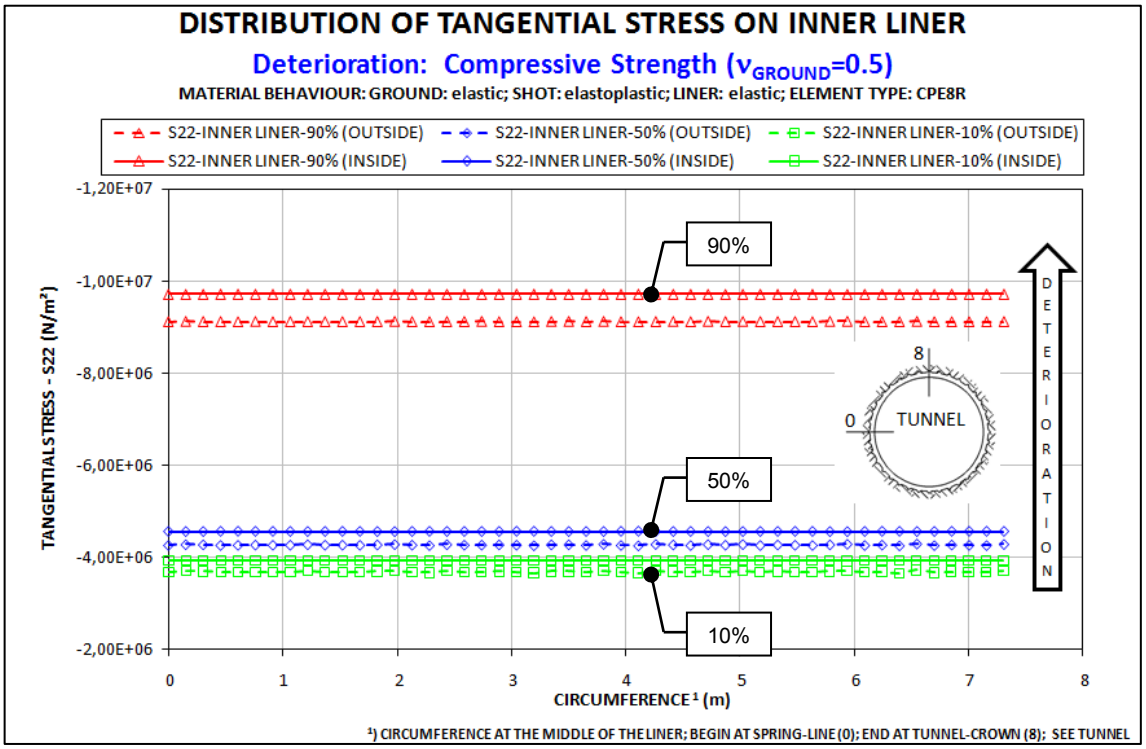

Fig. A–45: Results C15; Stresses at the outside and inside of the inner liner for three deterioration steps (10%, 50%, 90%); deterioration caused by degrading compressive strength;

Combination C16

- **Deterioration:** Compressive Strength
- **Element type:** CPE8R
- **Ground parameters:**
  - **Poisson's ratio:** $\nu = 0.4$
  - **Material behavior:** linear elastic
- **Shotcrete shell parameters:**
  - **Poisson's ratio:** $\nu = 0.2$
  - **Material behavior:** linear elastic
- **Inner liner parameters:**
  - **Poisson's ratio:** $\nu = 0.2$
  - **Material behavior:** linear elastic

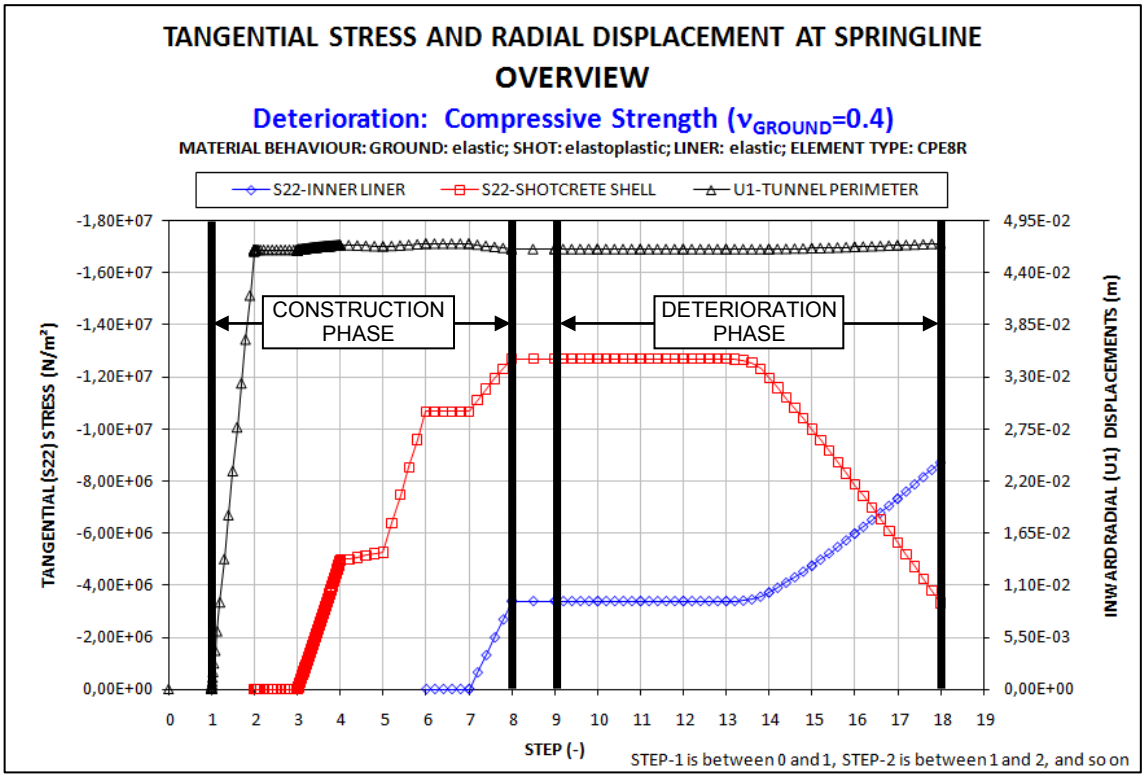

Fig. A–46: Results C16; Overview of stresses in the inner liner and shotcrete shell as well as radial displacements; all results are obtained at the spring-line; construction phase and deterioration phase;

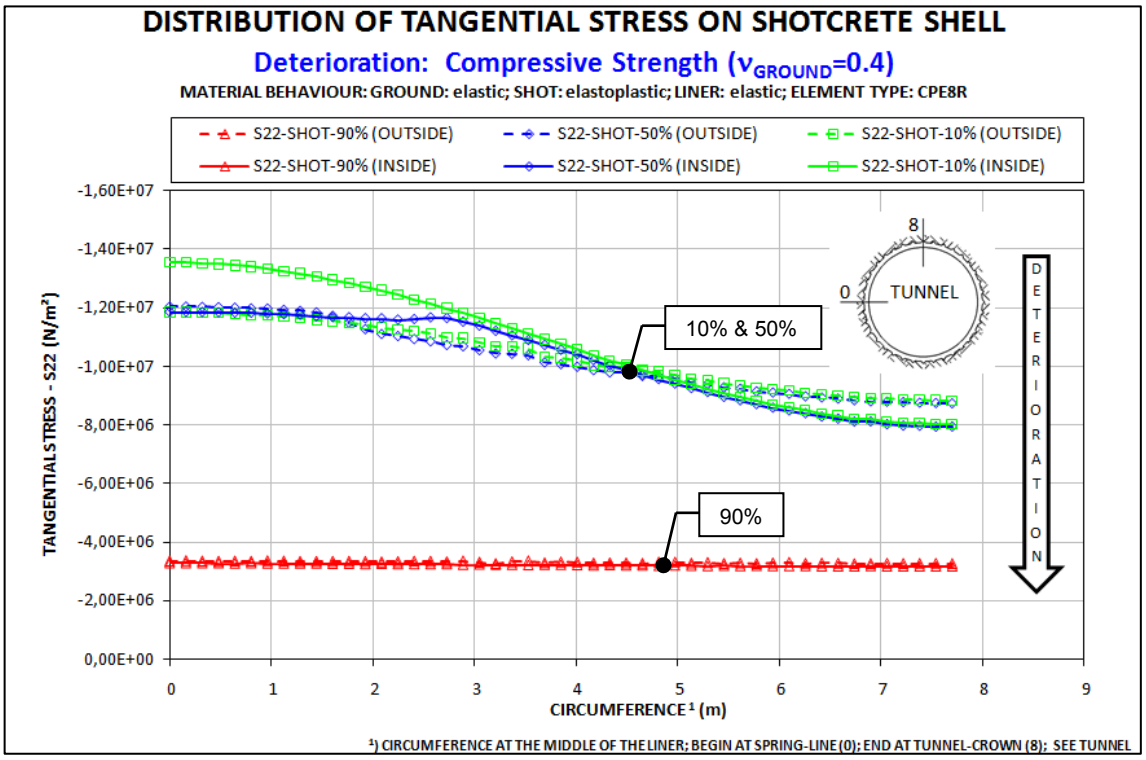

Fig. A–47: Results C16; Stresses at the outside and inside of the shotcrete shell for three deterioration steps (10%, 50%, 90%); deterioration caused by degrading compressive strength;

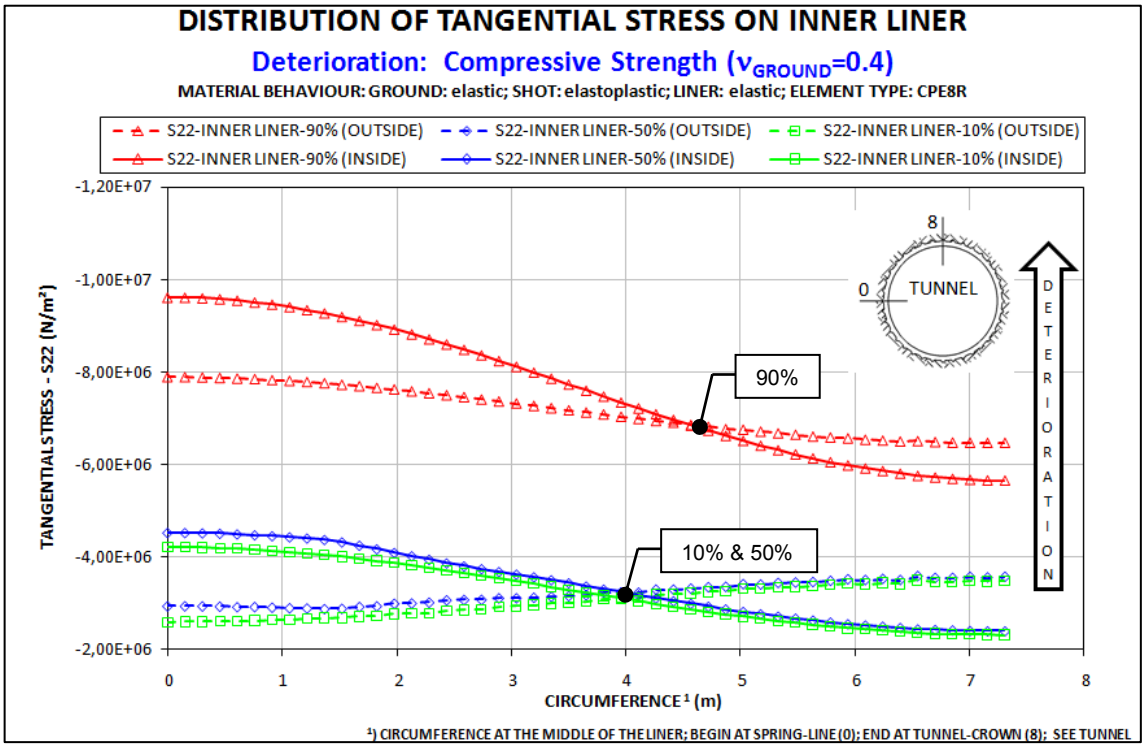

Fig. A–48: Results C16; Stresses at the outside and inside of the inner liner for three deterioration steps (10%, 50%, 90%); deterioration caused by degrading compressive strength;

Combination C17

- **Deterioration:** Young's Modulus & Compressive Strength
- **Element type:** CPE8R
- **Ground parameters:**
  - **Poisson's ratio:** $\nu = 0.5$
  - **Material behavior:** linear elastic
- **Shotcrete shell parameters:**
  - **Poisson's ratio:** $\nu = 0.2$
  - **Material behavior:** linear elastic
- **Inner liner parameters:**
  - **Poisson's ratio:** $\nu = 0.2$
  - **Material behavior:** linear elastic

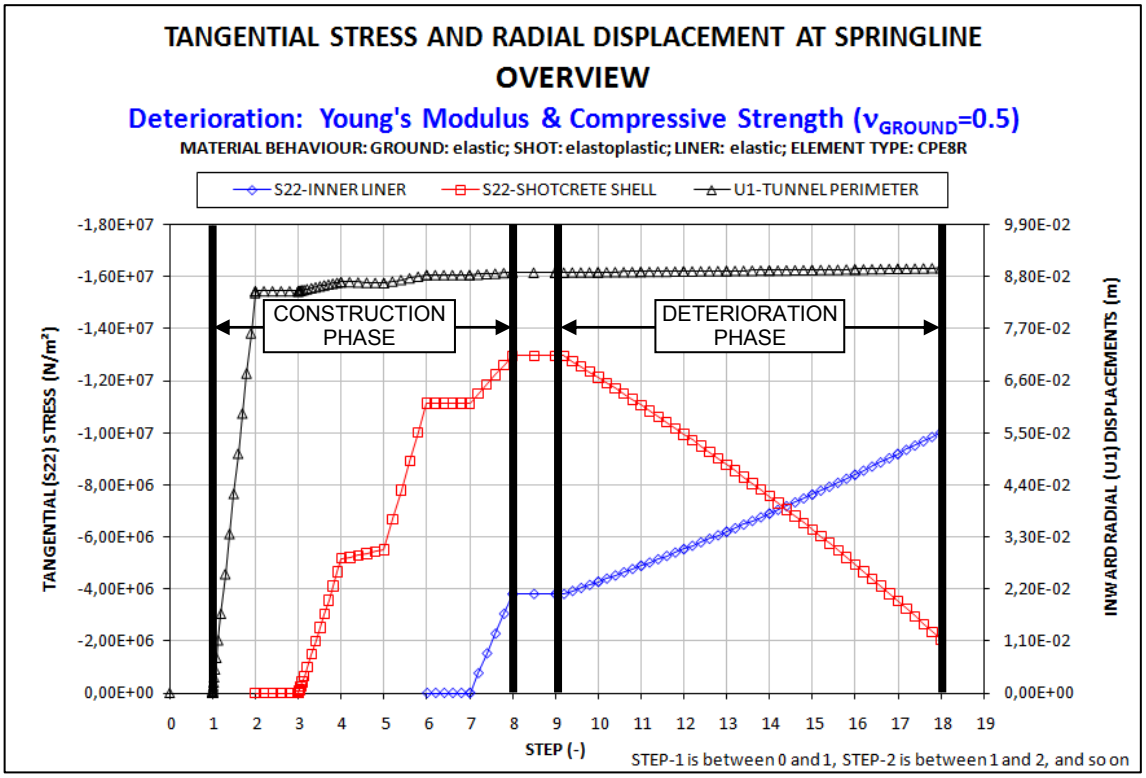

Fig. A–49: Results C17; Overview of stresses in the inner liner and shotcrete shell as well as radial displacements; all results are obtained at the spring-line; construction phase and deterioration phase;

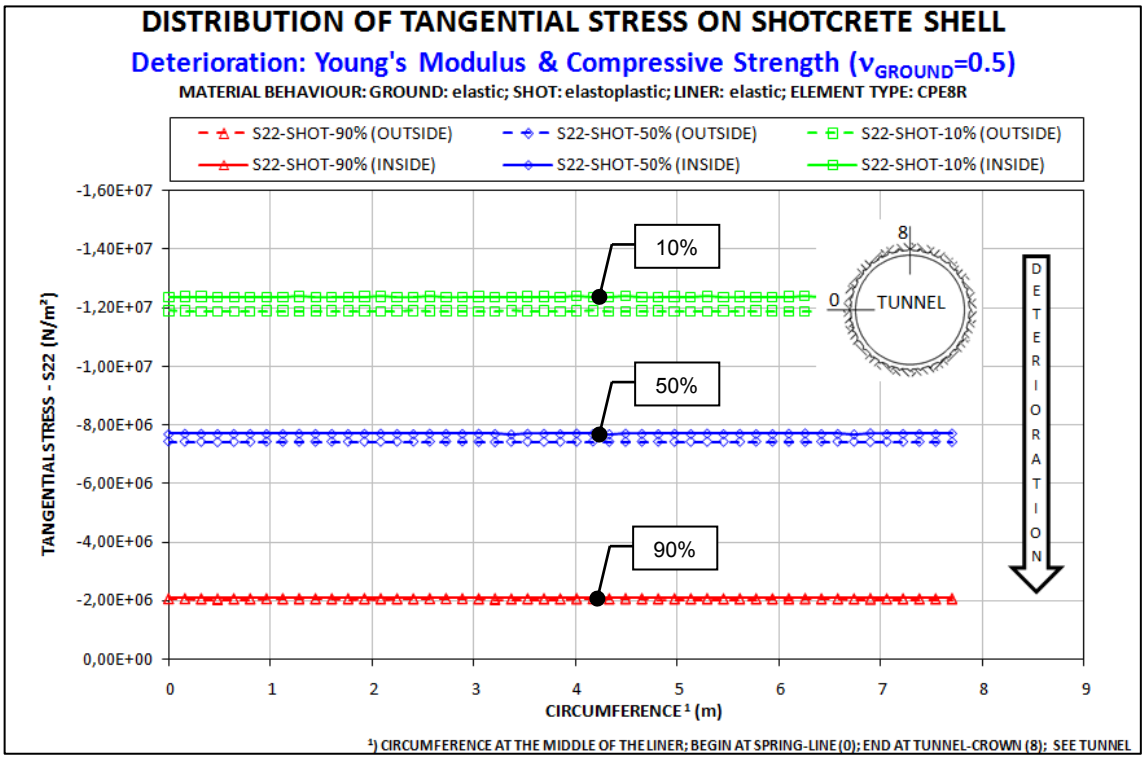

Fig. A–50: Results C17; Stresses at the outside and inside of the shotcrete shell for three deterioration steps (10%, 50%, 90%); deterioration caused by simultaneously degrading Young's modulus and compressive strength;

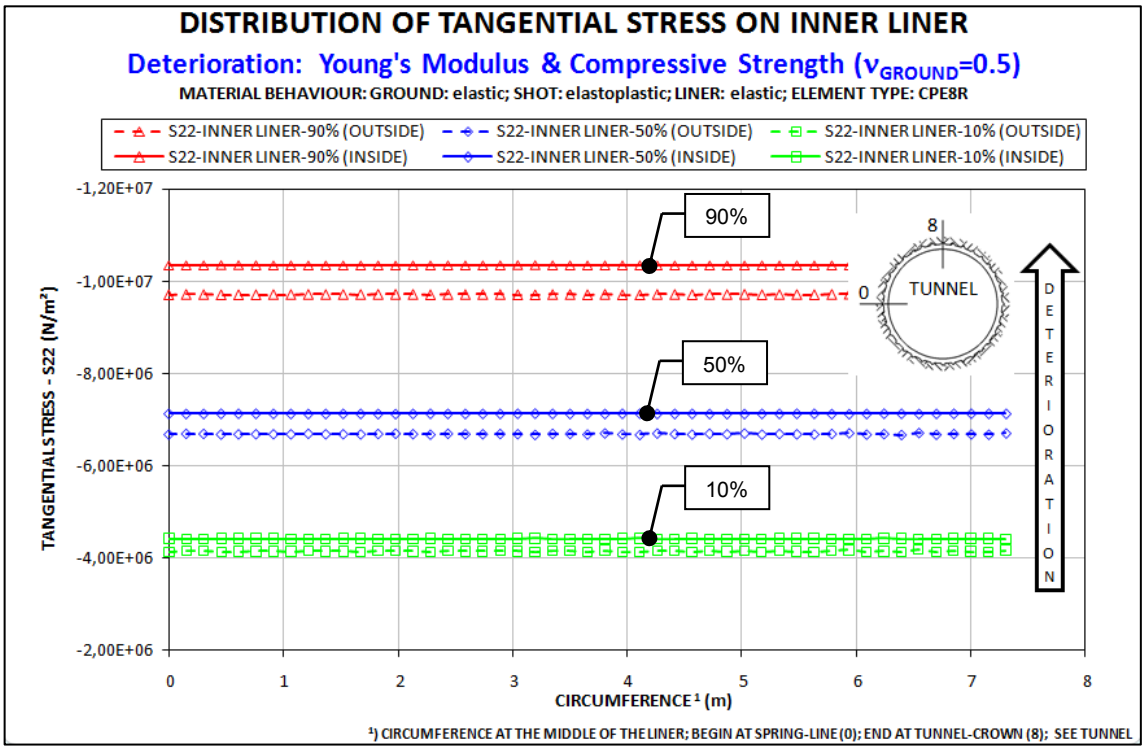

Fig. A–51: Results C17; Stresses at the outside and inside of the inner liner for three deterioration steps (10%, 50%, 90%); deterioration caused by simultaneously degrading Young's modulus and compressive strength;

Combination C18

- **Deterioration:** Young's Modulus & Compressive Strength
- **Element type:** CPE8R
- **Ground parameters:**
  - **Poisson's ratio:** $\nu = 0.4$
  - **Material behavior:** linear elastic
- **Shotcrete shell parameters:**
  - **Poisson's ratio:** $\nu = 0.2$
  - **Material behavior:** linear elastic
- **Inner liner parameters:**
  - **Poisson's ratio:** $\nu = 0.2$
  - **Material behavior:** linear elastic

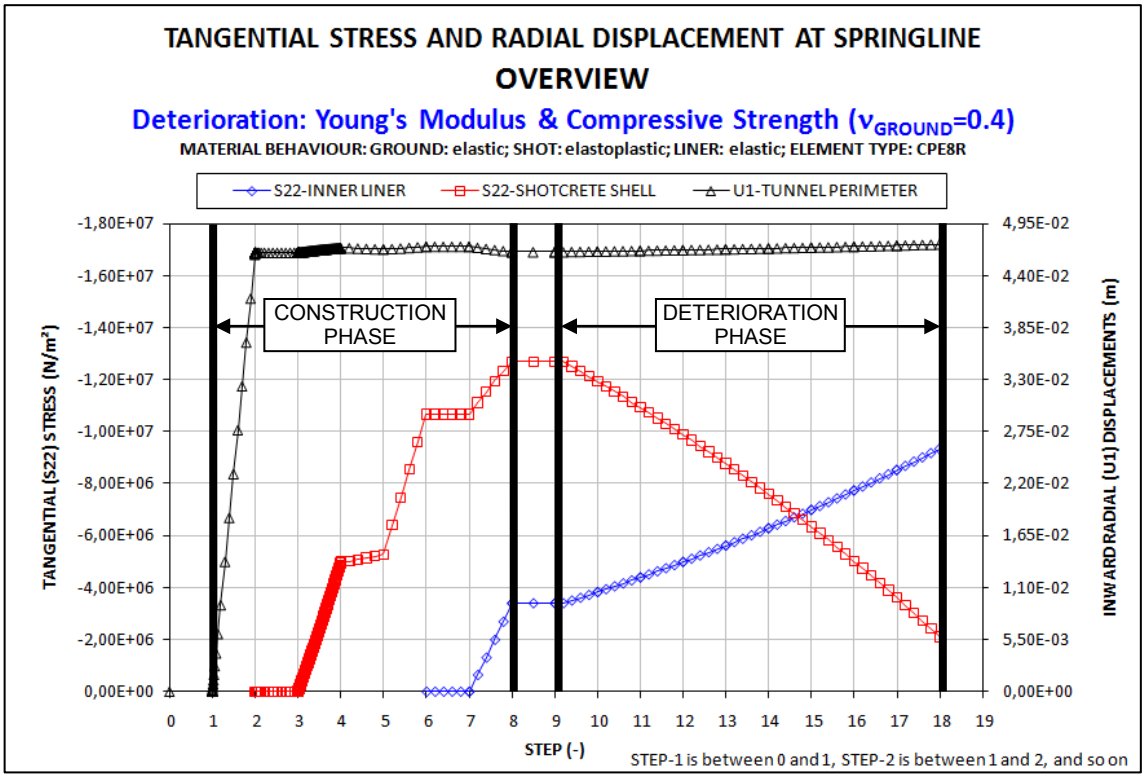

Fig. A–52: Results C18; Overview of stresses in the inner liner and shotcrete shell as well as radial displacements; all results are obtained at the spring-line; construction phase and deterioration phase;

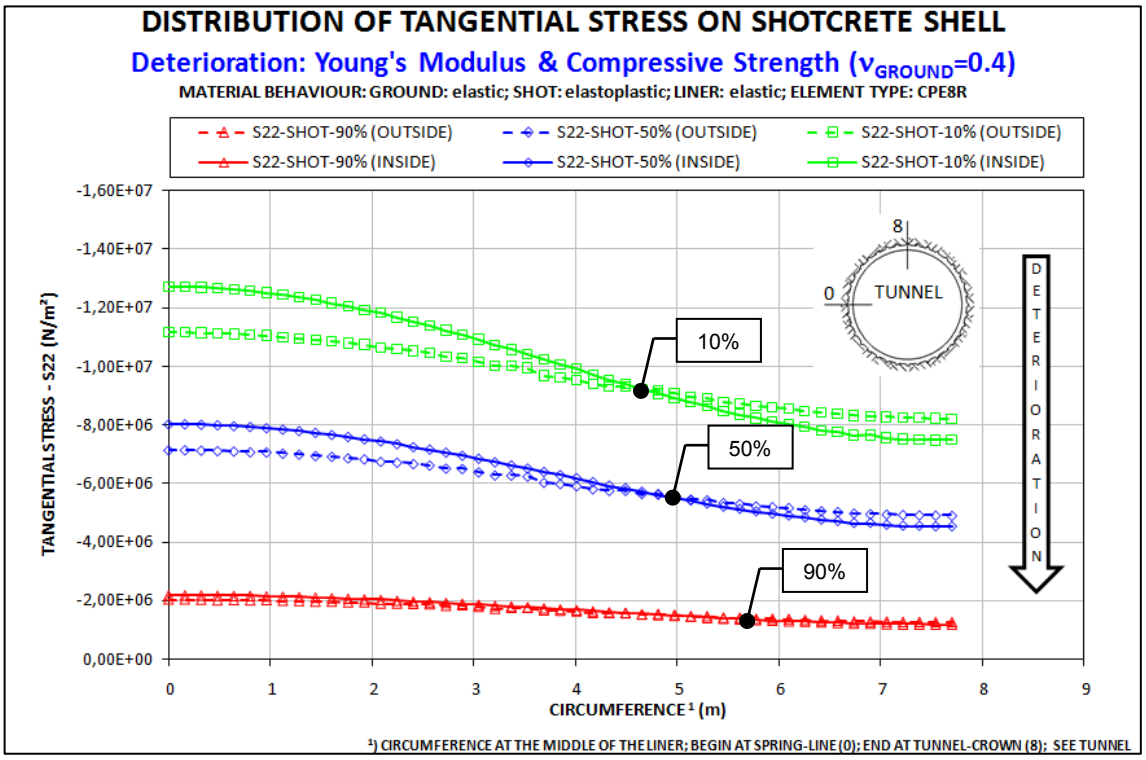

Fig. A–53: Results C18; Stresses at the outside and inside of the shotcrete shell for three deterioration steps (10%, 50%, 90%); deterioration caused by simultaneously degrading Young's modulus and compressive strength;

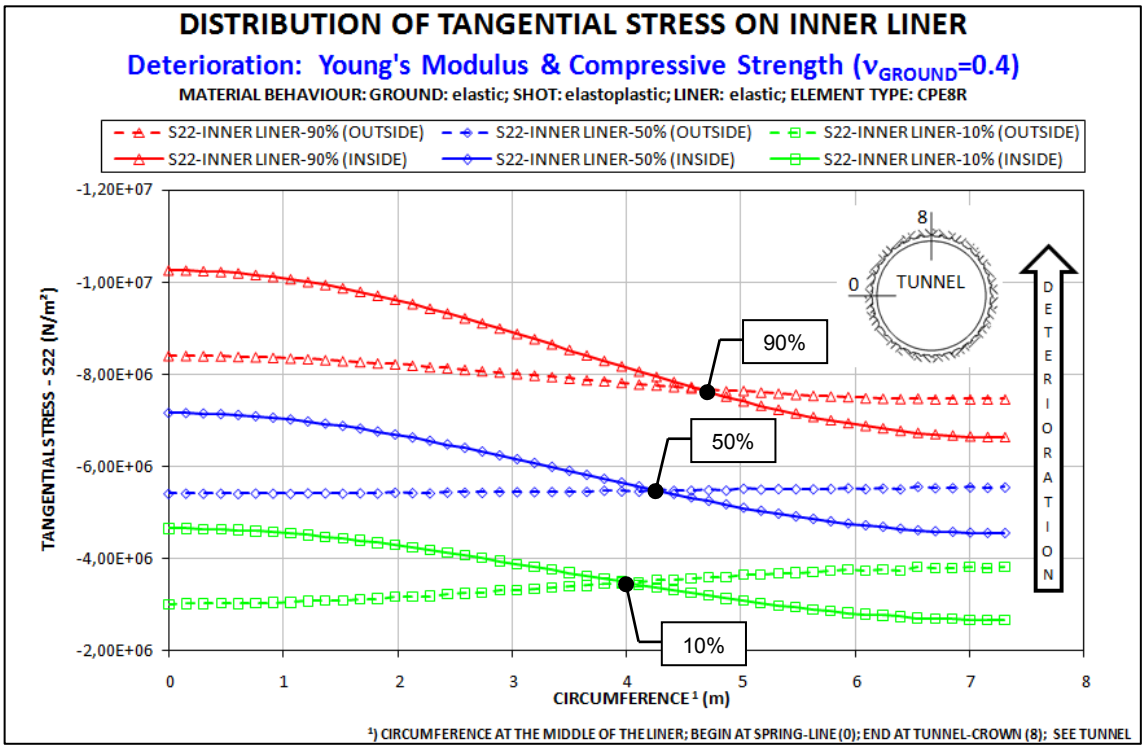

Fig. A–54: Results C18; Stresses at the outside and inside of the inner liner for three deterioration steps (10%, 50%, 90%); deterioration caused by simultaneously degrading Young's modulus and compressive strength;

Appendix B

INPUTFILE “ONE OF FOUR” – REACTION FORCES

```
*HEADING
 UNITS: N, m (SI-UNITS)
 ABAQUS/CAE 6.7-1
** Job name: REACTION FORCES Model name: C02-PART-1-OF-4
```

```
** GENERATION OF MODEL-PARTS
** PARTS
** GENERATION OF MODEL-PART: ROCK
*Part, name=ROCK
*Node
      1,          -55.,           0.
...
*Element, type=CPE4
  1,   1,  10, 148,  53
...
** GENERATION OF NODE AND ELEMENT SETS - MODEL-PART: ROCK
*Nset, nset=ROCK, generate
   1,  675,    1
*Elset, elset=ROCK, generate
   1,  624,    1
*Nset, nset=ROCK_BOT ** (EDGE: BOTTOM)
...
*Elset, elset=ROCK_BOT
...
*Nset, nset=ROCK_RHS ** (EDGE: RIGHT HAND SIDE)
...
*Elset, elset=ROCK_RHS
...
*Nset, nset=ROCK_TOP ** (EDGE: TOP SIDE)
...
*Elset, elset=ROCK_TOP, generate
...
*Nset, nset=ROCK_LHS ** (EDGE: LEFT HAND SIDE)
...
*Elset, elset=ROCK_LHS, generate
...
*Nset, nset=ROCK_SHOT ** (CONTACT SURFACE: ROCK-SHOT)
```

```
...
*Elset, elset=ROCK_SHOT
...
*Elset, elset=_ROCK_SHOT_S4, internal, generate
...
*Elset, elset=_ROCK_SHOT_S2, internal, generate
...
** GENERATION OF SURFACES - MODEL-PART: ROCK
*Surface, type=ELEMENT, name=ROCK_SHOT
_ROCK_SHOT_S4, S4
_ROCK_SHOT_S2, S2

*Elset, elset=_ROCK_TOP_S4, internal, generate
   1,  133,   12
*Surface, type=ELEMENT, name=ROCK_TOP
_ROCK_TOP_S4, S4

*Elset, elset=_ROCK_LHS_S2, internal, generate
 156,  288,   12
*Surface, type=ELEMENT, name=ROCK_LHS
_ROCK_LHS_S2, S2
```

```
** ASSIGN MATERIAL BEHAVIOR - MODEL-PART: ROCK
** Section: ROCK
*Solid Section, elset=ROCK, material=ROCK
1.,
*End Part
```

```
** ASSEMBLY OF PARTS
** ASSEMBLY
*Assembly, name=Assembly
*Instance, name=ROCK-1, part=ROCK
*End Instance
*End Assembly
```

```
** DEFINITION MATERIAL BEHAVIOR
** MATERIALS
*Material, name=ROCK
```

```
*Elastic
 5e+08, 0.4
```

```
** DEFINITION BOUNDARY CONDITIONS
** BOUNDARY CONDITIONS
** Name: BC-R_BOT Type: Symmetry/Antisymmetry/Encastre
*Boundary
 ROCK-1.ROCK_BOT, YSYMM
** Name: BC-R_RHS Type: Symmetry/Antisymmetry/Encastre
*Boundary
 ROCK-1.ROCK_RHS, XSYMM
** Name: BC-R_SHOT Type: Symmetry/Antisymmetry/Encastre
*Boundary
 ROCK-1.ROCK_SHOT, 1, 1
 ROCK-1.ROCK_SHOT, 2, 2
```

```
** DEFINITION INITIAL CONDITIONS
*INITIAL CONDITIONS, TYPE=STRESS, GEOSTATIC
 ROCK-1.ROCK, -6.75E6, 0.0, -6.75E6, -55.0, 0.667
```

```
** DEFINITION STEP-1: INITIAL CONDITIONS
** STEP: Step-1
*Step, name=Step-1, nlgeom=YES
Initial Stress Field; Apply SigmaV, SigmaH, P0*beta; Set beta
100%; Apply Boundary on BOT and RHS of Model (roller support and
mirror axes)
*Geostatic


** APPLY LOADS
** LOADS
** Name: SigmaH   Type: Pressure
*Dsload
ROCK-1.ROCK_LHS, P, 4.50e+06
** Name: SigmaV   Type: Pressure
*Dsload
ROCK-1.ROCK_TOP, P, 6.75e+06
```

```
** DEFINITION OUTPUT REQUESTS: DISPLACEMENTS, REACTION FORCES
** OUTPUT REQUESTS
*NODE PRINT, FREQUENCY=1, NSET=ROCK-1.ROCK_SHOT
 U, RF
...
*End Step
```

```
** DEFINITION STEP-2: OBTAIN REACTION FORCES
** STEP: Step-2
** OBTAIN REACTION FORCES
*Step, name=Step-2, nlgeom=YES
OBTAIN REACTION FORCES
*Static
0.2, 1., 1e-05, 0.2
...
*End Step
```

Appendix C

INPUTFILE “TWO OF FOUR” – SHOTCRETE SHELL

```
*Heading
 UNITS: N, m (SI-UNITS)
 ABAQUS/CAE 6.7-1
** Job name: SHOTCRETE_SHELL name: C02-PART-2-OF-4
*Preprint, echo=NO, model=NO, history=NO, contact=NO
```

```
** GENERATION OF MODEL-PARTS
** PARTS
** GENERATION OF MODEL-PART: ROCK
*Part, name=ROCK
*Node
      1,          -55.,           0.
...
*Element, type=CPE4
  1,   1,  10, 148,  53
...
** GENERATION OF NODE AND ELEMENT SETS - MODEL-PART: ROCK
*Nset, nset=ROCK, generate
   1,  675,    1
*Elset, elset=ROCK, generate
   1,  624,    1
*Nset, nset=ROCK_BOT ** (EDGE: BOTTOM)
...
*Elset, elset=ROCK_BOT
...
*Nset, nset=ROCK_RHS ** (EDGE: RIGHT HAND SIDE)
...
*Elset, elset=ROCK_RHS
...
*Nset, nset=ROCK_TOP ** (EDGE: TOP SIDE)
...
*Elset, elset=ROCK_TOP, generate
...
*Nset, nset=ROCK_LHS ** (EDGE: LEFT HAND SIDE)
...
*Elset, elset=ROCK_LHS, generate
...
```

```
*Nset, nset=ROCK_SHOT ** (CONTACT SURFACE: ROCK-SHOT)
...
*Elset, elset=ROCK_SHOT
...
*Elset, elset=_ROCK_SHOT_S4, internal, generate
...
*Elset, elset=_ROCK_SHOT_S2, internal, generate
...
** GENERATION OF SURFACES - MODEL-PART: ROCK
*Surface, type=ELEMENT, name=ROCK_SHOT
_ROCK_SHOT_S4, S4
_ROCK_SHOT_S2, S2

*Elset, elset=_ROCK_TOP_S4, internal, generate
   1,  133,   12
*Surface, type=ELEMENT, name=ROCK_TOP
_ROCK_TOP_S4, S4

*Elset, elset=_ROCK_LHS_S2, internal, generate
 156,  288,   12
*Surface, type=ELEMENT, name=ROCK_LHS
_ROCK_LHS_S2, S2
```

```
** ASSIGN MATERIAL BEHAVIOR - MODEL-PART: ROCK
** Section: ROCK
*Solid Section, elset=ROCK, material=ROCK
1.,
*End Part
```

```
** ASSEMBLY OF PARTS
** ASSEMBLY
*Assembly, name=Assembly
*Instance, name=ROCK-1, part=ROCK
*End Instance
*End Assembly
```

```
** DEFINITION MATERIAL BEHAVIOR
** MATERIALS
```

```
*Material, name=ROCK
*Elastic
 5e+08, 0.4
```

```
** DEFINITION BOUNDARY CONDITIONS
** BOUNDARY CONDITIONS
** Name: BC-R_BOT Type: Symmetry/Antisymmetry/Encastre
*Boundary
 ROCK-1.ROCK_BOT, YSYMM
** Name: BC-R_RHS Type: Symmetry/Antisymmetry/Encastre
*Boundary
 ROCK-1.ROCK_RHS, XSYMM
```

```
** DEFINITION INITIAL CONDITIONS
** INITIAL CONDITIONS
*INITIAL CONDITIONS, TYPE=STRESS, GEOSTATIC
 ROCK-1.ROCK, -6.75E6, 0.0, -6.75E6, -55.0, 0.667

** DEFINITION AMPLITUDE
** AMPLITUDE BETA
*AMPLITUDE, NAME=RELAX, TIME=TOTAL TIME
 0.0,1.0,  1.0,1.0,  2.0,0.15,  3.0,0.15,
 4.0,0.1,  5.0,0.1,  6.0,0.05,  7.0,0.05,
 8.0,0.0
```

```
** DEFINITION STEP-1: INITIAL CONDITIONS
** STEP: Step-1
*Step, name=Step-1, nlgeom=YES
Initial Stress Field; Apply SigmaV, SigmaH, P0*beta; Set beta
100%; Apply Boundary on BOT and RHS of Model (roller support and
mirror axes)
*Geostatic

** APPLY LOADS
** LOADS
** Name: P0   Type: CLOAD ** (CONCENTRATED LOAD)
*Cload, AMPLITUDE=RELAX
ROCK-1.7,   1,    -1040300
```

```
...
** (HORIZONTAL EARTH PRESSURE)
** Name: SigmaH   Type: Pressure
*Dsload
ROCK-1.ROCK_LHS, P, 4.5e+06

** (VERTICAL EARTH PRESSURE)
** Name: SigmaV   Type: Pressure
*Dsload
ROCK-1.ROCK_TOP, P, 6.75e+06

** DEFINITION OUTPUT REQUESTS: DISPLACEMENTS
** OUTPUT REQUESTS
*NODE PRINT, FREQUENCY=1, NSET=ROCK-1.ROCK_SHOT
 U
...
*End Step
```

```
** DEFINITION STEP-2: EXCAVATION (UNLOADING FACTOR BETA=85%)
** STEP: Step-2
*Step, name=Step-2, nlgeom=YES
EXCAVATION set beta=85%
*Static
0.2, 1., 1e-05, 0.2
...
*End Step
```

```
** DEFINITION STEP-3: OBTAIN NODAL COORDINATES SHOT
** STEP: Step-3
*Step, name=Step-3, nlgeom=YES
OBTAIN DISPLACEMENT FOR SUPPORT DELAY
*Static
0.2, 1., 1e-05, 0.2
...
*End Step
```

Appendix D

INPUTFILE “THREE OF FOUR” – INNER LINER

```
*Heading
 UNITS: N, m (SI-UNITS)
 ABAQUS/CAE 6.7-1
** Job name: INNER LINER name: C02-PART-3-OF-4
*Preprint, echo=NO, model=NO, history=NO, contact=NO
```

```
** GENERATION OF MODEL-PARTS
** PARTS
** GENERATION OF MODEL-PART: ROCK
*Part, name=ROCK
*Node
      1,          -55.,           0.
...
*Element, type=CPE4
  1,    1,   10, 148,   53
...
** GENERATION OF NODE AND ELEMENT SETS - MODEL-PART: ROCK
*Nset, nset=ROCK, generate
   1,  675,    1
*Elset, elset=ROCK, generate
   1,  624,    1
*Nset, nset=ROCK_BOT ** (EDGE: BOTTOM)
...
*Elset, elset=ROCK_BOT
...
*Nset, nset=ROCK_RHS ** (EDGE: RIGHT HAND SIDE)
...
*Elset, elset=ROCK_RHS
...
*Nset, nset=ROCK_TOP ** (EDGE: TOP SIDE)
...
*Elset, elset=ROCK_TOP, generate
...
*Nset, nset=ROCK_LHS ** (EDGE: LEFT HAND SIDE)
...
*Elset, elset=ROCK_LHS, generate
...
```

```
*Nset, nset=ROCK_SHOT ** (CONTACT SURFACE: ROCK-SHOT)
...
*Elset, elset=ROCK_SHOT
...
*Elset, elset=_ROCK_SHOT_S4, internal, generate
...
*Elset, elset=_ROCK_SHOT_S2, internal, generate
...
** GENERATION OF SURFACES - MODEL-PART: ROCK
*Surface, type=ELEMENT, name=ROCK_SHOT
_ROCK_SHOT_S4, S4
_ROCK_SHOT_S2, S2

*Elset, elset=_ROCK_TOP_S4, internal, generate
   1,  133,   12
*Surface, type=ELEMENT, name=ROCK_TOP
_ROCK_TOP_S4, S4

*Elset, elset=_ROCK_LHS_S2, internal, generate
 156,  288,   12
*Surface, type=ELEMENT, name=ROCK_LHS
_ROCK_LHS_S2, S2
```

```
** ASSIGN MATERIAL BEHAVIOR - MODEL-PART: ROCK
** Section: ROCK
*Solid Section, elset=ROCK, material=ROCK
1.,
*End Part
```

```
** GENERATION OF MODEL-PART: SHOT
*Part, name=SHOT
*Node
1,     -4.952361, -55
...
*Element, type=CPE4
 1,  1,  2,  5,  4
...
```

```
** GENERATION OF NODE AND ELEMENT SETS - MODEL-PART: SHOT
*Nset, nset=SHOT, generate
...
*Elset, elset=SHOT, generate
...
*Nset, nset=SHOT_ROCK, generate ** (CONTACT SURFACE: SHOT-ROCK)
...
*Elset, elset=SHOT_ROCK, generate
...
*Nset, nset=SHOT_LINER, generate ** (CONTACT SURF.: SHOT-LINER)
...
*Elset, elset=SHOT_LINER, generate
...
*Nset, nset=SHOT_BOT, generate ** (EDGE: BOTTOM)
...
*Elset, elset=SHOT_BOT
...
*Nset, nset=SHOT_RHS, generate ** (EDGE: RIGHT HAND SIDE)
...
*Elset, elset=SHOT_RHS
...
*Elset, elset=_SHOT_ROCK_S4, internal, generate
...
** GENERATION OF SURFACES – MODEL PART: SHOT
*Surface, type=ELEMENT, name=SHOT_ROCK
_SHOT_ROCK_S4, S4
*Elset, elset=_SHOT_LINER_S2, internal, generate
...
*Surface, type=ELEMENT, name=SHOT_LINER
_SHOT_LINER_S2, S2

** GENERATION COORDINATE SYSTEM – MODEL PART: SHOT
*Orientation, name=Ori-1, system=CYLINDRICAL
0.,-55.,   0.,0.,   -55.,1.
3, 0.
```

```
** ASSIGN MATERIAL BEHAVIOR - MODEL-PART: SHOT
** Section: SHOT
*Solid Section, elset=SHOT, orientation=Ori-1, material=SHOT
1.,
*End Part
```

```
** ASSIGN OF PARTS
** ASSEMBLY
*Assembly, name=Assembly

*Instance, name=ROCK-1, part=ROCK
*End Instance

*Instance, name=SHOT-1, part=SHOT
*End Instance
*End Assembly
```

```
** DEFINITION MATERIAL BEHAVIOR
** MATERIALS
*Material, name=ROCK
*Elastic
 5e+08, 0.4

*Material, name=SHOT
*Elastic, dependencies=1
    1e+10, 0.2, ,  0. ** (YOUNG SHOTCRETE)
    1e+10, 0.2, ,  3.
  1.5e+10, 0.2, ,  5. ** (CHANGE YOUNG TO HARDENED SHOTCRETE)

** ASSIGN USER DEFINED FIELD
*USER DEFINED FIELD
```

```
** DEFINITION CONTACT
** INTERACTION PROPERTIES
*Surface Interaction, name=CONTACT_RS **(CONTACT: ROCK-SHOT)
*Friction, elastic slip=0.001
 100.,
*Surface Behavior, no separation, pressure-overclosure=HARD
```

```
** DEFINITION BOUNDARY CONDITIONS
** BOUNDARY CONDITIONS

** BOUNDARY CONDITIONS: ROCK
** Name: BC-R_BOT Type: Symmetry/Antisymmetry/Encastre
*Boundary
ROCK-1.ROCK_BOT, YSYMM
** Name: BC-R_RHS Type: Symmetry/Antisymmetry/Encastre
*Boundary
ROCK-1.ROCK_RHS, XSYMM

** BOUNDARY CONDITIONS: SHOT
** Name: BC-S_BOT Type: Symmetry/Antisymmetry/Encastre
*Boundary
SHOT-1.SHOT_BOT, YSYMM
** Name: BC-S_RHS Type: Symmetry/Antisymmetry/Encastre
*Boundary
SHOT-1.SHOT_RHS, XSYMM
```

```
** APPLY CONTACT
** INTERACTIONS
** Interaction: CONTACT_RS
*Contact Pair, interaction=CONTACT_RS
SHOT-1.SHOT_ROCK, ROCK-1.ROCK_SHOT
```

```
** DEFINITION INITIAL CONDITIONS
*INITIAL CONDITIONS, TYPE=STRESS, GEOSTATIC
 ROCK-1.ROCK, -6.75E6, 0.0, -6.75E6, -55.0, 0.667

** DEFINITION AMPLITUDE
** AMPLITUDE BETA
*AMPLITUDE, NAME=RELAX, TIME=TOTAL TIME
 0.0,1.0,  1.0,1.0,  2.0,0.15,  3.0,0.15,
 4.0,0.1,  5.0,0.1,  6.0,0.05,  7.0,0.05
```

```
** DEFINITION STEP-1: INITIAL CONDITIONS
** STEP: Step-1
```

```
*Step, name=Step-1, nlgeom=YES
Initial Stress Field; Apply SigmaV, SigmaH, P0*beta; Set beta
100%; Apply Boundary on BOT and RHS of Model (roller support and
mirror axes)
*Geostatic

** APPLY LOADS
** LOADS
** Name: P0   Type: CLOAD ** (CONCENTRATED LOAD)
*Cload, AMPLITUDE=RELAX
ROCK-1.7,   1,    -1040300
...
** (HORIZONTAL EARTH PRESSURE)
** Name: SigmaH   Type: Pressure
*Dsload
ROCK-1.ROCK_LHS, P, 4.5e+06

** (VERTICAL EARTH PRESSURE)
** Name: SigmaV   Type: Pressure
*Dsload
ROCK-1.ROCK_TOP, P, 6.75e+06

** REMOVE CONTACT PAIR
** Interaction: CONTACT_RS
*Model Change, type=CONTACT PAIR, remove
 SHOT-1.SHOT_ROCK, ROCK-1.ROCK_SHOT

** REMOVE MODEL-PART: SHOT
*Model Change, remove
 SHOT-1.SHOT,

** DEFINITION OUTPUT REQUESTS: DISPLACEMENTS
** OUTPUT REQUESTS
*NODE PRINT, FREQUENCY=1, NSET=SHOT-1.SHOT_LINER
 U
...
*End Step
```

```
** DEFINITION STEP-2: EXCAVATION (UNLOADING FACTOR BETA=85%)
** STEP: Step-2
*Step, name=Step-2, nlgeom=YES
EXCAVATION (UNLOADING FACTOR BETA=85%)
*Static
0.2, 1., 1e-05, 0.2
...
*End Step
```

```
** DEFINITION STEP-3: CONTACT TO YOUNG SHOT
** STEP: Step-3
*Step, name=Step-3, nlgeom=YES
CONTACT TO YOUNG SHOT
*Static
0.2, 1., 1e-05, 0.2

** ADD CONTACT PAIR
** Interaction: CONTACT_RS
*Model Change, type=CONTACT PAIR, add
 SHOT-1.SHOT_ROCK, ROCK-1.ROCK_SHOT

** ADD MODEL-PART: SHOT
*Model Change, add
 SHOT-1.SHOT,
...
*End Step
```

```
** DEFINITION STEP-4: EXCAVATION (UNLOADING FACTOR BETA=90%)
** STEP: Step-4
*Step, name=Step-4, nlgeom=YES
EXCAVATION (UNLOADING FACTOR BETA=90%)
*Static
0.2, 1., 1e-05, 0.2
...
*End Step
```

```
** DEFINITION STEP-5: CHANGE PROPERTIES FROM A YOUNG TO HARDENED SHOTCRETE (USER DEFINED FIELD)
** STEP: Step-5
*Step, name=Step-5, nlgeom=YES
CHANGE PROPERTIES FROM YOUNG TO HARDENED SHOTCRETE (USER DEFINED FIELD)
*Static
0.2, 1., 1e-05, 0.2
...
*End Step
```

```
** DEFINITION STEP-6: EXCAVATION (UNLOADING FACTOR BETA=95%)
** STEP: Step-6
*Step, name=Step-6, nlgeom=YES
EXCAVATION (UNLOADING FACTOR BETA=95%)
*Static
0.2, 1., 1e-05, 0.2
...
*End Step
```

```
** DEFINITION STEP-7: OBTAIN NODAL COORDINATES LINER
** STEP: Step-7
*Step, name=Step-7, nlgeom=YES
OBTAIN NODE COORDINATES LINER
*Static
0.2, 1., 1e-05, 0.2
...
*End Step
```

Appendix E

INPUTFILE “FOUR OF FOUR” – DETERIORATION SHOTCRETE SHELL

```
*Heading
 UNITS: N, m (SI-UNITS)
 ABAQUS/CAE 6.7-1
** Job name: DETERIORATION SHOT Model name: C02-PART-4-OF-4
*Preprint, echo=NO, model=NO, history=NO, contact=NO
```

```
** GENERATION OF MODEL-PARTS
** PARTS
** GENERATION OF MODEL-PART: LINER
*Part, name=LINER
*Node
1,     -4.75054196,     -55
...
*Element, type=CPE4
 1,    1,    2,    6,    5
...
** GENERATION OF NODE AND ELEMENT SETS - MODEL-PART: LINER
*Nset, nset=LINER, generate
  1, 100,    1
*Elset, elset=LINER, generate
  1,  72,    1
*Nset, nset=LINER_SHOT, generate ** (CONTACT SURF.: LINER-SHOT)
...
*Elset, elset=LINER_SHOT, generate
...
*Nset, nset=LINER_BOT, generate ** (EDGE: BOTTOM)
...
*Elset, elset=LINER_BOT, generate
...
*Nset, nset=LINER_INS, generate ** (EDGE: INSIDE)
...
*Elset, elset=LINER_INS, generate
...
*Nset, nset=LINER_RHS, generate ** (EDGE: RIGHT HAND SIDE)
...
*Elset, elset=LINER_RHS, generate
...
```

```
*Elset, elset=_LINER_SHOT_S4, internal, generate
...
** GENERATION OF SURFACES - MODEL PART: LINER
*Surface, type=ELEMENT, name=LINER_SHOT
_LINER_SHOT_S4, S4

** GENERATION COORDINATE SYSTEM - MODEL PART: LINER
*Orientation, name=Ori-1, system=CYLINDRICAL
0.,-55.,   0.,0.,   -55.,1.
3, 0.
```

```
** ASSIGN MATERIAL BEHAVIOR - MODEL-PART: LINER
** Section: LINER
*Solid Section, elset=LINER, orientation=Ori-1, material=LINER
1.,
*End Part
```

```
** GENERATION OF MODEL-PART: ROCK
*Part, name=ROCK
*Node
      1,          -55.,           0.
...
*Element, type=CPE4
  1,   1,  10, 148,  53
...
** GENERATION OF NODE AND ELEMENT SETS - MODEL-PART: ROCK
*Nset, nset=ROCK, generate
...
*Elset, elset=ROCK, generate
...
*Nset, nset=ROCK_BOT ** (EDGE: BOTTOM)
...
*Elset, elset=ROCK_BOT
...
*Nset, nset=ROCK_RHS ** (EDGE: RIGHT HAND SIDE)
...
*Elset, elset=ROCK_RHS
...
```

```
*Nset, nset=ROCK_TOP ** (EDGE: TOP SIDE)
...
*Elset, elset=ROCK_TOP, generate
...
*Nset, nset=ROCK_LHS ** (EDGE: LEFT HAND SIDE)
...
*Elset, elset=ROCK_LHS, generate
...
*Nset, nset=ROCK_SHOT ** (CONTACT SURFACE: ROCK-SHOT)
...
*Elset, elset=ROCK_SHOT
...
*Elset, elset=_ROCK_SHOT_S4, internal, generate
...
*Elset, elset=_ROCK_SHOT_S2, internal, generate
...
** GENERATION OF SURFACES - MODEL-PART: ROCK
*Surface, type=ELEMENT, name=ROCK_SHOT
_ROCK_SHOT_S4, S4
_ROCK_SHOT_S2, S2

*Elset, elset=_ROCK_TOP_S4, internal, generate
   1,  133,   12
*Surface, type=ELEMENT, name=ROCK_TOP
_ROCK_TOP_S4, S4

*Elset, elset=_ROCK_LHS_S2, internal, generate
 156,  288,   12
*Surface, type=ELEMENT, name=ROCK_LHS
_ROCK_LHS_S2, S2

** ASSIGN MATERIAL BEHAVIOR - MODEL-PART: ROCK
** Section: ROCK
*Solid Section, elset=ROCK, material=ROCK
1.,
*End Part
```

```
** GENERATION OF MODEL-PART: SHOT
*Part, name=SHOT
*Node
1,     -4.952361, -55
...
*Element, type=CPE4
 1,  1,  2,  5,  4
...
** GENERATION OF NODE AND ELEMENT SETS - MODEL-PART: SHOT
*Nset, nset=SHOT, generate
...
*Elset, elset=SHOT, generate
...
*Nset, nset=SHOT_ROCK, generate ** (CONTACT SURFACE: SHOT-ROCK)
...
*Elset, elset=SHOT_ROCK, generate
...
*Nset, nset=SHOT_LINER, generate ** (CONTACT SURF.: SHOT-LINER)
...
*Elset, elset=SHOT_LINER, generate
...
*Nset, nset=SHOT_BOT, generate ** (EDGE: BOTTOM)
...
*Elset, elset=SHOT_BOT
...
*Nset, nset=SHOT_RHS, generate ** (EDGE: RIGHT HAND SIDE)
...
*Elset, elset=SHOT_RHS
...
*Elset, elset=_SHOT_ROCK_S4, internal, generate
...
** GENERATION OF SURFACES - MODEL PART: SHOT
*Surface, type=ELEMENT, name=SHOT_ROCK
_SHOT_ROCK_S4, S4
*Elset, elset=_SHOT_LINER_S2, internal, generate
...
*Surface, type=ELEMENT, name=SHOT_LINER
```

```
_SHOT_LINER_S2, S2

** GENERATION COORDINATE SYSTEM – MODEL PART: SHOT
*Orientation, name=Ori-1, system=CYLINDRICAL
0.,-55.,   0.,0.,   -55.,1.
3, 0.

** ASSIGN MATERIAL BEHAVIOR - MODEL-PART: SHOT
** Section: SHOT
*Solid Section, elset=SHOT, orientation=Ori-1, material=SHOT
1.,
*End Part

** ASSIGN OF PARTS
** ASSEMBLY
*Assembly, name=Assembly

*Instance, name=ROCK-1, part=ROCK
*End Instance

*Instance, name=SHOT-1, part=SHOT
*End Instance

*Instance, name=LINER-1, part=LINER
*End Instance
*End Assembly

** DEFINITION MATERIAL BEHAVIOR
** MATERIALS
*Material, name=LINER
*Elastic
 3.05e+10, 0.2

*Material, name=ROCK
*Elastic
 5e+08, 0.4

*Material, name=SHOT
```

```
*Elastic, dependencies=1
    1e+10, 0.2, ,  0. ** (YOUNG SHOTCRETE)
    1e+10, 0.2, ,  3.
  1.5e+10, 0.2, ,  5. ** (CHANGE YOUNG TO HARDENED SHOTCRETE)
  1.5e+10, 0.2, ,  9. ** (START DETERIORATION SHOTCRETE)
 1.35e+10, 0.2, , 10.
  1.2e+10, 0.2, , 11.
 1.05e+10, 0.2, , 12.
    9e+09, 0.2, , 13.
  7.5e+09, 0.2, , 14.
    6e+09, 0.2, , 15.
  4.5e+09, 0.2, , 16.
    3e+09, 0.2, , 17.
  1.5e+09, 0.2, , 18. ** (END DETERIORATION SHOTCRETE)

** ASSIGN USER DEFINED FIELD
*USER DEFINED FIELD

-------------------------------------------------------------------

** DEFINITION CONTACT
** INTERACTION PROPERTIES
**
*Surface Interaction, name=CONTACT_RS ** (CONTACT: ROCK-SHOT)
*Friction, elastic slip=0.001
100.,
*Surface Behavior, no separation, pressure-overclosure=HARD

*Surface Interaction, name=CONTACT_SL ** (CONTACT: SHOT-LINER)
*Friction, elastic slip=0.001
1.,
*Surface Behavior, pressure-overclosure=HARD

-------------------------------------------------------------------

** DEFINITION BOUNDARY CONDITIONS
** BOUNDARY CONDITIONS

** BOUNDARY CONDITIONS: LINER
** Name: BC-L_BOT Type: Symmetry/Antisymmetry/Encastre
*Boundary
LINER-1.LINER_BOT, YSYMM
```

```
** Name: BC-L_RHS Type: Symmetry/Antisymmetry/Encastre
*Boundary
LINER-1.LINER_RHS, XSYMM

** BOUNDARY CONDITIONS: ROCK
** Name: BC-R_BOT Type: Symmetry/Antisymmetry/Encastre
*Boundary
ROCK-1.ROCK_BOT, YSYMM
** Name: BC-R_RHS Type: Symmetry/Antisymmetry/Encastre
*Boundary
ROCK-1.ROCK_RHS, XSYMM

** BOUNDARY CONDITIONS: SHOT
** Name: BC-S_BOT Type: Symmetry/Antisymmetry/Encastre
*Boundary
SHOT-1.SHOT_BOT, YSYMM
** Name: BC-S_RHS Type: Symmetry/Antisymmetry/Encastre
*Boundary
SHOT-1.SHOT_RHS, XSYMM

** APPLY CONTACT
** INTERACTIONS
** Interaction: CONTACT_RS ** (CONTACT ROCK-SHOT)
*Contact Pair, interaction=CONTACT_RS
SHOT-1.SHOT_ROCK, ROCK-1.ROCK_SHOT

** Interaction: CONTACT_SL ** (CONTACT SHOT-LINER)
*Contact Pair, interaction=CONTACT_SL
LINER-1.LINER_SHOT, SHOT-1.SHOT_LINER

** DEFINITION INITIAL CONDITIONS
*INITIAL CONDITIONS, TYPE=STRESS, GEOSTATIC
 ROCK-1.ROCK, -6.75E6, 0.0, -6.75E6, -55.0, 0.667

** DEFINITION AMPLITUDE
*AMPLITUDE, NAME=RELAX, TIME=TOTAL TIME
 0.0,1.0,  1.0,1.0,  2.0,0.15,  3.0,0.15,
 4.0,0.1,  5.0,0.1,  6.0,0.05,  7.0,0.05,
```

```
 8.0,0.0
```

```
** DEFINITION STEP-1: INITIAL CONDITIONS
** STEP: Step-1
*Step, name=Step-1, nlgeom=YES
Initial Stress Field; Apply SigmaV, SigmaH, P0*beta; Set beta
100%; Apply Boundary on BOT and RHS of Model (roller support and
mirror axes)
*Geostatic

** APPLY LOADS
** LOADS
** Name: P0   Type: CLOAD ** (CONCENTRATED LOAD)
*Cload, AMPLITUDE=RELAX
ROCK-1.7,   1,    -1040300
...
** (HORIZONTAL EARTH PRESSURE)
** Name: SigmaH   Type: Pressure
*Dsload
ROCK-1.ROCK_LHS, P, 4.5e+06

** (VERTICAL EARTH PRESSURE)
** Name: SigmaV   Type: Pressure
*Dsload
ROCK-1.ROCK_TOP, P, 6.75e+06

** REMOVE CONTACT PAIRS
** Interaction: CONTACT_RS ** (CONTACT ROCK-SHOT)
*Model Change, type=CONTACT PAIR, remove
 SHOT-1.SHOT_ROCK, ROCK-1.ROCK_SHOT

** Interaction: CONTACT_SL ** (CONTACT SHOT-LINER)
*Model Change, type=CONTACT PAIR, remove
 LINER-1.LINER_SHOT, SHOT-1.SHOT_LINER

** REMOVE MODEL-PARTS
*Model Change, remove
 SHOT-1.SHOT,
```

```
 LINER-1.LINER,

** DEFINITION OUTPUT REQUESTS
** OUTPUT REQUESTS
** PRINT TO DATA

** (DISPLACEMENTS SURFACE ROCK-SHOT)
*NODE PRINT, FREQUENCY=1, NSET=ROCK-1.ROCK_SHOT
 U

** (DISPLACEMENTS SURFACE SHOT-LINER)
*NODE PRINT, FREQUENCY=1, NSET=SHOT-1.SHOT_LINER
 U

** (STRESSES SHOT)
*EL PRINT, FREQUENCY=1, ELSET=SHOT-1.SHOT,
 POSITION=AVERAGED AT NODES
 S,

** (STRESSES LINER)
*EL PRINT, FREQUENCY=1, ELSET=LINER-1.LINER,
 POSITION=AVERAGED AT NODES
 S,
...
*End Step
```

```
** DEFINITION STEP-2: EXCAVATION (UNLOADING FACTOR BETA=85%)
** STEP: Step-2
*Step, name=Step-2, nlgeom=YES
EXCAVATION (UNLOADING FACTOR BETA=85%)
*Static
0.2, 1., 1e-05, 0.2
...
*End Step
```

```
** DEFINITION STEP-3: CONTACT TO YOUNG SHOT
** STEP: Step-3
*Step, name=Step-3, nlgeom=YES
```

```
CONTACT TO YOUNG SHOT
*Static
0.2, 1., 1e-05, 0.2

** ADD CONTACT PAIR: ROCK-SHOT
** Interaction: CONTACT_RS
*Model Change, type=CONTACT PAIR, add
 SHOT-1.SHOT_ROCK, ROCK-1.ROCK_SHOT

** ADD MODEL-PART: SHOT
*Model Change, add
 SHOT-1.SHOT,
...
*End Step
```

```
** DEFINITION STEP-4: EXCAVATION (UNLOADING FACTOR BETA=90%)
** STEP: Step-4
*Step, name=Step-4, nlgeom=YES
EXCAVATION (UNLOADING FACTOR BETA=90%)
*Static
0.2, 1., 1e-05, 0.2
...
*End Step
```

```
** DEFINITION STEP-5: CHANGE PROPERTIES FROM A YOUNG TO HARDENED
SHOTCRETE (USER DEFINED FIELD)
** STEP: Step-5
*Step, name=Step-5, nlgeom=YES
CHANGE PROPERTIES FROM YOUNG TO HARDENED SHOTCRETE (USER DEFINED
FIELD)
*Static
0.2, 1., 1e-05, 0.2
...
*End Step
```

```
** DEFINITION STEP-6: EXCAVATION (UNLOADING FACTOR BETA=95%)
*Step, name=Step-6, nlgeom=YES
EXCAVATION (UNLOADING FACTOR BETA=95%)
```

```
*Static
0.2, 1., 1e-05, 0.2
...
*End Step
```

```
** DEFINITION STEP-7: CONTACT TO LINER
** STEP: Step-7
*Step, name=Step-7, nlgeom=YES
CONTACT TO LINER
*Static
0.2, 1., 1e-05, 0.2

** ADD CONTACT PAIR: SHOT-LINER
** Interaction: CONTACT_SL
*Model Change, type=CONTACT PAIR, add
 LINER-1.LINER_SHOT, SHOT-1.SHOT_LINER

** ADD MODEL-PART: LINER
*Model Change, add
 LINER-1.LINER,
...
*End Step
```

```
** DEFINITION STEP-8: EXCAVATION (UNLOADING FACTOR BETA=100%)
** STEP: Step-8
*Step, name=Step-8, nlgeom=YES
EXCAVATION (UNLOADING FACTOR BETA=100%)
*Static
0.2, 1., 1e-05, 0.2
...
*End Step
```

```
** DEFINITION STEP-9: IDLE STEP (FOR EVALUATION PURPOSES)
** STEP: Step-9
*Step, name=Step-9, nlgeom=YES
IDLE STEP (FOR EVALUATION PURPOSES)
*Static
0.2, 1., 1e-05, 0.2
```

```
...
*End Step
```

```
** DEFINITION STEP-10: DETERIORATION OF SHOTCRETE 10% (USER DEFINED FIELD)
** STEP: Step-10
*Step, name=Step-10, nlgeom=YES
DETERIORATION OF SHOTCRETE: 10% (USER DEFINED FIELD)
*Static
0.2, 1., 1e-05, 0.2
...
*End Step
```

```
** DEFINITION STEP-11: DETERIORATION OF SHOTCRETE 20% (USER DEFINED FIELD)
** STEP: Step-11
*Step, name=Step-11, nlgeom=YES
DETERIORATION OF SHOTCRETE: 20% (USER DEFINED FIELD)
*Static
0.2, 1., 1e-05, 0.2
...
*End Step
```

```
** DEFINITION STEP-12: DETERIORATION OF SHOTCRETE 30% (USER DEFINED FIELD)
** STEP: Step-12
*Step, name=Step-12, nlgeom=YES
DETERIORATION OF SHOTCRETE: 30% (USER DEFINED FIELD)
*Static
0.2, 1., 1e-05, 0.2
...
*End Step
```

```
** DEFINITION STEP-13: DETERIORATION OF SHOTCRETE 40% (USER DEFINED FIELD)
** STEP: Step-13
*Step, name=Step-13, nlgeom=YES
DETERIORATION OF SHOTCRETE: 40% (USER DEFINED FIELD)
*Static
```

```
0.2, 1., 1e-05, 0.2
...
*End Step
```

```
** DEFINITION STEP-14: DETERIORATION OF SHOTCRETE 50% (USER DEFINED FIELD)
** STEP: Step-14
*Step, name=Step-14, nlgeom=YES
DETERIORATION OF SHOTCRETE: 50% (USER DEFINED FIELD)
*Static
0.2, 1., 1e-05, 0.2
...
*End Step
```

```
** DEFINITION STEP-15: DETERIORATION OF SHOTCRETE 60% (USER DEFINED FIELD)
** STEP: Step-15
*Step, name=Step-15, nlgeom=YES
DETERIORATION OF SHOTCRETE: 60% (USER DEFINED FIELD)
*Static
0.2, 1., 1e-05, 0.2
...
*End Step
```

```
** DEFINITION STEP-16: DETERIORATION OF SHOTCRETE 70% (USER DEFINED FIELD)
** STEP: Step-16
*Step, name=Step-16, nlgeom=YES
DETERIORATION of initial support 70%
*Static
0.2, 1., 1e-05, 0.2
...
*End Step
```

```
** DEFINITION STEP-17: DETERIORATION OF SHOTCRETE 80% (USER DEFINED FIELD)
** STEP: Step-17
*Step, name=Step-17, nlgeom=YES
DETERIORATION OF SHOTCRETE: 80% (USER DEFINED FIELD)
```

```
*Static
0.2, 1., 1e-05, 0.2
...
*End Step
```

```
** DEFINITION STEP-18: DETERIORATION OF SHOTCRETE 90% (USER DEFINED FIELD)
** STEP: Step-18
*Step, name=Step-18, nlgeom=YES
DETERIORATION OF SHOTCRETE: 90% (USER DEFINED FIELD)
*Static
0.2, 1., 1e-05, 0.2
...
*End Step
```

Appendix F

INPUTFILE "USER SUBROUTINE" – USER DEFINED FIELD (FORTRAN)

```
C23456789012345678901234567890123456789012345678901234567890123456789012
C
      SUBROUTINE USDFLD(FIELD,STATEV,PNEWDT,DIRECT,T,CELENT,
     1 TIME,DTIME,CMNAME,ORNAME,NFIELD,NSTATV,NOEL,NPT,LAYER,
     2 KSPT,KSTEP,KINC,NDI,NSHR,COORD,JMAC,JMATYP,MATLAYO,LACCFLA)
C
      INCLUDE 'ABA_PARAM.INC'
C
C     The following line must be included in the material description
C     *USER DEFINED FIELD
C     Do not forget to make your material property dependent on Field
C     Variable(s), e.g.
C     *ELASTIC, DEPENDENCIES=1
C      210000., 0.31, , 0.
C      130000., 0.28, , 1.
C
      CHARACTER*80 CMNAME,ORNAME
      CHARACTER*3  FLGRAY(15)
      DIMENSION FIELD(NFIELD),STATEV(NSTATV),DIRECT(3,3),
     1 T(3,3),TIME(2)
      DIMENSION ARRAY(15),JARRAY(15),JMAC(*),JMATYP(*),COORD(*)
C
C     Set Field variable equal to total time
C     at the beginning of the current increment
      FIELD(1) = TIME(2)
C     Store the total time as a solution dependend state varialbe
C     STATEV(1) = FIELD(1)
C
      RETURN

           END
```